UNIVERSITY OF BIRMINGHAM

Harmony in Early Visual Cortex: Uncovering the Complementary Roles of Gamma & Alpha Oscillations in Local & Global Processing

by

Katharina Duecker

A thesis submitted to the University of Birmingham for the degree of

DOCTOR OF PHILOSOPHY

Centre for Human Brain Health

School of Psychology

College of Life and Environmental Sciences

University of Birmingham

November 2023

Abstract

Upon opening our eyes, we immediately perceive the world around us. Our remarkably seamless visual perception is a major source of information when interacting with our surroundings. Indeed, the dominance of vision over other senses is so significant that the brain allocates more resources to it than to any other sensory modality (Colavita, 1974; Van Essen et al., 1992). Yet, our seemingly effortless visual experience relies on a complex network of intricately interconnected cortical and sub-cortical structures performing real-time computations.

A central question in neuroscience is how the visual system optimally processes and routes incoming information. Popular ideas posit that neuronal oscillations, specifically gamma (> 30 Hz) and alpha oscillations (8 - 12 Hz), coordinate visual processing and attention (Fries, 2005, 2015; Jensen, 2023; Jensen & Mazaheri, 2010; Klimesch, 2012; Klimesch et al., 2007).

In this thesis, I will present findings based on empirical and computational work showing how gamma and alpha oscillations modulate visual inputs. The empirical part of my thesis consists of two studies using Magnetoencephalography (MEG) in combination with a high-frequency (subliminal) visual flicker. I will reveal that gamma oscillations in early visual regions are robust against this external, high-frequency stimulation and do not synchronise to the visual flicker. As I will discuss, this finding challenges the prevalent notion that gamma oscillations are critical for inter-areal communication in the visual system (also see Schneider et al., 2021, 2023; Vinck et al., 2023).

Following my experience with high-frequency stimulation gained in the first empirical chapter, I will use Rapid Invisible Frequency Tagging (RIFT) in the third chapter to investigate the neural correlates of feature-guided visual search. RIFT is a novel, subliminal stimulation

technique used to probe cortical excitability to visual inputs (Zhigalov et al., 2019). I will demonstrate that alpha oscillations globally modulate the cortical excitability to the visual search display, which was further linked to improved search performance. This suggests that gain modulation by alpha oscillations can support performance in visual attention tasks with a high number of distracting stimuli. However, I will also discuss a set of analyses suggesting that the response time modulation by the alpha rhythm may be linked to task duration. I will offer different perspectives on these multi-faceted results, as well as future research directions to understand the relationship between inhibition by alpha oscillations and visual search performance.

Inspired by these empirical results, I will finally present a *dynamical artificial neural network* — a computer vision algorithm embracing the rhythmic dynamics of the visual cortex. I will demonstrate that this network, despite not being explicitly trained for the task, can handle multiple concurrent visual inputs by segregating them in time.

In summary, my thesis combines empirical and computational methods to explore how gamma and alpha oscillations contribute to computational processes in the visual system. I will conclude that while gamma oscillations reflect localised neural processes, alpha oscillations operate at a more global scale.

To my family. Danke für alles.

Acknowledgements

Throughout my time as a PhD student, I had the privilege to meet amazingly smart and kind mentors, colleagues, and friends. I feel incredibly lucky for all the support I have received.
First and foremost, my biggest gratitude goes to my lead PhD supervisor.

Ole, I cannot thank you enough for your guidance through the good times, the bad times, the COVID times, and the times-on-task. You have really gone out of your way to train me and I have learned so much working on such a wide range of projects with you. Thank you for always making time for me and for being extra encouraging when things got tough; for never allowing any amount of bugs or mistakes to stop you from believing in me. Thank you for always finding ways to support my scientific endeavours, and for writing countless letters of recommendation for me. Your commitment has opened many doors for me, and I am so grateful for your support.

Thank you to my secondary advisor, **Kim**. I would not have considered a career in science if it wasn't for the project on the Attentional Blink that I worked on during my undergraduate. Needless to say, it has been an honour to learn from you. I am grateful for our many conversations that always left me inspired and motivated. Thank you for always finding time to rewrite my convoluted thoughts into eloquent sentences. And many thanks for all the reference letters you have written for me - sometimes in as little as half an hour.

My collaborators and co-authors

Simon, somehow you always managed to pull rabbits out of your science hat whenever I needed a solution. Thank you for your tireless support over the years, for all the thought-provoking discussions, and for suggesting the visual search project in the first place. I hope we can find

ways for me to join your group at some point in my science life.

Jeremy, I feel very lucky to have the chance to work with you on one of my favourite paradigms in all of vision science - visual search. Thank you for sharing your incredible wisdom with me, and for always being the first one to send your edits, comments, and recommendation letters - even at the most impossible times. Your support has been invaluable.

Yali, without your help and expertise, the visual search project would not be what it is today. Thank you for generously sharing your scripts, and for always being available for a chat. You are an amazing colleague, and it's always been great fun working with you.

Tjerk, thank you for never minding my head popping through your office door whenever I needed advice (which was a lot), and for often dropping everything to help me. Your witty comments have always made work fun, and I feel very lucky to have had your support.

Christoph, your fantastic lectures have sparked my excitement for neuronal oscillations when I first started in Oldenburg. The set-up and training you provide for your MSc students is the perfect preparation for a PhD, and I am grateful to have benefited from that. Most importantly, thank you for setting up the contact with Ole in the first instance, and thus laying the foundation for this thesis.

Marco, thank you for patiently teaching me so much about computational neuroscience, dynamical systems, and linear stability. Despite my non-STEM background, I always felt like we spoke the same language. Your strategies and support when solving problems have been truly instrumental in forming my new aspirations to becoming a computational neuroscientist.

Marcel, thank you for editing my work in record time, for making sure the ANN stayed on course, and for the many solutions you have offered to our problems. It has been fantastic to work with you.

The (new and old) Neuronal Oscillations group, especially: Thank you to **Geoff** for being an incredibly rigorous scientific role model, for guiding my way to Python land, for editing numerous application letters, and for always making time to chat about statistics, batch jobs, and brains. It has been amazing to work with you! Thanks to **Alex** for involving me in the gamma-

echo project, for helping me set up my experiments, and for answering my many questions. A big thank you to **Iris**, the kindest and most selfless research assistant there ever was. You always went the extra mile to ensure we had what we needed, be it MRI scans, participant money, or birthday presents. Thank you for making everyone's workday that little bit better. **Dorottya**, thank you for being such a great support - both as an RA in the lab and as a friend. You always find the right words when the self-doubts take over, and I am so grateful to be able to come to you with all the good and bad news.

CHBH support staff A huge thank you to **Caroline** for always going out of your way to support us, the CHBH would be a mess without you. Thanks to **Chris** who *ran* the extra mile to get CHBH up and running, you were without a doubt the hardest working person in the centre! Thank you to **Jonathan** for all your tireless efforts to keep the MEG lab working and always making sure our data have the best possible quality. A big thank you to **Katia**, **Brandon**, **Alex**, **Davide**, **Roya**, and **Nina** for collecting MRI scans with me - there would be no source localisation results in the thesis without your help.

CHBH friends I have met many great people whilst working at the CHBH who, though not formally involved in my work, made the centre an amazing place to work. **Ben**, a big thank you for always listening to my data analysis miseries, for never minding me turning up at the office with loads of questions, for offering solutions where I didn't see any, and for super productive writing sessions. You make it all look so easy! Thank you to my great friend **Emma** for always being there for me, for continuously providing me with the soundtrack to my work and life, and for planning the checkpoints leading to my thesis submission. I'm so glad I sent you that Spotify link! **Mel**, I could not have made it through lockdown 1-10 without you! Thank you for showing me how to relax, for all the DMCs, and all the fun nights in and out! **Romy**, thank you for always making time to chat with me about postdocs, careers, and funding, and for regularly checking in to make sure that I'm doing alright. Your support has truly been amazing. **Andrew**, thank you for all the tea-point banter which more often than not turned into super helpful discussions about data analysis and statistics. Your rigour is truly inspiring. Thank you to **Todd** for letting me

vent about the stress of the final PhD sprint (and the sprints in between), and for the tyrannical think-tank writing sessions that allowed me to get more done in an hour than I usually did in a day. Thank you to **Jack**, **Alicia**, and **Foyzul** for making 119 an amazing office to work in - including a continuous biscuit supply.

...and finally A big thank you to my British family, **James M**, **James B**, **Liz**, and **Wendy** for adopting me from the moment I arrived in England for the first time, for curry nights and love island marathons. **Liz**, thank you for letting me stay with you and making Birmingham feel like home from the first day of my PhD. Thank you to **James M**, for the countless lifts and lessons in British culture. And a huge thank you to my wonderful friend **James B**, for never getting tired of my drama and for always sharing your life wisdom.

Thank you to **Bo**, for being the best housemate ever - for all the graphic design advice, the styling tips, the life lessons, the banter, for sharing your fancy clothes and my love for electronic music. Our friendship has been invaluable to my personal growth.

Jo and **Susie**, thank you for making Flat 4 feel like home right from the start, for all the banter and laughter, and for not only making the first lockdown bearable but surprisingly enjoyable at times. **Izaskun** and **Thomas**, thank you for making life in our mainland Europe houseshare so effortless, for crêpes Sundays and pizza dinners, and for keeping our little houseplant jungle growing.

Thank you to my brain camp besties **Laura**, **Cody**, and **Daniel** for making Kavli even more amazing than it already was, and for the most special 30th birthday weekend in New York.

A big thank you to my friend **Amanda** for clicking with me at first sight, for lovely countryside walks, coffee dates and G&T evenings, and for always finding the right words. Thank you to my life-long friend **Tanah** who has been cheering me on from the first day of the BSc to the end of my PhD, and for bringing home closer with daily phone calls during the lockdown. I feel incredibly lucky to have your support.

And finally, thank you to my parents for supporting my education from my first day at school, for the many hours of practising English vocabulary and solving equations for x. You both laid

the foundation for the work in this thesis. **Mama** und **Papa**, danke für alles.

Funding acknowledgement Lastly, I'd like to thank the School of Psychology for supporting me with a monthly scholarship and course waiver.

Publications and Contributions

Parts of this thesis contain material that has been published in an academic journal, posted on pre-print servers, and presented at academic conferences. The figures have been adjusted to achieve a common aesthetic for the thesis.

Chapter 2 I proposed the research idea. The project was designed in collaboration with Tjerk Gutteling, Christoph Herrmann, and Ole Jensen. Data was collected and analysed by myself. Ole Jensen and Tjerk Gutteling supervised the data anlaysis and data collection. The paper was written by myself under the supervision of Ole Jensen, the paper in its current form was edited by myself, Tjerk Gutteling, Christoph Herrmann, and Ole Jensen.

The pilot study of this project was reported in my thesis for the MSc degree Neurocognitive Psychology at the University of Oldenburg. The chapter presented here has been fully re-written, a new full data set (N=30) has been collected, and new analysis methods and results are presented.

Chapter 3 Simon Hanslmayr proposed the research idea following the PhD work by Aleksandra Pastuzsak. The experiment was designed by myself, Kimron Shapiro, Simon Hanslmayr, Jeremy Wolfe, and Ole Jensen. The data were acquired and analysed by myself. Jeremy Wolfe helped with the analysis of the behavioural data, Yali Pan supported the coherence analysis, Simon Hanslmayr provided guidance for the statistical analyses, Ole Jensen supervised all presented analyses. The chapter was written by myself and Ole Jensen, and edited by Kimron Shapiro, Simon Hanslmayr, Jeremy Wolfe, and Yali Pan.

Chapter 4 Ole Jensen proposed the research idea. The project was designed by myself, Ole Jensen, and Marco Idiart. The network architecture was developed by myself, with support from Marcel van Gerven. Marco Idiart developed the ordinary differential equations used for the dynamical system. Network simulations and parameter tuning were performed by myself under the supervision of Ole Jensen and Marco Idiart. The chapter was written by myself and Ole Jensen, and edited by all collaborators.

Journal articles and pre-prints

Chapter 2

Duecker, K., Gutteling, T. P., Herrmann, C. S., & Jensen, O. (2021). No evidence for entrainment: Endogenous gamma oscillations and rhythmic flicker responses coexist in visual cortex [Publisher: Society for Neuroscience Section: Research Articles]. *Journal of Neuroscience*, *41*(31), 6684–6698. https://doi.org/10.1523/JNEUROSCI.3134-20.2021

and the corresponding pre-print on BioRxiv:

Duecker, K., Gutteling, T. P., Herrmann, C. S., & Jensen, O. (2020, September 26). No evidence for entrainment: Endogenous gamma oscillations and rhythmic flicker responses coexist in visual cortex [Pages: 2020.09.02.279497 Section: Contradictory Results]. https://doi.org/10.1101/2020.09.02.279497

Chapter 3

Duecker, K., Shapiro, K. L., Hanslmayr, S., Wolfe, J., Pan, Y., & Jensen, O. (2023, August 3). Alpha oscillations support the efficiency of guided visual search by inhibiting both target and distractor features in early visual cortex [Pages: 2023.08.03.551520 Section: New Results]. https://doi.org/10.1101/2023.08.03.551520

Note that the text has been updated since posting this work on the pre-print server, and new results have been added in the current version of chapter 3.

Conference presentations and abstracts

Chapter 2

Duecker, K., Gutteling, T. P., Herrmann, C. S., & Jensen, O. (2020). No evidence for entrainment: Endogenous gamma oscillations and rhythmic flicker responses coexist in visual cortex [Neuromatch Conference 3 (virtual poster)]

Duecker, K., Gutteling, T. P., Herrmann, C. S., & Jensen, O. (2019). Does rapid frequency tagging entrain neuronal gamma oscillations? [British Association for Cognitive Neuroscience (poster)]

Chapter 3

Duecker, K., Shapiro, K. L., Hanslmayr, S., Wolfe, J., Pan, Y., & Jensen, O. (2023). Alpha oscillations in early visual cortex support visual search through blanket inhibition [European Society for Cognitive Psychology, Porto, Portugal (talk in Symposium Flicker & Flutter: recent advances in studying cognition using frequency tagging)]

Duecker, K., Shapiro, K. L., Hanslmayr, S., Wolfe, J., Pan, Y., & Jensen, O. (2023). Alpha oscillations in early visual cortex support visual search through inhibition of neuronal excitability to target and distractor features [Vision Science Society conference, St. Pete Beach, Florida, USA (talk)]

Duecker, K., Shapiro, K. L., Hanslmayr, S., Wolfe, J., Pan, Y., & Jensen, O. (2022). Alpha oscillations support modulation of neuronal excitability to target and distractor features in guided search [The 22nd International Conference on Biomagnetism (poster)]

Duecker, K., Shapiro, K. L., Hanslmayr, S., Wolfe, J., Pan, Y., & Jensen, O. (2022). Guided search is associated with modulated neuronal excitability to target and distractor features in early visual regions [International Conference of Cognitive Neuroscience (poster)]

Chapter 4

Duecker, K., Idiart, M., & Jensen, O. (2021). Space-to-time-conversion: Oscillations in an artificial neural network generate a temporal code representing simultaneous visual inputs [Montreal

AI & Neuroscience (conference abstract)]

Contents

Abstract **i**

Acknowledgements **v**

Publications and Contributions **xi**

Contents **xv**

List of Figures **xxi**

List of Tables **xxiii**

List of Acronyms **xxv**

1 Introduction **1**

1.1 A brief history of electrophysiology 2

1.1.1 The discovery of electric currents in the nervous system 2

1.2 Neuronal Oscillations 6

1.2.1 Oscillations conduct the orchestra of neuronal firing 7

1.3 Gamma oscillations: perceptual binding, neuronal computation, and neuroprotection 9

1.3.1 Binding by Synchrony 9

1.3.2 Communication through Coherence 12

1.3.3 Gamma oscillations in cognitive tasks 14

1.3.4 Photic stimulation in the gamma band to counter neuro-degeneration . . 15
1.3.5 Challenges to the involvement of gamma oscillations in perceptual binding and neuronal communication 16
1.4 Alpha oscillations: Idling vs. Functional Inhibition 19
1.4.1 Early views: alpha oscillations as neuronal "idling" 19
1.4.2 Evidence for the functional relevance of alpha oscillations 20
1.4.3 Alpha oscillations facilitate attention through inhibition. 21
1.4.4 Alpha oscillations in spatial attention 22
1.4.5 The role of alpha inhibition in attention to low-level features is undetermined 24
1.4.6 Questions surrounding gain modulation by alpha oscillations 25
1.4.7 Phasic modulation of neuronal excitability by alpha oscillations 26
1.4.8 Alpha oscillations may implement a processing pipeline in the visual system 28
1.4.9 Linking computational models of the visual system to Computer Vision 29
1.5 Questions addressed in this thesis 31

2 No evidence for entrainment: endogenous gamma oscillations & rhythmic flicker responses coexist in visual cortex 33

2.1 Abstract 34
2.2 Introduction 35
2.3 Materials and Methods 38
2.3.1 Experimental Procedure & Apparatus 38
2.3.2 Rapid photic stimulation 39
2.3.3 Experimental paradigm 39
2.3.4 Participants 42
2.3.5 MEG sensor analysis 43
2.3.6 MEG source analysis 45
2.3.7 Experimental Design & Statistical Analyses 46

2.4 Results . . . 49
2.4.1 Identifying Individual Gamma Frequencies . . . 49
2.4.2 Photic drive induces responses up to 80 Hz . . . 51
2.4.3 Magnitude of flicker response decreases as a function of frequency . . . 54
2.4.4 Gamma oscillations and flicker response coexist . . . 55
2.4.5 Frequency analyses with a longer time window confirm robustness of the reported results . . . 57
2.4.6 Oscillatory gamma dynamics cannot be captured by frequency entrainment 58
2.4.7 Photic drive does not reliably modulate gamma phase . . . 60
2.4.8 The sources of the gamma oscillations and the flicker responses peak at different locations . . . 62
2.5 Discussion . . . 65
2.5.1 Flicker responses do not entrain the gamma oscillator . . . 65
2.5.2 Coexistence of flicker responses and oscillations versus oscillatory entrainment . . . 67
2.5.3 Limitations & Generalizability . . . 68
2.6 Conclusion . . . 71

3 Alpha oscillations may support the efficiency of guided visual search by inhibiting both target and distractor features in early visual cortex 73

3.1 Abstract . . . 74
3.2 Introduction . . . 75
3.3 Methods . . . 79
3.3.1 Experimental design & stimuli . . . 79
3.3.2 Apparatus for data acquisition . . . 80
3.3.3 Participants . . . 80
3.3.4 Behavioural performance . . . 81
3.3.5 MEG pre-processing . . . 81
3.3.6 RIFT response magnitude . . . 82

3.3.7 RIFT response sensor selection . . . 83
3.3.8 Power at the Individual Alpha Frequency . . . 84
3.3.9 Source localisation . . . 84
3.4 Results . . . 87
3.4.1 Rapid Invisible Frequency Tagging responses indicate target boosting and distractor suppression . . . 87
3.4.2 Strong pre-search alpha oscillations predict enhanced search performance and reduced Rapid Invisible Frequency Tagging (RIFT) responses in guided search . . . 90
3.4.3 Strong alpha power during search is linked to faster reaction times and reduced RIFT responses in *guided* and *unguided* search . . . 93
3.4.4 Time-on-task as a confounding variable in search performance and cortical excitability - exploratory analyses . . . 95
3.5 Discussion . . . 98
3.5.1 Limitations & Outlook . . . 101
3.6 Conclusion . . . 103

4 Oscillations in an Artificial Neural Network convert competing inputs into a temporal code 105

4.1 Abstract . . . 106
4.2 Introduction . . . 107
4.3 Methods . . . 111
4.3.1 Network architecture . . . 111
4.3.2 Network dynamics in the hidden layers . . . 113
4.3.3 Fixed points of the system . . . 114
4.4 Results . . . 115
4.4.1 Network stability and parameters . . . 115
4.4.2 Alpha oscillations stabilise dynamics in a two-layer Neural Network . . . 118
4.4.3 Simultaneous presentation of two inputs produces a temporal code . . . 120

4.4.4 Making and breaking the temporal code: the effect of phase delay between the layers . . . 124
4.5 Discussion . . . 126
4.6 Conclusion . . . 131

5 Discussion **133**
5.1 Summary of the core findings . . . 135
5.2 Novel insights & future directions . . . 138
5.2.1 The low-pass filter properties of neuronal integration attenuate the propagation of gamma oscillations along the visual hierarchy. . . . 138
5.2.2 Gamma oscillations may still support vision by increasing the information represented by individual spikes. . . . 141
5.2.3 Gamma oscillations may support local neuronal processing. . . . 142
5.2.4 Gating by alpha oscillations may flexibly operate in different areas for the different forms of attention. . . . 144
5.2.5 The link between blanket inhibition and the temporal code . . . 146
5.2.6 Extensions of the dynamical artificial neural network could embrace the local and global dynamics of the visual system. . . . 148

6 General conclusion **151**

A Appendix Chapter 3 **153**
A.1 Supplementary Analyses . . . 154
A.1.1 Behavioural results: Guided Search is associated with better performance 154
A.1.2 RIFT responses for fast compared to slow trials . . . 155
A.1.3 Ocular artefacts and gaze bias not linked to reaction time or alpha power 156
A.2 Supplementary Figures . . . 159
A.3 Supplementary Tables . . . 169

B Appendix Chapter 4 **175**

List of Figures

1.1 The synapse and action potential 5
1.2 Binding by Synchrony and Communication Through Coherence 12
1.3 Gating by inhibition, duty cycle, and temporal code. 22

2.1 Experimental paradigm 40
2.2 Identification of Individual Gamma Frequencies and Sensors-of-Interest 50
2.3 Topographies of the response to the rhythmic flicker 51
2.4 Averaged power spectra per *frequency*×*condition* combination 52
2.5 Magnitude of the flicker response as a function of frequency 53
2.6 Single-subject Time-Frequency Representations of the *flicker&gratings* condition 56
2.7 Grand average Time-Frequency Representations of the *flicker&gratings* condition 57
2.8 Power change at the Individual Gamma Frequency (IGF) as an indicator of frequency entrainment 58
2.9 Phase angle and phase plateaus 61
2.10 Source localisation of the gamma oscillations and flicker response 63

3.1 Models of visual search considering a priority map and inhibition by alpha oscillations. 77
3.2 Experimental paradigm, Rapid Invisible Frequency Tagging and search performance. 88
3.3 Rapid Invisible Frequency Tagging responses reflect a priority-map based mechanism. 89

3.4 Alpha oscillations pre visual search predict better performance and reduced RIFT responses. 91
3.5 Alpha oscillations during visual search predict faster response times and reduced RIFT responses. 94
3.6 The blanket inhibition confound with time-on-task: behaviour and RIFT responses. 96

4.1 Concept: An interplay between object-based attention and neuronal alpha oscillations implements a pipelining mechanism reflected by a temporal code. . . 108
4.2 The classification problem and network architecture. 112
4.3 Dynamics of H and R in a single node and dependence on key parameters. . . . 116
4.4 Dynamics in the neural network in response to a single input (here letter A) in absence and presence of the alpha inhibition. 119
4.5 The bottleneck problem when the network receives two inputs simultaneously. . 120
4.6 The oscillatory neural network multiplexes simultaneously presented stimuli. . 121
4.7 Segmentation of the competing inputs along the network layers 123
4.8 The read-out of two simultaneous stimuli as a function of phase delay between the layers. 125

A.1 Individual topoplots of the RIFT response 160
A.2 RIFT responses for fast vs slow trials 161
A.3 Indiviudal topoplots of power at the Individual Alpha Frequency 162
A.4 Individual alpha frequency per participant 163
A.5 Alpha power pre- and during search does not differ between conditions. 164
A.6 Spectra of alpha power pre-search high vs. low 165
A.7 RIFT responses for set size 16, alpha high vs. low. 166
A.8 Spectra of alpha power during search high vs. low 167
A.9 Ocular artefacts for fast vs. slow trials, and trials with high and low alpha power. 168

B.1 Examples of the temporal code for all input combinations. 176

List of Tables

2.1 Estimated simple linear regression models: Flicker response as a function of frequency 55

A.1 Results of the hierarchical regression on reaction time. 169

A.2 Reaction time contrasts between conditions 170

A.3 Hierarchical regression on accuracy 171

A.4 Sensitivity contrasts between conditions 172

A.5 Number of saccades for fast vs slow trials 173

A.6 Number of saccades for high vs low pre-search alpha power 173

A.7 Number of saccades for high vs low alpha power during search 173

List of Acronyms

ANN Artificial Neural Network.

ANOVA Analysis of Variance.

CNN Convolutional Neural Network.

DICS Dynamic Imaging of Coherent Sources.

DNN Deep Neural Network.

ECG Electrocardiography.

ECoG Electrocorticography.

EEG Electroencephalography.

EOG Electrooculography.

fMRI functional Magnetic Resonance Imaging.

fMRI functional Magnetic Resonance Imaging.

GABA Gamma Aminobutyric acid.

HPI Head-Position-Indicator.

ICA Independent Component Analysis.

IGF Individual Gamma Frequency.

IT Inferior Temporal cortex.

LFP Local Field Potential.

MEG Magnetoencephalography.

MNI Montreal Neurologic Institute.

ODE Ordinary Differential Equation.

ReLU Rectified Linear Unit.

RFT Rapid Frequency Tagging.

RIFT Rapid Invisible Frequency Tagging.

RNN Recurrent Neural Network.

TFR Time-Frequency Representation.

V1 Primary Visual Cortex.

V2 Secondary Visual Cortex.

V4 Visual Area 4.

1

Introduction

Every sensation, every perception, even that which arises in us from the observation of a beautiful landscape, a beautiful painting, or from seeing a friend's visage, is due to the flow of tiny electric signals. Like an "electric storm," these signals incessantly flow along the fibers of our peripheral nerves or the central circuits of our brain.

SHERRINGTON (1949)

1.1 A brief history of electrophysiology

Neuronal activity is fundamentally electric. Although this concept has been understood for more than a century, it took approximately 150 years from the initial recordings of electric activity in animal muscle fibres to secure measurements of neural currents in the human brain. The narrative of electrophysiology is both intricate and expansive; it encompasses contributions from scientists in Italy, Germany, America, and England, the invention of the battery, and several Nobel Prizes. Here, I offer a brief, albeit not exhaustive, outline of key events and figures that paved the way for the first recordings of rhythmic electric current flow—neuronal oscillations—in the human brain.

1.1.1 The discovery of electric currents in the nervous system

Scientists of the 18th century were widely fascinated with electricity, a term coined by William Gilbert ca. 1600 (Finger, 2005b). Experimentation with electricity was the trend among aspiring scientists; particularly the field of electrotherapy - the use of electricity to treat sickness and injuries – drew widespread attention (Finger, 2005b; Piccolino & Bresadola, 2013). These medical applications, often performed by individuals without any formal training, led to the notion that electricity was the "fluid of the nerve" (Finger, 2005b).

Aloisio Luigi Galvani (1737-1798), an Italian physician practising in Bologna in the second half of the 18th century, was inspired by these advances. He studied the *fluido elettrico* (electrical fluid) in frog preparations (Finger, 2005b; Piccolino & Bresadola, 2013). His landmark 1791 publication entitled Commentary on the Effects of Electricity on Muscular Motion (*De viribus electricitatis in motu musculari commentarius*) was among the first documentations of what he termed *animal electricity*. In this work, Galvani reported that administering an electric spark to a deceased frog's leg muscle led to "violent contractions". Based on these observations, and several follow-up experiments, Galvani hypothesised that the electric spark activated inherent currents in the nerve fibres (Fara, 1995; Finger, 2005b; Piccolino & Bresadola, 2013;

Underwood, 1955) [1].

Galvani's remarkable findings, although later confirmed by a series of experiments, did not immediately win the approval of his peers. One notable sceptic was Alessandro Volta, who refuted Galvani's idea that muscle contractions were generated by innate neural currents (Piccolino et al., 2013). Volta argued that the observed electrical activity was due to the electromotive properties of the metals used in Galvani's experiments connecting the nerves and muscle fibres. This debate persisted for years, lasting until Galvani's death in 1798, and was instrumental in the development of the first electric battery—the voltaic pile (Finger, 2005b). Despite—or perhaps thanks to—the prolonged discourse between Galvani, Volta, and other scientists, experiments in the early 19th century would conclusively affirm that nerves are electrically excitable and that nervous energy is, indeed, electric (Finger, 2005b; Piccolino et al., 2013).

The development of the galvanometer - named in honour of Galvani's work and credited to German physicisist, chemist, and mathematician Johann Schweigger (Landman, 2004; Schweigger, 1836) – would lead to fundamental advances in the study of nervous conduction in the late 19th and early 20th century. Around 1850, Hermann von Helmholtz employed the galvanometer to quantify the time delay between applying an electric spark to a muscle fibre and the onset of the resultant muscular contraction. This experiment allowed him to reliably estimate neural signal speed (Schmidgen, 2014; von Helmholtz, 2021).

Following his mentor's lead, Helmholtz's student Julius Bernstein advanced the galvanometer ca. 1868 to measure changes in time and accomplished the first measurements of electric discharge in neurons (Seyfarth, 2006). Moreover, he proposed notably accurate hypotheses about the changes in intra- and extra-cellular charges in neuronal firing (Piccolino & Bresadola,

[1] Various theories surround Galvani's first observations of "animal electricity," all suggesting that the initial discovery was more serendipitous than systematic. According to some reports, Galvani made this observation when touching a frog's leg with a metal instrument during a thunderstorm (Fara, 1995; Finger, 2005b; Piccolino & Bresadola, 2013). Others describe that Galvani observed said muscle contractions in the frog when preparing a frog soup for his bedridden wife Lucia (Piccolino & Bresadola, 2013). Yet others claim that it was not Galvani himself, who applied the electric current to the frog preparation, but his assistants who found amusement in playing with the devices in the laboratory (Finger, 2005b), or a servant who had hung a dead frog up on a copper hook on the balcony, causing muscle contractions every time the lifeless frog's legs touched the iron railing (Piccolino & Bresadola, 2013).

2013). These ideas were later corroborated in in-depth studies of action potentials (Box 1.1 Hodgkin & Huxley, 1952; Piccolino & Bresadola, 2013).

Following the First World War, ca. 1917, Sir Edgar Adrian published seminal work that had been started by his mentor Keith Lucas, describing several characteristics of neuronal firing, which were again explored using an improved version of the galvanometer (Lucas & Adrian, 1917)[2]. Fast forward to another seminal moment in the history of electrophysiology, Alan Hodgkin and Andrew Fielding Huxley utilised the galvanometer to measure transmembrane currents in squid axons (Hodgkin & Huxley, 1952). Their work led to the creation of the Hodgkin-Huxley model, a mathematical formula describing how action potentials initiate and propagate, that is still used today (Hodgkin & Huxley, 1952; McCormick et al., 2007). The action potential is described in detail in Box 1.1.

And, importantly, it was a galvanometer that was used for the first non-invasive recordings of electric current from the human brain, famously performed by Hans Berger ca. 1924, a professor of neurology and psychiatry in Jena, Germany (Berger, 1929, 1931, 1932, 1933a, 1933b, 1933c, 1934, 1935)

[2] A key figure in the development of an amplified galvanometer was American scientist Alexander Forbes, who would become a close collaborator of Lucas' and Adrian's. In fact, Forbes was so engrossed in his work with Lucas and Adrian, that he delayed his return from Liverpool to Boston and cancelled his ticket for the ill-fated Titanic (Finger, 2005a).

Box 1.1: The action potential (spike)

Neurons communicate via synapses, i.e. connections between one neuron's axon and another neuron's dendrite (Figure 1.1a). At rest, the ion concentrations between the intra- and extracellular spaces maintain a stable charge of approximately -70mV. If a synaptic excitation is sufficiently strong to depolarise the membrane potential to around -50 mV, an action potential is initiated near the axon hillock (Figure 1.1a and b). This event surges the transmembrane potential to approximately +40 mV (Figure 1.1b). The action potential, or spike, then travels down the axon to the synapse where the neuron connects to a neighbouring neuron (Figure 1.1a). Following the spike, the cell repolarises, to the point where the transmembrane potential drops below the resting potential of -70 mV. Following this refractory period, the transmembrane current recovers back to its resting potential (Figure 1.1b, see Gazzaniga, 2009; Pinel & Barnes, 2017). Depending on the strength of the transmitted signal, the receiving neuron may perpetuate the process. Although the action potential is known to be an "all-or-nothing" response, inputs that do not trigger a spike may still increase or reduce the transmembrane current such that a subsequent input may be more or less likely to cause a spike. Throughout the thesis, I will repeatedly argue that neuronal oscillations increase or decrease the excitability within a population, thus offering "windows of opportunity" for a spike (Moore et al., 2010). This is based on the notion that the membrane potential of the neurons participating in the oscillation decreases and increases rhythmically (Anderson & Strowbridge, 2014; Buzsáki & Draguhn, 2004; Llinás, 1988).

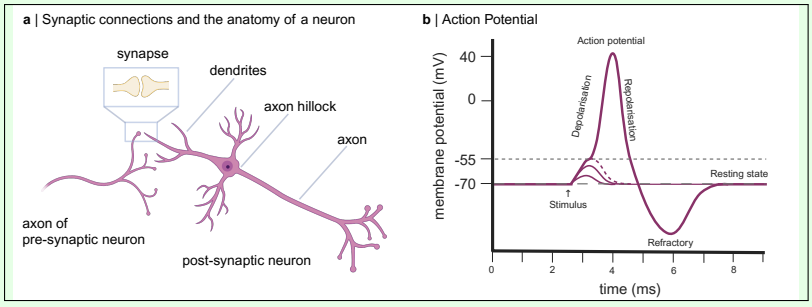

Figure 1.1: The synapse and action potential. **a** The anatomy of a pyramidal neuron and synaptic connection with neighbouring neuron. **b** The time course of the action potential.

1.2 Neuronal Oscillations

Clocks tick, bridges and skyscrapers vibrate, neuronal networks oscillate.

Buzsáki and Draguhn (2004)

In a series of seminal papers, Hans Berger describes a series of invasive and non-invasive electrophysiological recordings from human participants, laying the foundation for the electroencephalogram (EEG; Berger, 1929, 1931, 1932, 1933a, 1933c, 1934, 1935). Berger reported rhythmic high-amplitude oscillations with a period of 90-100 ms, which he famously termed the "alpha" rhythm (in early works also referred to as "Berger rhythm", Adrian & Matthews, 1934). This activity was often overlaid by or alternated with faster, lower-amplitude oscillations with a period of about 35 ms, termed "beta" rhythm (Berger, 1929). Due to its prominence and high amplitude, most early reports focused on studying the alpha rhythm (Adrian & Matthews, 1934; Adrian & Yamagiwa, 1935; Berger, 1929, 1931, 1932, 1933c, 1934, 1935).

While many researchers were convinced about the cerebral origin of these oscillations (Adrian & Yamagiwa, 1935; Berger, 1929; Hogan & Fitzpatrick, 1988), others questioned whether they were indeed generated by the brain and did not reflect artefacts from muscular activity (Lippold, 1970; Upton & Payan, 1970). Today, it is well-established that neuronal oscillations are produced by transmembrane currents underlying both spiking and non-spiking activity (Buzsáki & Watson, 2012; Einevoll et al., 2013; Lopes Da Silva & Storm Van Leeuwen, 1977).

In human participants, oscillations are generally studied non-invasively using EEG or magnetoencephalography (MEG), or via electrocorticography (ECoG), an array of electrodes directly placed the brain's surface to identify seizures in patients with treatment-resistant epilepsy (Buzsáki & Watson, 2012; Lopes da Silva, 2022). In non-human primates, oscillations can be observed in intracranial recordings of extracellular currents, known as the Local Field Potential (LFP, Buzsáki & Watson, 2012).

Over the last three decades, research on neuronal oscillations in cognition (Başar et al., 2000;

Jensen & Hanslmayr, 2020; Jensen, Spaak, & Zumer, 2014; Jensen et al., 2007), psychiatric and neurological disorders (Başar, 2013; Schnitzler & Gross, 2005; Uhlhaas & Singer, 2006, 2010), and neuronal computation has attracted great interest (Akam & Kullmann, 2014; Buzsáki & Vöröslakos, 2023; Salinas & Sejnowski, 2001; Varela et al., 2001). Following Berger's terminology (Berger, 1929), researchers still follow the convention to categorise neuronal oscillations according to their frequency bands and distinguish between rhythms in the delta (0.1 – 3 Hz), theta (4 – 8 Hz), alpha (8 – 12 Hz), beta (13 – 25 Hz), and gamma-band (>30 Hz), which are conserved across different species—from rodents and primates to humans and even insects (Buzsáki & Vöröslakos, 2023).

This thesis focuses on the role of gamma and alpha oscillations in visual perception and attention.

1.2.1 Oscillations conduct the orchestra of neuronal firing

> *When an axon of cell A is near enough to excite a cell B and repeatedly or persistently takes part in firing It, some growth process or metabolic change takes place in one or both cells such that A's efficiency, as one of the cells firing B, is increased.*
>
> – Donald Hebb, 1949, p. 62, available at: pure.mpg.de, but see Hebb (2002)[3]

In "The Organization of Behavior," one of the most influential works in modern neuroscience, Donald Hebb posits that cell assemblies—reciprocal neuronal connections—emerge when adjacent neurons recurrently stimulate each other (Hebb, 2002). While Hebb explicitly linked these connections to synaptic plasticity, the computational benefit of synchronised neuronal activity has also been discussed in the context of neuronal communication and visual perception. For instance, the coincident firing of several neurons, e.g. in the form of coherent feedforward inputs (Peter et al., 2021; Singer, 2018) or proximal and distal feedforward and feedback inputs (Larkum, 2013), has been argued to increase the impact of individual spikes on the receiving

[3]This quote is often used in its summarized form: "Neurons that fire together, wire together". However, it was not Hebb who first used these words, but Carla Shatz (Collins, 2017)

cell.

Moreover, transient synchronous activity between neurons has been suggested to create a "neural word", that can be read out by a receiving population (Buzsáki, 2010; Engel & Singer, 2001). As I will detail below, this has been linked to the binding of low-level visual features into coherent object representations (Singer, 1999; von der Malsburg, 1985, 1995). Neuronal oscillations have long been theorised to facilitate the creation of cell assemblies by synchronising neurons aiming to collaborate, and may thus play a role in efficient neuronal communication (Buzsáki, 2010; Singer & Gray, 1995; Singer, 1999, 2018). These ideas indicate a computational benefit of neuronal synchronisation (Buzsáki, 2010; Engel & Singer, 2001).

The complexity of cognitive and behavioural tasks demands more than just localised neuronal assemblies; it also calls for coordinated interactions among distributed neural networks (Buzsáki et al., 2013). In addition to their involvement in the formation of local neuronal partnerships, oscillations have long been proposed to enable inter-areal communication (Bressler & Kelso, 2001; Bressler et al., 1993; Buzsáki & Watson, 2012; Buzsáki et al., 2013; Engel et al., 2001; Varela et al., 2001). Synchronous rhythms in anatomically distant areas are often interpreted as indicators of long-range neural connectivity, whereby the oscillations are believed to effectively convey information between the regions (Fries, 2005, 2015; Hoppensteadt & Izhikevich, 1998; Varela et al., 2001). The notion that long-range connections modulate neuronal activity in distinct regions underpins the concept that cognition is an active, orchestrated process, rather than a mere byproduct of local, sequential neuronal activation.

Two highly influential theories, known as *Binding by Synchrony* (Engel et al., 1991; Gray, 1994; Singer & Gray, 1995; Singer, 1999) and *Communication Through Coherence* (Fries, 2005, 2015), underscore the role of gamma oscillations (>30 Hz) in both the formation of cell assemblies and inter-regional communication.

1.3 Gamma oscillations: perceptual binding, neuronal computation, and neuro-protection

In his pioneering paper on human EEG recordings, Hans Berger reported brief bursts of high-frequency activity, lasting around 30 ms, that were prominent when participants were engaged in cognitively demanding tasks (Berger, 1929). Consistent with these initial findings, gamma oscillations have been frequently linked to sensory perception and cognition (Cardin, 2016; Herrmann & Mecklinger, 2001; Herrmann et al., 2004; Jensen et al., 2007; Sohal, 2016).

In the late 1980s, the hypothesis emerged that these oscillations serve to orchestrate the formation of cell assemblies (Gray & Singer, 1989; Gray, 1994; Singer & Gray, 1995). This notion has since been extensively studied in a multitude of experiments, particularly in the context of perceptual binding and neuronal communication (for review see Buzsáki & Wang, 2012; Engel et al., 2001; Fries, 2005, 2015; Gray, 1994; Singer & Gray, 1995; Singer, 1999, 2018).

1.3.1 Binding by Synchrony

As soon as an object enters our visual field, we can quickly perceive and segregate it from its surroundings. This seamless perception relies on an intricate hierarchical visual system that binds the neuronal representations of simple features into a unified percept of each object.

The visual ventral stream, extending from the primary visual cortex to the inferior temporal cortex, plays a pivotal role in object recognition (DiCarlo & Cox, 2007). By relating electrophysiological recordings and neuroimaging data to the representations emerging in Deep Neural Networks (DNNs) for image classification, it has been repeatedly demonstrated that the complexity of the neural representations increases along this hierarchically structured system (Güçlü & van Gerven, 2015; Kruger et al., 2013; Yamins & DiCarlo, 2016; Yamins et al., 2014). Neurons in the primary visual cortex have been consistently shown to respond to simple features such as the orientation of contours, while neurons in higher-order areas respond to more

complex feature conjunctions (Carandini, 2005; Felleman & Van Essen, 1991; Van Essen et al., 1991). The increasing complexity of the neural representations along the visual hierarchy is further coupled to increasing receptive field sizes (Reynolds & Desimone, 1999; Rolls & Baylis, 1986; Rolls et al., 2003; Tovee et al., 1994). This structure gives rise to the binding problem: the neuronal representations of the low-level features belonging to the same object must converge along the hierarchy such that they are integrated into a coherent percept.

Considering the complexity of our visual system, and the abundance of stimuli in our visual world, feature binding is not a trivial task (Roelfsema, 2023). It has been proposed that the brain might solve the binding problem with neurons that are responsive to feature conjunctions (Reynolds & Desimone, 1999; Shadlen & Movshon, 1999). A neuron that is responsive to the conjunction "blue triangle", could integrate the responses of one neuron responding to triangular shapes, and another neuron responding to the colour blue. However, the feasibility of this coding scheme is limited, as it requires the neurons to have overlapping receptive fields. Moreover, the number of possible feature combinations in the world is likely to exceed the number of neurons in the visual cortex (Roelfsema, 2023; Shadlen & Movshon, 1999).

The *Binding by Synchrony* model proposes a complementary mechanism, suggesting that complex objects are represented by the synchronous activity of distributed neurons, each favouring different features of the same object (Aertsen & Arndt, 1993; Milner, 1974; von der Malsburg, 1995, 1999) . Originally proposed by von der Malsburg (1981), this model has been updated in the late 1980s by Singer and colleagues who hypothesised that gamma oscillations orchestrated spiking activity in cortical areas and thus facilitated the binding (Engel et al., 2001; Gray & Singer, 1989; Singer & Gray, 1995) . Consider the example in Figure 1.2 a, showing a scientist focusing her gaze on an Erlenmeyer flask. According to the *Binding by Synchrony* model, the flask is represented and communicated across the visual cortex through synchronous spiking of all neurons responding to the contours of the object within a gamma cycle (Figure 1.2c, Engel et al., 2001; Gray, 1994; Singer & Gray, 1995; Singer, 1999). Gamma oscillations have been repeatedly shown to underlie a balance of excitation and inhibition (Börgers & Kopell, 2003; Börgers et al., 2008; Olufsen et al., 2003; Traub et al., 1997; Whittington et al., 2011). The

up-state of the gamma cycle has been argued to reflect a state of high excitation, thus providing a "window of opportunity" for the neurons to discharge (Fries et al., 2007; Nikolić et al., 2013). By concentrating the spikes within a short time window, it has been argued that the receiving area can read them out as a coherent neuronal representation of the visual input (Engel et al., 2001; Gray, 1994; Singer & Gray, 1995; Singer, 1999). The *Binding by Synchrony* model was initially developed based on intracranial recordings in cat visual cortex showing that neurons in early visual cortex synchronised their firing to ongoing gamma oscillations in response to visual stimuli (Eckhorn et al., 1988; Gray & Singer, 1989). This notion was supported by further subsequent studies based on intracranial recordings in the visual cortex of cats (Engel et al., 1990; Fries, Neuenschwander, et al., 2001; Gray & Prisco, 1997; Gray et al., 1990; König et al., 1995; Roelfsema et al., 1997) and non-human primates (Fries, Reynolds, et al., 2001; Havenith et al., 2011; Maldonado et al., 2000; Womelsdorf et al., 2007).

Following the excitement generated by the *Binding by Synchrony* hypothesis, gamma oscillations and gamma-band activity have been extensively studied in the visual cortex of humans and non-human primates (Brunet et al., 2015; Brunet & Fries, 2019; Gieselmann & Thiele, 2008; Hoogenboom et al., 2010; Jia et al., 2011; Müller et al., 1997; Muthukumaraswamy et al., 2010; Stauch et al., 2022; Tallon et al., 1995; Vidal et al., 2006). Moreover, several studies have claimed that activity in the gamma-band carries stimulus- and feature-specific information (Brunet et al., 2014; Brunet & Fries, 2019; Fries, Neuenschwander, et al., 2001; Peter et al., 2019; Stauch et al., 2022). In line with these findings, visual attention has been linked to enhanced gamma synchrony in visual and prefrontal areas, suggesting that these oscillations are involved in processing the attended stimulus (Bichot et al., 2005; Buschman & Miller, 2007; Fries, Reynolds, et al., 2001; Gregoriou et al., 2009; Kim et al., 2016; Vinck et al., 2013).

In sum, the *Binding by Synchrony* model, and the multitude of studies supporting its predictions, have generated considerable enthusiasm over the role of gamma oscillations in visual perception. However, the excitement about the importance of gamma oscillations for neuronal processing is juxtaposed by a number of reports questioning the plausibility of the *Binding by Synchony* hypothesis (Roelfsema, 2023; Roelfsema et al., 2004; Shadlen & Movshon, 1999). As

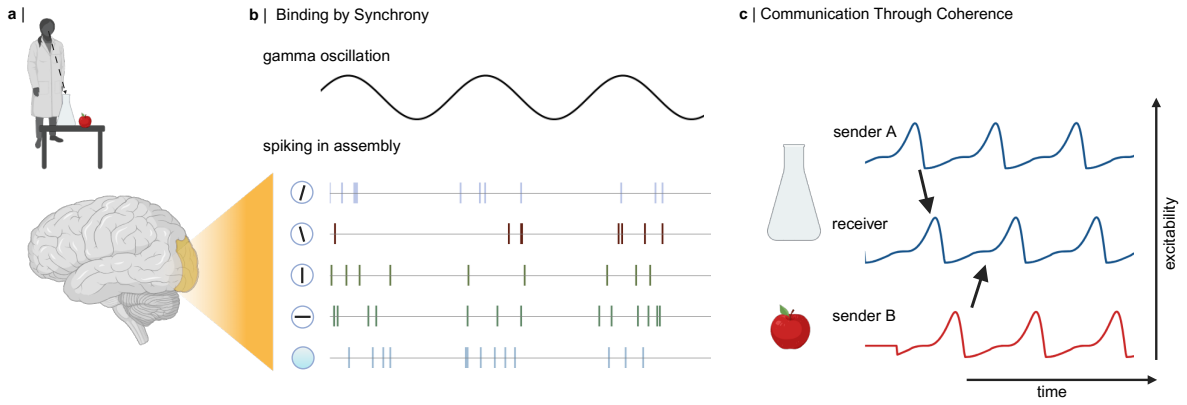

Figure 1.2: **a** Example: A scientist looking at an Erlenmeyer flask. **b** The *Binding by Synchony* hypothesis predicts that features belonging to the same object are bound through synchronous spiking in feature-selective neurons. (top) Ongoing gamma oscillation in the population, (bottom) spike raster of the neurons responding to the contours and colour of the flask. The circles signify that each feature is encoded by neurons with different receptive fields. The neurons fire only during the excitable state of the oscillation. (This figure is strongly inspired by Engel et al., 2001 and Roelfsema, 2023) **c** The *Communication Through Coherence* hypothesis predicts that synchronous oscillatory activity between two populations acts as a channel for communication between them. The blue trace associated with sender A reflects collective activity within a neuronal population in response to the Erlenmeyer flask, the red trace reflects neuronal activity in response to the apple. The phase relationship between sender A and the receiver is optimal for communication, as the excitatory input from A arrives at an excitatory state in the receiver. The signal from sender B, on the other hand, reaches the receiver in an inhibitory state, and is unable to activate the neurons in the receiving population.

I will outline at the end of this section, this criticism has recently gained momentum.

1.3.2 Communication through Coherence

Building on concepts analogous to the *Binding by Synchrony* model, the *Communication through Coherence* theory proposes that synchronisation between neuronal populations—typically quantified using coherence metrics—facilitates communication between cortical regions (Fries, 2005, 2015). The rhythmic modulation of neuronal excitability in the gamma range is again central to this model: Strong gamma oscillations in the "sender" neurons have been argued to concentrate the neuronal spiking within the gamma cycle (Fries et al., 2007; Singer, 1999). If the gamma oscillations in the sending and receiving population are synchronous, the inputs from the sending population will reach the "receiver" neurons in a state of heightened excitability (Fries, 2005, 2015). In turn, the sender will be able to drive the receiver effectively (Başar-Eroglu et al., 1996;

Fries, 2005, 2015; Salinas & Sejnowski, 2000).

To visualise these concepts, consider again the example motivated in Figure 1.2, whereby the scientist focuses her gaze and attention on the flask, while the apple on the table is outside her attentional focus. The blue and red traces in Figure 1.2c depict the gamma-band activity in response to the flask and the apple in three different neuronal populations sender A, sender B, and a receiver population. All areas show oscillations in the gamma band, reflected as a balanced interplay of excitation (sawtooth-shaped peak) and inhibition (trough). According to the *Communication Through Coherence* theory, as sender A wants to communicate the representation of the flask to the receiver, the two regions will synchronise their activity in the gamma band such that their phase relationship is optimal for communication (Fries, 2005, 2015). As the excitation triggers local inhibition in both the sender and the receiver (Börgers et al., 2008), the excitatory inputs from sender B reach the receiver in an inhibitory state and will be insufficient to excite the neurons in that area in order to trigger spiking. As a result, the representations of the apple are not communicated between sender B and the receiver.

Inter-areal coherence at gamma frequencies has been especially well-documented within the macaque visual system (Bastos, Vezoli, & Fries, 2015; Bosman et al., 2012; Grothe et al., 2012; Womelsdorf et al., 2007). Several studies have proposed that gamma oscillations facilitate feedforward communication by synchronising population activity across successive regions within the visual ventral stream (Bastos, Vezoli, & Fries, 2015; Shin et al., 2023; van Kerkoerle et al., 2014; Womelsdorf et al., 2007). This aligns well with the core premise of the *Communication through Coherence* model, according to which the inter-areal synchrony orchestrates the activity between visual areas in a manner that is conducive to effective communication. This type of oscillatory communication has been metaphorically linked to radio signals, transmitting information from a sender to a receiver (Hoppensteadt & Izhikevich, 1998).

Much like the *Binding by Synchrony* hypothesis, *Communication through Coherence* has generated great excitement about gamma oscillations and a rich body of literature arguing in favour of its predictions (Bastos, Vezoli, & Fries, 2015; Bastos, Vezoli, Bosman, et al., 2015; Bosman et al., 2012; Michalareas et al., 2016; Womelsdorf et al., 2007). However, recent

reports have questioned whether the coherence measure is feasible to infer that two populations have synchronised their activity (Schneider et al., 2021; Vinck et al., 2013). I will outline the counter-arguments to this theory in the final part of this section.

1.3.3 Gamma oscillations in cognitive tasks

Beginning in the late 1990s and extending into the early 2000s, research on gamma oscillations has attracted great interest, generating an extensive body of literature spanning rodent, non-human primate, and human studies (for review, see Başar et al., 2000; Başar-Eroglu et al., 1996; Buzsáki & Wang, 2012; Herrmann et al., 2004, 2010). Attention to visual objects has been consistently associated with an amplification of gamma oscillations, particularly in visual area V4 (Bichot et al., 2005; Fries, Neuenschwander, et al., 2001; Fries et al., 2008; Taylor et al., 2005; Vinck et al., 2013), and in prefrontal regions (Kim et al., 2016; Rouhinen et al., 2013), as well as enhanced coherence between sensory and frontal areas in the gamma frequency band (Gregoriou et al., 2009). These findings reinforce the relevance of gamma oscillations for perception and attention.

Gamma oscillations in the MEG and intracranial recordings from the human and macaque cortex have further been linked to working memory maintenance in both the visual and auditory domains (Howard et al., 2003; Kaiser et al., 2003; Mainy et al., 2007; Roux et al., 2012). Following the notion that oscillations coordinate the formation of cell assemblies (Buzsáki, 2010), gamma oscillations have also been argued to control synaptic plasticity (Galuske et al., 2019; Salinas & Sejnowski, 2001). Indeed, gamma oscillations have been linked to long-term memory formation and retrieval (Griffiths et al., 2019; Gruber et al., 2004; Osipova et al., 2006; Sederberg, Schulze-Bonhage, Madsen, Bromfield, Litt, et al., 2007; Sederberg, Schulze-Bonhage, Madsen, Bromfield, McCarthy, et al., 2007). These findings suggest that gamma oscillations play a significant role in broader cognitive functions (Başar-Eroglu et al., 1996; Herrmann et al., 2004; Jensen et al., 2007).

In sum, several decades of research encompassing diverse animal models and cognitive tasks have accumulated evidence in support of the concept that gamma oscillations serve critical

functions in neuronal communication (Fries, 2005; Fries et al., 2007). This, in turn, underscores their importance in shaping perception, attention, and memory, among other cognitive processes (for review see Başar-Eroglu et al., 1996; Buzsáki & Wang, 2012; Cardin, 2016; Herrmann & Mecklinger, 2001; Herrmann et al., 2010; Jensen et al., 2007).

1.3.4 Photic stimulation in the gamma band to counter neuro-degeneration

Gamma oscillations have not only attracted attention in normal brain function but have also been intensely investigated in clinical populations, particularly those with cognitive impairments (Başar, 2013; Grützner et al., 2013; Uhlhaas & Singer, 2010; Uhlhaas et al., 2008). Alzheimer's Dementia has been shown to be marked by alterations in network activations, particularly affecting inhibitory interneurons (Andrade-Talavera et al., 2023; Verret et al., 2012). As mentioned above, gamma oscillations reflect a balanced state of excitation and inhibition, that has been proposed to underlie the interplay between pyramidal neurons and inhibitory interneurons (Cardin, 2016; Whittington et al., 2011). In line with that, gamma oscillatory power and rhythmicity have been found to be compromised in Alzheimer's patients (see Traikapi & Konstantinou, 2021, for review) as well as biological models of Alzheimer's Dementia (see Andrade-Talavera et al., 2023, for review).

A series of innovative studies have tested whether modulating neuronal gamma oscillations through sensory stimulation could mitigate the neuropathological changes seen in Alzheimer's Disease (Adaikkan & Tsai, 2020; Adaikkan et al., 2019; Iaccarino et al., 2016; Singer et al., 2018). Indeed, these studies suggest that daily optogenetic and non-invasive photic stimulation at 40 Hz might lead to an activation of neuroprotective mechanisms in mouse models of Alzheimer's Dementia (see Adaikkan & Tsai, 2020, for review). These effects have been attributed to the 40 Hz flicker driving gamma oscillations throughout the visual hierarchy to the hippocampus (Adaikkan et al., 2019). The feasibility and efficacy of 40 Hz photic stimulation as a therapeutic strategy for Alzheimer's Disease have since been explored in preliminary human trials, yielding encouraging results (Chan et al., 2022; He et al., 2021; Liu, Han, et al., 2022; McNett et al., 2023). In line with the aforementioned criticism targeting the *Binding by Synchrony* and

Communication through Coherence theories, these findings have also been questioned by recent reports that were unable to replicate the neuroprotective effects on neurons and glia cells (Soula et al., 2023).

To conclude, there is a rich body of literature supporting the involvement of gamma oscillations in visual perception, neuronal communication, and cognition. At the time of writing this thesis, however, gamma oscillations and in particular the *Binding by Synchrony* and *Communication through Coherence* models are facing serious criticism.

1.3.5 Challenges to the involvement of gamma oscillations in perceptual binding and neuronal communication

The first line of criticism addresses the paradigms and stimuli employed to study gamma oscillations in the visual cortex (Hermes et al., 2015b; Ray & Maunsell, 2010). The temporal and spectral properties of cortical gamma-band activity, particularly in non-invasive recordings obtained with EEG and MEG, have been shown to markedly vary with task requirements and visual inputs. For instance, short-lived, event-related gamma bursts and prolonged, narrow-band gamma oscillations have been noted to reflect different underlying processes of visual perception (Herrmann et al., 2004; Ray & Maunsell, 2011; Tallon-Baudry et al., 1999). Yet, both types of gamma activity are often discussed interchangeably to argue for the pivotal role of gamma oscillations in perception (but see Ray & Maunsell, 2011). Gamma bursts are evoked in response to naturalistic stimuli and have been reported to be modulated by attention (Busch et al., 2004; Lachaux et al., 2000, 2005). However, they have not been linked to perceptual binding (Tallon-Baudry et al., 1999). Narrow-band gamma oscillations, reflecting stronger synchrony within neuronal populations, are typically elicited using grating stimuli (Hoogenboom et al., 2006, 2010) but are not robustly observed in response to natural stimuli (Hermes et al., 2015b). Additionally, while the frequency of the oscillations has been shown to have a genetic component (van Pelt et al., 2012), gamma oscillations have also been shown to be modulated specific stimulus properties, such as spatial frequency and contrast (Muthukumaraswamy & Singh, 2013; Muthukumaraswamy et al., 2010; van Pelt & Fries, 2013).

This poses difficulties on both the *Binding by Synchrony* and *Communication through Coherence* hypotheses: If different stimulus properties induce rhythms at different frequencies, how can a person wearing a striped cardigan over a dress with polka dots be perceived as an entity? If gamma oscillations are mainly induced by unnatural stimuli, how can we conclude that they have a general relevance for visual perception? The variability of the gamma oscillations and frequency in response to different stimuli complicates generalisable claims about their role in visual perception (Ray & Maunsell, 2010; Sohal, 2016).

Another series of concerns have been raised based on single- and multi-unit recordings from macaque and rodent brains (Roelfsema, 2023; Shadlen & Movshon, 1999). For example, it has been argued that noise correlations, meaning neural synchrony, between neurons do not necessarily change the information content encoded within the population (Averbeck et al., 2006). Furthermore, even weak neuronal correlations can manifest as oscillatory activity in the LFP, potentially leading to inflated interpretations of population synchrony (Mazurek & Shadlen, 2002). Neuronal correlations have further been reported to be reduced by attention (Cohen & Maunsell, 2009). These arguments are at odds with the *Binding by Synchrony* hypothesis.

A third line of critique specifically targets the studies that have informed the *Communication through Coherence* theory. Several methodological issues have been raised in the context of studying and interpreting communication between two populations. For instance, coherence between two recording sites could emerge if the LFP measured by one electrode contains afferent synaptic inputs from the population near the second electrode (Buzsáki & Schomburg, 2015). This problem has been argued to be exacerbated by volume conduction which further complicates interference regarding the origin of the signal (Buzsáki & Schomburg, 2015; Buzsáki et al., 2012). As such, coherence may therefore not reflect unequivocal evidence for inter-regional synchrony (Buzsáki & Schomburg, 2015; Schneider et al., 2021).

Moreover, the *Communication through Coherence* hypothesis predicts that gamma oscillations carry visual inputs from the primary visual cortex along the visual ventral stream (Fries, 2015). However, it has been pointed out that gamma oscillations are more prominent in the superficial layers 2/3 of visual cortical areas and comparably weak in the input layer 4 (Ray

& Maunsell, 2015; Smith et al., 2013; Xing et al., 2012). The superficial layers have been suggested to be more strongly involved in gain control of the deep layer neurons, rather than feedforward communication (Quiquempoix et al., 2018).

The mounting evidence in support of the relevance of gamma oscillations in visual perception and cognition is juxtaposed by a growing body of research questioning the predictions of *Binding by Synchrony* and *Communication through Coherence* theories. This ongoing debate underscores the complexity and nuance that underlie the neurophysiological processes in visual perception and neuronal communication. In chapter 2, I will present the results of an MEG study, in which I systematically tested whether endogenous gamma oscillations can be synchronised to a high-frequency visual flicker. Considering the contradictory evidence regarding gamma oscillations in the visual system outlined above, developing a tool that can modulate these oscillations would allow causal inferences over the functional role of gamma oscillations in visual perception and cognition. As I will demonstrate, we did not find any evidence that the gamma oscillations were modulated by the visual stimulation. These findings were surprising considering the link between gamma oscillations and communication along the visual hierarchy (van Kerkoerle et al., 2014). In the final chapter, I will discuss replications of these findings based on intracranial recordings in rodents, which have supported the main conclusions in the chapter (Schneider et al., 2023; Soula et al., 2023). As I will discuss, these findings have important implications for the role of gamma oscillations in inter-areal communication.

1.4 Alpha oscillations: Idling vs. Functional Inhibition

Berger's EEG recordings were dominated by periodic activity at 10 Hz, which he famously referred to as the alpha rhythm (Berger, 1929). This observation was later replicated by Adrian and Matthews (1934):

> *There is often [. . .] variation in the size of the waves and sometimes the rhythm only appears intermittently, but its frequency is so characteristic and so constant that there is never any doubt as to its presence.*
>
> – Adrian and Matthews (1934)

1.4.1 Early views: alpha oscillations as neuronal "idling"

Berger (1929) hypothesised that cells spanning the entire cortex generated the alpha rhythm. Adrian and Matthews (1934), however, reported that the rhythm was strongest in the occipital lobe, and disappeared in response to visual stimuli (also see Adrian & Yamagiwa, 1935). While Berger (1929) and Adrian and Matthews (1934) were convinced about the cerebral origin of the rhythm, it was only shown four decades later that alpha oscillations emerge from thalamic and cortical generators (e.g. layer 4 and 5 in primary visual cortex V1, Hogan & Fitzpatrick, 1988; Lopes Da Silva & Storm Van Leeuwen, 1977; Lopes da Silva, 2022).

Early reports have posited that alpha oscillations signify a state of "idling" or inactivity within the visual system (Pfurtscheller, 2001). This notion was based on the observation that alpha oscillations are most robustly observed during relaxed wakefulness, particularly when the eyes are closed (Adrian & Matthews, 1934; Adrian & Yamagiwa, 1935; Pfurtscheller, 2001; Pfurtscheller et al., 1996).

> *It is true that, in our view, the rhythm shows the negative rather than the positive side of cerebral activity, it shows what happens in an area of cortex which has nothing to do, and it disappears as soon as the area resumes its normal work.*
>
> – Adrian and Matthews (1934)

This notion conforms with electrophysiological studies that linked strong alpha oscillations to reduced neuronal excitability, quantified by reduced spiking activity (Bollimunta et al., 2008, 2011; Dougherty et al., 2017; Haegens et al., 2011) and reduced high-frequency broadband and gamma band activity in the LFP (Iemi et al., 2022; Spaak et al., 2012), as well as phosphenes induced using transcranial magnetic stimulation (Romei et al., 2008, 2010). Moreover, EEG-fMRI studies have revealed an inverse relationship between alpha power and the BOLD response in prefrontal (Sadaghiani et al., 2012) and occipital areas (Scheeringa et al., 2012; Zumer et al., 2014). In line with these observations, signal detection tasks have repeatedly associated strong occipital alpha oscillations with reduced visual performance (e.g. Dijk et al., 2008; Ergenoglu et al., 2004; Hanslmayr et al., 2007; Iemi et al., 2017; Limbach & Corballis, 2016). These studies suggest that strong alpha oscillations may be detrimental to neuronal processing and perception.

1.4.2 Evidence for the functional relevance of alpha oscillations

Even though the idling hypothesis prevailed in the literature up until the beginning of the 21st century (Cooper et al., 2003; Pfurtscheller, 2001) some early reports have also suggested a functional role for alpha oscillations in cortical processing and perception. Berger posited that the disappearance of the alpha rhythm in response to visual stimuli could reflect an activation of the visual cortex, which simultaneously inhibits other brain areas (Berger, 1929). This implies that alpha oscillations may be involved in the dynamic allocation of computational resources (Ray & Cole, 1985).

This perspective has gained support from studies investigating modality- and task-specific attention. For instance, multimodal attention studies have demonstrated increases in alpha power in the occipital lobe when participants were instructed to focus on the auditory component of an audio-visual stimulus (Brickwedde, Limachya, et al., 2022; Foxe et al., 1998; Fu et al., 2001; Mazaheri et al., 2014). In visual attention and perception tasks, reduced alpha power is often associated with improved performance (Legewie et al., 1969; Ray & Cole, 1985; Schupp et al., 1994). However, tasks requiring "internal attention", such as mental arithmetic, mental imagery,

or working memory maintenance have been shown to benefit from increased alpha power (Jensen et al., 2002; Klimesch et al., 1999; Ray & Cole, 1985; Schupp et al., 1994). These findings have been explained by the notion that the power of the alpha oscillations in visual cortex can be modulated depending on whether the task benefits from attention being guided toward or away from sensory information (Klimesch et al., 2007; Ray & Cole, 1985; Schupp et al., 1994).

This line of work suggests that these oscillations are more actively involved in perception and cognition than predicted by the idling account (Jensen & Mazaheri, 2010; Klimesch, 2012; Klimesch et al., 2007; Palva & Palva, 2007). As I will detail in the following, decades of research have also argued for a functional role of the inhibitory alpha oscillations in visual attention.

1.4.3 Alpha oscillations facilitate attention through inhibition.

The capacity of our visual system is limited (Allport, 2011; Broadbent, 1958; Bundesen, 1990; Kahneman, 1973; Wolfe et al., 2006). This circumstance becomes apparent in everyday situations such as searching for our keys: if we were able to process all objects in a visual scene in parallel, we would find our keys immediately, regardless of the number of stimuli in the environment. However, we have all experienced that we take longer to search for objects in cluttered compared to tidy spaces. This everyday task is typically operationalised in visual search experiments, which have led to a quantification of our visual (and attentional) capacity to about 20-50 objects/second (Wolfe, 1998; Wolfe & Horowitz, 2017).

Attention has long been posited as the mechanism that enables us to effectively interact with our environment despite these limitations (Allport, 2011; Broadbent, 1958; Treisman et al., 1980). Based on early proposals, attention is often understood as a mechanism for stimulus selection (Broadbent, 1958; Treisman et al., 1980) or as a channel that gates resources towards areas that are relevant for the current behaviour (Allport, 2011). As I will outline below, inhibition by alpha oscillations has long been proposed to facilitate both of these aspects of attention: the selection of task-relevant stimuli (Klimesch, 2012) and the gating of cortical resources towards task-relevant areas (Jensen & Mazaheri, 2010).

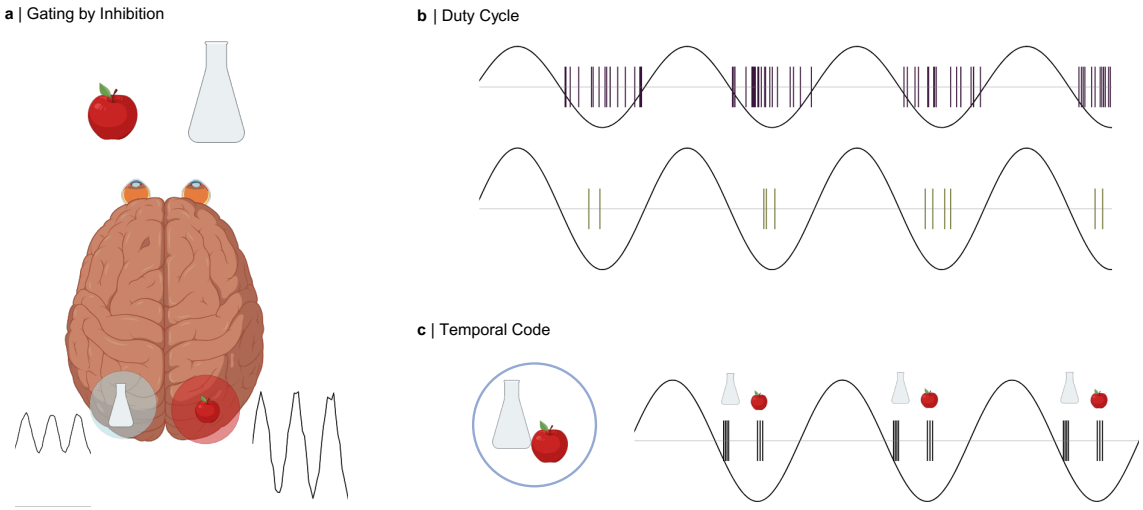

Figure 1.3: **a** The *Gating by Inhibition* theory proposes that an increase of alpha oscillations reduces neuronal processing of the unattended stimulus (here, the apple). In turn, this funnels resources toward the cortical areas processing the attended stimulus (here, the Erlenmeyer flask) (Jensen, 2023; Jensen & Mazaheri, 2010). **b** Alpha oscillations have been argued to implement a duty cycle in neuronal processing. (top) During the trough of the alpha cycle, the neuronal population is able to activate, as indicated by the spike raster. (bottom) A higher amplitude results in a shortened duty cycle, with fewer spikes in the population (see Jensen et al., 2012; VanRullen, 2016). **c** Alpha oscillations might support visual processing by converting competing inputs into a temporal code. For this example, imagine the Erlenmeyer flask and the apple are placed close to each other, such that they are within the same receptive field in, for instance, the object-selective IT cortex. As attention is directed toward the flask, the excitatory inputs to all neurons representing this item will be stronger than the inputs to neurons responding to the features of the apple. Consequently, the neural representation of the flask should overcome the inhibition by the alpha oscillation at an earlier phase. Through this mechanism, the flask receives a temporal advantage over the apple (Jensen, Gips, et al., 2014; Jensen et al., 2021).

1.4.4 Alpha oscillations in spatial attention

Numerous studies using lateralised attention tasks have suggested that occipital alpha oscillations facilitate the allocation of attentional resources (see, for review Foster & Awh, 2019; Jensen, 2023; Jensen & Mazaheri, 2010; Klimesch et al., 2007, 2011). Spatial attention robustly triggers an increase in alpha power in the hemisphere contralateral to the unattended side (Bahramisharif et al., 2010; Gutteling et al., 2022; Kelly et al., 2006; Sauseng et al., 2005; van Gerven & Jensen, 2009; Vissers et al., 2016; Worden et al., 2000; Zhigalov et al., 2019). The magnitude of this modulation has further been linked to the participant's ability to ignore task-irrelevant

stimuli (Händel & Jensen, 2014; Händel et al., 2011; van Zoest et al., 2021; Zhao et al., 2023). More recently, it has been shown that alpha oscillations can even be modulated with retinotopic precision, whereby a decrease in alpha power is observed over receptive fields representing the attended spatial location (Foster et al., 2017; Popov et al., 2019; Yuasa et al., 2023). These studies underpin the hypothesis that alpha oscillations selectively reduce neural activity in sensory regions corresponding to task-irrelevant stimuli (Jensen & Mazaheri, 2010; Klimesch, 2012).

These observations have been reconciled in the *Gating by Inhibition* theory which postulates that the inhibition of task-irrelevant areas facilitates the transfer of information toward task-relevant areas (Jensen, 2023; Jensen & Mazaheri, 2010). Figure1.3a presents this notion based on the scenario of the scientist attending to the Erlenmeyer flask placed next to an apple introduced in Figure 1.2a. Imagine, for simplicity, that the scientist covertly attends to the flask, without moving her eyes. As a result of this attention shift, the amplitude of the alpha oscillations will increase in the right hemisphere, where the apple is processed, reducing cortical excitability in this area. According to the *Gating by Inhibition* hypothesis, this inhibition will in turn funnel computational resources toward the cortical region processing the attended stimulus (here, the left hemisphere, Jensen & Mazaheri, 2010). This is reflected in an increase in neuronal excitability to the attended stimulus, as shown in a myriad of studies in humans (e.g. Appelbaum & Norcia, 2009; Chen et al., 2003; Kastner et al., 1999; Morgan et al., 1996; Saenz et al., 2002) and non-human primates (e.g. Martinez-Trujillo & Treue, 2004; McAdams & Maunsell, 2000; Moran & Desimone, 1985; Seidemann & Newsome, 1999).

As such, while strong alpha oscillations have been associated with reduced cortical processing, these ideas argue that they can be modulated in a functional way, to enhance the processing of task-relevant stimuli.

1.4.5 The role of alpha inhibition in attention to low-level features is undetermined

While alpha oscillations have been most extensively studied in the context of signal detection and spatial attention, previous work has also argued that alpha oscillations may be modulated to facilitate the selection of visually overlapping stimuli based on their features. Snyder and Foxe (2010) presented participants with a display of spatially overlapping, coloured, moving dots. The authors demonstrated that when participants were cued to attend to the colour, alpha amplitude increased in parietal areas, i.e. the dorsal stream, that has traditionally been argued to predominantly process spatial relations and direction of movement (Milner & Goodale, 2008; Ungerleider & Haxby, 1994). When participants were asked to attend to the colour of the stimuli, alpha oscillations emerged from occipital sources, arguably the ventral stream that has a preference for low-level features such as colour (Milner & Goodale, 2008; Ungerleider & Haxby, 1994). These findings imply that alpha oscillations may be modulated to reduce the processing of the unattended modality, and are generally conform with previous of reports on modality-specific and spatial attention outlined above (e.g. Foxe et al., 1998; Ray & Cole, 1985; Worden et al., 2000).

While the modulation of alpha oscillations in separate cortical areas is well-studied, fewer insights exist on whether alpha oscillations support attention when the task-relevant and -irrelevant features are processed in spatially proximal neuronal populations. For instance, in visual search, the location of the search target is, by definition, unknown. However, it has been repeatedly shown that observers complete the search faster and with higher accuracy when they have been informed about the low-level features of the target or the distractors, such as colour or shape (Thayer et al., 2022; Wolfe, 1994, 2021; Wolfe et al., 1989), both of which have been shown to be processed in early visual areas V1 and V2 (Horwitz, 2020; Hubel & Livingstone, 1987; Livingstone & Hubel, 1988). These findings can be explained by the rationale that attention can be directed at features in a spatially unspecific way (Maunsell & Treue, 2006; Treue, 2001). For instance, we can speed up the search for our keys when focusing on objects sharing the

colour of the ornament on the key chain. Like spatial attention, feature-based attention has been associated with increased excitability to target features and reduced responses to distractor features (Martinez-Trujillo & Treue, 2004; Maunsell & Treue, 2006).

A series of preliminary studies has proposed a negative correlation between occipital alpha oscillations and reaction time in a visual search task (Pastuszak et al., 2018, PhD thesis, chapter 4-6) – the higher the power in the alpha-band, the faster were the responses. This outcome has been rationalised by the theory that alpha oscillations act as a uniform filter on the visual inputs that reduces the excitability of neuronal representations across visual cortex. As attentional modulation enhances the cortical excitability to the target, this stimulus will be able to surpass the threshold, while the inhibition of the distractors is facilitated (Pastuszak et al., 2018, chapter 5). This idea provides an explanation of how alpha oscillations could support a visual search task in which many distracting stimuli are present. In chapter 3, I will directly test this hypothesis using MEG in combination with Rapid Invisible Frequency Tagging (RIFT), a novel, subliminal visual stimulation technique, that can be used to probe neuronal excitability in visual cortex to different stimuli on the screen (Zhigalov et al., 2019).

1.4.6 Questions surrounding gain modulation by alpha oscillations

Despite growing empirical support for the notion that alpha oscillations attenuate distracting inputs, recent studies employing visual flicker to study spatial attention and visual search could not reliably establish a correlation between the magnitude of the alpha oscillations and cortical excitability (Antonov et al., 2020; Gundlach et al., 2020; Morrow et al., 2023; Zhigalov & Jensen, 2020). Furthermore, it has been argued that the alpha rhythm observed during spatial attention emerges from parietal, rather than occipital sources, and may therefore not be feasible to modulate the gain of visual inputs (Zhigalov & Jensen, 2020). These findings stand in contrast to the theories positing that alpha oscillations gate visual processing through inhibition of task-irrelevant information (Jensen & Mazaheri, 2010).

As an alternative hypothesis, it has been argued that the visual system may rely on desynchronisation in the alpha band to track and maintain the locus of attention (Foster & Awh, 2019).

Indeed, recent work has found a link between alpha power and distractor inhibition in tasks that demand enhanced target processing (Gutteling et al., 2022; Noonan et al., 2016). The increased need for target processing could indirectly require a reduction of computational resources for the distracting stimuli, manifesting as relatively enhanced alpha amplitude in task-irrelevant cortical regions (Jensen, 2023; Peylo et al., 2021).

In chapter 3, I will link alpha oscillations to reduced cortical responses in a feature-based attention task (Duecker et al., 2023). As I will elucidate, the discrepancies between this outcome and those that contradict the involvement of alpha oscillations in gain modulation may be attributable to differences between spatial and feature-based attention. Specifically, feature-based attention may benefit from an inhibitory gating mechanism situated in early visual regions (also see Snyder & Foxe, 2010), while spatial attention predominantly engages parietal cortical areas (Ungerleider & Haxby, 1994).

1.4.7 Phasic modulation of neuronal excitability by alpha oscillations

As described above, many reports have investigated a somewhat continuous inhibition of task-irrelevant cortical regions by alpha oscillations. A related body of literature has targeted the periodicity of the alpha rhythm, and its effect on perception and attention in time (for review see VanRullen, 2016; VanRullen et al., 2014).

Early EEG research by Lindsley (1952) has posited that the alpha rhythm creates a time window for neural integration. In this context, the author discusses theories about the relevance of alpha oscillations in the coordination of eye movements, a topic that has only recently rekindled interest (Liu et al., 2023; Pan et al., 2023; Popov et al., 2021; Staudigl et al., 2017). Lindsley postulated that the thalamic and cortical alpha rhythms periodically regulate the excitability of visual neurons (Lindsley, 1952). These ideas predict that the perceptibility of a sensory input changes according to the phase of the alpha cycle. Consistent with this hypothesis, several studies have linked the pre-stimulus alpha phase to stimulus detectability (Busch & VanRullen, 2010; Callaway & Yeager, 1960; Dugué et al., 2011; Dustman & Beck, 1965; Mathewson et al., 2009; Nunn & Osselton, 1974). These behavioural indications have been corroborated by

evidence showing that visual evoked responses also vary with alpha phase (Dugué et al., 2011; Gruber et al., 2014; Jansen & Brandt, 1991).

In conformity with Lindsley's ideas, further experiments have evidenced that the perception of two consecutively presented stimuli, such as light pulses on a screen or phosphenes induced by transcranial magnetic stimulation, is influenced by the phase and frequency of alpha oscillations in occipital cortex (Gulbinaite et al., 2017; Samaha & Postle, 2015; Valera et al., 1981). For example, two flashes within the same alpha cycle integrate into a single perceptual event, while flashes presented in separate cycles are perceived as distinct (e.g. Gulbinaite et al., 2017; Sharp et al., 2022; VanRullen, 2016; Wutz et al., 2018), also see Buergers and Noppeney (2022) for a critical account.

Based on these observations, alpha oscillations have been proposed to implement a duty cycle, i.e. a time frame for periodic activation and inactivation that rhythmically modulates perception (Jensen et al., 2012; VanRullen, 2016). Figure 1.3b depicts how the spiking activity in a neuronal population may be modulated by an ongoing alpha oscillation. Note that the amplitude in the panel is lower than in the bottom panel. At the peak of the oscillation, inhibition is high, which reduces the probability of neuronal firing (Bollimunta et al., 2008; Dougherty et al., 2017; Haegens et al., 2011; Iemi et al., 2022; Watson et al., 2018). As the inhibition reduces toward the trough of the cycle, the neurons are able to fire, as indicated by the spike raster (Jensen et al., 2012). An increase in amplitude, as shown in the bottom panel, shortens the duty cycle, reflected in the reduced number of spikes within the alpha cycle (Jensen et al., 2012).

This line of research has argued that our visual perception is not continuous but changes along the phase of the alpha oscillations (VanRullen, 2016). Why would evolution yield a visual system whose effectiveness is not constant, but modulated rhythmically?

1.4.8 Alpha oscillations may implement a processing pipeline in the visual system

The cyclic modulation of cortical excitability along the alpha cycle has been suggested to facilitate stimulus selection (Jensen, Gips, et al., 2014; Jensen et al., 2012) - one of the key functions of attention (Carrasco, 2011). This proposal is based on the notion that a high alpha amplitude reflects strong inhibition, that can only be overcome by sufficiently excited neurons. As neuronal excitability has been shown to be enhanced as a result of attention (e.g. Kastner et al., 1999; Moran & Desimone, 1985) and stimulus salience (Beck & Kastner, 2005; Morris et al., 1997) neurons representing potentially important stimuli will be able to overcome this inhibition, while neurons representing irrelevant stimuli may remain silent (Jensen et al., 2012). This mechanism may be particularly relevant in the context of spatial attention: even when reducing computational resources in the hemisphere associated with the unattended side by increasing the amplitude of the alpha oscillations, a sufficiently salient stimulus - signifying potential danger - would still be able to elicit a response (Jensen et al., 2012). As such, the periodic nature of the inhibition by alpha oscillations may be superior to a uniform inhibition, as it allows a window of opportunity for potentially important stimuli to be processed.

A more recent extension of this idea suggests that this mechanism supports the processing of multiple competing stimuli in time, by organising neuronal representations along the phase of ongoing alpha oscillations in visual cortex (Jensen, Gips, et al., 2014; Jensen et al., 2021). At the peak of the alpha oscillation, when inhibition is high, only neurons responding to attended or highly salient stimuli would be able to reach the criticial membrane potential to initiate a spike (Jensen, Gips, et al., 2014). As the inhibition wanes toward the trough of the alpha cycle, weaker excitatory inputs may be able to trigger a spike. This results in a phase code, whereby the neuronal representations of attended or salient stimuli activate before unattended stimuli (Jensen, Gips, et al., 2014). In this way, alpha oscillations may facilitate the processing of competing stimuli in our visual world by organising them in time (Jensen, Gips, et al., 2014; Jensen et al., 2021).

Consider again the example of the Erlenmeyer flask and the apple within the scientist's visual field. Imagine now that the two objects are placed close together and compete for processing resources in the same cortical areas (Figure 1.3c). Object-based attention will enhance the excitatory inputs to all neurons responding to the features of the flask. Consequently, these neurons will be able to fire at an earlier phase of the alpha oscillations than the neurons representing the apple. The result is a temporal code, that organises the neuronal representations along the phase of the alpha oscillation (Figure 1.3c Jensen, Gips, et al., 2014). Furthermore, this code may give priority to the attended stimulus, whose representations may reach higher-order areas with a temporal advantage over the unattended stimulus (Jensen et al., 2021). As such, this model explains why we are able to efficiently interact with out environment despite the multitude of stimuli in our visual world.

The temporal code model is strongly inspired by intracranial recordings from the rodent and human hippocampus, where distributed firing patterns have been shown to be organised by the phase of ongoing theta oscillations (Jezek et al., 2011; Liebe et al., 2022; O'Keefe & Recce, 1993; Skaggs et al., 1996). In the visual system, such a temporal code could be implemented by a coupling of spike times to the phase of the ongoing alpha oscillations (Bollimunta et al., 2008; Haegens et al., 2011), or as phase-amplitude-coupling between alpha and gamma oscillations (Spaak et al., 2012; van Kerkoerle et al., 2014).

The outlined framework rationalises the series of studies showing that the perceptability of visual inputs and their associated event-related responses, change along the alpha cycle. While it seems counter-intuitive that our continuous perception would underlie a mechanism that reduces the efficacy of visual inputs periodically, the proposed model shows how such a mechanism can support computationally efficient selection and processing of attended and salient stimuli.

1.4.9 Linking computational models of the visual system to Computer Vision

Despite the limited capacity and bottleneck problems associated with our hierarchically organised visual system, our perception of the visual world is virtually seamless. This is just one testament

of the remarkable computational efficiency of the neocortex (Diehl et al., 2018). Historically, the field of Machine Learning has drawn many inspirations from neuroscience to improve the computational efficiency and performance of Artificial Neural Networks (ANNs, LeCun & Bengio, 1995; Rosenblatt, 1958). However, the temporal dynamics of the human visual system, despite their posited relevance for cortical computation, are rarely used to inform ANNs.

While the temporal code model presented in Figure 1.3c and outlined above elegantly describes how inhibitory alpha oscillations may facilitate the selection and processing of attended stimuli, the proposed computational efficiency of this mechanism has so far not been demonstrated. In chapter 4, I will draw inspiration from the rich body of research on the importance of alpha oscillations for visual processing and attention. Specifically, I will present an ANN trained on a computer vision problem that embraces biologically semi-realistic alpha oscillations. As I will show, these dynamics allow the network to segregate competing visual inputs and convert them into a temporal code as depicted in Figure 1.3.

1.5 Questions addressed in this thesis

Gamma and alpha oscillations in the visual system have been studied for decades (Fries, 2015; Jensen & Hanslmayr, 2020). While a rich body of literature has argued that gamma oscillations facilitate inter-areal communication along the visual hierarchy, recent reports have raised concerns regarding the credibility of these findings. Alpha oscillations have been extensively studied in the context of spatial attention, however, their involvement in feature-guided visual search has so far only been implicated by preliminary studies (Pastuszak et al., 2018). Lastly, while previous work has argued that alpha oscillations facilitate the processing of competing visual stimuli in time, their computational efficiency has so far not been explicitly tested. To address these uncertainties, this thesis tackles the following questions:

Can ongoing gamma oscillations in visual cortex be modulated by a high-frequency, rhythmic visual flicker?

In chapter 2, I will present the results of a MEG study, in which I have systematically investigated cortical responses to rhythmic photic stimulation in absence and presence of endogenous gamma oscillations in early visual regions (Duecker et al., 2021). The key finding of this study is that despite overlapping frequency ranges, the gamma oscillation and the visual responses coexist in visual cortex, without any indication that the external drive modulates the endogenous rhythm. These findings challenge the *Communication through Coherence* hypothesis, as they suggest that high-frequency oscillatory activity does not propagate between cortical regions. As I will discuss, the presented results have been supported by recent reports on intracranial recordings in mice (Schneider et al., 2021; Soula et al., 2023). I will conclude that a high-frequency visual flicker can still be used for Rapid Invisible Frequency Tagging (RIFT) to probe cortical excitability to visually presented stimuli, without interfering with potentially task-relevant cortical activity in the gamma-band.

Do cortical alpha oscillations facilitate feature-guided visual search through functional inhibition, and, if so, how selective is this inhibition?

Chapter 3, builds on my insights from the previous chapter, and presents an MEG study in which I used RIFT in a classic visual search paradigm the understand the neural processes underlying feature guidance. My results reveal that the RIFT response serves as a reliable, continuous measure of cortical excitability to visual features that is modulated to boost targets and suppress distractors. Moreover, I will show that strong alpha oscillations correlate with improved search performance and a globally reduced excitability to all visual inputs. I will discuss the idea that alpha oscillations act as a threshold on the cortical responses to the visual inputs, that can only be overcome by boosted stimuli. Through this mechanism, which I will refer to as *blanket inhibition*, the observer may be enabled to focus her search on the task-relevant stimuli (Duecker et al., 2023). I will further report some limitations in this study, that suggest that the relationship between the magnitude of the alpha oscillations with reaction time and the RIFT response may be confounded by task duration. An alternative explanation to the thresholding account may be that the observed effects are a consequence of practice, fatigue, and neural adaption. To further understand these confounds, I will discuss the results of preliminary analyses both in favour and in contrast to the blanket inhibition account.

Do oscillatory dynamics in Artificial Neural Network generate a temporal code in response to multiple stimuli?

In chapter 4, I will integrate concepts from Computational Neuroscience and Machine Learning, to explore how alpha oscillations might enhance the computational efficiency of visual processing in the context of object-based attention. This algorithm is rooted in the idea outlined above that alpha oscillations segregated simultaneous visual inputs into a temporal code (Jensen, Gips, et al., 2014). The dynamics enable this *dynamical ANN* to convert simultaneous stimuli into a temporal code, despite only being trained on individual inputs. These simulations show how embracing the dynamics of the human visual system can enhance the abilities of computer vision algorithms without explicit training.

2

No evidence for entrainment:

endogenous gamma oscillations & rhythmic flicker responses coexist in visual cortex

Published in: Duecker, K., Gutteling, T. P., Herrmann, C. S., & Jensen, O. (2021). No evidence for entrainment: Endogenous gamma oscillations and rhythmic flicker responses coexist in visual cortex [Publisher: Society for Neuroscience Section: Research Articles]. *Journal of Neuroscience*, *41*(31), 6684–6698. https://doi.org/10.1523/JNEUROSCI.3134-20.2021

This chapter is written in American English, in accordance with the regulations of the Journal of Neuroscience.

2.1 Abstract

Over the past decades, numerous studies have linked cortical gamma oscillations (~30-100 Hz) to neurocomputational mechanisms. Their functional relevance, however, is still passionately debated. Here, we asked if endogenous gamma oscillations in the human brain can be entrained by a rhythmic photic drive >50 Hz. Such a noninvasive modulation of endogenous brain rhythms would allow conclusions about their causal involvement in neurocognition.

To this end, we systematically investigated oscillatory responses to a rapid sinusoidal flicker in the absence and presence of endogenous gamma oscillations using magnetoencephalography (MEG) in combination with a high-frequency projector. The photic drive produced a robust response over visual cortex to stimulation frequencies of up to 80 Hz. Strong, endogenous gamma oscillations were induced using moving grating stimuli as repeatedly done in previous research.

When superimposing the flicker and the gratings, there was no evidence for phase or frequency entrainment of the endogenous gamma oscillations by the photic drive. Unexpectedly, we did not observe an amplification of the flicker response around participants' individual gamma frequencies; rather, the magnitude of the response decreased monotonically with increasing frequency. Source reconstruction suggests that the flicker response and the gamma oscillations were produced by separate, coexistent generators in visual cortex.

The presented findings challenge the notion that cortical gamma oscillations can be entrained by rhythmic visual stimulation. Instead, the mechanism generating endogenous gamma oscillations seems to be resilient to external perturbation.

2.2 Introduction

Cortical gamma oscillations have been repeatedly linked to the formation of neuronal ensembles through synchronization of spiking activity in rodents and primates (Brosch et al., 2002; Eckhorn et al., 1988; Engel et al., 1991; Gray & Singer, 1989; Wehr & Laurent, 1996), including humans (Hoogenboom et al., 2006; Müller et al., 1997; Rodriguez et al., 1999; Tallon et al., 1995). Accordingly, they have been ascribed a supporting role for neuronal computations within populations (Engel et al., 2001; Nikolić et al., 2013; Singer & Gray, 1995; Singer, 1999, 2009; von der Malsburg, 1999) as well as inter-regional functional connectivity (Bressler, 1990; Fries et al., 2007; Varela et al., 2001). Indeed, numerous studies have been able to link gamma oscillations in the human brain to cognitive processes and perception (for review see Başar-Eroglu et al., 1996; Herrmann & Mecklinger, 2001; Jensen et al., 2007; Tallon-Baudry, 2009; Uhlhaas et al., 2009), whereas anomalous gamma-band activity has been associated with impaired cognition and awareness, as in e.g. autism spectrum disorder, schizophrenia and Alzheimer's dementia (see Grützner et al., 2013; Herrmann & Demiralp, 2005; Traub & Whittington, 2010; Uhlhaas et al., 2009; Uhlhaas & Singer, 2006, for review).

In this study, we aimed to entrain, i.e. synchronize, gamma oscillations in the human visual cortex to a rhythmic photic drive at frequencies above 50 Hz. Stimulation at such high frequencies has recently been applied in Rapid Frequency Tagging (RFT) protocols, to investigate spatial attention (Zhigalov et al., 2019) and audiovisual integration in speech (Drijvers et al., 2020), with minimal visibility of the flicker. The ability to non-invasively modulate gamma rhythms would allow to study their causal role in neuronal processing and cognition, as well as their therapeutic potential, as recently proposed by (Adaikkan & Tsai, 2020; Iaccarino et al., 2016).

It is widely accepted that rhythmic inhibition imposed by inhibitory interneurons forms the backbone of neuronal gamma oscillations (Bartos et al., 2007; Buzsáki & Watson, 2012; Lozano-Soldevilla et al., 2014; Traub et al., 1996). Indeed, Cardin et al. (2009) demonstrate evidence for resonance, i.e. a targeted amplification, in the gamma band, in response to optogenetic stimulation of GABAergic interneurons, but not when driving excitatory pyramidal cells (also

see Tiesinga, 2012).

Here, we ask if a rapid photic flicker can hijack human visual gamma oscillations; a positive outcome would suggest that visual stimulation can modulate pyramidal-inhibitory-network-gamma (PING) activity. To this end, we designed a paradigm that embraces the definition of resonance and entrainment as stated in dynamical systems theory. While neuroscientific studies widely rely on this terminology (e.g. Hutcheon & Yarom, 2000; Lakatos et al., 2019; Notbohm et al., 2016; Schwab et al., 2006), the prerequisites of entrainment are often not sufficiently accounted for, as pointed out by Helfrich et al. (2019). Entrainment requires the presence of a self-sustained oscillator that synchronizes to an external drive (Pikovsky et al., 2003; Thut et al., 2011). This synchronization is reflected by a convergence of the frequency and phase of the endogenous oscillator to the driving force (Pikovsky et al., 2003). Similarly, resonance is reflected by periodic responses to a rhythmic drive and an amplification of individually preferred rhythms, but does not require the presence of self-sustained oscillations per se (Helfrich et al., 2019; Pikovsky et al., 2003). Indeed, studies on photic stimulation at a broad range of frequencies (Gulbinaite et al., 2019; Herrmann, 2001) including the alpha-band (Notbohm et al., 2016) have provided evidence for both resonance and entrainment in the visual system (also see Rager & Singer, 1998, for resonance phenomena in cat visual cortex).

In this study, oscillatory MEG responses to photic stimulation from 52 to 90 Hz were investigated in the presence and absence of visually induced gamma oscillations. In the *flicker* condition, a rhythmic flicker was applied to a circular, invisible patch. In the *flicker&gratings* condition, the flicker was superimposed on moving grating stimuli that have been shown to reliably induce strong, narrow-band gamma oscillations (Hoogenboom et al., 2006, 2010; van Pelt & Fries, 2013). These oscillations reflect individual neuronal dynamics (Hoogenboom et al., 2006; van Pelt & Fries, 2013) and have been shown to propagate to downstream areas in the visual hierarchy (Bastos, Vezoli, Bosman, et al., 2015; Bosman et al., 2012; Buffalo et al., 2011; Michalareas et al., 2016). Therefore, we will use the terms *induced* and *endogenous* gamma oscillations interchangeably in the following. We chose moving grating stimuli to elicit narrow-band endogenous gamma oscillations since more complex stimuli induce a broad-band

gamma response which might not reflect oscillations (Hermes et al., 2015a; Hermes et al., 2015b).

We expected the visual system to resonate to frequencies close the endogenous gamma rhythm elicited by the gratings, as well as a synchronization of the gamma oscillations and the rhythmic flicker. As we will demonstrate, the moving gratings did generate strong endogenous gamma oscillations, and the photic drive did produce robust responses at frequencies up to 80 Hz. However, to our great surprise, there was no evidence that the rhythmic stimulation entrains endogenous gamma oscillations.

2.3 Materials and Methods

2.3.1 Experimental Procedure & Apparatus

The MEG data were recorded using a MEGIN Triux system housed in a magnetically shielded room (MSR; Vacuumschmelze GmbH & co., Hanau, Germany). Neuromagnetic signals were acquired from 204 orthogonal planar gradiometers and 102 magnetometers at 102 sensor positions. Horizontal and vertical EOG, the cardiac ECG signals, stimulus markers as well as luminance changes recorded by a photodiode were acquired together with the neuromagnetic signal. The data were sampled at 1,000 Hz and low-pass filtered online at 330 Hz. Structural magnetic resonance images (MRIs), for later co-registration with the MEG data, were acquired using a 3 Tesla Siemens MAGNETOM Prisma whole-body scanner (Siemens AG, Muenchen, Germany), TE = 2 ms, and TR = 2 s). For two subjects, the T1-weighted images obtained in previous experiments, using a 3 Tesla Philips Achieva Scanner (Philips North America Corporation, Andover, USA), were used (scanned at the former Birmingham University Imaging Centre). Participants were invited to two separate sessions during which the MEG data and the anatomical images were acquired, respectively. Whenever possible, the MEG recording preceded the fMRI scan; otherwise, the MEG session was scheduled at least 48 hours after the fMRI session to avoid any residual magnetization from the fMRI system.

Volunteers were requested to remove all metal items (e.g. jewelry) before entering the MSR. To enable later co-registration between fMRI and MEG data, four to five head-position-indicator (HPI) coils were attached to the participants' foreheads. Along with the position of the coils, three fiducial landmarks (nasion, left and right tragus) and over 200 head-shape samples were digitized using a Polhemus Fastrak (Polhemus, Colchester, USA). Following the preparation, the participants were seated in upright position under the dewar, with orientation set to 60°.

The MEG experiment consisted of fifteen blocks lasting 4 min 30 s each. Participants were offered breaks every ~20 min but remained seated. At the beginning of each of these recording blocks, subjects were instructed to sit with the top and backside of their head touching the sensor

helmet. The positions of the HPI coils relative to the sensors was gathered at the beginning of each recording block, but not continuously. The MEG experiment lasted ~75 min in total.

2.3.2 Rapid photic stimulation

Stimuli were presented using a Propixx lite projector (VPixx Technologies Inc, Saint-Bruno, QC Canada) which allows refresh rates of up to 1440 Hz. To achieve this high-frequency mode, the projector separates the screen (initial resolution: 1920×1080 pixels) into quadrants and treats them as separate frames, resulting in a display resolution of 960×540 pixels. The RGB color codes for each quadrant, viz. red, green and blue, are converted to a gray scale, separately for each frame and color, and presented consecutively within one refresh interval. The twelve frames are presented at a refresh rate of 120 Hz, resulting in 12×120 Hz = 1440 Hz. This approach allows to drive the luminance of each pixel with high temporal precision, allowing for smooth sinusoidal modulations, reducing unwanted harmonics (see Figure 2.1c,d). In this study, we applied rapid rhythmic stimulation at frequencies ranging from 52 to 90 Hz in 2 Hz increments.

2.3.3 Experimental paradigm

Stimuli were created in MATLAB 2017a (The MathWorks, Inc. Natick, MA, USA) and presented using the Psychophysics Toolbox Version 3 (Brainard, 1997).

Conditions The experiment consisted of two conditions that will be referred to as the *flicker* and the *flicker&gratings* condition, respectively. Each trial began with a one-second interval, in which a central white fixation cross was presented on a dark gray background. In the *flicker* trials, a photic drive in the shape of a circular patch of diameter 2.62° was presented for 2 s. Therefor, the patch's luminance was modulated sinusoidally at frequencies between 52 and 90 Hz (Figure 2.1a). To minimize the visibility of the flicker, the mean luminance of the patch was

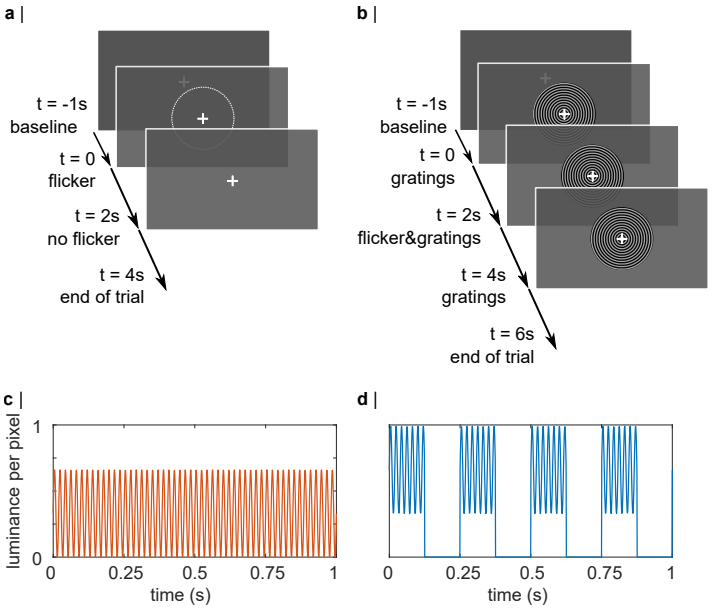

Figure 2.1: The experimental paradigm. **a** Trials in the *flicker* condition. A 1 s baseline interval with a central fixation cross was followed by a 2 s interval of the rapid flicker applied to a circular patch of size 2.62°. The average luminance in the flickering patch was equal to the surrounding grey colour, making the photic drive almost unperceivable. The trials ended with 2 s of the fixation cross only. **b** The trials in the *flicker&gratings* condition. The 1 s baseline interval was followed by 2 s of grating stimuli presented centrally on the screen, contracting inwards. Subsequently, the flicker was imposed onto the stimuli for 2 s. The trial ended with a 2 s presentation of the moving gratings without photic stimulation. **c** Sinusoidal luminance change in one pixel induced by the photic drive at 52 Hz in the *flicker* condition. **d** Luminance change in one pixel as a result of the flicker and the gratings moving concentrically with a velocity of 4 cycles/s. To maintain a similar mean luminance between conditions, photic modulation of the invisible patch in **a** ranged from 0 to 66% (mean RGB [84 84 84]), while the light grey rings of the grating, that is 50% of the stimulus' surface, were flickered between 33 and 99% (mean RGB [168 168 168] per ring).

matched with the background (33% luminance, 213.5 cd/m^2, RGB [84 84 84]). Frequencies were randomized and balanced across trials. The patch was centered on the fixation cross, such that it was presented both foveally and parafoveally. Each trial ended with a two-second interval in which only the fixation cross was presented.

In the *flicker&gratings* condition, the baseline interval was followed by a 2 s presentation of a moving grating stimulus that has been shown to reliably elicit gamma oscillations in visual cortex (e.g. Hoogenboom et al., 2006, 2010; Muthukumaraswamy & Singh, 2013; Tan et al., 2016). The stimulus was the same size as the patch (2.62°) and had a spatial frequency of 9.1 rings/° (see Figure 2.1b); the individual rings' width was 0.11°. The rings contracted towards

the center of the screen with a velocity of 0.56 °/s, i.e. ~4 cycles/s. In the subsequent 2 s interval, the gratings were flickered at the respective frequencies, by sinusoidally modulating the luminance of the entire stimulus with each screen refresh. The trial concluded with a 2 s interval in which the concentric moving circles remained on the screen without photic stimulation. To keep the overall brightness of the stimulation similar between conditions, the luminance of the circular patch in the *flicker* condition ranged from 0 to 66% (of the projector's maximum), while the brightness of the gratings in the *flicker&gratings* ranged from 33 to 99%, with an average luminance of 214.5 cd/m^2 during the presentation of the flicker. The resulting contrast between the gray and black rings, of 66%, has been previously demonstrated to induce clearly identifiable gamma oscillations (Self et al., 2016). The flicker was replicated in the lower right corner of the screen, to acquire the stimulation signal with a photodiode.

The rationale of this design was to investigate if and how the resonance properties of the visual system change when an endogenous gamma oscillator in visual cortex is activated; and whether the flicker response modulates the ongoing oscillatory activity. Studying these two phenomena in the *flicker&gratings* condition required a characterization of both the gamma oscillations and flicker response in isolation. The former was achieved by presenting the gratings without the flicker. To extract the flicker response, we aimed to avoid any gamma-band activity in visual cortex. This was implemented by applying the flicker to a texture-free, invisible patch. Given the filter properties of the visual system (see Cormack, 2005, for review), we were further interested in identifying an upper limit of the frequencies inducing reliable responses. As we expect these results to guide future studies employing the rapid flicker for frequency tagging, we chose an invisible patch to avoid any confounds by response enhancement, e.g. by object-based attention or figure-ground segregation (Self et al., 2016).

Task & time course Participants were kept vigilant by performing a simple visual detection task that required them to respond to a 45° rotation of the fixation cross at the center of the screen, which occurred once every minute (e.g. Zaehle et al., 2010). Data including the target and/or the responses were discarded and not considered in the analysis. The rotation took place

after a trial in the majority, i.e. 60%, of the cases. The remaining 40% of rotations took place at any point during a trial. The experiment was divided into 15 blocks of 4.5 min, resulting in a recording time of 75 min in total.

The 40 frequency×condition combinations were presented once in each block, in randomized order, resulting in a total of 15 trials per flicker frequency and condition. To minimize the amount of trials rejected by eye-blink artifacts, 3 s breaks, indicated by a motivating catchphrase or happy face on the screen, were incorporated every five trials, i.e. every 25 - 35 seconds. Participants were instructed to utilize these breaks to rest their eyes.

2.3.4 Participants

This project was reviewed and approved by the local Ethics Committee at the University of Birmingham, UK. Thirty-one students of the University of Birmingham participated in the experiment. One experimental session was terminated prematurely due to the participant not being cooperative, resulting in a sample of thirty participants (15 female), aged 25.7 ± 3.4 years. This sample size was decided upon based on a conceptually similar study investigating entrainment of neuronal alpha oscillations by Notbohm et al. (2016).

All volunteers declared not to have had a history of neuropsychiatric or psychological disorders, reported to be medication-free and had normal or corrected-to-normal vision. For safety reasons, volunteers with metal items inside their bodies were excluded at the selection state. Prior to taking part in the study, participants gave informed consent, in accordance with the declaration of Helsinki, to both the MEG recording and the fMRI scan and were explicitly apprised of their right to abort the experiment at any point. The reimbursement amounted to £15 per hour.

To allow analysis of flicker responses at frequencies with a sufficient distance to the individual gamma frequency (IGF; see 2.4.1), i.e. ±6 Hz, 8 participants were excluded due to their IGF being below 58 Hz. Thus, the data of 22 participants were included in the following analyses (11 female; mean age 25.7 years).

2.3.5 MEG sensor analysis

Analyses were performed in MATLAB 2017a and 2019b (The MathWorks, Inc. Natick, MA, USA) using the `FieldTrip` toolbox (Oostenveld et al., 2010).

At the sensor level, the analysis was confined to the planar gradiometer signals, as these provided the best signal-to-noise ratio. The sensor positions relative to the HPI coils were loaded in from the data files and averaged for each subject.

MEG preprocessing Trials containing the target or button presses were excluded. The data were read into MATLAB as 5 s and 7 s trials for the *flicker* and *flicker&gratings* conditions, respectively. Artefactual sensors were identified visually during and after the recordings for each participant, and interpolated with the data of their neighboring sensors (0 to 2 sensors per participant). The individual trials were linearly detrended. Trials containing head movements and/or multiple eye blinks were discarded using a semi-automatic approach. An ICA approach ('runica' implemented in `FieldTrip`) was used to project out cardiac signals, eye blinks and eye movement.

Time-Frequency Representation of Power Time-Frequency Representations (TFRs) of power were calculated using a sliding time-window approach ($\Delta T = 0.5s; 0.05$ s steps). A Hanning taper (0.5 s) was applied prior to the Fourier transform. This approach induced spectral smoothing of ±3 Hz. Relative power change in response to the stimulation, i.e. the moving grating and/or the photic drive, was calculated as:

$$P_{\text{normalized}} = \frac{P_{\text{stim}}}{P_{\text{base}}} - 1 \tag{2.1}$$

with P_{stim} being the power during stimulation and P_{base} being the power in the baseline interval. The baseline interval was 0.75 - 0.25 s prior to the onset of the flicker (*flicker* condition) or the moving grating stimulus (*flicker&gratings* condition).

Individual Gamma Frequency The frequency band of the oscillatory activity elicited in response to the moving grating stimulus was identified individually per participant. TFRs of power were calculated over the first 3 seconds of each trial, that is, the baseline interval and the presentation of the moving grating in the *flicker&gratings* condition and averaged over trials. The normalized power was averaged over the 0.25 - 1.75 s interval, and the frequency bin with the maximum relative power was considered the Individual Gamma Frequency (IGF). For each participant, the 4 to 6 gradiometers with the strongest gamma response to the moving gratings were selected as the Sensors-of-Interest (SOI).

Phase-Locking The average phase-synchrony between the photodiode (recording the visual flicker) and the neuromagnetic signal at the SOI was quantified by the Phase-Locking Value (PLV) (Bastos & Schoffelen, 2016; Lachaux et al., 1999) calculated using a 0.5 s sliding window multiplied with a Hanning taper of equal length. The phases of both signals were calculated from Fourier transformations, applied to the tapered segments. The PLV was computed separately for each *frequency*×*condition* combination:

$$PLV = \frac{1}{n}|\sum_{n=1}^{N} exp(j\theta(t,n))| \tag{2.2}$$

where $\theta(t,n) = \phi_{\mathrm{m}}(t,n) - \phi_{\mathrm{p}}(t,n)$ is the phase difference between the MEG (m) and the photodiode (p) signal at time bin t in trial n (see Lachaux et al., 1999, p.195 and Figure 2.5 and 2.9).

Phase difference as a measure of entrainment Additionally, we investigated changes in phase difference between the photodiode and neuromagnetic signal over time for flicker frequencies of IGF±6 Hz, to identify intervals of strong synchrony, so-called *phase plateaus*. MEG and photodiode signals (ΔT = 3 cycles = $\frac{3}{f_{flicker}}$ s) were convolved with a complex Hanning taper using the sliding time window approach. Phase angles were derived from the Fourier transformed time series, unwrapped and subtracted to estimate the phase difference over time for each trial. Plateaus were defined as a constant phase angle (maximum average gradient < 0.01 rad/ms) over

the duration of one cycle of the stimulation frequency:

$$\frac{\sum_{i=1}^{\Delta T} |\nabla \theta_i|}{n} \leqslant 0.01 rad/ms \tag{2.3}$$

with $\nabla\theta_i$ being the gradient, i.e. slope, of the phase angle between MEG and photodiode signal at a given sample i; n being the length of the cycle in ms, rounded up to the next integer, e.g. 17 ms for a flicker frequency of 60 Hz. This approach allowed to identify intermittent phase plateaus in each trial. In comparison, the PLV analysis described above quantifies the phase-similarity of the two signals over trials, and is therefore not feasible to capture brief episodes of synchrony between the MEG signal and the stimulation.

Statistical analysis The statistical analysis was performed in RStudio Version 1.2.1355 (RStudio Inc., Northern Ave, Boston, MA; R version 3.6.1., The R Foundation for Statistical Computing).

2.3.6 MEG source analysis

MRI preprocessing The raw T1 weighted images were converted from DICOM to NIFTI. The coordinate system of the participants' individual fMRI was aligned to the anatomical landmarks using the head-surface obtained from the fMRI and the scalp shapes digitized prior to the recordings. Realignment was done automatically using the Iterative Closest Point (ICP) algorithm (Besl & McKay, 1992) implemented in the `FieldTrip` toolbox and corrected manually as necessary. The digitized headshape of one participant, for whom there was no anatomical image available, was aligned to a standardized template brain.

Linearly Constrained Minimum Variance Beamforming The neuroanatomical origins of the visually induced gamma oscillations and the response induced by the photic drive condition were estimated using Linearly Constrained Minimum Variance spatial filters (LCMV; Veen et al., 1992), implemented in the `Fieldtrip` Toolbox (Oostenveld et al., 2010). The MEG

forward model was calculated using single-shell head-models, estimated based on the aligned anatomical images, and an equally spaced 4-mm grid, warped into MNI (Montreal Neurologic Institute) space (Nolte, 2003; Oostenveld et al., 2010; Stenroos et al., 2012); yielding 37,163 dipoles inside the brain.

The pre-processed data, epoched in 7 and 5-second trials for the respective conditions, were band-pass filtered at 50 to 92 Hz, by applying second order Butterworth two-pass high- and low-pass filters. To identify the peak locations of the endogenous gamma oscillations and flicker response, respectively, segments of 0.5 s of the baseline interval (0.75 - 0.25 s prior to stimulation) and the stimulation interval (0.75 - 1.25 s after flicker/grating onset) were extracted from the data in both conditions. The peak source of the flicker response to the flickering gratings was isolated based on the 2.75 to 3.25 interval, when the photic drive was superimposed on the gratings, contrasted with the 0.75 to 1.25 interval during which the gratings were presented.

For each participant, a common covariance matrix for the 204 planar gradiometers was computed based on the extracted time series and used to estimate the spatial filter coefficients for each dipole location, whereby only the direction with the highest dipole moment was considered. Data in the baseline and stimulation intervals were projected to source space by multiplying each filter coefficient with the sensor time series. Fast Fourier Transforms of the resulting time series, multiplied with a Hanning taper, were computed for each of the 37,163 virtual channels, separately for the baseline and stimulation intervals, and averaged over trials. Relative power change at the IGF and flicker frequencies was computed by applying equation (2.1) to the Fourier-transformed baseline and stimulation intervals. The source-localized power change values at flicker frequencies up to 78 Hz were averaged to identify a common source for the oscillatory response to the photic drive.

2.3.7 Experimental Design & Statistical Analyses

Using the experimental set up outlined above, this study aimed to explore resonance properties of the visual cortex, reflecting oscillatory dynamics in each participant. Furthermore, we asked if responses to a visual flicker close to and at the IGF are enhanced when the flicker is

superimposed on the moving grating stimuli. This would reflect a change in the oscillatory dynamics in presence of the endogenous gamma oscillations. In this context, we hypothesized that these oscillations would synchronize to the flicker.

The 40 frequency×condition combinations were tested in a within-subject design. Resonance at individually preferred rhythms would be revealed by a relatively high response magnitude to stimulation at the preferred frequency in comparison to the surrounding frequencies (Herrmann, 2001; Notbohm et al., 2016; Schwab et al., 2006) (H_1). A general decrease in response to the flicker as a function of frequency would suggest an absence of such an amplification (H_0). Entrainment of the ongoing gamma rhythm by the flicker response would result in the peak frequency of the gamma oscillator being synchronized to the stimulation frequency. This is reflected by a reduction in power at the IGF during the application of the flicker to the gratings, at frequencies different from the IGF, compared to the presentation of the gratings alone (H_1).

Statistical analyses were performed in R (R Core Team, 2020, version 3.6.3., using RStudio version 1.2.5033, RStudio Inc., Boston, Massachusetts). The statistical power of the individual tests was evaluated using Bayes Factors, computed using the `Bayes Factor` package in R (Morey & Rouder, 2018). As the identified IGF was found to be higher than the frequency inducing the strongest flicker response in the majority of participants, we quantified their relationship using a simple Binomial test with an a priori defined alpha level of 0.01. The linearity of the flicker response power as a function of flicker frequency, i.e. evidence for the H_0 as observed in the results reported below, was corroborated using linear regression models implemented in the R base package. Changes in the power at the IGF, with the onset of the flicker in the *flicker&gratings* condition, were examined using a repeated measures ANOVA on the factors time (pre and during flicker) and flicker frequency (above and below IGF).

Lastly, we compared the peak sources of the gamma oscillations and flicker responses, identified using LCMV beamforming, in both conditions using dependent sample t-tests. As the direction of the distances was not known a priori, the alpha level was set to 0.025. To reduce the dimensionality of the comparisons, the obtained 3D coordinates were first projected along their first Principal Component (Herrmann et al., 2011). The p-values of the three comparisons were

corrected using the Benjamini-Hochberg procedure.

2.4 Results

The aim of the current study was to characterize entrainment and resonance properties in the visual cortex in absence and presence of gamma-band oscillations induced by visual gratings. To this end, we drove the visual cortex with a rapid flicker at frequencies ranging from 52 to 90 Hz, in steps of 2 Hz. The photic drive was applied either to a circular patch (the *flicker* condition, Figure 2.1a,c) or to the light gray rings of a moving grating stimulus (the *flicker&gratings* condition, Figure 2.1b,d). We hypothesized that a photic drive in the *flicker&gratings* condition would entrain the grating-induced oscillations. This would be observed as the endogenous gamma oscillation synchronizing with the flicker. Synchronization would be reflected by a constant phase angle between the neuromagnetic signal and the stimulation ('phase entrainment'), as well as a reduction in power at the IGF, indicating a change in the peak frequency of the gamma oscillator towards the flicker frequency ('frequency entrainment'; Pikovsky et al., 2003). Moreover, we expected the presence of the induced gamma oscillator to change the resonance properties (compared to the *flicker* condition), reflected by an amplification of responses to stimulation frequencies equal to the endogenous gamma rhythm.

Response magnitudes in the *flicker* condition were expected to reveal resonance properties of the visual system in absence of gamma oscillations, demonstrating favorable stimulation frequencies to be used in future experiments applying Rapid Frequency Tagging (RFT; Drijvers et al., 2020; Zhigalov et al., 2019).

2.4.1 Identifying Individual Gamma Frequencies

The frequency of the endogenous gamma rhythm is known to vary between participants (Hoogenboom et al., 2006, 2010; Muthukumaraswamy et al., 2010; van Pelt et al., 2012). Therefore, each subject's Individual Gamma Frequency (IGF) was identified first, based on the 0 - 2 s interval in the *flicker&gratings* condition during which the moving grating stimuli were presented without the visual flicker (Figure 2.1c).

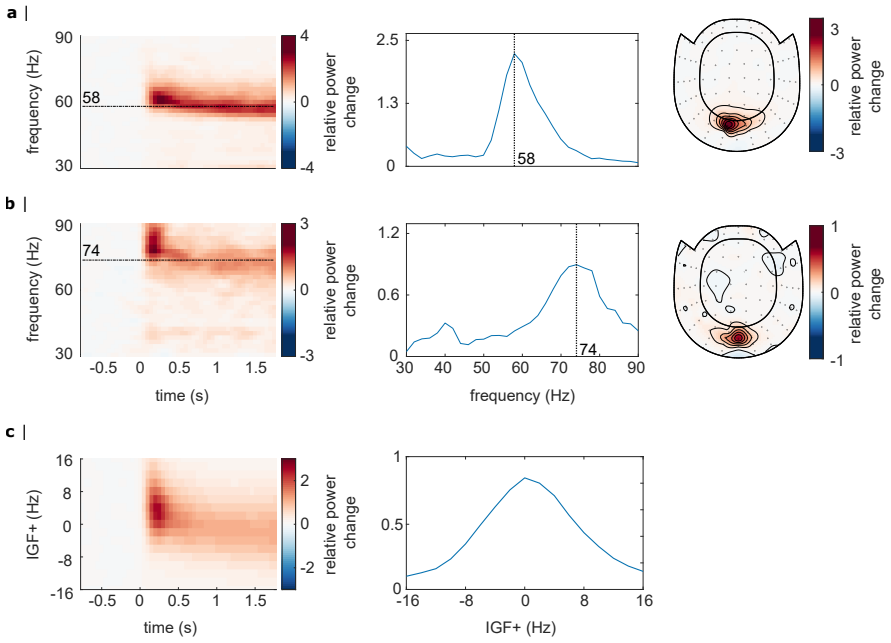

Figure 2.2: Identification of Individual Gamma Frequencies (IGF) and Sensors-of-Interest (SOI). **A, B** The TFRs of power, power spectra (averaged over 0.25 - 1.75 s) and topographic representations (combined planar gradiometers) of the IGF for two representative participants. The TFRs of power were calculated from the Fourier Transforms using a 500 ms sliding window, resulting in spectral smoothing of ±3 Hz. The IGFs were identified from the spectral peak in 0.25 - 1.75s interval of the TFRs. Identified IGFs are indicated by dashed lines. **c** The grand average of the power analysis after aligning the individual TFRs and spectra to the IGF (N=22).

The Time-Frequency Representations (TFRs) of power are depicted in Figure 2.2a,b for two representative participants. The center column shows the power averaged over time (0.25 - 1.75 s after the stimulus onset to avoid any event-related field confounds) demonstrating distinct peaks at 58 and 74 Hz for these participants. The topographies in the right column depict relative power change at the identified frequencies, focally in sensors over the occipital cortex. For each subject, the 2 - 3 combined planar gradiometers showing maximum relative power change in the gamma band were selected for further analysis (Sensors-of-Interest; SOI) per visual inspection. These sensors strongly overlapped between participants. The data of participants with an IGF closer than 6 Hz to the lowest (52 Hz) drive, i.e. IGF<58 Hz, were not considered for further analyses.

Figure 2.2c depicts the averaged TFRs of power as well as the power spectrum for the remaining subjects (N=22), aligned to each participant's IGF prior to averaging. The moving

grating stimulus induced sustained oscillatory activity constrained to the IGF ± 8 Hz, with an average relative power change of 80% in the 0.25 - 1.75 s interval compared to baseline. In short, the moving gratings produced robust gamma oscillations observable in the individual participants which reliably allowed us to identify the individual gamma frequencies.

2.4.2 Photic drive induces responses up to 80 Hz

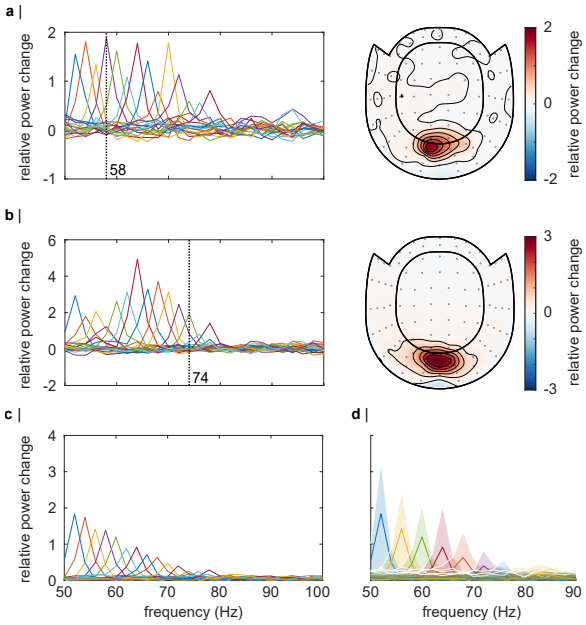

Figure 2.3: **a,b** The response to the photic drive in the *flicker* condition and the corresponding topographies for two representative subjects. Spectra were estimated from the TFRs of power averaged in the 0.25 - 1.75 s interval. Dashed vertical lines indicate the participants' IGF. The topographies (combined planar gradiometers) demonstrate a strong overlap with the ones in Figure 2.2. **c** grand average of the responses to the photic drive for each flicker frequency. On average, the magnitude of the flicker response decreases with increasing frequency and is identifiable for stimulation below 80 Hz. **d** grand average flicker responses for frequencies from 52 to 90 Hz in steps of 4 Hz. The shaded areas, illustrating the standard deviation, indicate a substantial inter-subject variability.

We next set out to quantify the rhythmic response to the flicker as a function of frequency in the *flicker* condition, in which stimulation was applied to an invisible patch. Figure 2.3a and b, left panel, depicts the overlaid power spectra for the different stimulation frequencies in two representative participants (the same as in Figure 2.2). The spectra were estimated by averaging the TFRs of power in the 0.25 - 1.75s interval after flicker onset. Due to the overlap of the sensors detecting the gamma oscillations and photic drive response (compare Figure 2.2 and 2.3 right columns) the same SOI were used as in the *flicker&gratings* condition.

Both individuals showed strong responses at the respective stimulation frequencies, with a maximum relative power change of 200% and 500% in subject A and B, respectively. The identified IGFs (indicated by vertical dashed lines) were higher than the frequencies inducing the strongest flicker response in

20 out of 22 participants (exact Binomial Test against H_0: $p = 0.00012$, probability of successes (IGF>flicker freq) = 0.91, Bayes Factor $BF_{10} = 309.3$). When averaged over all participants, the magnitude of the flicker response decreased systematically with frequency (Figure 2.3c). Figure 2.4a displays the power spectra in the *flicker* condition, estimated from the TFRs as explained above, averaged over all participants, as a function of stimulation frequency. These are equivalent to Figure 2.3c. Diagonal values indicate the magnitude of the oscillatory responses (relative to baseline) at the stimulation frequencies, reaching values of up to 300% and decreasing monotonically with frequency. This confirms an upper limit for the stimulation of around 80 Hz. Off-diagonal values indicate oscillatory activity at frequencies different from the stimulation frequency. Figure 2.4b shows the same spectra after aligning to the IGFs, prior to averaging.

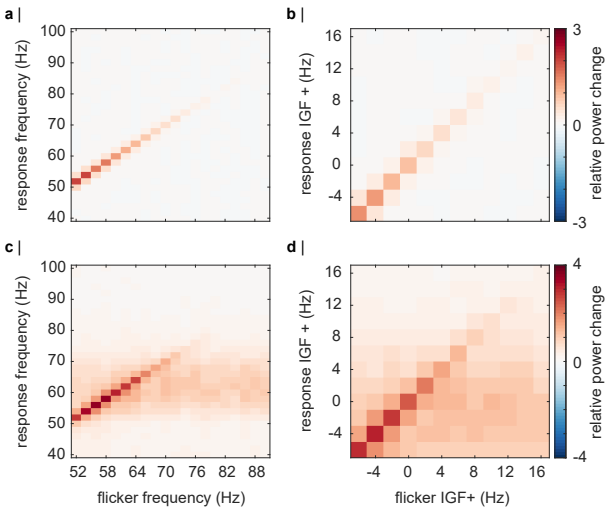

Figure 2.4: Average relative power change to the photic drive (y-axis) with respect to the driving frequencies (x-axis). **a** The *flicker* condition. Note that the power changes mirror Figure 2.3c. Power decreases with increasing frequency, from a relative change of ~3 at 52 HZ to ~.5 at 80 Hz. **b** The *flicker* condition after the spectra were aligned to the IGF. **c** The *flicker&gratings* condition. All spectra demonstrate both the flicker response and induced gamma oscillation (observed as the light red horizontal band). Again, the amplitude of the rhythmic stimulation response appears to decrease with increasing frequency. **d** The spectra for the *flicker&gratings* condition aligned to the IGF. There is no indication that the rhythmic flicker captures the endogenous gamma oscillations.

Figure 2.4c and d display the spectra in the *flicker&gratings* condition (averaged in the 2.25 - 3.75s interval), during which the photic drive was applied to the moving grating stimulus (see Figure 2.1b). The induced gamma band activity can be observed as the horizontal light red band at ~60 Hz. When aligning the spectra to the IGF (Figure 2.4d), we observe a decrease in the flicker response but no evidence for an amplification at or close to the IGF.

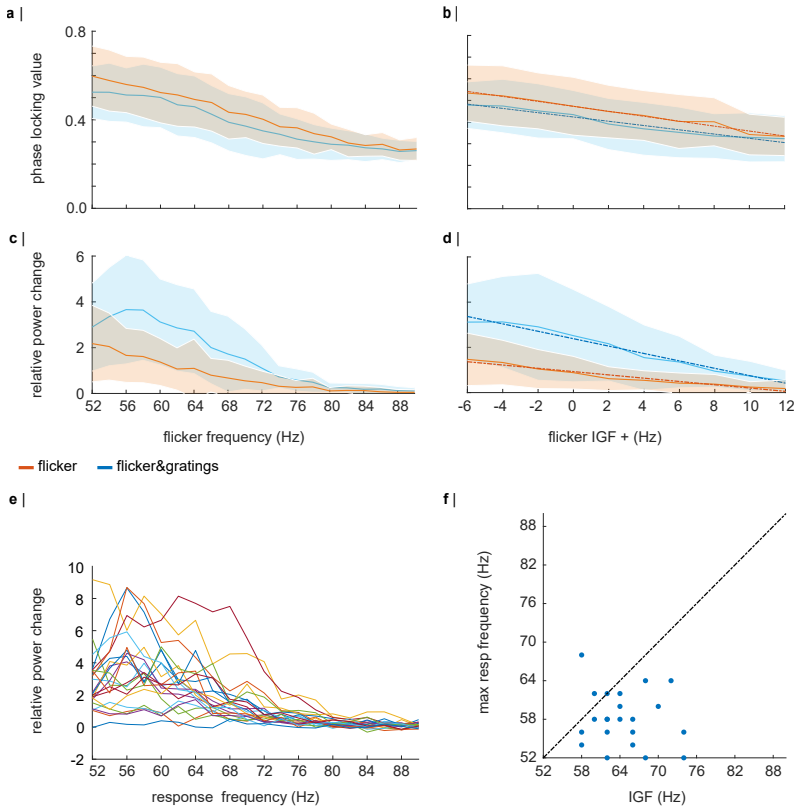

Figure 2.5: Magnitude of the flicker response as a function of frequency in the *flicker* (orange line plots) and *flicker&gratings* (blue graphs) condition. Shaded areas indicate the standard deviation. **a** The phase-locking values between the photodiode and the MEG signal over the SOIs as a function of driving frequency. **b** The phase-locking values between the photodiode and the MEG signals as a function of frequency after the spectra were aligned to the IGF. Again, the phase-locking decreases with increasing frequency (see Table 2.1 for a statistical quantification of the simple linear regression models). **c** Relative power change with respect to baseline as a function of frequency. Generally, the power decreased with frequency, however, in the *flicker&gratings* condition there is an apparent peak at ~56 Hz. The shaded areas (standard deviation) indicate considerable variance between participants. **d** Relative power change as a function of frequency after the individual spectra were aligned in frequency according to the IGF, demonstrating that responses to a photic drive at the IGF are not amplified. **e** Relative power change as a function of frequency for each individual subject (N = 22), indicates that the peak at ~56 Hz in **c** is driven by comparably high power in that frequency range in just a few individuals. **f** Flicker frequency inducing highest power values versus IGF, demonstrating the IGF to be higher than the frequency inducing maximum power change in the majority of participants.

2.4.3 Magnitude of flicker response decreases as a function of frequency

The averaged TFRs of power in Figure 2.4 point to an approximately linear decrease in power of the flicker response with increasing frequency. Literature on neural resonance and entrainment, however, suggests the existence of a preferred rhythm at which oscillatory responses are amplified (Gulbinaite et al., 2019; Herrmann, 2001; Hutcheon & Yarom, 2000; Notbohm et al., 2016; Pikovsky et al., 2003). As argued in Pikovsky et al. (2003) phase-locking between the driving signal and the self-sustained oscillator is the most appropriate metric to investigate entrainment.

Figure 2.5a,b depicts the phase-locking value (PLV) between the photodiode and the MEG signal at the SOI (planar gradiometers, not combined). This measure reveals a systematic decrease in phase-locking with increasing flicker frequency for both the *flicker* (orange) and *flicker&gratings* (blue) condition (Figure 2.5a). The observed relationship is preserved when aligning the frequencies to the IGF (2.5b, also see Table 2.1). Note the absence of increased phase-locking at the IGF.

The magnitude of the flicker response, quantified by power change compared to baseline, as a function of frequency, is demonstrated in Figure 2.5c-f and depicts a similar relationship to the one observed for the PLV. The *flicker* condition (2.5c, orange line) revealed a systematic decrease with frequency, whereas the *flicker&gratings* condition did show a peak at 56 Hz. However, this observed increase appeared to be caused by considerable variance between the power estimates of the individual participants (see Figure 2.5e, with each line graph depicting power estimates per individual participant). We again aligned the spectra to the IGF before computing the grand-average (Figure 2.5d). The absence of a peak at 0 Hz suggests no evidence for resonance at the IGF, confirming the peak at 56 Hz in Figure 2.5c to be the result of inter-subject variability.

Indeed, simple linear regression models, fit individually to PLV and power as a function of frequency aligned to the IGF, separately for each condition, explain a considerable amount of the variance (see Table 2.1 and dotted lines in Figure 2.5). We then identified the individual peak frequencies, eliciting the strongest response to the flicker in the *flicker&gratings* condition, and related those to the IGF, as seen in Figure 2.5f. As observed in the *flicker* condition, the

frequency inducing the strongest response to the flicker was lower than the IGF in the majority of participants, i.e. 19 out of 22 (exact Binomial Test against $H_0 : p = 0.0008$, Bayes Factor $BF_{10} = 67.5$).

Table 2.1: Simple linear regression models: Flicker response magnitude, quantified by phase-locking value and relative power change as a function of distance to Individual Gamma Frequency (IGF).

Model	**Estimates**				
	β_1	t	p ***	R^2	F(1,218)
$flicker_{plv}$	−.01	−8.07	$< 2.2e-16$	.23	65.07
$flicker\&gratings_{plv}$	−.01	−7.24	$< 2.2e-16$	.19	52.44
$flicker_{pow}$	−.07	−9.01	$4.80e-14$	.27	81.14
$flicker\&gratings_{pow}$	−.16	−8.95	$7.51e-12$	.27	80.13

2.4.4 Gamma oscillations and flicker response coexist

We initially hypothesized that entrainment of the gamma oscillations in the *flicker&gratings* condition would result in the photic drive capturing the oscillatory dynamics when the driving frequency was close to the IGF. Figure 2.6 depicts the TFRs of power relative to a 0.5 s baseline, for one representative subject (also shown in Figures 2.2 and 2.3a). The averaged trials for a photic drive at 52 Hz are shown in Figure 2.6a and separately for each flicker frequency in Figure 2.6b. The IGF (58 Hz for this subject) and the respective stimulation frequencies are indicated by dashed lines. The endogenous gamma oscillations, induced by the moving grating stimulus, are observed as the sustained power increase from 0 - 6 s whereas the flicker response is demonstrated by a power increase at 2 - 4 s.

The plots reveal that gamma oscillations persist at the IGF and coexist with the response to the photic drive, which is particularly apparent for stimulation at 52 Hz (Figure 2.6a). Furthermore, the power increase at the flicker frequency does not appear to outlast termination of the drive at t = 4 s. In the subsequent step, we frequency-aligned the TFRs of power according to the IGF before averaging over participants. Again, the analyses were constrained to individuals with an

IGF above 56 Hz (N = 22).

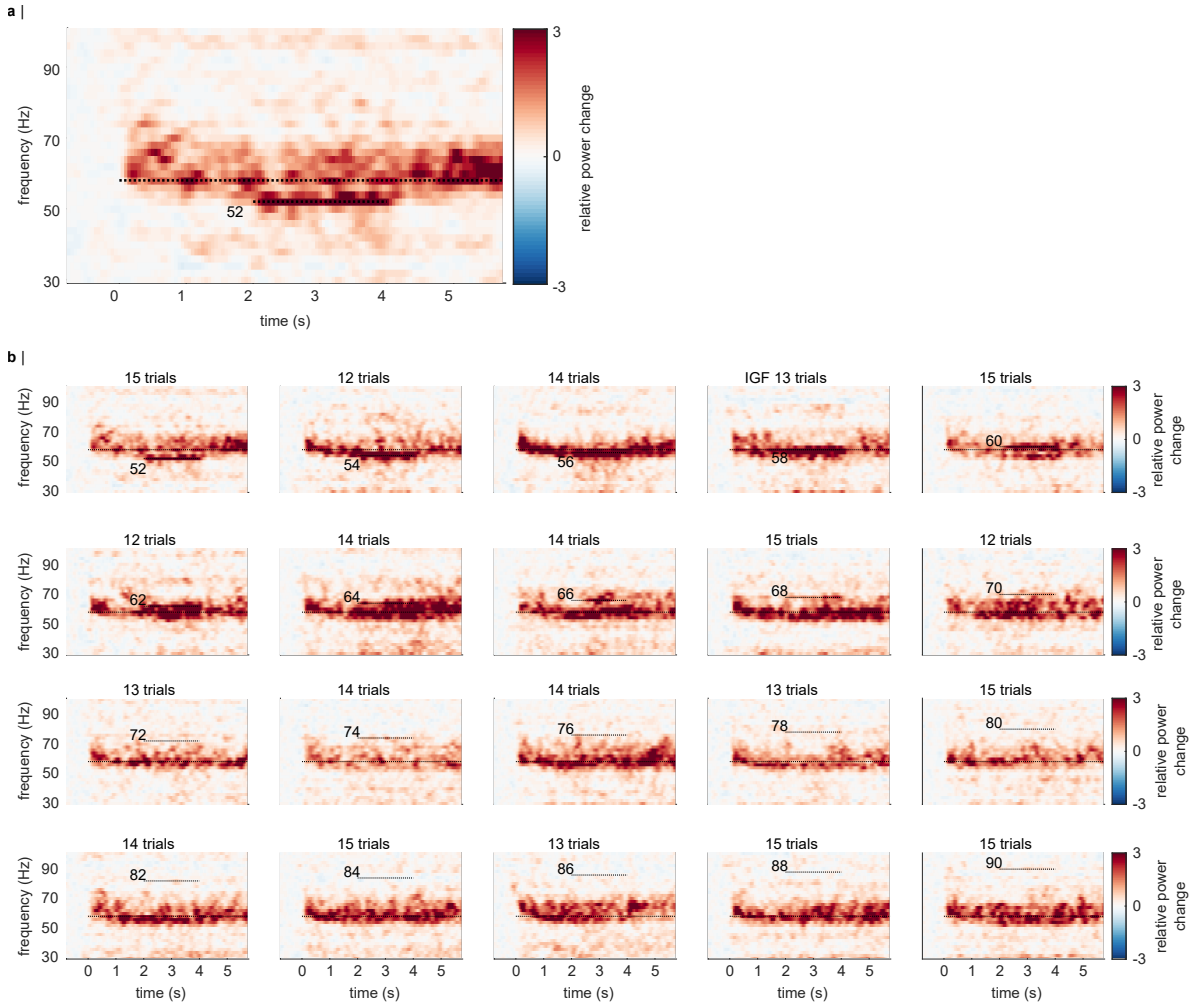

Figure 2.6: The time-frequency representations (IGFs) of power for one representative subject, showing relative power change averaged over trials and SOIs in the *flicker&gratings* condition. **a** Photic drive at 52 Hz. The moving grating stimuli were presented for 0 - 6 s, with the flicker superimposed from 2 to 4 s. Sustained gamma-band activity is clearly observable throughout the presentation of the stimuli, with a power increase of 300% relative to baseline. Additionally, the rhythmic stimulation elicited a response at 52 Hz, which seems to coexist with the gamma oscillations, indicating that the photic drive is unable to capture the dynamics of the gamma oscillation. **b** The plots for the frequencies from 52 to 90 Hz. Stimulation frequencies and IGF (here 58 Hz) are indicated by horizontal dashed lines. The flicker induced responses up to 66 Hz in this participant. Gamma oscillations persist in presence of flicker responses, suggesting that they coexist.

The group averaged, aligned IGFs are shown in Figure 2.7 for frequencies ranging from IGF-6 Hz to IGF+16 Hz. The endogenous gamma oscillations are observed as the power increase extending from 0 - 6 s, and the flicker response as the power change in the 2 - 4 s interval

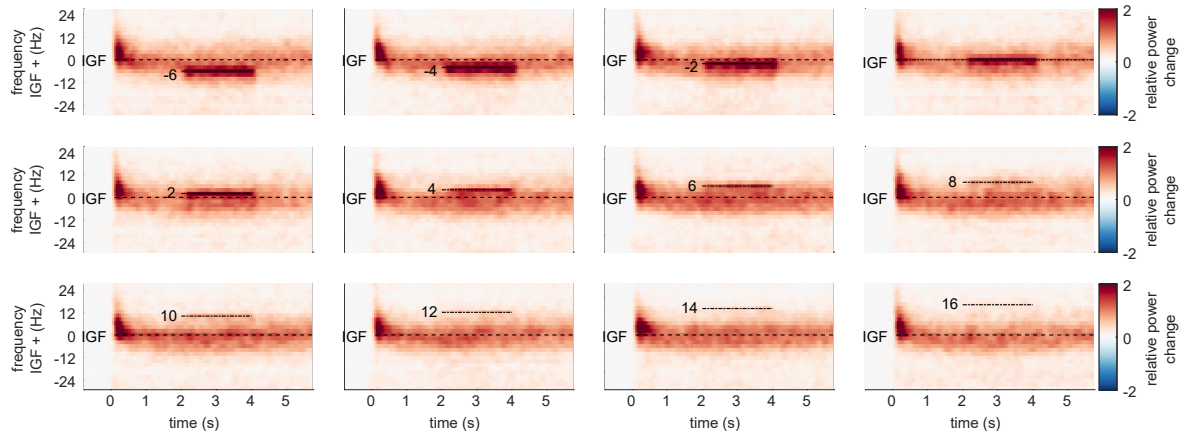

Figure 2.7: Grand average IGFs of power after aligning to the IGF for each subject in the *flicker&gratings* condition. The stimulation frequencies (from -6 to 16 Hz relative to the IGF) are indicated by dashed horizontal lines. As suggested by the single subject IGFs in Figure 2.6, the endogenous gamma oscillations and the flicker response seem to be coexistent. Thus, there is no obvious indication of the photic drive being able to capture the dynamics of the gamma oscillations.

marked by dashed lines, respectively. The photic stimulation induces a reliable response that decreases toward 12 Hz above the IGF. Despite the representation of the gamma oscillations being smoothed due to inter-individual differences, the averaged aligned IGFs of power support the observations in the single subject data: both the gamma oscillations and flicker response coexist in the 2 - 4 s interval. Furthermore, there is no indication of the gamma power being reduced during the presentaiton of the flicker at frequencies close to, but different from, the IGF.

In addition to the narrow-band gamma oscillations, the gratings elicited a rhythmic response at 4 Hz, i.e. the velocity of the concentric drift (not shown). We did not find any evidence for an intermodulation between the frequency of the movement and the photic drive.

2.4.5 Frequency analyses with a longer time window confirm robustness of the reported results

To assess the robustness of our results, we repeated the frequency analyses in the *flicker* and *flicker&gratings* condition with a 2s sliding time window. The longer window substantially increased the signal-to-noise ratio of the flicker response, to up to over 400% relative power change in the *flicker* condition and more than 600% in the *flicker&gratings* condition (not

shown). Besides that, the analyses replicated our reported main finding: a reduction in response magnitude (power) with increasing frequency, in both conditions, following the same trend as depicted in Figure 2.5c and d. The 2 s sliding time-window did however not optimally capture the gamma power, which has a broader peak than the response to the photic drive. The 500 ms sliding window used in our reported analyses is therefore a good compromise, allowing both a reliable identification of a gamma peak frequency and a sufficiently high signal-to-noise ratio and frequency resolution of the flicker response (see Figure 2.6a).

2.4.6 Oscillatory gamma dynamics cannot be captured by frequency entrainment

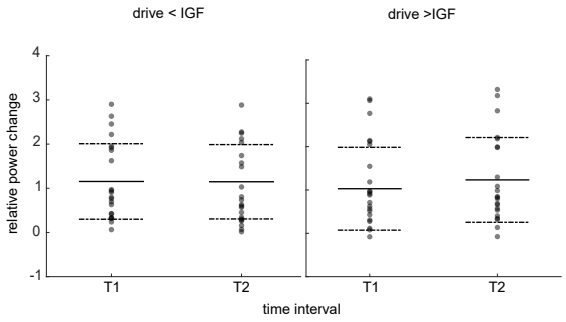

Figure 2.8: Power change relative to baseline at IGF in response to the moving grating stimuli before (T1; 0.5 - 1.5 s) and during application of the flicker (T2; 2.5 - 3.5 s), at frequencies below and above IGF (drive<IGF [-6, -4 Hz] and drive>IGF [+4, +6 Hz], respectively). Scatters demonstrate individual values, solid and dashed lines depict mean and standard deviation, respectively. The key finding is that power at T2 is not decreased compared to T1 for either of the frequency ranges, which is supported by a Bayesian repeated measures ANOVA ($BF_{10} = 0.274$).

Synchronisation of neuronal oscillations by rhythmic stimulation could be conceptualized as the entrainment of a self-sustained oscillator by an external force (e.g. Helfrich et al., 2019; Notbohm et al., 2016). Frequency entrainment is reflected by a change in frequency of the ongoing oscillations towards the rhythm of the drive. Visual inspection of the IGFs of power in Figure 2.6 and 2.7 do not indicate any modulation of the peak frequency of the gamma oscillations by the flicker response, suggesting that they do not synchronize.

To quantify these observations, we investigated the power of the gamma oscillations before and during the photic drive (Figure 2.8) in the *flicker&gratings* condition. A central assumption of oscillatory entrainment is the existence of a 'synchronization region' in the frequency range around the endogenous frequency of the oscillator, the so-called Arnold tongue (e.g. Pikovsky et al., 2003). Driving frequencies falling

inside this synchronization region, will be able to modulate the dynamics of the self-sustained oscillator (also see Hutt et al., 2018). With this in mind, the following analyses only included flicker frequencies in the vicinity of the IGF. For each participant, we considered the relative power change induced by the moving gratings in the 0.5 - 1.5 s interval (T1) before the flicker onset and in the 2.5 - 3.5 s interval (T2) in which both the moving gratings and the photic drive were present. We investigated this for stimulation frequencies below the IGF (averaged power for -6 and -4 Hz) and above (averaged power for +4 and +6 Hz). Assuming a symmetric Arnold tongue centered at the IGF, as shown for entrainment in the alpha-band (Notbohm et al., 2016), we expected a reduction in power at the IGF in interval T2 compared to interval T1 for both higher and lower driving frequencies, i.e. an effect of time, but not frequency.

Figure 2.8 depicts power change at the IGF for the factors stimulation frequency (drive<IGF and drive>IGF) and time interval (T1 and T2), averaged over the SOIs for each subject. In accordance with the IGFs in Figure 2.7, there is no meaningful indication for gamma power being reduced during the T2 interval as compared to the T1 interval, affirming the coexistence of the two responses. A factorial repeated-measures ANOVA did not reveal any significant main effects of the factors time (T1 vs T2) and frequency (drive<IGF vs drive>IGF), but a significant interaction effect ($F(1, 21) = 5.09$, $p = 0.003$, $\eta^2 = .003$). These results were further investigated using a Bayesian repeated-measure ANOVA. The obtained Bayes factors (BF_{10}) indicate that the variance in the data underlies the variability between participants, while the factor *time* ($BF_{10} = 0.233$) and both factors *time* and *frequency* ($BF_{10} = 0.274$) do not add any explanatory value. Evidence for the interaction effect *time:frequency* was found to be inconclusive ($BF_{10} = 0.53$), as was the main effect of frequency alone $BF_{10} = 1.146$). These results provide evidence against the expected reduction in gamma power during rhythmic photic stimulation at frequencies different from the IGF; suggesting that the flicker did not capture the oscillatory gamma dynamics.

2.4.7 Photic drive does not reliably modulate gamma phase

Synchronization of a self-sustained oscillator by an external force, can not only be described by a change in frequency, but also 'phase approximation' or 'phase entrainment' (Pikovsky et al., 2003). This phenomenon is reflected by a constant phase angle between the two oscillators over extended intervals, so-called *phase plateaus*. These might occur when the frequency of the driver is close to the endogenous frequency of the oscillator, i.e. within its Arnold Tongue (Notbohm et al., 2016; Pikovsky et al., 2003; Tass et al., 1998). When approaching the edge of the synchronization region, episodes of constant phase angles are interrupted by so-called *phase slips* that emerge when the self-sustained oscillator briefly unlocks from the driving force and oscillates at its own frequency. These phase slips will be observed as steps between the phase plateaus.

The phase plateau analysis was implemented to complement the PLV analysis shown in Figure 2.5. The PLV quantifies the average synchrony between photodiode and neuromagnetic signal over trials using a 500 ms sliding time window. We hypothesized that in the case of oscillatory entrainment, the gamma oscillator in the *flicker&gratings* condition would alternate between locking on to the photic drive for a few cycles and slipping back to its endogenous rhythm. Due to the short duration of the gamma cycle (~17.2 ms for a 58 Hz IGF), this intermittency would be smeared out by the sliding window. As there was no endogenous gamma oscillator in the flicker condition, such an intermittency was not expected.

To investigate phase entrainment of the gamma oscillations by the photic drive, we inspected the phase angle between the photodiode and one, individually selected, occipital gradiometer of interest per participant. The time series of the phase were estimated per trial, separately for the two sensors, using a sliding time-window Fourier transform approach (ΔT = 3 cycles = $3/f_{flicker}$s; Hanning taper). Phase differences per trial were obtained by subtracting the unwrapped phase angle time series.

Phase angle between photodiode and MEG signal over time Figure 2.9 illustrates the unwrapped phase angles between the MEG and photodiode signal during the photic drive at the IGF (here 58 Hz), in the *flicker* (A) and *flicker&gratings* condition (B), respectively, for the same representative participant shown in Figure 2.2a, 2.3a and 2.6.

The colored line graphs depict individual trials. In both conditions, the MEG signal drifts apart from the photic drive, towards a maximum difference of 60 radians, i.e. a phase difference of about 9.5 cycles, by the end of the trial (Figure 2.9a and b, top panel). Interestingly, the direction of the phase angle appears to change during some of the trials, suggesting spectral instability of the gamma oscillations. Furthermore, the graphs demonstrate a substantial inter-trial variability. This diffusion between trials, quantified for each participant as the standard deviation over trials at the end of the photic stimulation (t=2 in *flicker* and t=4 in *flicker&gratings* condition), converted from radian to ms, is juxtapositioned in Figure 2.9c for the two conditions. It can be readily seen that the phase angles between the stimulation and MEG signal fan out highly similarly in absence and presence

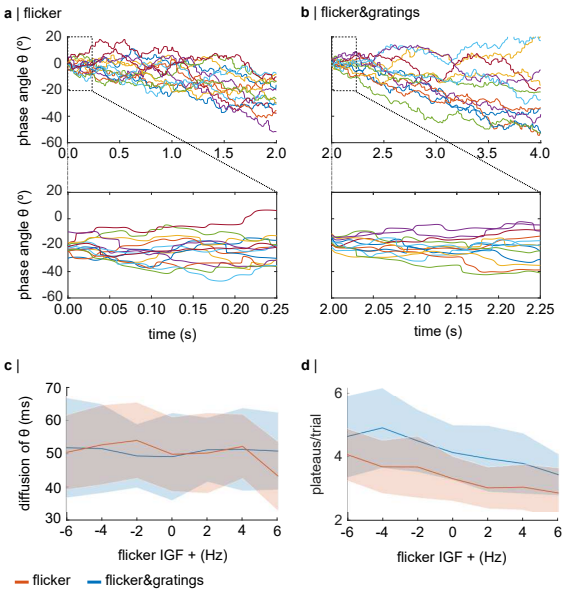

Figure 2.9: **a,b** Phase angle between photodiode and the MEG signal (one gradiometer of interest) at the IGF, for one representative participant; colored lines depict individual trials. **a** Phase angle θ in the *flicker* condition over the duration of the flicker presentation (upper panel) and the first 250 ms (lower panel). The MEG signal drifts apart from the stimulation and can reach a maximum accumulated phase difference of 60 rad, i.e. 9.54 cycles, at the end of the stimulation and up to 15 rad, i.e. 2.39 cycles, in 250 ms. **b** The increase in phase difference over the time of the stimulation for the *flicker&gratings* condition (upper panel) and in the first 250 ms (lower panel). The diffusion of the phase difference across trials is similar to the *flicker* condition. Moreover, there is no clear difference in the number and length of phase plateaus between conditions, implying that the presence of the gamma oscillations does not facilitate entrainment at the IGF. **c** Fanning out across trials as a function of frequency aligned to IGF. Trials diffuse to a highly similar extent in both conditions and across frequencies. **d** Number of plateaus per trial as a function of frequency. While the *flicker&gratings* conditions exhibits more plateaus for all flicker frequencies, there is no indication that stimulation at the IGF results in comparably strong synchronization.

of the endogenous gamma oscillations.

Phase plateaus Visual inspection of the first 0.25 s of the phase angle times series, depicted in Figure 2.9a,b lower panel, does not suggest a relatively high number of phase plateaus in the *flicker&gratings* compared to the *flicker* condition, that would have been expected if the photic drive was able to entrain the endogenous gamma oscillator. Importantly, the graphs demonstrate the phase angles to reach values of over 2π, i.e. more than one cycle, within the duration of the first gamma cycle (17.2 ms), suggesting that even stimulation at the endogenous frequency of the oscillator cannot capture the gamma dynamics. To verify these observations for the entire sample, plateaus during stimulation at the IGF were identified based on the mean absolute gradient ($\leqslant$0.01 rad/ms, see Equation 2.3) over the duration of one cycle of stimulation, i.e. 18 consecutive samples for a flicker frequency of 58 Hz. Figure 2.9d shows the average number of plateaus per trial as a function of flicker frequency aligned to IGF, averaged over participants. The shaded areas indicate the standard deviation. While the *flicker&gratings* condition exhibits more phase plateaus than *flicker* for all stimulation frequencies, the number of plateaus decreases similarly in both conditions with increasing frequency. Importantly, stimulation at the IGF did not result in the highest number of plateaus in either condition. These results are in line with the reported frequency analyses: responses to the photic drive in *flicker&gratings* show strong similarity to the *flicker* condition despite the presence of the gamma oscillator. The results affirm the observations presented in Figure 2.5a and b.

2.4.8 The sources of the gamma oscillations and the flicker responses peak at different locations

The coexistence of the endogenous gamma oscillations and flicker response suggest that these two signals are generated by different neuronal populations; possibly in different regions. To test this assumption we localized the respective sources using Linearly Constrained Minimum Variance spatial filters (LCMV; Veen et al., 1992). The covariance matrix for the spatial filters was estimated based on the -0.75 to -0.25 s baseline in both conditions, the 0.75 to 1.25 s interval

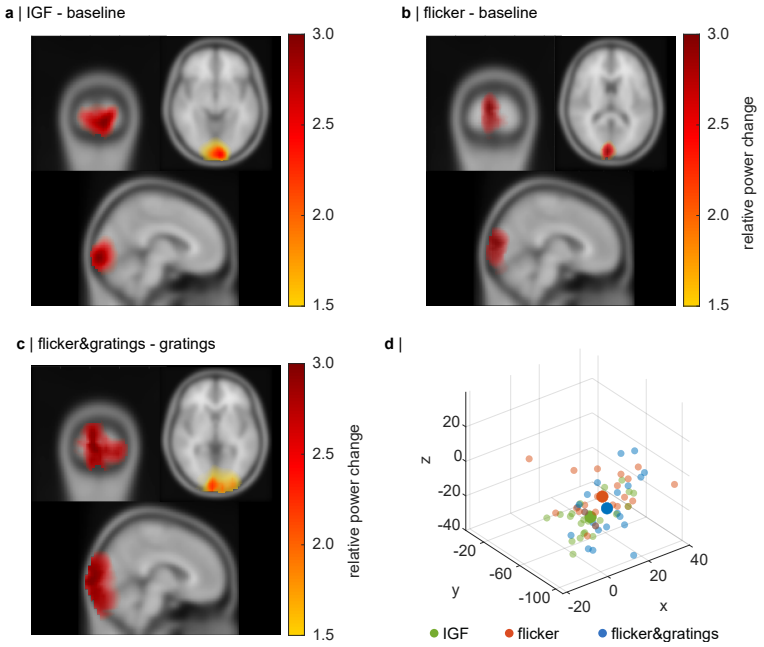

Figure 2.10: Source estimates using the LCMV beamformer approach mapped on a standardized MNI brain. **a** Source estimation of the visually induced gamma oscillations (power change relative to baseline), with the peak of the source identified at MNI coordinates [-6mm -100mm -8mm]. **b** Source estimation of the flicker response (relative to baseline), with the average peak source at [6mm -96mm 12mm] (in Calcarine Fissure). **c** Source estimation of the flicker response in the *flicker&gratings* condition (relative to the gratings interval), with the average peak source at [6mm -100mm 0mm] (in Calcarine Fissure). **d** Coordinates of the identified peak sources for all participants (small scatters) and grand average (large scatters) for the IGF, and the flicker responses in the *flicker* and *flicker&gratings* condition (green, orange and blue, respectively). The peak sources of the flicker responses are adjacent, while the gamma sources tend to peak at inferior locations.

with the moving gratings in *flicker&gratings* and the invisible flicker in the *flicker* condition, as well as the 2.75 to 3.25 interval in the *flicker&gratings* condition in which the flicker was applied to the grating stimulus.

Note that for each participant, one common filter was used for source estimation in both conditions. Power values at the IGF and flicker frequencies, averaged up to 78 Hz, respectively for the *flicker&gratings* and *flicker* condition, were estimated based on the Fourier Transform. To extract power at the IGF and flicker frequencies, power change was computed relative to the baseline interval at each of the 37,163 grid points using Equation 2.1. To isolate the flicker response on the *flicker&gratings* condition, the flicker&gratings interval was contrasted to the moving grating interval. Figure 2.10 illustrates the grandaverage of the source localization for

the gamma oscillations (a), the invisible flicker response (b) and the response to the flickering gratings (c). Consistent with previous work, the responses originate from mid-occipital regions (Hoogenboom et al., 2006; Zhigalov et al., 2019). It is worth noting that the sources of the gamma oscillations and response to the invisible flicker are relatively focal, while the activity induced by the flickering gratings extends more broadly over visual cortex. Using the MNI to Talaraich mapping online tool by Biomag Suite Web (MNI2TAL Tool) (see Lacadie et al., 2007, 2008), the peak of the gamma oscillations was located in the ventral part of the secondary visual cortex (V2, Brodmann area 18; MNI coordinates = [-6mm -100mm -8mm], grandaverage). The peak sources of the flicker responses in both conditions were found in the Calcarine Fissure, at a 2mm distance to the border of the primary (V1) and secondary visual cortex (in dorsal direction); suggesting that they are generated by neighboring, coherent sources in both hemispheres in and close to V1 (Belardinelli et al., 2012) (MNI coordinates: flicker [6mm -96mm 12mm]; flicker&gratings [6mm -100mm 0mm]). To compare the peak locations between the sources in a lower dimensional space, the identified 3D coordinates were projected along their first Principal Component (Herrmann et al., 2011). Dependent sample t-tests revealed a significant difference in location between the peak sources of the IGF and the invisible flicker responses, $t(21) = -3.091, p = 0.017$, Cohen's $d = -0.845$, 95% CI $[-1.5 - 0.2]$, $B_{10} = 8.2$, as well as to the flickering gratings relative to gratings, $t(21) = -2.633, p = 0.023$, Cohen's $d = -0.495$, 95% CI $[-0.89 - 0.09]$, $B_{10} = 3.45$; with the Bayes Factors B_{10} revealing moderate evidence for the H_1 (Quintana & Williams, 2018). There was no significant difference in location between the sources of the flicker responses in both conditions, $t(21) = 0.732, p = 0.472$, $B_{10} = 0.28$, with the Bayes Factor providing moderate evidence for the H_0. Note that all t-values were Benjamini-Hochberg-corrected for multiple comparisons. In light of the coexistence of the two responses observed in Figure 2.6 and 2.7, these results support the notion that gamma oscillations and flicker responses are generated by different neuronal populations.

2.5 Discussion

In this MEG study, we explored resonance and entrainment in the human visual system in response to a rapid photic drive >50 Hz. Strong, sustained gamma oscillations were induced using moving grating stimuli (Hoogenboom et al., 2006, 2010; Muthukumaraswamy & Singh, 2013; van Pelt & Fries, 2013) and used to identify each participant's gamma frequency. The superposition of the flicker and the gratings allowed us to investigate whether the flicker is able to entrain endogenous gamma oscillations.

The photic drive induced responses for frequencies up to ~80 Hz, both in presence and absence of grating-induced endogenous gamma oscillations. To our surprise, we did not find evidence for resonance, i.e. an amplification of an individually preferred frequency in the range of the rhythmic stimulation, in either condition, despite the IGF being above 50 Hz in all participants. Moreover, there was no indication that the endogenous gamma oscillations synchronized with the rhythmic stimulation, i.e. no evidence for entrainment. Despite their differences, the flicker responses in the two conditions show strong similarities in the phase and frequency measures, supporting the notion that the flicker response coexists with the grating-induced oscillations. In accordance with these results, source estimation using Linearly Constrained Minimum Variance (LCMV) spatial filters (Veen et al., 1992), suggests that the neuronal sources of the flicker responses in both conditions and the endogenous gamma oscillations peak at different locations in visual cortex.

2.5.1 Flicker responses do not entrain the gamma oscillator

While the sources of the gamma oscillations and the response to the (nearly) invisible flicker did overlap in occipital cortex, their peak coordinates were found to be significantly different. Relative power change at the IGF peaked at sources inferior to the flicker responses in both conditions, and was located in the left secondary visual cortex (V2) using the MNI2TAL online tool (see Lacadie et al., 2007, 2008). The flicker peak sources were located in the Calcarine Fissure, in close proximity to the primary visual cortex (V1). These results are in line with the

coexistence of the endogenous oscillations indicated by the time-frequency analyses and might be the result of the filter properties of synaptic transmission as the flicker response propagates in the visual system (see Carandini et al., 1997; Cormack, 2005; Hawken et al., 1996; Kuffler, 1953; Ringach, 2004; Shadlen & Movshon, 1999).

Low-pass filtering at the transition from the thalamus to V1 (Connelly et al., 2016) might attenuate the photic drive at frequencies above 80 Hz, leading to an absence of measurable responses in this range. Low-pass filter properties in V1 in projections from granular layers (L4a, 4cα and 4cβ) to supragranular (L2/3, 4b) and infragranular layers (L5,6) (Douglas & Martin, 2004; Fröhlich, 2016; Hawken et al., 1996) might have prevented the flicker response to converge to the neuronal circuits generating the endogenous gamma rhythms. This idea is supported by intracranial recordings in macaques showing the strongest gamma synchronization in response to drifting grating stimuli in V1 in supragranular layers (L2/3 and 4B) (Xing et al., 2012), whereas steady-state responses to a 60 Hz photic flicker have been localized in granular layer 4cα (Williams et al., 2004).

While plausible, these interpretations are conjectural based on the present data. Recent findings by Drijvers et al. (2020), providing evidence for non-linear integration of visual and auditory rapid frequency tagging signals in frontal and temporal regions, challenge the notion that the flicker response might not propagate beyond V1. Pairing the current paradigm with intracranial recordings in non-human primates would allow to test the filtering properties without the limitations imposed by the inverse problem in the source localization of neuromagnetic signals (Baillet, 2013).

Flicker responses might not be wired to inhibitory interneurons orchestrating the endogenous gamma rhythm Computational models, as the one demonstrated by Lee and Jones (2013) and Tiesinga (2012), would be suitable to investigate whether the grating-induced gamma oscillations and flicker response are likely to be generated by neuronal circuits whose wiring is not conducive to entrainment. As the properties of neuronal gamma oscillations have been repeatedly shown to depend on rhythmic inhibition imposed by inhibitory interneurons (e.g.

Bartos et al., 2007; Buzsáki & Wang, 2012; Kujala et al., 2015; Lozano-Soldevilla et al., 2014; Wilson & Cowan, 1972), entrainment should only be achieved when the flicker response is able to modulate their activity. Indeed, Cardin et al. (2009) show resonance in the gamma range to optogenetic stimulation of fast-spiking interneurons, but not to stimulation of pyramidal cells (also see Tiesinga, 2012). We therefore suggest that the photic stimulation applied in our study drives the pyramidal cells in early visual cortex. As in the optogenetic study by Cardin et al. (2009), this drive is not sufficiently strong to entrain the GABAergic interneurons.

This interpretation is contrasted to the findings of Adaikkan and Tsai (2020) who demonstrate that a non-invasive 40 Hz flicker evokes neuronal processes counteracting neuro-degeneration (Adaikkan & Tsai, 2020; Singer et al., 2018). However, it should be noted that the authors understand entrainment as the neural response to rhythmic stimulation, rather than a synchronization of ongoing oscillations to an external drive (Adaikkan & Tsai, 2020). While our findings do not question the authors' compelling evidence that fast photic stimulation impacts neurocircuits and glia, the current study shows that it is not trivial to attribute these effects to entrainment of endogenous gamma oscillations.

2.5.2 Coexistence of flicker responses and oscillations versus oscillatory entrainment

The current study was inspired by studies reporting that a visual flicker in the alpha-band can capture the oscillatory dynamics of the visual system: resonance at distinct frequencies (Gulbinaite et al., 2019; Herrmann, 2001; Schwab et al., 2006)[1], amplitude and phase effects outlasting the stimulation interval (Otero et al., 2020; Spaak et al., 2014) and an "Arnold Tongue" relationship between stimulation intensity, distance to the individual alpha frequency and flicker-response-synchrony (Notbohm et al., 2016).

Unlike the works listed above, we did not find any indication for a synchronization or resonance of endogenous oscillations in the gamma band to the visual stimulation. Recent studies applying photic stimulation in the alpha band, have pointed to a coexistence of endogenous

[1] see (Rager & Singer, 1998) for flicker responses in cat visual cortex

alpha oscillations and flicker responses, similar to the one we report here for the gamma band. While retinotopic alpha modulation has been associated with suppression of unattended stimuli, allocating attention to a stimulus flickering in the alpha band results in enhanced, phase-locked activity (Antonov et al., 2020; Friedl & Keil, 2020; Gundlach et al., 2020; Keitel et al., 2019). While the presented study does not allow nor aim to make generalized claims in favor or against neuronal entrainment, it is worth noting that the ability of rhythmic sensory stimulation to entrain endogenous oscillations is still a matter of debate.

2.5.3 Limitations & Generalizability

Interpretation of the different locations of the peak sources The results of the LCMV beamforming are in line with the notion that gamma oscillations and flicker response are generated by sources at different locations. Yet, due to the ill-posed inverse problem (Baillet, 2013) and the merging of coherent sources when using the LCMV approach (Belardinelli et al., 2012) these source estimates should be interpreted with caution. Figure 2.10 illustrates that the sources of the flicker response in the *flicker&gratings* condition extended more broadly over visual cortex than the sources of the gamma oscillations and invisible flicker response, which might be the result of the flickering rings stimulating different receptive fields (Gur & Nodderly, 1997). While our results suggest a coexistence of the gamma oscillations and flicker response, we do not exclude that they interact.

These limitations do not seriously challenge our interpretation that the neuronal populations generating the flicker response do not entrain the activity of the neurons engaging in the endogenous gamma rhythm. Firstly, it is reasonable to assume that the peak sources reflect the flicker response, which tends to be stronger than the endogenous gamma oscillations (see Figure 2.6 and 2.7). Secondly, the significant difference between the peak locations of the gamma oscillations and flicker response in the *flicker&gratings* condition provides circumstantial evidence for the notion that the two responses emerge from different neuronal populations, despite being elicited by the same stimulus; albeit there is also an overlap between the sources. Intracranial recordings

in nonhuman primates or humans would be useful to substantiate this interpretation.

Strong flicker responses despite limited stimulation strength The number of conditions that have been tested in this paradigm, i.e. 40 frequency×condition combinations, imposed limitations on the maximum number of trials per condition (N=15) and the duration of the stimulation (2 seconds). Stimulation strength was limited to a contrast of 66% peak to trough, ensuring equal luminance across conditions. Due to these limitations, one might be concerned that the absence of oscillatory entrainment was caused by the limited magnitude of the photic drive. However, we found the flicker to induce strong responses of up to 400% in the *flicker&gratings* condition and over 200% in the flicker condition (e.g. see Figures 2.4 and 2.5). In light of these response magnitudes, we argue that the absence of evidence for entrainment cannot be explained by the photic drive being too weak.

Generalizability of the current findings to gamma oscillations associated with visual perception The use of drifting gratings is a standard approach to induce strong narrow-band gamma oscillations in humans (e.g. Hoogenboom et al., 2006, 2010; Michalareas et al., 2016; Muthukumaraswamy et al., 2010; van Pelt & Fries, 2013; van Pelt et al., 2012) and nonhuman primates (e.g. Bosman et al., 2012; Buffalo et al., 2011; Womelsdorf et al., 2006). One might argue that the conclusions presented here only apply to these stimuli and that entrainment could have been achieved using more complex stimuli such as natural images or faces. We find this very unlikely for the following reasons:

Natural stimuli have been argued to induce gamma-band responses that are characterized by broadband activity (Hermes et al., 2015a; Hermes et al., 2015b; Ray & Maunsell, 2010), but also see (Bartoli et al., 2019; Brunet et al., 2014; Brunet & Fries, 2019). This is likely explained by the fact that gamma power and frequency depend on stimulus properties such as contrast, size and orientation (Jia et al., 2013; Muthukumaraswamy & Singh, 2013; Ray & Maunsell, 2010; Schadow et al., 2007). As these factors vary greatly within a natural image, the net result of the oscillatory activity in the gamma-band is a broadband response. Moving gratings have been shown to induce stronger gamma oscillations than their stationary

counterparts (Muthukumaraswamy & Singh, 2013; Perry et al., 2013) and were therefore chosen for the current paradigm. We expected the flicker responses to be substantially stronger than the grating-induced gamma oscillations, which is confirmed by Figure 2.6 and 2.7. Had we relied on stationary gratings, the photic drive might have overshadowed weaker gamma-band activity. Moreover, the frequencies of the endogenous gamma rhythms have been found to be higher for moving than for stationary gratings (Muthukumaraswamy & Singh, 2013; Perry et al., 2013). As our study aimed to investigate entrainment by a flicker with minimal visibility, the IGFs had to be relatively high to be in the range of feasible stimulation frequencies. While the gratings' concentric drift in our study did induce a rhythmic response at 4 Hz, there was no evidence for an intermodulation with the flicker frequencies, nor an indication that the *flicker&gratings* condition was lacking spectral precision. In line with our findings, recent work by Bauer et al. (2012), using a superposition of a 60 Hz flicker and static gratings, has demonstrated the coexistence of the grating-induced broadband gamma activity and the flicker response. Furthermore, the authors report that behavior only correlated with the broadband gamma activity in absence of the flicker. When the photic drive was applied to the static grating, the flicker response correlated with reaction time, but behaviour did no longer relate to the broadband gamma activity.

Another concern might be that grating stimuli do not engage downstream regions to the same extent as complex stimuli; as such they might be generated in specialized neuronal circuits. However, a number of studies in both human and non-human primates have demonstrated that attended as well as unattended gratings induce gamma oscillations that propagate to downstream areas along the ventral (V4 and inferotemporal cortex) and dorsal stream (area V5 and V7) (Bastos, Vezoli, Bosman, et al., 2015; Bosman et al., 2012; Buffalo et al., 2011; Michalareas et al., 2016). For the reasons outlined above, we argue that moving grating stimuli created the optimal conditions to investigate gamma-band entrainment, as these induced strong, sustained, narrow-band gamma oscillations reflecting individual oscillatory dynamics (also see Hoogenboom et al., 2006; van Pelt & Fries, 2013).

2.6 Conclusion

Our results suggest that rapid photic stimulation does not entrain endogenous gamma oscillations and can therefore not be used as a tool to probe the causal role of gamma oscillations in cognition and perception. However, the approach can be applied in Rapid Frequency Tagging (RFT) to track neuronal responses without interfering, for instance, to investigate covert spatial attention (Zhigalov et al., 2019), multisensory integration (Drijvers et al., 2020) and parafoveal reading (Pan et al., 2020).

3

Alpha oscillations may support the efficiency of guided visual search by inhibiting both target and distractor features in early visual cortex

This chapter largely overlaps with: Duecker, K., Shapiro, K. L., Hanslmayr, S., Wolfe, J., Pan, Y., & Jensen, O. (2023, August 3). Alpha oscillations support the efficiency of guided visual search by inhibiting both target and distractor features in early visual cortex [Pages: 2023.08.03.551520 Section: New Results]. https://doi.org/10.1101/2023.08.03.551520

3.1 Abstract

Visual search models have long emphasised that task-relevant items must be prioritised for optimal performance. While it is known that search efficiency also benefits from active distractor inhibition, the underlying neuronal mechanisms are debated. Here, we used MEG in combination with Rapid Invisible Frequency Tagging (RIFT) to understand the neural correlates of feature-guided visual search.

RIFT served as a continuous read-out of the neuronal excitability to the search stimuli and revealed evidence for target boosting and distractor suppression in early visual cortex. These findings were complemented by an increase in occipital alpha power predicting faster responses and higher hit rates, as well as reduced RIFT responses to all stimuli, regardless of their task relevance. However, additional exploratory analysis revealed that observed effects on reaction time may be confounded by time-on-task.

In light of these mutli-facted results, we will discuss the idea alpha oscillations in early visual regions may implement a *blanket inhibition* that reduces neuronal excitability to both target and distractor features. As the excitability of neurons encoding the target features is boosted, these neurons may overcome the inhibition, facilitating guidance towards task-relevant stimuli. These results provide novel insights on a mechanism in early visual regions that may support selective attention through inhibition.

3.2 Introduction

Visual search is a widely used paradigm, applied to operationalise the everyday task of finding a pre-defined stimulus (target) among distracting stimuli (distractors), for instance, a friend in a crowd. Search is more efficient when low-level features of the target, e.g., colour or shape, are known to the observer (Egeth et al., 1984; Wolfe, 1994, 2021). For example, when we know that our friend is wearing a yellow raincoat, we will pay less attention to people wearing blue jackets (Figure 3.1a). The allocation of visual attention has long been suggested to involve a priority map: a representation of the visual field in which locations are weighted based on their salience and task-relevance (Awh et al., 2012; Koch & Ullman, 1985; Navalpakkam & Itti, 2005; Serences & Yantis, 2006; Thompson & Bichot, 2005). Priority maps have become a central component of models of selective attention (Awh et al., 2012; Bisley, 2011; Fecteau & Munoz, 2006) and visual search Wolfe, 1994, 2021. In the example above, this map would assign high priority to locations containing the colour yellow and low priority to the colour blue (Figure3.1b).

Evidence from behavioural, electrophysiological, and neuroimaging studies leaves little doubt that visual attention and search are guided by a mechanism akin to a priority map, whereby neural responses to the target are boosted, and responses to the distractors are reduced or suppressed (Andersen et al., 2008; Bayguinov et al., 2015; Bichot & Schall, 1999; Bisley & Goldberg, 2010; Bisley & Mirpour, 2019; Chelazzi et al., 1993; Cosman et al., 2018; Fecteau & Munoz, 2006; Gottlieb et al., 1998; Hickey et al., 2009; Ipata, Gee, Goldberg, & Bisley, 2006; Klink et al., 2023; Luck & Hillyard, 1994a, 1994b; Mirpour et al., 2009; Motter, 1994; Müller et al., 2006; Ptak, 2012; Serences & Yantis, 2006; Sprague & Serences, 2013; Thompson & Bichot, 2005; Thompson et al., 2005). While target boosting is known to largely underlie gain modulation of the neural representations (Desimone & Duncan, 1995; Kastner & Ungerleider, 2000, 2001; Mehrpour et al., 2020), it is still debated how distractor suppression is implemented (Gaspelin & Luck, 2018a; Geng, 2014; Luck et al., 2021).

Numerous studies on spatial and temporal attention have linked neuronal alpha oscillations

(8-12 Hz) to functional inhibition (for review see Jensen & Mazaheri, 2010; Klimesch, 2012; Klimesch et al., 2007). Motivated by these findings, we here sought to uncover to what extent they support distractor suppression in visual search. Alpha oscillations were long associated with a state of inattention or idling (Adrian & Matthews, 1934; Pfurtscheller et al., 1996). In line with that, signal detection tasks have repeatedly linked high alpha power to a higher number of misses (Dijk et al., 2008; Hanslmayr et al., 2007; Iemi et al., 2017). However, a series of electrophysiological studies have demonstrated that alpha power is also reliably modulated by attention (Gutteling et al., 2022; Hanslmayr et al., 2007; Kelly et al., 2006; Sauseng et al., 2005; Vissers et al., 2016; Worden et al., 2000). For instance, in spatial attention tasks, alpha power has been shown to retinotopically track the locus of attention (Foster et al., 2017; Popov et al., 2019; Yuasa et al., 2023). Strong alpha oscillations in the visuo-cortical areas processing unattended locations has further been linked to the participant's ability to ignore task-irrelevant stimuli (Händel & Jensen, 2014; Händel et al., 2011; Spaak et al., 2016; van Zoest et al., 2021; Zhao et al., 2023). Moreover, intracranial recordings in monkeys and humans have related the phase of the alpha oscillations to a rhythmic inhibition of neuronal excitability (Haegens et al., 2011; Iemi et al., 2022). These studies have converged on the notion that alpha oscillations reflect pulses of inhibition (Foxe & Snyder, 2011; Jensen & Mazaheri, 2010; Klimesch et al., 2007; Payne & Sekuler, 2014; Van Diepen et al., 2019).

Both the idling and functional inhibition accounts predict that strong alpha oscillations are detrimental to visual processing. However, it has also been hypothesised that alpha oscillations facilitate performance in tasks with a lot of distracting information (Klimesch, 2012); such as visual search among a high number of stimuli. So far, there are only preliminary results linking strong alpha oscillations in a classic visual search experiment to faster responses (Pastuszak et al., 2018). This relationship was found for alpha oscillations before the onset of the search display.

Based on evidence from spatial attention tasks, one might suggest that alpha oscillations support such a search task by selectively inhibiting distractor locations (Figure. 3.1c). This spatially specific inhibition could however only be imposed after the display onset, when the

locations of the distractors are known, and would therefore be unhelpful in a visual search task. Research on feature-based attention has led to the hypothesis that attention can also be guided by spatially unspecific feature maps (Maunsell & Treue, 2006). These feature maps could assist in the implementation of the priority map, and thus distractor inhibition. As alpha oscillations have so far mainly been investigated in the context of spatial and modality-specific attention (Foxe et al., 1998; Mazaheri et al., 2014; Ray & Cole, 1985), it is unknown if and how they would support distractor suppression in a feature map.

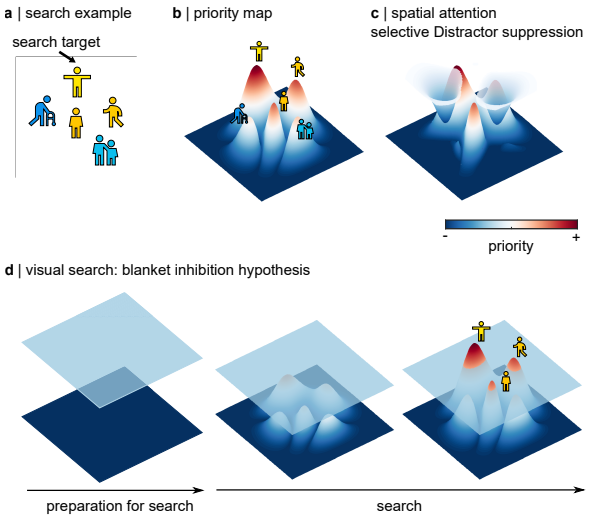

Figure 3.1: Models of visual search considering a priority map and inhibition by alpha oscillations. **a** Search example: finding a person who is dressed in yellow in a crowd of people who are dressed in yellow and blue. **b** Visual search models typically assume that search is guided by a priority map, i.e., a representation of the visual world, whereby each location is weighted based on its relevance for the current search. In this example, the location of the people dressed in yellow is assigned a higher priority than people dressed in blue. **c** Studies on spatial attention have tested the hypothesis that alpha oscillations selectively inhibit distractors. In electrophysiological recordings, this would show as a targeted reduction of neuronal activity in areas representing locations of people dressed in blue. **d** Alternative hypothesis for visual search: alpha oscillations implement a blanket inhibition mechanism, whereby an inhibitory threshold is set up in preparation for the search (left). With the onset of the display, this threshold subsides as the priority map is built (middle). Once the priority map is established, only the boosted items in the visual field can overcome the threshold, focusing the search on locations that are likely to contain a target stimulus (right).

We consider the alternative hypothesis that instead of selectively inhibiting distractors, alpha oscillations support visual search by applying an inhibitory threshold to the neural representations of all stimuli in the visual field; we refer to this as *blanket inhibition* (Figure3.1d). This threshold is set in anticipation of the search display, represented by an increase in pre-search alpha power (Figure 3.1d, left). With the onset of the search display, the threshold subsides, as reflected by a decrease in alpha power in response to visual stimuli (Pfurtscheller & Lopes da Silva, 1999, 3.1d, middle). We argue that as the *blanket inhibition* is applied to the priority

map, only the boosted representations will overcome the threshold, reducing the number of high-priority locations; thus, facilitating guidance (Figure 3.1d, right). This relationship would be reflected by increases in alpha power paired with a reduction of the neuronal excitability to stimuli sharing both target and distractor features.

We tested the hypotheses outlined in Figure 3.1c and d using MEG in combination with Rapid Invisible Frequency Tagging (RIFT) (link to preregistration). MEG allows to both localise and quantify changes in human neuronal activity with a fast temporal resolution. RIFT is a novel, subliminal stimulation method to probe neuronal excitability in early visual regions, while leaving endogenous spontaneous oscillations unperturbed (Duecker et al., 2021; Zhigalov & Jensen, 2020; Zhigalov et al., 2019). The RIFT responses served as a read-out of the excitability in early visual neurons to target and distractor features (also see Bouwkamp et al., 2023). Relating the magnitude of the RIFT responses to alpha power before and during the search allowed us to investigate how alpha oscillations operate on a priority map.

The neural dynamics of distractor suppression in humans and non-human primates are typically investigated in the context of actively ignoring a singleton distractor presented among four to six spatially organised stimuli (Donohue et al., 2020; Feldmann-Wüstefeld & Awh, 2020; Feldmann-Wüstefeld et al., 2021; Ferrante et al., 2023; Forschack et al., 2022; Gaspar & McDonald, 2014; Gaspelin & Luck, 2018b; Hickey et al., 2009; Jannati et al., 2013; Sawaki & Luck, 2010; Serences et al., 2004; van Zoest et al., 2021), and have so far not led to an agreement on the underlying mechanism (Luck et al., 2021). Using RIFT, we were able to read out the neuronal excitability to target and distractor features in a complex visual search display, without any pop-out stimuli; in the tradition of early behavioural studies that motivated the hypotheses that search is guided by a map of the visual field (Treisman et al., 1980; Wolfe, 1994, 2021, Figure 3.2a).

3.3 Methods

3.3.1 Experimental design & stimuli

Task

We applied Rapid Invisible Frequency Tagging (RIFT) in a classic visual search paradigm to probe the neuronal excitability to the target and distractor colour in *guided* and *unguided search*. The participants' task was to indicate whether a cyan or yellow letter "T" was present or absent amongst several cyan and yellow "Ls" (Figure 3.2a). The experiment was designed in blocks of 40 trials with set sizes of either 16 or 32 items. At the beginning of a block in the *guided search* condition, the letter "T" was presented in yellow or cyan, indicating the colour of the target for the following block (Figure 3.2a). In blocks in the *unguided search* condition a white "T" was shown, and the color of the target was randomised over trials. Each search display was preceded by a 1.5-s baseline interval in which a white fixation dot was presented in the centre of the screen. The trials were terminated with the participants' button press, or automatically after 4 seconds. The button press was followed by a black screen, presented for 500 ms, before the start of the pre-search interval of the following trial. All participants complete four practice blocks consisting of 10 trials each before the experiment. Participants were instructed to find the target without moving their eyes. The experiment and MEG recording were paused every 10 minutes and participants were encouraged to rest their eyes and move their heads.

Display physics

The stimuli were presented using a Propixx lite projector (VPixx Technologies Inc, Quebec, Canada), set to a refresh rate of 480 Hz. The luminance of the yellow and cyan stimuli in the search display was modulated sinusoidally, respectively at 60 and 67 Hz (Figure3.2b, target and distractor colours, tagging frequencies, and set sizes were randomized within participants). The stimuli were created using the Psychophysics Toolbox version 3 (Brainard, 1997) in MATLAB 2017a (The Mathworks, Natick, MA, USA).

3.3.2 Apparatus for data acquisition

The MEG data were acquired using a MEGIN Triux (MEGIN Oy, Espoo, Finland), with 204 planar gradiometers and 102 magnetometers at 102 sensor positions, housed in a magnetically shielded room (Vacuumschmelze GmbH & Co, Hanau, Germany). Data were filtered online between 0.1 and 330 Hz using anti-aliasing filters and then sampled at 1,000 Hz. The dewar orientation was set to 60° to allow the participants to comfortably rest their heads against the back of the sensor helmet, optimizing the recording of the neuromagnetic signals in the occipital cortex.

The three fiducial landmarks (nasion and left and right periauricular points), the participant's head shape (>200 samples), and the location of four head-position-indicator (HPI) coils were digitized using a Polhemus Fastrack (Polhemus Inc, Vermont, USA) prior to the recording. The location of the HPI coils was acquired at the beginning of each new recording block, but not continuously throughout the experiment.

The RIFT signals at 60 and 67 Hz were further applied to two squares at the outer corners of the screen and recorded using two custom-made photodiodes (Aalto NeuroImaging Centre, Aalto University, Finland), connected to the MEG system.

Eye movements and blinks were tracked using an EyeLink® eye tracker (SR Research Ltd, Ottawa, Canada), positioned at the minimum possible distance from the participant. The conversion of the EyeLink® Edf files was done with the Edf2Mat Matlab Toolbox designed and developed by Adrian Etter and Marc Biedermann at the University of Zurich.

The T1-weighted anatomical scans were obtained using a whole-body 3-Tesla Philips Achieva scanner (echo time TE=0.002s, repetition time TR=2s).

3.3.3 Participants

This study was carried out in accordance with the declaration of Helsinki and the COVID-19 related safety measures at the University of Birmingham in place between April 2021 and January 2022. A telephone screening was conducted 48 hours before the experiment to ensure

that all participants were safe for fMRI and free of COVID-19 symptoms. 48 volunteers with no history of neurological disorders participated in the experiment. The participants' colour vision was assessed prior to the experiment using 14 Ishihara plates (Clark, 1924). Participants for whom the eye tracking recording was missing due to technical errors were not considered for the analysis (N=6). Three additional participants were excluded as their button presses often exceeded into the following trials (in 160-300 trials), resulting in a total sample size of N=39. Participants who did not show a significant tagging response (N=8) were excluded at a later stage (see RIFT response sensor selection below), leaving 31 data sets (20 female, see below).

3.3.4 Behavioural performance

The participants' performance on correctly detecting the presence and absence of the target was quantified based on average reaction time and perceptual sensitivity (d'), calculated as:

$$d' = z(H) - z(FA) \tag{3.1}$$

with $z(H)$ being the z-scored portion of hits in target present trials and $z(FA)$ being the z-scored portion of false alarms in target absent trials.

3.3.5 MEG pre-processing

Signal Space Separation (SSS, "Maxfilter") implemented in MNE Python was applied to suppress magnetic signals emerging from sources outside the participant's brain. The remaining pre-processing of the MEG data, frequency and source analyses, and cluster-based permutation test were performed using the Fieldtrip toolbox (Oostenveld et al., 2010) in MATLAB 2019b. Statistical analyses of the behavioural and eye tracking data were carried out in RStudio 1.1.456 with R version 3.6.1. (The R Foundation for Statistical Computing).

Faulty sensors were identified and corrected prior to the SSS using MNE python. The filtered data were divided into intervals of 4.5 s, starting 2.5 s before, and extending to 2s after the onset of the search display in each trial. Semi-automatic artefact rejection was performed on the

4.5 s intervals, by manually identifying and rejecting epochs with a comparably high variance, separately for gradiometers and magnetometers.

Independent Component Analysis (ICA) was used to suppress oculomotor and cardiac artefacts based on the 68 components that were identified for each participant. Trials with unreasonably short reaction times of up to 200ms, as well as trials without a response were rejected (Wolfe et al., 2010). When comparing performance for high and low alpha trials and fast vs slow response times, we further discarded trials with a response time of ±3 standard deviations above the mean, separately for each condition.

3.3.6 RIFT response magnitude

The photodiode signals were replaced with a perfect sine wave with low-amplitude white noise (SE= 0.05) for the offline analyses, extending into the baseline interval. The magnitude of the RIFT response was quantified by calculating the spectral coherence between the MEG sensors of interest, identified as described above, and RIFT signal. The data were bandpass-filtered using a two-pass Butterworth filter at 60 and 67 Hz ± 5 Hz, respectively. The analytic signal was obtained from the filtered data using the Hilbert transform. The spectral coherence was then calculated as (Cohen, 2014, pp. 343–344):

$$coh_{MEG,diode}(t) = \frac{\mid \sum_{k=1}^{n} m_{MEG}(t) \cdot m_{diode}(t) \cdot e^{i\phi(t)} \mid}{\left(n^{-1} \sum_{k=1}^{n} \mid m_{MEG} \mid\right) \cdot \left(n^{-1} \sum_{k=1}^{n} \mid m_{diode} \mid\right)} \tag{3.2}$$

with m_{MEG} and m_{diode} being the analytic MEG and RIFT amplitude, respectively, ϕ being the phase difference between the two signals, and n being the number of trials. To obtain the coherence to the RIFT signal of the target colour, for instance, we split the data into trials in which the target colour was tagged at 60 and 67 Hz, and calculated the coherence separately over these trials. Afterwards, the coherence was averaged over the two frequencies.

3.3.7 RIFT response sensor selection

The MEG sensors containing a reliable frequency tagging response were identified using non-parametric (Monte Carlo) statistical testing, proposed by (Maris & Oostenveld, 2007) and implemented in the Fieldtrip toolbox. The pre-processed data were divided into a baseline (0.7 to 0.2 s before stimulus onset) and stimulation interval (0.5 s following the onset of the search display). Coherence between a given MEG sensor and the 60 Hz photodiode signal over trials was estimated separately for the pre-search and the search interval. The difference between the coherence in the baseline and search interval was z-transformed using the following equation:

$$Z = \frac{\left(tanh^{-1}\left(\mid coh_{search}\right) \mid -bias\right) - \left(tanh^{-1}\left(\mid coh_{bsl} \mid\right) - bias\right)}{\sqrt{(2 \cdot bias)}} \tag{3.3}$$

Whereby coh_{search} and coh_{bsl} are the coherence between the respective MEG sensor and the photodiode at 60 Hz during the search and pre-search interval, respectively. The bias is calculated as $bias = \frac{1}{2n-2}$ with n being the number of trials.

The statistical significance of the z-transformed coherence difference (the empirical z-value) was estimated using a permutation procedure. To this end, a null distribution for the empirical z-value was estimated by generating 10,000 random permutations of the trial labels and calculating the z-values for the shuffled pre-search and search interval, using Equation 3.3. If the coherence difference obtained for the unshuffled data in the respective sensor was larger than 99% of the null distribution, the sensor was considered to show a significant tagging response at a 1% significance level. This procedure was completed for a total of 81 occipital and occipito-parietal sensors to identify the sensors of interest for each participant. 31 out of 39 participants had at least one significant gradiometer. As only 27 participants showed a significant response in at least one magnetometer, only gradiometers were considered for the sensor and source analyses. In total, we used the data from 31 volunteers for further analyses (20 female; aged 23.4 years ± 3.18). All participants were right-handed according to the Edinburgh Inventory (augmented handedness score: M=84.08; STD=14.37 Oldfield, 1971).

3.3.8 Power at the Individual Alpha Frequency

To identify the individual alpha frequency and the sensors acquiring alpha oscillations, we calculated the Time Frequency Representation (TFR) of power over all trials for frequencies from 4 to 30 Hz, by means of Fourier transformation applied by sliding 0.5 s windows (in 50 ms steps) multiplied by a Hanning taper. To identify each participant's *alpha sensors of interest*, the TFRs were averaged in the -1 to 0 s interval over trials. For each participant, the four sensors exhibiting the highest power peak in the 4-14 Hz range were selected as the *alpha sensors of interest* (combined planar gradiometers). We did not use the *RIFT sensors of interest* to investigate alpha power, as the alpha oscillations and RIFT response do not emerge from the same brain areas per se (Zhigalov & Jensen, 2020). The Individual Alpha Frequency was identified as the peak in the power spectra averaged over these sensors (see Figure A.4).

3.3.9 Source localisation

The anatomical sources of the pre-search alpha oscillations and the RIFT response were estimated using the Dynamic Imaging of Coherent Sources beamformer (Gross et al., 2001), implemented in the Fieldtrip toolbox (Oostenveld et al., 2010).

MEG leadfield

To calculate the MEG lead field, we first aligned the fiducial landmarks in the individual T1-weighted images with the digitised points taken prior to the experiment. The coordinate system of the participant's T1-weighted scan was then automatically aligned to the digitised head shape using the iterative closest point (ICP) algorithm(Besl & McKay, 1992), implemented in the Fieldtrip toolbox, and corrected manually as necessary. For the two participants for whom there was no T1 scan available, the digitised fiducial landmark and head shape were aligned with a standardised template brain provided with the Fieldtrip toolbox.

Next, the brain volume was discretised into a source grid of the equivalent current dipoles by warping each participant's realigned anatomical scan to the Montreal Neurologic Institute

(MNI) coordinate system; using a template MRI scan, and an equally spaced 8 mm grid, with 5,798 locations inside the brain. The lead field was then estimated at each point in the source grid using a semi-realistic headmodel (Nolte, 2003).

Dynamic Imaging of Coherent Sources

The sources of the RIFT response and alpha oscillations were localised using Dynamic Imaging of Coherent Sources (DICS, Gross et al., 2001). The spatial filters for this beamformer are calculated as a function of the forward model (estimated using the lead field matrix) and the cross-spectral density matrix of the sensor data. Here, we used the cross-spectral matrix of the gradiometers only. The SSS ("Maxfilter") caused the data to be rank deficient, making the estimate of the sensor cross-spectral density matrix unreliable. To ensure numerical stability, we calculated the truncated singular value decomposition (SVD) pseudoinverse (Gencer & Williamson, 1998; Westner et al., 2022) of the sensor cross-spectral density matrix. This method decomposes the covariance matrix using SVD, selects a subset of singular values (the subset size is defined by the numerical rank) and calculates a normalised cross-spectral density matrix using this subset. The spatial filters are then estimated based on the normalised cross-spectral density matrix using unit-noise gain minimum variance beamforming(Borgiotti & Kaplan, 1979; Westner et al., 2022).

To estimate the cross-spectral density matrix for the RIFT response, we first extracted data segments from 0 to 0.5 s (the minimum reaction time for all participants). The complex cross-spectral density between the signal in the (uncombined) planar gradiometers and the RIFT signal was computed based on the Fourier-transformed data segments (Hanning taper, separately for the 60 Hz and the 67 Hz photodiode signal). The cross-spectral density matrices were used to estimate the forward model to create a spatial filter for each frequency. The spatial filters were then applied to the cross-spectral density matrix to estimate the RIFT response as the coherence between each point in the source grid and the photodiode signal.

The spatial filters of the alpha oscillations were estimated based on the cross spectral density matrix of the gradiometers at the individual alpha frequency, calculated based on the -1 to 0

s interval (Hanning taper). Analogously to the RIFT response, the filters were than applied to calculate power at the individual alpha frequency at each grid point.

3.4 Results

Our experimental paradigm featured two search conditions (*guided* and *unguided search*) and two set sizes (16 and 32), presented in a block design, with each block consisting of 40 trials (Figure 3.2a). Participants were requested to indicate if a single iteration of the letter "T" was presented among several iterations of the letter "L". In the *guided search* condition, participants were cued to the colour of the target "T" (either yellow or cyan) at the beginning of the block. Importantly, as only these two colours were used throughout the experiment, participants were able to infer the distractor colour from this cue. In the *unguided search* condition, a white "T" was presented at the beginning of the block, meaning the target and distractor colours were not cued, and the colour of the T was randomised over trials. Set size was kept constant within each block. The target and distractor colours were frequency-tagged by modulating their luminance sinusoidally, at 67Hz and 60Hz respectively (randomised over trials; Figure 3.2b). Participants were instructed to perform the task while fixating a centrally presented dot.

Based on the extensive literature on visual search, we predicted search performance to be worse (indicated by reaction time and accuracy) for more difficult searches, i.e., *set size 32* relative to *16* and *unguided* compared to *guided search* (Egeth et al., 1984; Palmer, 1994; Wolfe, 1994, 2021). Indeed, these hypotheses were confirmed by the statistical analyses on the reaction time and sensitivity (d') outlined in the Supplementary analyses and shown in Figure 3.2c and d. Furthermore, we found that reaction time and sensitivity did not differ for *unguided search, set size 16* and *guided search, set size 32*, indicating that the difficulty of these searches was similar (see Table A.2 and Table A.4). This suggests that the participants used the colour cue at the beginning of the block to focus their search on the target colour.

3.4.1 Rapid Invisible Frequency Tagging responses indicate target boosting and distractor suppression

RIFT elicited brain responses at the respective stimulation frequencies detected in a small number of MEG sensors over the occipital cortex (Figure 3.3a, see Figure A.1 for individual

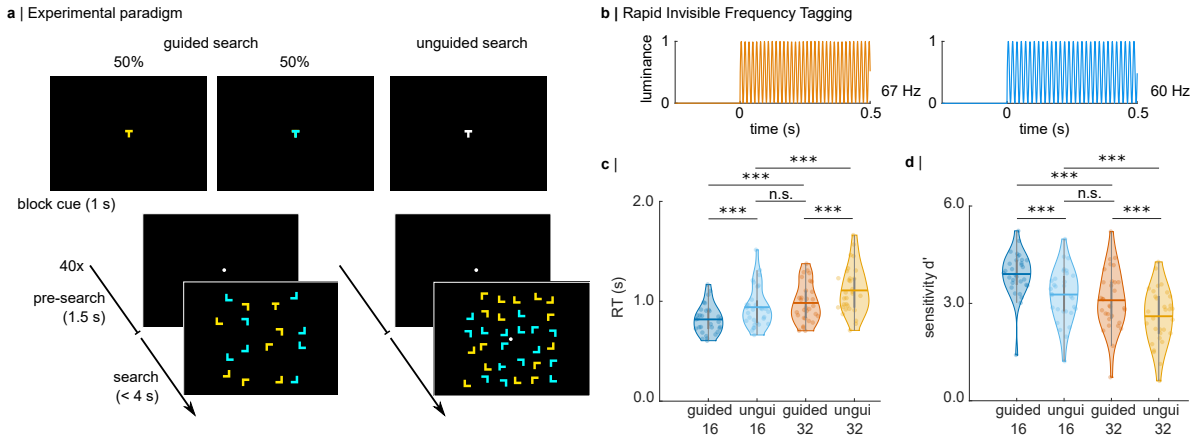

Figure 3.2: Experimental paradigm, Rapid Invisible Frequency Tagging (RIFT), and search performance. **a** Trials were presented in a blocked design. Each block contained 20 target absent and 20 target present trials. Set sizes (16 or 32) were the same within each block. At the start of a block in the guided search condition, a "T" was presented in yellow or cyan, revealing the target colour for the following 40 trials. A block in the unguided search condition began with the presentation of a white "T", and the target colour was randomized over trials. Note that the search displays are not true to scale; the eccentricity of the search array amounted to 10° visual angle, 5° on either side of the fixation dot. **b** RIFT at 60 and 67 Hz was applied to the colour of the stimuli by modulating the luminance sinusoidally. In this example, yellow stimuli were tagged at 67 Hz and cyan stimuli were tagged at 60 Hz. **c** Search performance decreases for more difficult searches. A hierarchical regression approach reveals a significant main effect for set size ($\beta = 0.18$) and guided/unguided ($\beta = -0.14$). Indicating that larger set sizes are associated with slower responses, while guided searches are faster than unguided searches. Pairwise comparisons reveal no significant difference in reaction time between unguided search set size 16 and guided search set size 32 ($V = 134, z = 2.24, r = 0.4, p = 0.14$), suggesting that participants focused their search on task-relevant items in the guided search condition. **d** Analogously, for accuracy (as measured by d'), hierarchical regression reveals a significant main effect for set size ($\beta = -0.74$) and guided/unguided ($\beta = 0.56$), indicating that accuracy is higher in guided searches and for set size 16 compared to 32. Again, there is no significant difference in sensitivity for unguided search set size 16 and guided search set size 32 ($t(30) = 2.2, d = 0.2, p = 0.23$).

topographic representations per participant). Source modelling based on Dynamic Imaging of Coherent Sources (DICS) demonstrated that the responses emerged from early visual regions (V1, MNI coordinates [0 -92 -4], Figure 3.3b).

As outlined in our pre-registration, we hypothesised that the RIFT response reflects a priority-map-based search strategy, indicating target boosting and distractor suppression in the *guided search* condition. Figure 3.3c and d show the RIFT response as quantified by the coherence (R^2) between the MEG response (*RIFT sensors of interest*) and the frequency tagging signal, averaged over participants (see 3.3 for details on the RIFT analysis). Note that the immediate increase in

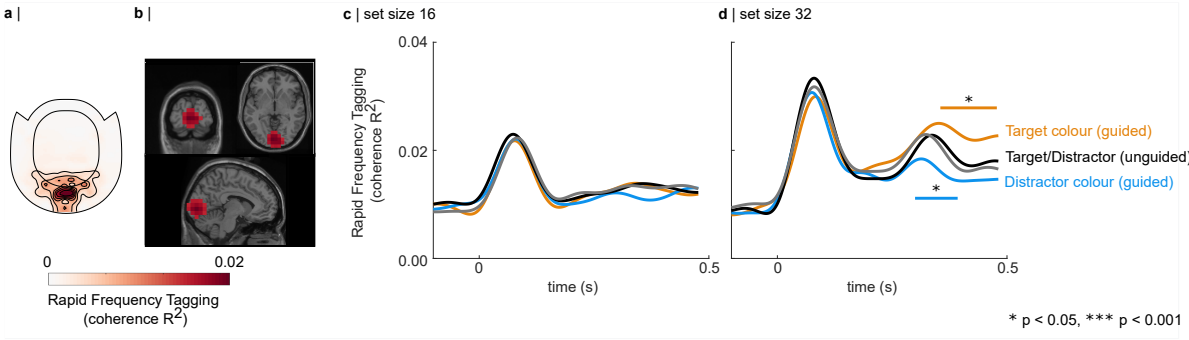

Figure 3.3: Rapid Invisible Frequency Tagging (RIFT) responses reflect a priority-map based mechanism. **a** Topographic representation of the 60 Hz RIFT signal, averaged over participants in the 0 to 0.5 s interval (t = 0 s is the onset of the search display). The RIFT response is confined to the occipital sensors. **b** Source modelling demonstrates that the RIFT response was primarily generated in the early visual cortex. The source grid has been masked to show the 1% most strongly activated grid points (MNI coordinates [0 -92 -4]). **c,d** Coherence to the RIFT signal reveals target boosting and distractor suppression in guided search. **c** set size 16. There was no difference in RIFT responses between target and distractor colours; nor guided versus unguided search. **d** set size 32. The RIFT responses to the guided target colour are significantly enhanced and the responses to the guided distractor colour are significantly reduced compared to the unguided search condition ($p < 0.05$; multiple comparison controlled using a cluster-based permutation test in the 0 to 0.5 s interval).

coherence after the search display onset reflects a broad-band evoked response, rather than the frequency-specific flicker signal. The RIFT responses for *set size 16* were noticeably weak and did not show any modulation to the target and distractor colour (Figure 3.3c). Considering that the coherence drops to baseline after the event-related response, we argue that this is the result of an insufficient signal-to-noise ratio caused by a comparably small number of pixels flickering (but see 3.5).

For *set size 32*, we find that the RIFT responses to the target colour in the *guided search* condition were significantly enhanced compared to the *unguided search* condition (Figure 3.3d). This suggests a boosting of the neuronal excitability to all items sharing the known target colour. Importantly, the responses to the distractor colour when comparing *guided* to *unguided search* were significantly reduced, providing evidence for distractor suppression (Figure 3.3d, $p < 0.05$; multiple comparisons were controlled using a Monto-Carlo cluster-based dependent sample t-test on the 0 to 0.5 interval, 5,000 permutations). Our findings demonstrate that knowledge about the target and distractor colour in the *guided search* condition results in a modulation of

the RIFT response consistent with the concept of a priority map, whereby target representations are boosted, and distractor representations are suppressed. Importantly, these results serve as a proof-of-principle, showing that RIFT is suitable to measure the neuronal excitability associated with the priority map in visual search (also see Bouwkamp et al., 2023).

We further tested whether this modulation was relevant for performance, by sorting the trials based on a median split of reaction time into fast and slow trials. The analyses only revealed a weak relationship between reaction time and RIFT responses which are described in detail in the A.1 and Figure A.2.

3.4.2 Strong pre-search alpha oscillations predict enhanced search performance and reduced RIFT responses in guided search

We next aimed to identify if alpha oscillations facilitate search by modulating the neuronal excitability associated with the visual inputs. As part of the pre-processing, we identified the sensors showing the highest peak in the alpha-band, averaged over all conditions and trials, as the *alpha sensors of interest.* We did not use the *RIFT sensors of interest*, as RIFT responses and alpha oscillations do not emerge from the same brain areas *per se* (Zhigalov & Jensen, 2020, see 3.3 and Figure A.3 for individual topographies of pre-search alpha power). Fiure 3.4a shows the Time-Frequency Representation (TFR) of power in the identified alpha sensors, aligned to each individual's alpha frequency before calculating the grand average (see Figure A.4 for individual spectra). The TFR demonstrates that visual search was preceded by high power in the alpha band, which was sustained during the search albeit weakened.

We hypothesised that more demanding conditions would require stronger inhibition to suppress a larger portion of the search display. Therefore, we expected alpha power to be stronger for *set size 32* compared to *16*. A repeated measures ANOVA using the factors condition (*guided* vs *unguided search*) and *set size* did not reveal any main effects or interactions of the alpha power before or during the search (Figure A.5). This result suggests that pre-search alpha is not modulated by the anticipated difficulty of the search task. To test our hypothesis that alpha oscillations facilitate search, we next investigated the effect of the pre-search alpha power on

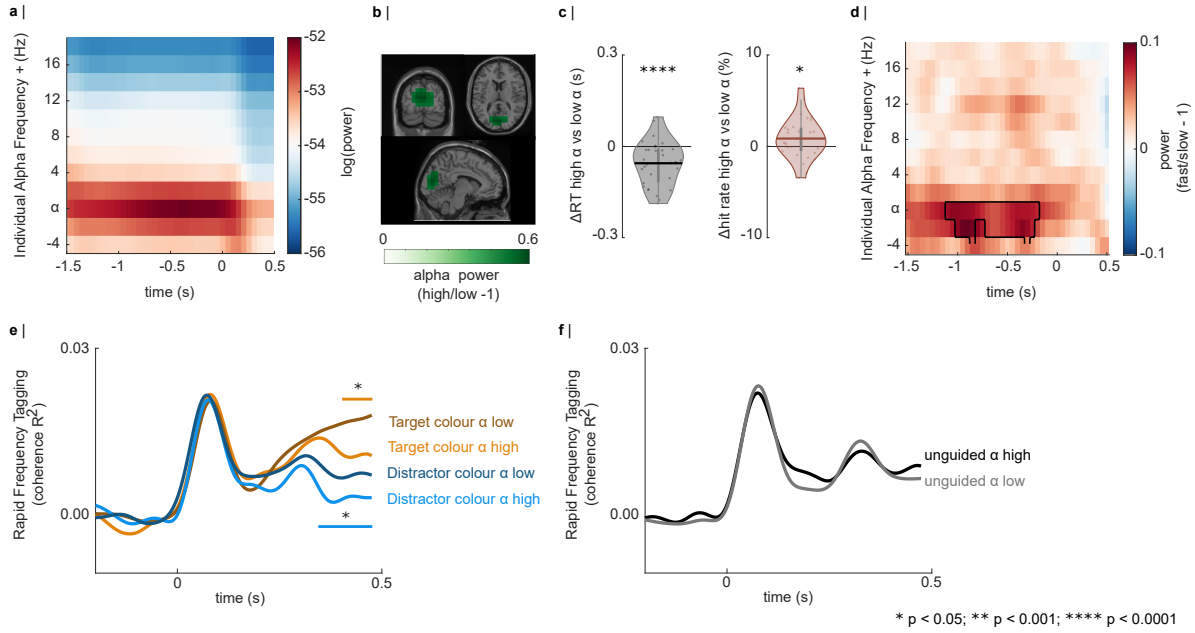

Figure 3.4: Alpha oscillations pre visual search predict better performance and reduced RIFT responses. **a-f** median split based on pre-search alpha power. **a** Time-Frequency Representation (TFR) of power, aligned to each participant's individual alpha frequency, revealing strong alpha oscillations in the baseline that persisted during the search. **b** Source localisation of the contrast between high and low alpha power (relative change), showing the 1% most strongly activated grid points. Alpha power peaks in V1, MNI coordinates [-8 -84 12]. **c** (left) Reaction time is significantly faster in trials with high compared to low alpha power (Wilcoxon signed rank test: $z = -3.53, p = 0.0001$). (right) High alpha is associated with a higher number of hits, i.e., a correct indication of target present or absent ($z = 2.12, p = 0.017$). **d** TFR contrast between fast and slow trials shows that fast trials were preceded by significantly stronger power in the alpha-band – and not in any other frequency band (controlled for multiple comparisons using Monte Carlo cluster-based permutation dependent sample t-test, one-sided, $p < 0.01, 5,000$ permutations). **e** High alpha trials in the guided search condition (*set size 32*) are associated with reduced RIFT responses to both the target and distractor colour ($p < 0.05$, permutation test applied to the 0.15 to 0.5 s interval, 5,000 permutations) **f** The finding in **e** did not replicate for the unguided search condition.

search performance and neuronal excitability measured by the RIFT response. Pre-search alpha power was estimated by averaging the TFR of power of every trial over the -1 to 0 s interval. The trials were then sorted based on the median split on power at the individual alpha frequency, separately for each condition, i.e., *set size 16* vs. *32*, *guided* vs. *unguided search,* and *target present* vs. *absent* trials. After performing the median split, the data of all conditions were combined into *high alpha* and *low* alpha trials. The averaged spectra for each participant for the high and low alpha trials are shown in Figure A.6, and demonstrate a clear peak in the alpha-

band for all participants. Source localisation using a DICS beamformer revealed the maximum difference in alpha power between high and low alpha trials in early visual areas as demonstrated in Figure 3.4b (V1, MNI coordinates [-8 -84 12], masked to show the top 1% most strongly activated grid points).

Figure 3.4c shows the difference in performance for trials with high compared to low pre-search alpha power. Trials with high alpha power were associated with significantly reduced reaction times (left, Wilcoxon signed rank test: $V = 68, z = -3.53, p = 0.0001, r = 0.63, SE = 0.013$). Moreover, hit rates (correct indication of target absent or present) were significantly higher for high compared to low alpha trials, indicating that the response time effect was not driven by a speed-accuracy trade-off (right, $V = 356, z = 2.12, p = 0.017, r = 0.38, SE = 0.004$). These results suggest that high alpha power in preparation for the search predicts significantly better performance. To confirm that there was indeed a negative correlation between reaction time and pre-search alpha power across trials, we conducted an additional analysis, whereby we fitted a linear regression model to the reaction time data for each participant, as a function of set size, *guided* vs *unguided*, target present/absent, and alpha power in the -1 to 0 s interval (both reaction time and alpha power were z-scored for each participant). Indeed, we find that the regression coefficient associated with the alpha power was significantly smaller than zero ($t(30) = -4.14, d = -0.74, p = 0.00013, SE = 0.011$), and the difference in R^2 between the full model including alpha power, and the model just including set size, guided/unguided, target absent/present was significantly larger than zero ($t(30) = 4.6, p = 4x10^{-5}, d = 0.82, SE = 0.001$, data not shown).

To corroborate that these results are based on frequency-specific increases in the alpha-band, and not broadband power changes, we performed a confirmatory analysis step, whereby we sorted the trials in each condition based on a median split on reaction time, into *fast* and *slow* trials. The TFRs for the fast and slow trials of each participant were averaged over the *alpha sensors of interest* and compared using a Monte Carlo dependent sample t-test. Indeed, fast trials were associated with significantly enhanced power in the alpha-band, in the pre-search interval, as indicated by the black outline in Figure 3.4d ($p < 0.01, 5,000$ permutations).

Next, we asked to what extent pre-search alpha power links to modulations in the RIFT response. Figure 3.4e shows the grand average RIFT responses in *guided search*, *set size 32*, separated for trials with high and low pre-search alpha power. Notably, trials with high alpha power appeared to be associated with overall reduced RIFT responses. In line with that, we found a significant reduction in RIFT responses to both the target and distractor colour for high compared to low alpha trials, using cluster-based permutation Monte Carlo t-tests ($p < 0.05, 5,000$ permutations, note that the tests were applied to the 0.15 to 0.5 s interval, as the attentional modulation of the RIFT responses in Figure 3.3d was observed after about 200 ms). This demonstrates that high alpha power before the search is associated with reduced RIFT responses to all stimuli in the visual field. Surprisingly, there was no link between pre-search alpha power and RIFT responses in *unguided search*, *set size 32*. As we did not observe a RIFT response for *set size 16* (Figure 3.3c), we did not expect to find any evidence for a modulation of the RIFT signal by alpha power in this condition; which was indeed confirmed by our A.1 (but see Figure A.7a,b).

The presented analyses link strong pre-search alpha oscillations in early visual areas to enhanced performance, as indicated by faster and more accurate responses, as well as reduced neuronal excitability to both target and distractor features in *guided search, set size 32*. This finding supports the *blanket inhibition* hypothesis indicated in Figure 3.1d. It should be emphasised that these results were not related to ocular artefacts or targeted eye movements, as confirmed by control analyses outlined in the A.1 and Figure A.9.

3.4.3 Strong alpha power during search is linked to faster reaction times and reduced RIFT responses in *guided* and *unguided* search

Considering the link between pre-search alpha power, behaviour, and RIFT responses, we next set out to quantify the effect of alpha power during the search. We divided the trials based on alpha power in the 0.25 to 0.5 s interval (median split performed separately for each condition as described above), avoiding an extension of the sliding window into the baseline interval. The spectra of the trials with high and low alpha power during search are shown in Figure A.8,

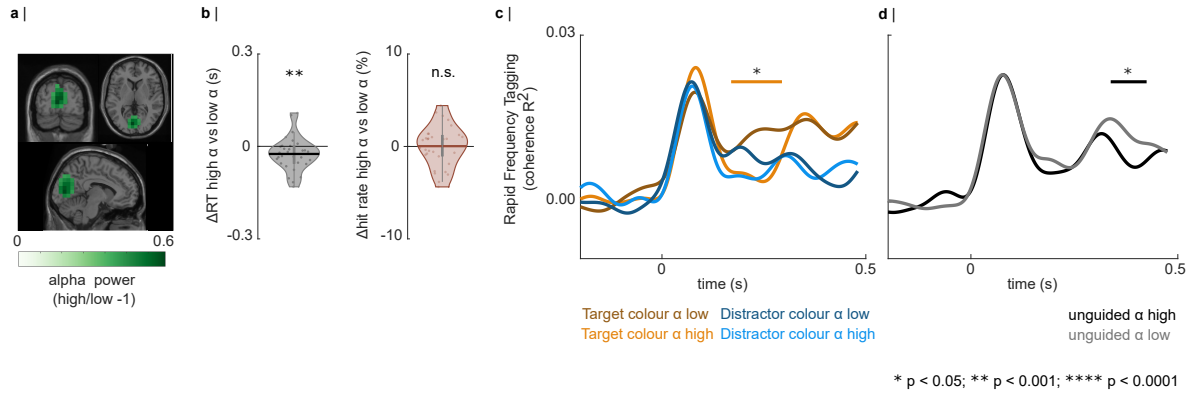

Figure 3.5: Alpha oscillations during visual search predict faster response times and reduced RIFT responses.**a** Source localized contrast between high and low alpha power during search, showing the 1% most strongly activated grid points, again revealing strongest activation in early visual cortex (MNI coordinates [-8 -84 4]). **b** (left) Trials with high alpha power during search are associated with significantly faster reaction time (z = -2.7, p = 0.0026). (right) There is no significant difference in hit rate between trials with high and low alpha power during search (z = 0.43, p = 0.33). **c** Trials with high alpha power during guided search, set size 32 are associated with reduced RIFT responses to the target colour (p<0.05, sign.) and the distractor colour (p=0.1, trend). **d** Trials with high alpha power in unguided search, set size 32, were also associated with significantly reduced RIFT responses (p < 0.05).

demonstrating a pronounced peak at the individual alpha frequency for all participants. The source of the alpha oscillation was again located in early visual regions, as indicated by a contrast between high and low alpha power (Figure 3.5a, MNI coordinates [-8 -84 4]).

In line with the findings reported above, we again found that response times were significantly faster in trials with high compared to low power in the alpha-band during search (Figure 3.5b, left, $V = 110, z = -2.7, p = 0.003, r = 0.49, SE = 0.01$). However, there was no significant difference in hit rate between high and low alpha trials (Figure 3.5b, right, $V = 270$, $z = 0.43$, $p = 0.34, r = 0.08, SE = 0.004$).

We then tested if the magnitude of the RIFT response was related to alpha power during the search. For *guided search, set size 32*, we find that the responses to both the targets and distractors are again reduced for trials with high compared to low alpha power during search (Figure 3.5c); with a significant difference for the target colour ($p < 0.05$) and a trend effect for the distractor colour ($p = 0.1$). Interestingly, we found that high alpha power during *unguided search, set size 32*, was also associated with significantly reduced RIFT responses (Figure 3.5d).

The RIFT responses for *set size 16*, *guided* and *unguided search* are shown in Figure A.7c,d. The results only indicate a reduced event-related response to the distractor colour in the high alpha trials, but no modulation in the later (frequency-specific) response.

The presented results demonstrate that strong alpha oscillations are present during visual search. Moreover, the magnitude of these oscillations was associated with faster reaction times and reduced RIFT responses in *guided* and *unguided search, set size 32*. These results again support a *blanket inhibition* mechanism, that facilitates visual search through inhibition of all visual inputs, regardless of their task-relevance.

3.4.4 Time-on-task as a confounding variable in search performance and cortical excitability - exploratory analyses

Previous studies employing visual paradigms have reported that alpha power tends to increase over task duration (Benwell et al., 2019). Such changes in alpha power over time have been associated with fluctuations in visual performance (Benwell et al., 2018) and fatigue (Cajochen et al., 1995; Craig et al., 2012; Daniel, 1967). Therefore, the observed link between increased alpha power and search performance, and alpha power and RIFT responses, could be confounded by time-on-task. Figure 3.6 shows the Spearman correlation between time-on-task and alpha power in the interval pre- (left plot) and during search (right plot), suggesting that alpha power indeed increases with task time for the majority of participants. We tested the correlation coefficients against zero using a permutation procedure, whereby the null distribution was obtained by randomly flipping the sign of the correlation coefficients for 5,000 iterations, and calculating the t-values at each iteration (Nichols & Holmes, 2002). Comparing the t-statistics obtained from the original values to this null distribution disclosed that the correlation with time-on-task was significant for both pre-search alpha power ($p < 0.0001, d = 1.25$) and alpha power during the search ($p = 0.004, d = 0.56$).

We next performed a balanced median split to control for the potential confound of time-on-task on search performance and RIFT response. To this end, we first divided the data into four equal time-on-task bins. Within each bin, we then split the data based on high and low

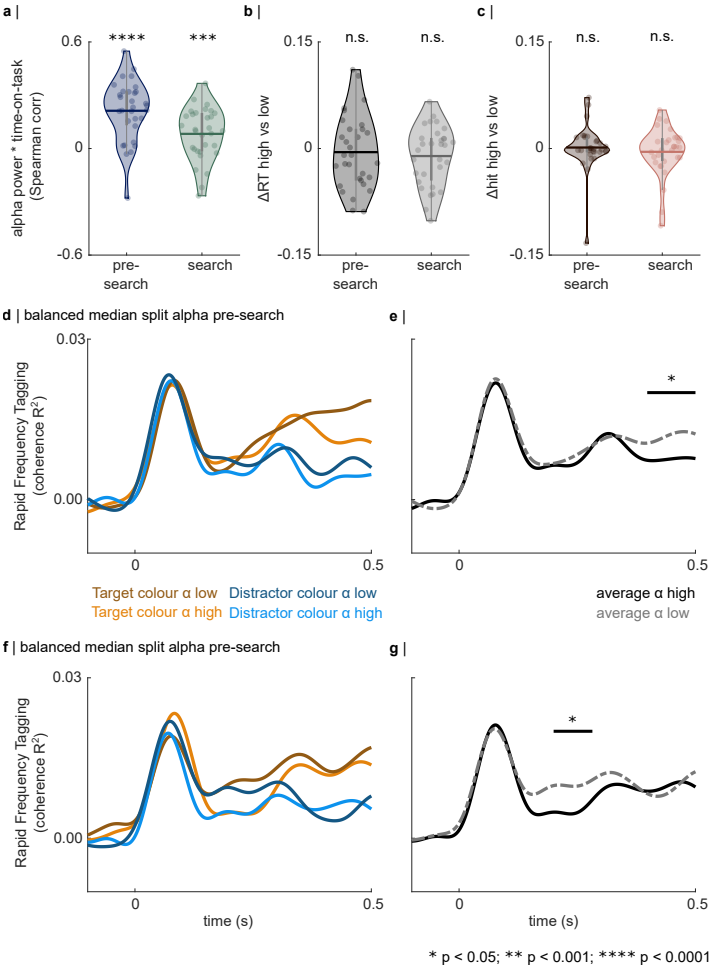

Figure 3.6: The blanket inhibition confound with time-on-task: behaviour and RIFT responses. **a** Spearman correlation coefficient for alpha power and time-on-task for individual participants (indicated by the scatters). A permutation test reveals a significant correlation for both alpha power pre- and during the search. **b** Reaction time sorted into high and low alpha power according to a balanced median split did not replicate the previously described relationship between alpha power and reaction time. **c** Similarly, the balanced median split on hit rate yielded inconclusive results. **d** RIFT responses in *guided search, set size 32* sorted using a balanced median split on pre-search alpha power. **e** The balanced split reveals a significant reduction of the RIFT response for trials with high alpha power. Notably, this effect appears to be largely driven by the response to the target. **f,g** RIFT responses sorted into high and low alpha during the search based on a balanced median split again reveal significantly reduced responses in high compared to low alpha trials.

alpha power, separately for *guided* and *unguided search*, and *set size 16* and *32*. We combined the trials with high alpha power from the separate bins to create a group of *high alpha* trials, and did the same for low alpha power trials. Figures 3.6b and c present the comparison in between the *high* and *low alpha* trials for reaction time and hit rate, respectively. Our analysis

revealed no significant effect of alpha power neither on reaction time (Figure 3.6b, Wilcoxon signed-rank test: pre-search $V(30) = 211, z = -0.73, p = 0.48, r = -0.13$, during search $V(30) = 194, z = -1.5, p = 0.48, r = -0.19$, after Benjamini-Hochberg correction) nor hit rate (Figure 3.6c, dependent sample t-test: pre-search $t(30) = -0.55, p = 0.58, d = -0.1$, during search: $t(30) = -1.43, p = 0.33, r = -0.26$, Benjamini-Hochberg corrected). These findings suggest that the link between alpha power and search performance cannot clearly be dissociated from effects of time-on-task on both of these variables.

Next, we looked at how the RIFT responses varied when we applied the balanced median split based on alpha power. Figure 3.6d shows the RIFT responses to target and distractor colours in *guided search set size 32*, split according to pre-search alpha power. The graphs suggest a reduction in RIFT responses for high alpha trials. To test the main effect of alpha power on RIFT responses, we first averaged the responses to target and distractor colours for both high and low alpha trials. A cluster-based permutation test revealed a significant reduction in RIFT responses for high alpha trials compared to low (Figure 3.6e, one-sided Monte Carlo test, $p < 0.05$, 5,000 permutations). This result was replicated for the balanced median split based on alpha power during the search (Figure 3.6g, $p < 0.05$, 5,000 permutations). However, we were unable to replicate the reduction in RIFT response with high alpha power for the *unguided search* condition (data not shown).

In summary, while the balanced median split approach indicated that search performance is not robustly affected by alpha power when controlling for time-on-task, the impact on RIFT responses in *guided search, set size 32* remained significant.

3.5 Discussion

We used Rapid Invisible Frequency Tagging (RIFT), a novel approach to probe neuronal excitability in visual cortex, in combination with MEG, to investigate feature-guided visual search. In the *guided search* condition, the target colour was cued, and in the *unguided search* condition, the target colour was unknown. As expected, search performance was reduced for higher set sizes and for *unguided* compared to *guided* search; the latter confirming that participants used the colour cue at the beginning of the block to guide their search. The RIFT responses in the *guided search* condition, *set size 32*, demonstrated an increase in neuronal excitability in early visual cortex associated with the target colour and a suppression associated with the distractor colour. Furthermore, we find that high pre-search alpha power predicts significantly faster and more accurate responses. However, these results were not robust when accounting for time-on-task using a balanced median split approach. Yet, high alpha power before and during the search was associated with reduced RIFT responses to all stimuli, even when controlling for time-on-task. In sum, we here provide neural evidence for a priority-map-based mechanism in early visual regions that may be supported by alpha oscillations.

Our results demonstrate that a mechanism akin to a priority map guides visual search by modulating neuronal activity in early visual regions, as indicated by increased RIFT responses associated with the target colour and suppressed responses to distractors. Considering that the modulation starts 200 ms after the onset of the search display, we argue that this mechanism underlies top-down control by the ventral stream (but see below), and operates in a feature-specific manner (Maunsell & Treue, 2006). Importantly, we provide novel insight relating alpha oscillations to this priority-map-based mechanism. As alpha oscillations are associated with functional inhibition, we propose that they reduce the firing of excitatory neurons in early visual cortex in preparation for the search through a *blanket inhibition* mechanism. As the inhibition subsides with the onset of the search display, the neurons associated with the boosted target features will be able to surpass this inhibitory threshold (as depicted in Figure 3.1d). This model explains the enhanced performance in trials with high compared to low pre-search alpha power,

as the alpha inhibition promotes more efficient search (Figure 3.4c and 3.5a).

Our work complements previous electrophysiological recordings in humans and non-human primates investigating visual search paradigms with smaller set sizes of up to six items (Donohue et al., 2018, 2020; Forschack et al., 2022; Hickey et al., 2009; Ipata et al., 2009; Klink et al., 2023; van Zoest et al., 2021), and selective attention to moving stimuli(Andersen & Müller, 2010; Andersen et al., 2008; Müller et al., 2006). Here, we used a complex display with a large set size, in the tradition of psychophysical research on visual search (Treisman et al., 1980; Wolfe, 1994, 2021). Recent studies have suggested that the RIFT signal does not propagate beyond V1/V2 (Duecker et al., 2021; Schneider et al., 2023; Soula et al., 2023), which is consistent with our source modelling results. We therefore propose that our findings provide evidence for a retinotopically organised priority map supported by early visual regions.

Electrophysiological recordings in non-human primates have shown target boosting and distractor suppression in the frontal eye field and lateral intraparietal cortex about 90 ms after stimulus onset (Cosman et al., 2018; Ipata, Gee, Goldberg, & Bisley, 2006; Ipata, Gee, Gottlieb, et al., 2006) and after about 110 ms in V4 (Klink et al., 2023). As the modulation of the RIFT signal in this was observed at about 200 ms after search display onset, we argue that this priority map underlies top-down control from higher-order areas in the ventral stream (Chen & Seidemann, 2012; Kamiyama et al., 2016; Muckli, 2010; Muckli & Petro, 2013). This time course is in line with the observation that guidance by colour takes about 200-300 ms to be effective(Palmer et al., 2019). Our results add to the literature by demonstrating that activity in early visual cortex contributes to priority maps in addition to e.g. lateral intraparietal cortex(Ipata, Gee, Goldberg, & Bisley, 2006; Ipata, Gee, Gottlieb, et al., 2006; Ipata et al., 2009; Mirpour et al., 2009), the frontal eye field (Bichot & Schall, 1999; Cosman et al., 2018; Thompson & Bichot, 2005), V4 (Klink et al., 2023; Reynolds et al., 1999), and superior colliculus(Bayguinov et al., 2015).

Using a feature-guided search paradigm, we associate increases in alpha power to enhanced performance and reduced neuronal excitability to the stimuli's colour. This result challenges the early notion of alpha oscillations reflecting a state of inattention or idling (Pfurtscheller et al.,

1996). Furthermore, our results show that strong alpha power is not always detrimental in visual tasks, as suggested by signal detection paradigms (Dijk et al., 2008; Ergenoglu et al., 2004; Hanslmayr et al., 2007). Our finding can be explained by the notion that a substantial fraction of the items needs to be supressed to optimise the search (Liesefeld & Müller, 2019); which we refer to as *blanket inhibition*. This interpretation is in line with previous work demonstrating that alpha oscillations reflect functional inhibition (Dugué et al., 2011; Haegens et al., 2011; Iemi et al., 2022; Zumer et al., 2014).

Nevertheless, the correlation between alpha power and time-on-task, paired with its influence on reaction time, could suggest an alternative interpretation: Increases in alpha power over the course of the task may not be directly task-related but rather a signature of increased fatigue (Benwell et al., 2019; Cajochen et al., 1995; Craig et al., 2012; Daniel, 1967), activation of the Default Mode Network (Knyazev et al., 2011), or a decrease in cortical excitability caused by neural adaptation (Katyal et al., 2019). However, while previous studies have found a connection between increased alpha power and mental fatigue during visual search, this was typically tied to a drop in task performance (Fan et al., 2015; Hanna et al., 2018). Conversely, our results suggest an increase, or, in the case of the balanced split, no change in task performance with enhanced alpha power. Accordingly, the association between alpha power and time-on-task might imply that participants learn to use inhibition to reduce the distractibility of task-irrelevant stimuli. To explore this hypothesis, we are currently developing analyses that examine the link between reaction time and spectral power across various frequencies and time points at a single-trial level, while controlling for time-on-task. This approach of keeping the data in its continuous form reduces the risks of information loss and the introduction of random errors that come with dichotomising continuous variables (McClelland et al., 2015) and may thus allow us to better understand how alpha oscillations support visual search. At the time of writing this thesis, the outcomes of these analyses are at a preliminary stage and, as such, are not yet ready for dissemination.

Our findings seem inconsistent with previous studies that did not find a relationship between flicker responses and alpha oscillations in the context of spatial attention(Antonov et al., 2020;

Gundlach et al., 2020; Zhigalov & Jensen, 2020). We argue that this discrepancy may be explained by the notion that feature-based attention, as required in the present task, does not benefit from the allocation of spatial attention (Maunsell & Treue, 2006) and therefore involves different neural mechanisms and cortical regions to the ones investigated in previous work. For instance, spatial location and configural information have been suggested to involve the dorsal stream (Ayzenberg & Behrmann, 2022; Konen & Kastner, 2008; Mishkin et al., 1983). Accordingly, spatial attention paradigms have shown a modulation of alpha power in parietal cortex(Zhigalov & Jensen, 2020). In the *guided search* task presented here, the search could be sped up by using information about the target colour, which is processed in the ventral stream (Conway, 2014; Mishkin et al., 1983). The participants further needed to distinguish between T's and L's, which are defined by the spatial arrangement of the vertical and horizontal bars. These visual stimulus properties have been argued to be processed in caudal-medial areas of the dorsal pathway (V7), which are strongly connected to early visual and ventral regions (Freud et al., 2016). Accordingly, the generator of the alpha oscillations in our study was found in early visual cortex. The discrepancies between our findings and previous work could therefore underlie the fact that feature-guided search would benefit from a gating mechanism in early visual cortex, while spatial attention requires inhibition of task-irrelevant locations, which are processed in the dorsal stream.

3.5.1 Limitations & Outlook

We did not find evidence for target boosting and distractor suppression for the lower set size of 16 items. Considering that the coherence drops to baseline after the event-related, frequency-unspecific response, this most likely reflects an insufficient signal-to-noise ratio of the RIFT response, caused by a larger distance between the stimuli and half as many pixels flickering for *set size 16* compared to *32*. In future studies, it would be interesting to investigate whether this is indeed the cause, by placing the 16 stimuli on a smaller search array or increasing the stimulus size.

Target boosting and distractor suppression have been argued to be implemented by distinct

mechanisms (Donohue et al., 2018; Noonan et al., 2016). In this study, participants were able to infer the distractor colour from the cue provided at the beginning of the block, thus preventing us from disentangling these mechanisms. In future studies, it would be useful to use RIFT in a paradigm relying solely on distractor inhibition (Thayer et al., 2022), in which the participants are only informed about the distractor colour, while the target colour varies. This would clarify if and how alpha oscillations can support distractor-specific inhibition.

Our *blanket inhibition* model links strong alpha power to an unselective suppression of all stimuli in the visual field. While we did not find a link between pre-search alpha power and RIFT responses in the *unguided search* condition, we demonstrate this relationship for alpha power during search. This suggests that the *blanket inhibition* mechanism might only be effective when the participants have a strategy in place regarding the stimuli they want to boost and suppress. Importantly, the negative correlation was established between the magnitude of the RIFT response and alpha power in the same interval, showing that blanket inhibition is effective during the search.

3.6 Conclusion

In conclusion, our work demonstrates that guided search is associated with a modulation of neuronal excitability in early visual regions according to a priority map. Based on previous work, we argue that this mechanism underlies top-down control by the ventral stream. We propose that guided search relies on a priority map affecting neuronal excitability as early as primary visual cortex. Furthermore, we have presented evidence suggesting that occipital alpha oscillations may facilitate the search by a *blanket inhibition* mechanism, that is laid out in preparation for the search. Our working hypothesis is that alpha oscillations in early visual regions may apply an inhibitory threshold to the entire priority map, which can only be exceeded by boosted stimuli. This might enable the observer to focus the search on task-relevant items while reducing the distractibility of irrelevant stimuli, as reflected by improved search performance for higher alpha power. An alternative interpretation could be that the increase in alpha power over time may reflect a reduction in excitability due to fatigue or neural adaptation, and could thus not be instrumental for the task. As such, additional analyses controlling for time-on-task will be conducted to understand the mechanisms through alpha oscillations support visual search.

4

Oscillations in an Artificial Neural Network convert competing inputs into a temporal code

Prelimiary results of this project have been previously shared in: Duecker, K., Idiart, M., & Jensen, O. (2021). Space-to-time-conversion: Oscillations in an artificial neural network generate a temporal code representing simultaneous visual inputs [Montreal AI & Neuroscience (conference abstract)]

This chapter has been developed in collaboration with Marco Idiart, Marcel van Gerven, and Ole Jensen.

4.1 Abstract

Deep convolutional neural networks (CNNs) resemble the hierarchically organised neural representations in the primate visual ventral stream. However, these models typically disregard the temporal dynamics experimentally observed in these areas. For instance, alpha oscillations dominate the dynamics of the human visual cortex, yet the computational relevance of oscillations is rarely considered in artificial neural networks (ANNs). We propose an ANN that embraces oscillatory dynamics with the computational purpose of converting simultaneous inputs, presented at two different locations, into a temporal code. The network was trained to classify three individually presented letters. Post-training, we added semi-realistic temporal dynamics to the hidden layer, introducing relaxation dynamics in the hidden units as well as pulsed inhibition mimicking neuronal alpha oscillations. Without these dynamics, the trained network correctly classified individual letters but produced a mixed output when presented with two letters simultaneously, elucidating a bottleneck problem. When introducing refraction and oscillatory inhibition, the output nodes corresponding to the two stimuli activated sequentially, ordered along the phase of the inhibitory oscillations. Our model provides a novel approach for implementing multiplexing in ANNs. It further produces experimentally testable predictions of how the primate visual system handles competing stimuli.

4.2 Introduction

The inclusion of convolution in artificial neural networks (ANNs) marked a significant milestone in computer vision (LeCun & Bengio, 1995). Building on this innovation, deep convolutional neural networks (CNNs) have successfully addressed a wide range of image classification challenges, as demonstrated by Krizhevsky et al (Krizhevsky et al., 2012) in the ImageNet competition [see (Voulodimos et al., 2018) for review]. Originally inspired by the receptive fields of neurons in visual cortex, the hierarchically organised representations emerging in these networks have been repeatedly shown to map on to those identified from human MEG and fMRI recordings of the visual ventral stream (Cichy et al., 2016, 2017; Güçlü & van Gerven, 2015) and intracranial recordings from the non-human primate brain (Kriegeskorte, 2015; Marques et al., 2021; Schrimpf et al., 2020; Yamins & DiCarlo, 2016; Yamins et al., 2014). Despite the parallels between CNNs and the primate visual system, there are only few examples of ANNs for computer vision that have drawn inspiration from the temporal dynamics of cortical activity (Effenberger et al., 2022; Vinken et al., 2020). For instance, alpha oscillations (8-12 Hz) dominate electrophysiological recordings from the human occipital lobe (Adrian & Matthews, 1934; Berger, 1929), however, their computational benefit has so far not been explicitly explored in ANNs. Here, we show how embracing dynamic activations in the hidden nodes of an ANN allows the network to process competing visual inputs. This work proposes a new framework combining principles from computational neuroscience and machine learning. We show that embedding biologically inspired neural dynamics in an ANN trained for image classification, enables the network to overcome bottleneck problems when presented with multiple stimuli.

Both CNNs and the visual system of primates have a converging architecture, wherein receptive field sizes expand progressively along the hierarchy (DiCarlo et al., 2012; Felleman & Van Essen, 1991; Gattass et al., 2005; Hubel & Wiesel, 1962; Smith et al., 2001). Neurons in the early layers of CNNs resemble simple cells in the primary visual cortex and possess small receptive fields that detect edges and contours in the visual input (Carandini, 2005; LeCun & Bengio, 1995). The receptive fields of neurons in later layers of the CNN have more expansive

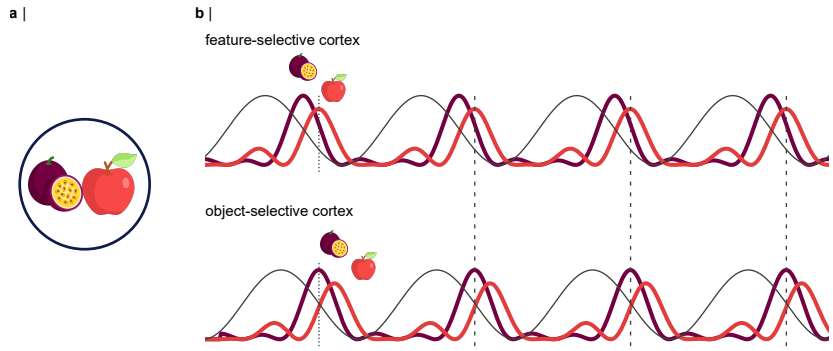

Figure 4.1: Concept: An interplay between object-based attention and neuronal alpha oscillations implements a pipelining mechanism reflected by a temporal code. **a** Example: A passionfruit and an apple are competing for the processing resources of the visual system. **b** Inhibitory alpha oscillations modulate neuronal firing rhythmically. The alpha oscillations are illustrated by the black line, the aggregate neuronal responses to the passionfruit and the apple are shown as the deep purple and red lines, respectively. As the neurons responding to the passionfruit will receive stronger excitatory inputs, they will activate at an earlier phase of the alpha cycle compared to the apple. Refraction causes a momentary inactivation of the neural representation, allowing the neurons encoding the features of the apple to activate. As the apple is processed in feature-selective cortex (e.g. V4), its representation has already been passed on to the next stage of the hierarchy, the object-selective cortex (e.g. IT).

receptive fields, akin to the inferior temporal (IT) cortex that has been shown to be critically involved in core object recognition (DiCarlo & Cox, 2007; Goodale & Milner, 1992; Milner & Goodale, 2008; Ungerleider & Haxby, 1994). This hierarchical architecture has been argued to give rise to a bottleneck problem (Broadbent, 1958): while early visual cortex has been shown to process visual features in parallel (Chen & Seidemann, 2012; White et al., 2017, 2019), object recognition has been argued have a limited capacity, which implies that the semantics of multiple visual stimuli are extracted serially (Kahneman, 1973; Popovkina et al., 2021). It has been posited that the visual and auditory systems in human and non-human primates handle simultaneously presented stimuli through "multiplexing" (Akam & Kullmann, 2014), that is, by dynamically switching between the activity patterns associated with each stimulus (Caruso et al., 2018; Li et al., 2016) (also see Panzeri et al., 2010, 2015, for review). Through this mechanism, a single neuron can contribute to the neural code of multiple stimuli (Kristan & Shaw, 1997). This dynamic interleaving of neural responses to simultaneous stimuli requires precise temporal coordination.

One mechanism through which the neural representations of multiple objects are organised

in time is phase coding, which underlies a modulation of spiking activity by ongoing low-frequency neuronal oscillations (Liebe et al., 2022; O'Keefe & Recce, 1993; Skaggs et al., 1996) [also see (Panzeri et al., 2010, 2015) for review]. For example, place representations, encoded in spatially distributed firing patterns, have been shown to be ordered along the phase of hippocampal theta (4-8 Hz) oscillations (Jensen & Lisman, 1996, 2000; Jezek et al., 2011; O'Keefe & Recce, 1993; Skaggs et al., 1996). Several conceptual and computational models have extended on these ideas, suggesting that the items in working memory could be segregated into cycles of ongoing gamma oscillations (Lisman & Buzsáki, 2008; Lisman & Idiart, 1995; Lisman & Jensen, 2013). This represents a multiplexed coding scheme (Lisman & Jensen, 2013).

It has been proposed that visual perception is supported by a similar mechanism, that underlies neuronal alpha oscillations. Alpha oscillations have long been known to reflect functional inhibition (Jensen & Mazaheri, 2010; Klimesch et al., 2007). The strength of the inhibition waxes and wanes along the alpha cycle, such that at the peak of the oscillation, strong inhibition reduces the probability of neuronal firing in the population (Haegens et al., 2011; Iemi et al., 2022). It has been proposed that only neurons receiving sufficiently strong excitatory inputs will be able to fire at the early phases of the alpha cycle (Jensen, Gips, et al., 2014; Jensen et al., 2012, 2021). As the inhibition reduces toward the trough of the cycle, the neurons may fire successively according to their excitability (Jensen, Spaak, & Zumer, 2014; Jensen et al., 2012, 2021). In this way, the interplay between inhibition by alpha oscillations and neuronal excitability generates a temporal code.

To visualise this process, imagine the following scenario at the supermarket: While searching for the ingredients for a passionfruit martini, your gaze lands on the key element: a passionfruit, placed next to an apple (Figure 4.1a). With your gaze fixating on both pieces of fruit, your visual system needs to find a way to represent and process them as coherent but separate objects. As alluded to above, it has been proposed that ongoing inhibitory alpha oscillations in visual cortex serve to organise the representations of simultaneously presented stimuli competing for processing resources.

It is well-documented that object-based attention is associated with increased neuronal excitability (Appelbaum & Norcia, 2009; Chen et al., 2003; Kastner et al., 1999; McAdams & Maunsell, 2000; Moran & Desimone, 1985; Seidemann & Newsome, 1999). Consequently, all neurons responding to the features of the passionfruit receive stronger excitatory inputs than the neurons responding to the apple and will thus overcome the alpha inhibition at an earlier phase (Figure 4.1b, top panel). Following the burst of activation associated with the passionfruit, refractory dynamics will momentarily deactivate its neural representation. In other words, excitation triggers inhibition, for instance, due to the activation of GABAergic (Anderson et al., 2000; Kopell & Ermentrout, 2004) or membrane properties such as the calcium-activated potassium current (Storm, 1990). As the alpha inhibition decreases further, the neurons attuned to the apple will take over. As Figure 4.1b illustrates, these dynamics implement a temporal code, whereby the signals corresponding to the competing items activate successively along the alpha cycle. As the passionfruit is processed earlier in the alpha cycle, it will reach the next layer of the hierarchy with a temporal advantage over the apple. As the apple is processed in feature-selective cortex, e.g. V4, the passionfruit has already reached the object-selective cortex, e.g. IT cortex. In this way, the visual system might solve bottleneck problems through pipelining: multiple stimuli are processed in parallel, while their representations are segmented in time.

In the following, we will present how a mechanism inspired by these concepts can be integrated into an ANN, to allow a successive read-out of competing inputs. We will refer to our model as a dynamical artificial neural network (dynamical ANN). This work serves as a proof of principle to demonstrate the basic principles and analyse the ensuing dynamics in the network. Our model relates to previous work investigating emergent dynamical and oscillatory properties in systems for information storage Hopfield, 1982 and Recurrent Neural Networks (RNNs) for image classification (Effenberger et al., 2022) and sequence learning (Liebe et al., 2022). In comparison to these works, we tune the dynamics of the system such that the network is able to segment the representations of competing stimuli along the phase of ongoing oscillations in the hidden units.

4.3 Methods

To implement a dynamical ANN we first trained a two-layer network on a simple image classification task. After training, we added biologically inspired dynamics to the hidden layers motivated by alpha oscillations in the human visual system. The dynamics were not included in the training process and did not change the weights of the network.

4.3.1 Network architecture

We consider a fully connected ANN with two hidden layers, consisting of 64 and 32 hidden nodes, respectively, and an output layer with three nodes (Figure 4.2a). A weight matrix of size 28×28 was applied to the input (56×56) with a stride of 28, such that each node in the first layer received $4 \times 28 \times 28$ inputs, ensuring representational invariance across the quadrants in the input. The activation h_j in each unit j of a hidden layer was calculated as:

$$h_j = \sigma\left(z_j\right) = \frac{1}{1 + e^{-a\left(z_j - b\right)}} \tag{4.1}$$

with z_j the input to each hidden unit. The input z_j arises from the activation in the previous layer according to $z_j = \sum_i w_{ji} z_i$, with w_{ji} being the weight matrix connecting nodes i and j. The slope of the sigmoid was set to $a = 2$, and the sigmoid was shifted by the bias term $b = 2.5$. These parameters were fixed, such that a small input ($z \approx 0$) would result in an activation h close to 0, while strong inputs well above 2.5, would result in an h close to 1. Consequently, the activations in the hidden layers were approximately binary ("all or none", see Figure 4.2d). The activation in each output node was calculated using the softmax function

$$o_j = \text{softmax}(z_j) = \frac{e^{z_j}}{\sum_{j=1}^{K} e^{z_j}} \tag{4.2}$$

converting the inputs z_j into K probabilities in the output layer (Goodfellow et al., 2016).

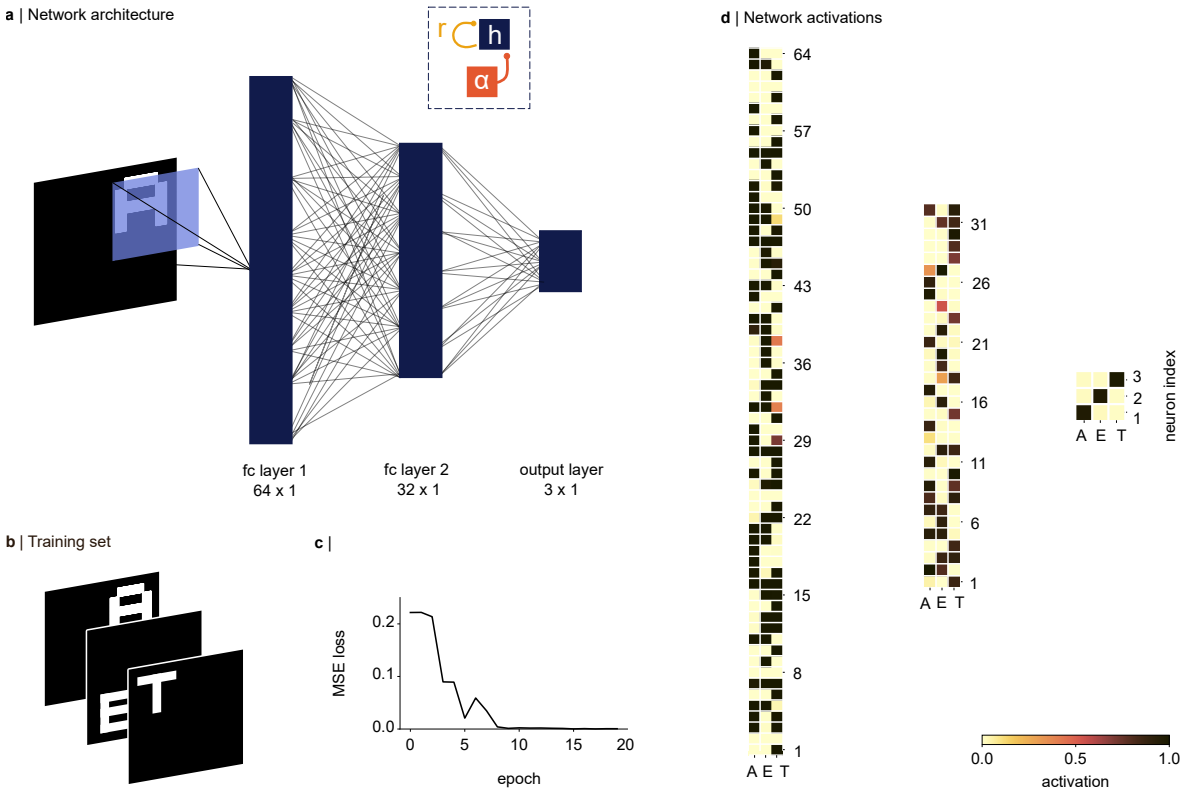

Figure 4.2: The classification problem and network architecture. **a** A network with two fully connected hidden layers was trained to classify three letters presented on a 56×56 image, in one of four quadrants (28×28). Convergence of the quadrants in the first hidden layer was implemented by sliding a 28×28 weight matrix over the image, with a stride of 28. After the training, we added a refractory term r, and pulses of inhibitory alpha oscillations $\alpha(t)$ to each hidden node h, as shown in the inset, and Equations 4.3 and 4.4. **b** Example inputs from the training set. **c** The network learned to classify the three letters within 10 epochs, as indicated by the mean-squared error (MSE) loss approaching 0. **d** Activations in the hidden layers and the output node in response to three inputs, presented in the three columns. The shifted sigmoid (see main text) resulted in approximately binary activations in the hidden layers. The activations in the output node demonstrate that the inputs are classified correctly.

The weights of the network were initialised according to a uniform distribution within the range $[-x, x]$, where $x = \sqrt{\frac{6}{n_{\text{in}}+n_{\text{out}}}}$ with n_{in} and n_{out} being the number of inputs and outputs to the current layer, respectively (Glorot initialization, Glorot & Bengio, 2010). The Adam optimiser was chosen to minimise the mean squared error loss using gradient descent (Kingma & Ba, 2017). The network weights were learned by backpropagating the error through the network layers (as mentioned above, the bias term was fixed at $b = -2.5$).

4.3.2 Network dynamics in the hidden layers

We aimed to implement multiplexing by oscillatory dynamics into a fully connected ANN. To this end, after training the network on an image classification task, we added biologically inspired non-spiking dynamics to each node in the hidden layer, expressed by non-linear ordinary differential equations (ODEs). The ODEs were solved using the Euler method with a fixed time step of $\Delta t = 0.001$ s. The rate of change in each hidden unit j was defined as:

$$\tau_h \frac{dh_j}{dt} = -h_j + \sigma\left(\frac{z_j - r_j - \alpha(t) + h_j}{s}\right) \tag{4.3}$$

where τ_h determines the timescale at which h_j approaches the sigmoid activation (see Equation 4.1). The relaxation term r_j was applied to reduce the activation of each hidden node, ensuring an intermittent activation. The dynamics of the relaxation term are given by

$$\tau_r \frac{dr_j}{dt} = -r_j + c \cdot h_j \tag{4.4}$$

with time constant τ_r defining the delay with which r approaches h. Rhythmic inhibition, mimicking inhibitory neuronal alpha oscillations in the visual system (Jensen, Gips, et al., 2014), was integrated into each h_j, implemented as a 10 Hz sine wave

$$\alpha(t) = m \cdot [1 + \sin(2\pi t \cdot 10)] \tag{4.5}$$

and subtracted from the input z_j; with amplitude m being adjustable to modulate the strength and offset of the inhibition.

The selection of the parameters was informed by electrophysiological and computational constraints. For instance, the timescale of the activation τ_h was set to 0.01 s, in accordance with the membrane time constant of excitatory neurons of 10-30 ms (Buzsáki, 2010; Harris et al., 2003; Vogels & Abbott, 2009). The time constant of the refractory term was chosen to be $\tau_r = 0.1$ s akin to afterhyperpolarization effects caused by calcium-activated potassium

currents (Sah & Louise Faber, 2002; Wong et al., 1979). The effect of parameters c and s on the dynamics will be explored below (see Figure 4.3).

4.3.3 Fixed points of the system

The fixed points (steady-state) of h and r are defined by setting Equations 4.3 and 4.4 to zero. Solving for h and r yields:

$$h^* = \frac{z}{c-1} + \frac{s}{c-1}\left[\frac{\log\left(\frac{1}{h^*}-1\right)}{a} - b\right] \tag{4.6}$$

$$r^* = c \cdot h^* \tag{4.7}$$

We found the fixed points numerically, using the function `fsolve` implemented in SciPy (Virtanen et al., 2020). For small values of $s \ll 1$, the equilibrium points could be approximated as $h^* = \frac{z}{c-1}$ and $r^* = \frac{c \cdot z}{c-1}$. Unless otherwise specified, the dynamics of all hidden nodes in the full network were initialised at these approximated fixed points with $z = 4$ (the average input size to the first layer).

4.4 Results

The aim of this project was to show that biologically inspired dynamics will allow a neural network to handle competing inputs, despite having been trained on one stimulus at a time. To illustrate these dynamics, we trained the network to classify three letters "A", "E", and "T" (Figure 4.2a,b). The network learned to read out the images correctly within 10 training epochs (Figure 4.2c), with the softmax activation in the output layer approaching an activation of 1 in the node of the corresponding image (Figure 4.2d). Post-training, we integrated the full dynamical system described in Equation 4.3 and Equation 4.4, into the hidden layers. We will first investigate the behaviour of the individual hidden nodes.

4.4.1 Network stability and parameters

Figure 4.3a demonstrates how the interplay between the input $z = 6.5$ and refraction by r (orange trace) resulted in dynamical activations in h (purple trace) with a period of approximately 100 ms. As h increases, r increases with a delay. As r opposes h, this results in refraction. The adjustable parameters c and s in Equation 4.3 and Equation 4.4 were explored to identify values resulting in robust self-sustained dynamics at a frequency of about 10 Hz in the hidden nodes. Figure 4.3b shows how the frequency of h changes as a function of c, for $s = 0.05$, for different levels of z (ranging from 0.5 to 6.5 as indicated by the yellow to dark brown colour scale). The parameter c influences how strongly r grows depending on h (see Equation 4.4). Consequently, the frequency of h increases monotonically for increasing values of c. For large values of z, the frequency changes approximately exponentially with c. To induce oscillations in the 10-12 Hz range for a broad range of inputs z, we selected $c = 10$ (indicated by the dotted box). Figure 4.3c demonstrates how the frequency changes as a function of input size z for $c = 10$, showing that the nodes tend to oscillate at faster rhythms for larger inputs. There is a slight tendency for the frequency to plateau for very large values of z. This is due to r having to oppose a strong input while growing as a function of activation h, which is bounded at 1 (Equation 4.1). As a result, the frequency does not increase further and eventually decreases for large values of z.

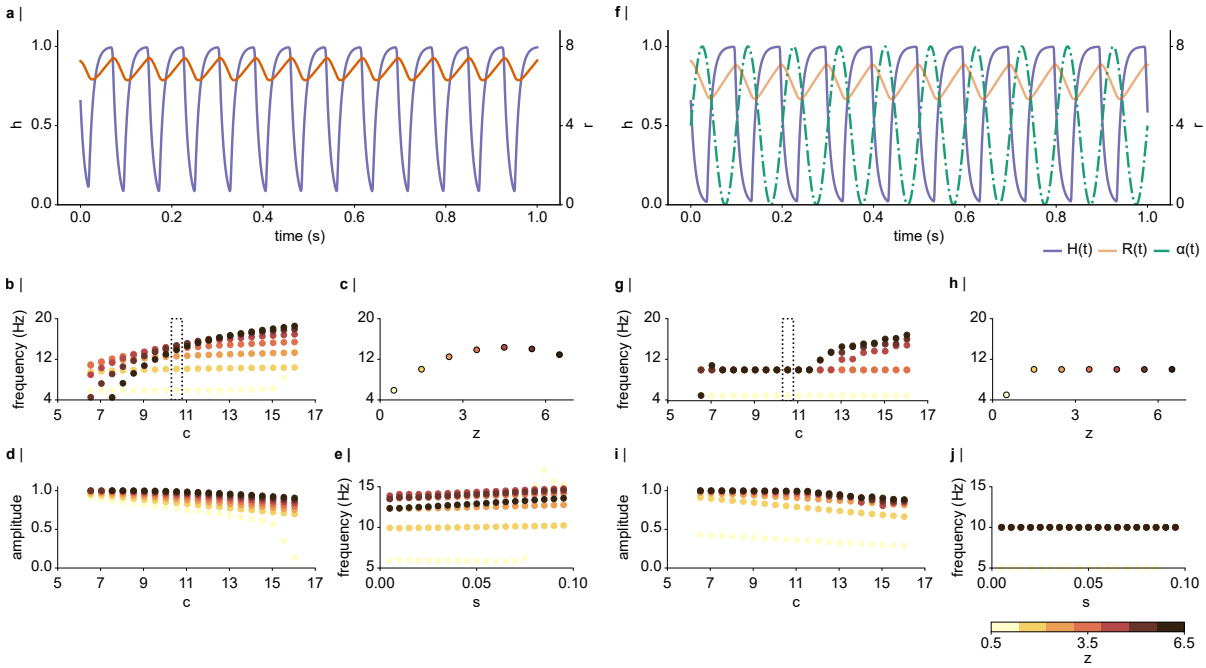

Figure 4.3: **a** Exemplary dynamics in h for one input $z = 6.5$, with $c = 10$ and $s = 0.05$. The interplay between h (purple trace) and r (orange trace) leads to dynamics with a period of approximately 100 ms. **b** Frequency as a function of c for different input values z (colour coded from 0.5 o 6.5). High values of z require larger values of c to generate oscillatory dynamics in h. **c** A value of $c = 10$ (indicated by the dotted box in **b**) leads to dynamics in the 8-12 Hz range for $z > 0.5$, whereby the frequency of the dynamics increases approximately monotonically with input size z. **d** Amplitude of h as a function of c, showing that for high values of c, h will not reach an activation of 1. Values of $c < 11$ seem appropriate to induce dynamics in the 10-12 Hz range that reach the sigmoid activation of 1. **e** Frequency of h as a function of s, indicating that the dynamics only change marginally for all values of s within a range of 0.005 to 0.1. Only for very small inputs ($z = 0.5$), a large s leads to fast dynamics of up to 15 Hz. **f** The dynamics of h and r shown in **a** are entrained by the 10 Hz alpha inhibition (dotted green line). **g-j** The alpha inhibition stabilises the dynamics in the 10 Hz range. **g** For large values of $c > 11$, the dynamics are able to escape the periodic inhibition and oscillate at a faster frequency. For small values of $z = 0.5$, the dynamics in h skip one alpha cycle, and oscillate at 5 Hz. **h** frequency as a function of z, for $c = 10$, showing that all nodes with inputs $z > 0.5$ are entrained by the 10 Hz rhythm. **i** The amplitude of h as a function of c in the presence of the alpha inhibition. The amplitude tends to be slightly larger than the sigmoid activation for small values of z. **j** In presence of alpha inhibition, h is robustly entrained to the 10 Hz rhythm, for all values of s.

Figure 4.3d demonstrates that the amplitude of h decreases as a function of c. We aimed to induce dynamics such that h would oscillate between 0 and the sigmoid activation of the current input, which for large values of z is close to 1. This amplitude was achieved for the selected $c = 10$. Note that for $z < 4.5$ the amplitude of h was slightly larger than the sigmoid activation of z. For instance, for $z = 1.5$ the activation is $h = \sigma(-2 \cdot (1.5 - 2.5)) \approx 0.12$, however, the

amplitude reached values of about 0.8 (see Figure 4.3d). We did not find this to cause problems when integrating the dynamics into the network, as most activations in the hidden layers were outside the linear part of the sigmoid, and thus approached an activation of 1 (Figure 4.2c, layer 1; see below for details).

Another instrumental parameter in Equation 4.3 is s, which serves to scale the various input parameters. A small s will effectively increase the steepness of the sigmoid, resulting in a more step-like response. Figure 4.3e depicts the frequency of the node as a function of s and suggests that values ranging from 0.005 to 0.1 result in dynamics of about 10 Hz for a range of inputs z. Based on these observations, we selected $s = 0.05$.

We next explored the effects of adding pulsed inhibition at 10 Hz to the hidden dynamics (α(t) in Equation 4.3). As depicted in Figure 4.3f, the alpha inhibition (green dashed line) entrained the dynamics, such that h activated in anti-phase to the 10 Hz rhythm. Another effect of the alpha inhibition is that r oscillates between lower values than before. This is sensible, as the alpha inhibition and refraction r work together to reduce the activations in h. Figure 4.3g depicts the frequency of h as a function of c, showing that in the presence of the alpha inhibition, all hidden nodes oscillate at a frequency of 10 Hz, when $5 < c \leq 11$, for the current input range of $0.5 < Z \leq 6.5$. For large values of c ($c > 11$) the dynamics escape the alpha rhythm when z is sufficiently large (> 5) and oscillate at a faster rate. For small inputs ($z = 0.5$), h appears to skip one alpha cycle at a time and follows a 5 Hz rhythm. The frequency in h as a function of input size z is shown in the right panel, confirming the 10 Hz entrainment. Figure 4.3i shows the amplitude of h as a function of c, demonstrating that the amplitude is most stable for $c < 11$. Notably, the amplitude of h again reaches values above the sigmoid activation of z (as described above), however, we did not find this to interfere with the dynamics in the full network. Lastly, the exact value of s within the 0.005 to 0.1 range did not change the frequency, for all $z > 0.5$ (Figure 4.3j).

We conclude that the entrainment and refractory dynamics of the nodes were stable for a large range of the parameters. Based on the presented simulations, we settled on the parameters $\tau_h = 0.01$, $\tau_y = 0.1$, $c = 10$, $s = 0.05$ in all following simulations, as these produced robust

dynamics at approximately 10 Hz and an activation h close to 1 for a wide range of inputs.

4.4.2 Alpha oscillations stabilise dynamics in a two-layer Neural Network

After training the network on the "A-E-T" classification problem and exploring the behaviour of the individual nodes shown in Figure 4.3, we simulated the dynamics in the full network while keeping the weights connecting the layers fixed.

Figure 4.4a and b show the dynamics in the output and hidden layers of the network, in response to a single input letter, A, with $\tau_h = 0.01$, $\tau_r = 0.1$, $c = 10$, $s = 0.05$, but without any drive from the alpha oscillation ($m = 0$, Equation 4.5). The output node corresponding to A (blue trace) oscillates at approximately 12 Hz (Figure 4.4a). The leftmost panel in Figure 4.4b depicts the activations in h in layer 1 as a function of time, for z's ranging from 0.5 to 6.5 (only unique values of z are shown). The dynamics demonstrate that the phase of the oscillations depends on the size of input z, leading to inconsistent phase delays between the network nodes. Due to the softmax activation introducing lateral inhibition in the output nodes, these phase delays cause a spurious intermittent activation of the output node corresponding to letters "E" and "T" (orange and green traces). The right panel in Figure 4.4b, depicting h as a function of r, shows the limit cycle and fixed points (indicated by the diamond-shaped scatters) for each input z. All units demonstrate a limit cycle behaviour but with different amplitudes.

The bottom panel shows the dynamics in the second layer. While the phase-locking between the hidden nodes in the second layer is slightly stronger compared to layer 1, activations in the nodes receiving smaller inputs appear to lag the nodes receiving larger inputs. The right-most plot, showing the relationship between h and r, again suggests a limit cycle behaviour, although the amplitude of each node appears to vary over the course of the simulation. This is likely due to the second layer receiving dynamical, non-phase-locked inputs from the first layer.

Introducing oscillatory entrainment by periodic inhibition into each layer of the network stabilises the dynamics in the entire network. Figure 4.4c shows the dynamics in the ouput layer, with the amplitude of the oscillatory drive set to $m = 0.5$, and a phase delay of $\Delta\phi = 0$ between the layers. Comparison to the dynamics without the oscillatory drive shows that the inhibition

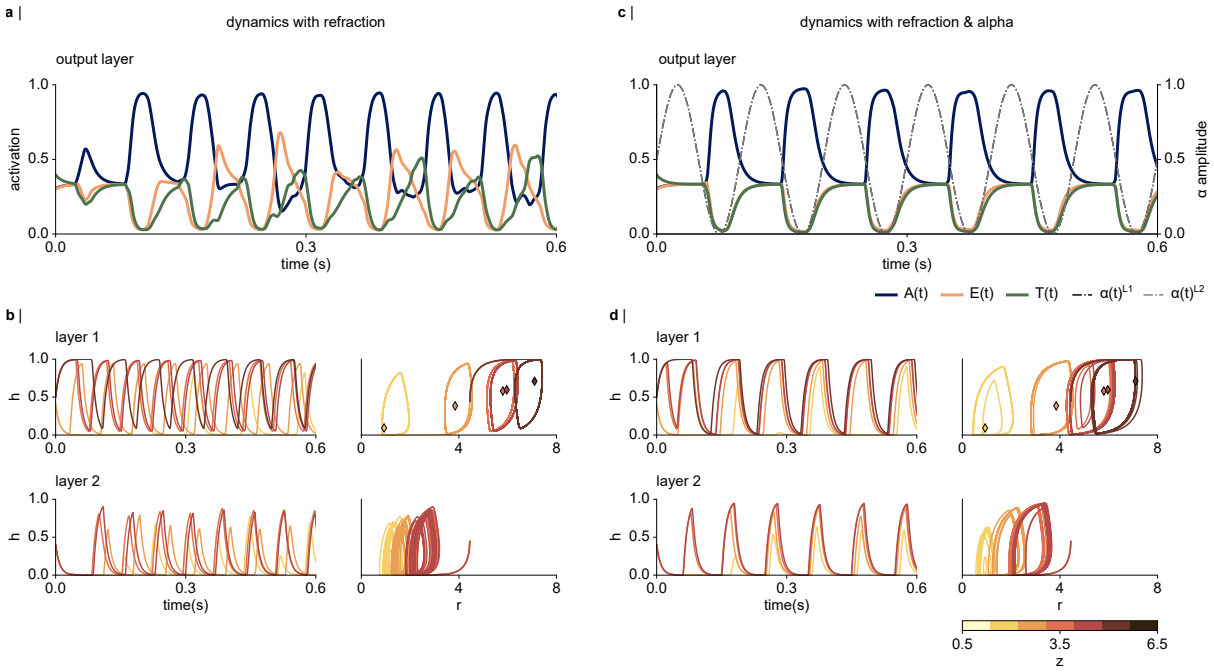

Figure 4.4: **a-b** Dynamics underlying the interplay between h and refraction r (Equation 4.3 and 4.4, without the alpha inhibition. **a** The output node corresponding to the letter A oscillates at about 12 Hz. The system spuriously activates the output node E and T. **b** (top left) The activations in the first hidden layer show that the frequency of the oscillation depends on the input size z, as suggested in Figure 3c. (top right) Trajectory of h as a function of r, with the fixed points indicated by the coloured diamonds. The dynamics are attracted towards a stable limit cycle, depending on the magnitudes of the input, and orbits around the fixed point. (bottom left) Activation of h in layer 2 as a function of time. There is a notable phase lag between the network nodes based on the input size z. (bottom right) The amplitude of the activation in each node appears to vary over time. **c-d** Periodic inhibition stabilises the dynamics in the system. **c** Periodic inhibition at 10 Hz with an amplitude of $m = 0.5$ was added to each layer. The read-out of the presented letter oscillates in anti-phase to the alpha inhibition. **d** Alpha oscillations notably stabilise the dynamics within and between the network layers, as indicated by the phase-locking between the nodes, and the stabilised H-R trajectories for the activations in layer 2.

removes the spurious activation in the output nodes corresponding to “E” and “T” (orange and green trace). This stabilisation of the read-out underlies increased synchrony both within and between the hidden layers, as indicated in Figure 4.4d. In particular, the phase-locking between the activations in the first layer has been notably increased by the oscillatory drive; as shown in the time course of the activations in h shown in Figure 4.4d, top left. Comparison of the limit cycles shown in Figure 4.4b top right, and Figure 4.4d top right, demonstrates a wider limit cycle in presence of the alpha oscillations, reflecting an increased amplitude of the

dynamics in h.

The dynamics in the second layer also show higher synchrony and stabilised trajectories h and r in presence of the alpha oscillations (Figure 4.4d, bottom right). This is explained by the more synchronous inputs from the first layer, and the alpha oscillations applied to the second layer. Comparison of the plots at the bottom right in Figure 4.4b and d reveals that the amplitude of the activation in the second layer varies less in presence of the alpha inhibition. These simulations show that the dynamics of the multi-layer network are dramatically stabilised by the oscillatory alpha inhibition.

4.4.3 Simultaneous presentation of two inputs produces a temporal code

The bottleneck problem in absence of the dynamics

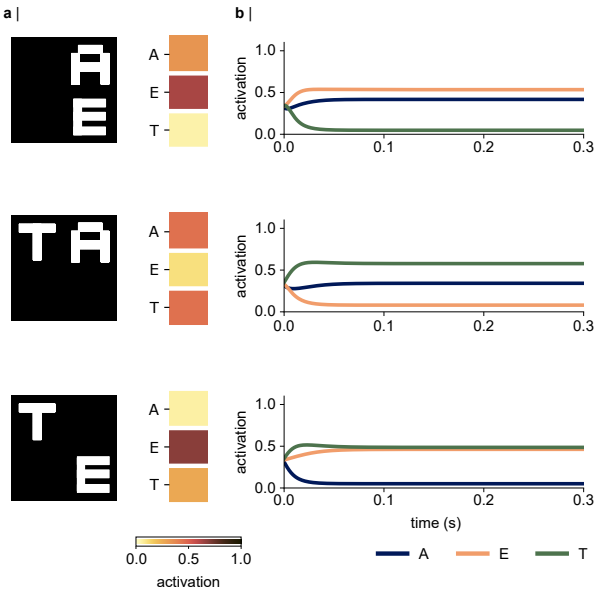

Figure 4.5: The bottleneck problem when the network receives two inputs simultaneously. **a** (left column) Exemplary input combinations of the two letters. (right) Activations in the output layer are distributed approximately evenly over the respective nodes. **b** Time course of the activation in the output layer, for $s = 1$, $r = 0$, and $\alpha(t) = 0$. The shared output is a consequence of the two items competing.

The network correctly classified individually presented stimuli after the training, as demonstrated in Figure 4.2c. However, when presented with two stimuli simultaneously (Figure 4.5a), the network produced a mixed output. The right panel in 4.5a shows the network activations in response to all possible inputs of stimuli. Figure 4.6b shows the corresponding time course to these simultaneous inputs, which was achieved using Equation 4.3, with $s = 1$, $r = 0$, $\alpha(t) = 0$, with the network dynamics initialised at $h = r = 0$ in all hidden nodes. The network distributes the activations in the output layer over the nodes corresponding to the respective inputs. This suggests that the output layer produces a weighted average

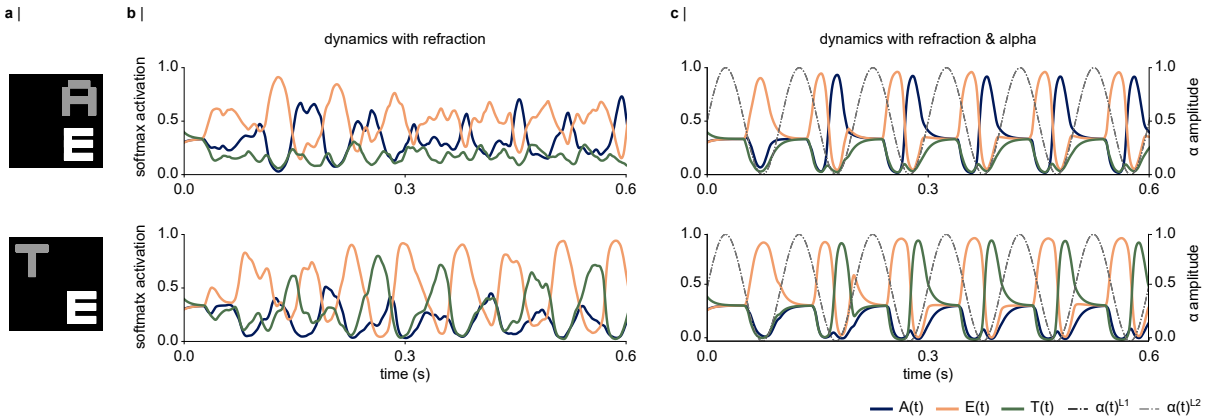

Figure 4.6: The dynamical artificial neural network (dynamical ANN) multiplexes simultaneously presented stimuli. **a** Examples of the simultaneous inputs. Attention towards the letter E was mimicked by increasing the input of all pixels belonging to E while reducing the inputs of the letters A and T. **b** The interplay between the excitation and refraction results in dynamic activations in the output layer, whereby one of the two letters is read-out at a time. However, the dynamics show notable instability, and the node corresponding to the "attended" input E activates over longer periods of time. **c** Introducing pulses of inhibition (alpha oscillations) into the network generates a temporal code in the output layer. The system first activates the node corresponding to the attended letter E. Following that, the letters are read out as a code, ordered along the phase of the alpha oscillation according to the input gain.

of the activations to both stimuli. This indicates a bottleneck problem when the network needs to classify two stimuli. In contrast, the abilities of our visual systems to recognise a stimulus do not decrease with the number of objects. As such, the visual system must be able to segment the representations of the different stimuli. As outlined above, it has been proposed that multiplexing in the visual system may underly oscillatory dynamics. In the following, we will explore how the complete dynamical network presented in Figure 4.4 and described by Equations 4.3 and 4.4 responds to simultaneous stimuli.

Refraction and alpha inhibition allow read-out of competing stimuli as a temporal code

Figure 4.6b shows how the output layer of the dynamical network responds to two simultaneous inputs ("A" and "E", and "T" and "E). To mimic spatial attention to letter E, we multiplied the pixels defining the letter E with 1.2, and the pixels defining the letters A and T with 0.8 (Figure 4.6a). Figure 4.6b shows the dynamics in the output layer, based on the simulations with parameters $\tau_h = 0.01$, $\tau_r = 0.1$, $c = 10$, $S = 0.05$, without any oscillatory drive. The

node corresponding to "E" activates first and dominates the dynamics in the first 150ms (orange trace). Subsequently, the network starts to alternate between the two inputs, whereby the nodes corresponding to the presented letters reach activation levels between 0.9 and 1. As such, the interplay between activation and refraction implements a multiplexing mechanism. However, the dynamics of the multiplexed representations are unstable. For instance, in Figure 4.6b, top panel, the node corresponding to the letter E (orange trace) activates over longer periods of time and reaches higher activations than the node representing A (blue).

Introducing the oscillatory alpha inhibition results in stabilised dynamics, whereby the simultaneous inputs are read out as a temporal code, organised along the alpha phase (Figure 4.6c). Notably, the attended stimulus "E" activates first, within the first alpha cycle. In the second cycle, the system starts to generate the phase code, which further stabilises with time. We replicated these dynamics for all combinations of simultaneous inputs (two letters at a time), as shown in Figure B.1.

A more detailed investigation of the multiplexing dynamics in the different layers is shown in Figure 4.7; for the exemplary simultaneous input E and T (as presented in Figure 4.6a, bottom panel). The top panels in Figure 4.7a and b indicate how strongly the hidden representations to the combined input correspond to the activations to the individually presented inputs. For instance, for letter "E" (orange trace) this measure of similarity was calculated as:

$$s_E(t) = \frac{\sum_{j=1}^{K} \left(h_j^{ET}(t) \odot h_j^E \right)}{\sum_{j=1}^{K} \left(h_j^E \odot h_j^E \right)} \tag{4.8}$$

with h_j^{ET} being the activation in hidden node j at time point t, to the simultaneously presented letters T and E, h_j^E being the activation in hidden node j to the letter E in the trained, non-dynamical network (see Figure 4.2c), and $\odot$ being the Hadamard operator (element-wise multiplication). This measure can be interpreted as a normalised dot product.

The time course of the normalized dot product indicates that the similarity between the activations in the first layer, and the representations to both letters E and T oscillates in anti-phase to the alpha inhibition (Figure 4.7a). Notably, the similarities to both letters follow the

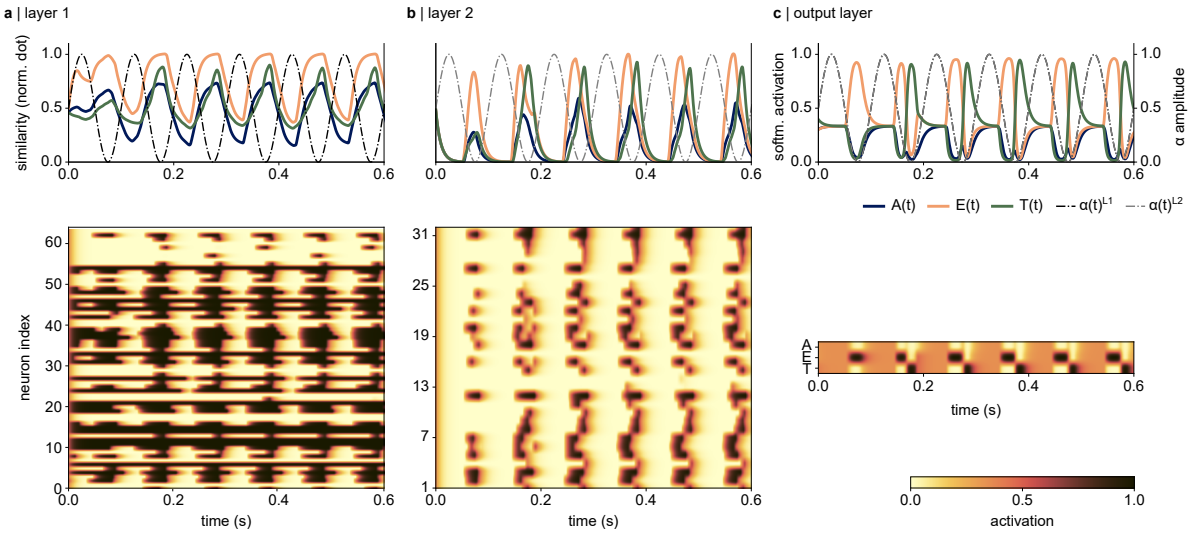

Figure 4.7: The representations of the competing inputs are segmented in the second layer of the dynamical Neural Network in response to an input image containing the letters E and T, as shown in Figure 5a, bottom. **a** (top) Layer 1: The nodes corresponding to both the letter E and the letter T activate in anti-phase to the alpha inhibition, with no segregation in time. Notably, the network activates the representations to the attended letter E more strongly, and over longer periods of time. (bottom) The network activations over time suggest that a large portion of the hidden nodes activates in anti-phase to the alpha inhibition. **b** Segregation of the simultaneous stimuli can be observed in the second hidden layer. (top) The normalised dot product suggests that the nodes corresponding to each input activate at different phases relative to the alpha inhibition. (bottom) The temporal segmentation observed in the top panel can also be observed as a successive activation of the nodes in the network. The alpha inhibition silences the activation in the entire layer. **c** The softmax activation and the output layer reflects a temporal code, whereby the inputs are read out along the phase of the alpha inhibition, ordered according to the magnitude of the input.

same time course,

indicating that the first layer does not segment the competing inputs. Moreover, the activations to the attended letter extend over the entire half-cycle, while the activations of the unattended letter are more short-lived. The bottom panel shows a raster plot of the magnitude of the activation in each neuron over time. The simultaneous presentation of two letters activates a large fraction of the hidden nodes in the first layer (Figure 4.7a, bottom). Note the rhythmic silencing of the network activations by the alpha inhibition, that affects most, but not all nodes. This implies that the first layer activates to both stimuli in parallel.

In comparison, the activations in the second layer demonstrate that the nodes responding to each letter are activated in succession: the normalised dot product between the current

representations and the activations to an individual letter “E” (orange trace) precede the ones corresponding to letter T (green trace, Figure 4.7b). The bottom panel in Figure 4.7b indicates that a smaller fraction of the network is activated at each time point, and the successive activation of the hidden nodes can be observed. Finally, Figure 4.7c shows the read-out in the output layer, confirming that the representations of E and T are fully separated after the second cycle of the alpha inhibition (also see Figure 4.6c).

In sum, our simulations show how integrating dynamics driven by excitation and refraction enables a fully connected neural network to multiplex simultaneous inputs – a task it has not been trained on explicitly. This mechanism is further stabilised by pulses of inhibition, akin to alpha oscillations in the human visual system.

4.4.4 Making and breaking the temporal code: the effect of phase delay between the layers

Previous research on neural codes in the visual and auditory system has suggested that the phase of low-frequency oscillations in electrophysiological recordings carries information about the sensory input (Kayser, 2009; Lopour et al., 2013; Montemurro et al., 2008). The *Communication Through Coherence* theory predicts that the phase relationship between two populations is critical for their communication (Fries, 2005, 2015) (also see (Akam & Kullmann, 2012; McLelland & VanRullen, 2016) for computational implementations). While *Communication Through Coherence* was initially proposed for oscillations in the gamma-band (Fries, 2005, 2015), related ideas have been explored for the alpha-band (Bonnefond et al., 2017). Based on these concepts, we next tested how different phase delays between the network layers impact the temporal code. Figure 4.8 shows the temporal codes for different phase delays between the alpha oscillations. Visual inspection suggests that the most robust temporal code of the two competing letters is achieved when the oscillations are synchronous in the two layers (top left), or when the second layer lags or precedes the first layer by 10 ms (top, second from left and bottom right). Notably, the temporal code breaks for larger phase delays between the layers. One might have expected an anti-phase delay between layers 1 and 2 to cut off all communication, however, the network

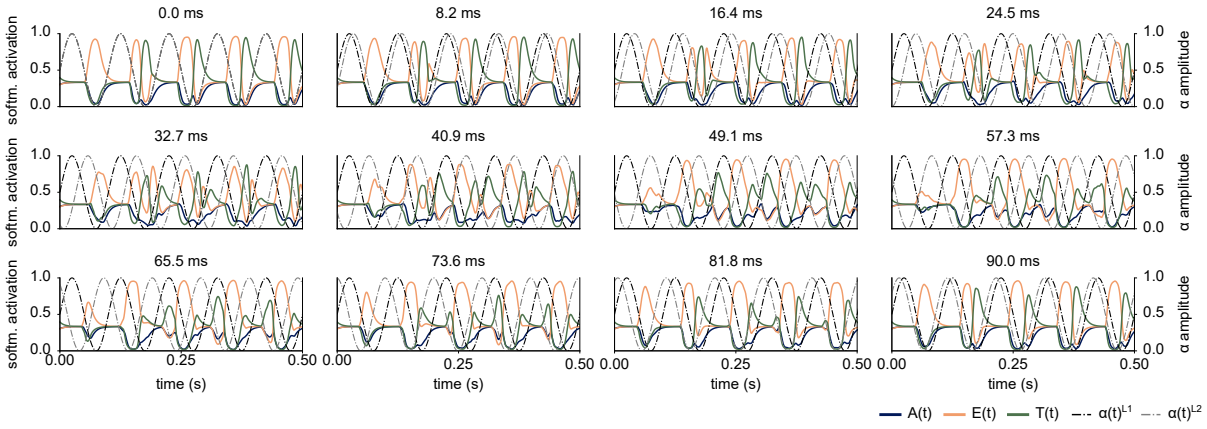

Figure 4.8: The temporal code as a function of phase delay between the layers, indicated in the title (in ms). The cleanest read-out of the two competing stimuli as a temporal code is achieved by a phase lag of zero (top left) and if the second layer precedes or lags the first layer by 10 ms.

is still able to identify at least one of the presented stimuli, albeit with high instability.

In sum, these simulations show that the shape of the temporal code, and the number of items that can be read-out, strongly varies based on the phase delay between the layers and is most robust for synchronous oscillations in both layers.

4.5 Discussion

We here demonstrate how integrating semi-realistic neuronal dynamics into an ANN enables multiplexing during image classification. The network was first trained to classify individual letters presented in quadrants. Post-training, the network correctly recognised the individual inputs. When presented with two letters simultaneously, however, the output layer produced a mixed representation of both stimuli due to the bottleneck in the network. Adding refractory dynamics to the nodes of the network resulted in alternating activations to the simultaneously presented inputs, suggesting that the network was able to segregate the representations. However, the dynamics expressed notable instability and asynchrony within and between layers. Adding oscillatory inhibition to the layers, akin to alpha oscillations in the visual system, stabilised the dynamics in the hidden layers. When two inputs were presented simultaneously, the interplay between activation, refraction, and pulses of inhibition resulted in a stable multiplexed code, whereby the output nodes were activated sequentially based on the strength of the input.

Our simulations provide an implementation of the idea that inhibitory alpha oscillations in visual cortex serve to support the processing of simultaneously presented stimuli, by segmenting them into a temporal code (Jensen, Gips, et al., 2014; Jensen et al., 2021). As the inhibition is strongest at the peak of the oscillations, only neurons receiving sufficiently strong excitatory inputs will be able to activate (Haegens et al., 2011; Iemi et al., 2022; Jensen et al., 2012). In turn, the neural representations associated with the attended stimulus will overcome the inhibition at an earlier phase of the alpha cycle than the unattended object. This allows temporal segmentation and thus multiplexing of simultaneously presented stimuli (Jensen, Spaak, & Zumer, 2014).

While it has been shown that simple visual features can largely be processed in parallel (Chen & Seidemann, 2012; White et al., 2017, 2019), object recognition has been demonstrated to be supported by serial processes (Kahneman et al., 1992; Popovkina et al., 2021). This indicates a bottleneck problem which has been argued to arise from the converging hierarchical structure of the visual system (Broadbent, 1958; Jensen et al., 2021; Popovkina et al., 2021; White et al., 2019). By segmenting individual object representations in time, alpha oscillations

have been suggested to allow the attended stimulus to pass through the network layers with a temporal advantage over the unattended stimulus (Figure 4.1, also see (Jensen et al., 2021)). These parallel and serial properties resulting from multiplexing can be observed in our network simulation as well. In the first layer, the stimuli are represented in parallel, while the second layer begins to segment them along the phase of the oscillation (Figure 4.7). These simulations show how integrating biologically inspired dynamics into a neural network results in a system that can multiplex simultaneous stimuli while embracing the parallel and serial properties of visual object recognition.

Evidence for a phase-coding mechanism similar to the one presented here has been robustly observed in recordings from the rodent and human hippocampus, whereby spiking activity has been shown to be modulated along the phase of ongoing theta oscillations (4-8 Hz (Jezek et al., 2011; Kamiński et al., 2020; O'Keefe & Recce, 1993; Rutishauser et al., 2010; Skaggs et al., 1996)). The order in which a sequence of inputs has been experienced, has further been proposed to be preserved in the spiking activity (Jezek et al., 2011; O'Keefe & Recce, 1993) but see (Liebe et al., 2022).

Intracranial recordings from the visual cortex in non-human primates have revealed that the phase of spontaneous alpha oscillations modulates spiking activity (Bollimunta et al., 2008, 2011; Dougherty et al., 2017; Haegens et al., 2011) and neuronal gamma oscillations (Bastos, Vezoli, & Fries, 2015; Bosman et al., 2012; Michalareas et al., 2016; Spaak et al., 2012). In this context, alpha oscillations have been argued to organize visual processing in a top-down manner (van Kerkoerle et al., 2014). Intracranial and MEG recordings from the human brain have replicated the observed phase-amplitude coupling between gamma and alpha oscillations during visual processing (Osipova et al., 2008; Voytek et al., 2010). Recent human EEG recordings have additionally posited that alpha waves travelling from occipital to frontal areas are actively involved in visual processing (Alamia & VanRullen, 2023; Alamia et al., 2023) (but see Zhigalov and Jensen, 2023 for a critical perspective). Similarly, ECoG recordings from marmoset visual cortex have revealed travelling waves in the dorsal and ventral stream that were linked to visual performance (Davis et al., 2020) and a modulation of neural processing

along the visual hierarchy following saccade initiation (Kaneko et al., 2022). These reports show that alpha oscillations may propagate over cortical areas involved in visual processing to coordinate neural activity. It has so far not been determined, however, if this modulation results in successive activations of the neural representations in line with our model simulations.

Our simulations result in two testable predictions. First, we propose that neural representations activate along the phase of spontaneous alpha oscillations, ordered according to attention or salience (Jensen, Gips, et al., 2014; Jensen et al., 2012). This prediction can be tested using electrophysiological recordings during visual tasks with more than one stimulus. The neural representations of each stimulus could be extracted from these data using decoding methods such as multivariate pattern analysis (Haxby et al., 2014) or linear discriminant analysis (Guggenmos et al., 2018). For instance, using MEG, van Es et al. (van Es et al., 2022) have recently investigated the effect of ongoing alpha oscillations on the decoding accuracy of visual stimuli in a spatial attention task. The authors have demonstrated that the phase of alpha oscillations in the frontal eye field and parietal cortex of the human brain modulated the performance of the decoder. However, a phase delay between the attended and unattended stimuli has not explicitly been reported. Alternatively, these predictions could be tested based on intracranial recordings from the mouse brain. Using Neuropixels probes, spiking activity and local field potentials can be simultaneously recorded intracranially from several cortical areas in mice (and non-human primates, (International Brain Laboratory et al., 2023; Steinmetz et al., 2021). It is well-established that the mouse visual system exhibits a hierarchical structure similar to the one observed in primates (de Vries et al., 2020; Siegle et al., 2021). As such, these data could be used to test whether spiking activity is segmented along the phase of ongoing alpha oscillations, for instance, to distinguish a figure from a background (Kirchberger et al., 2021).

The second prediction of our model is that a stable temporal code emerges from approximately synchronous oscillations in the consecutive network layers. Recent work using concurrent iEEG and MEG recordings has suggested that interactions between alpha oscillations in prefrontal cortex and mediodorsal thalamus mediate visual performance (Griffiths et al., 2022). In light of the literature on travelling alpha waves (Alamia & VanRullen, 2019, 2023; Alamia et al.,

2023; Bahramisharif et al., 2013; Davis et al., 2020; Kaneko et al., 2022; Zhang et al., 2018) this begs the question of whether neuronal processing along the visual hierarchy is controlled by one driving force as suggested by our simulations, e.g. the thalamus or prefrontal cortex, or a travelling wave propagating forward or backwards along the visual hierarchy. With recent advances in brain-wide recordings in mice using Neuropixels probes (International Brain Laboratory et al., 2023), it may be possible to investigate whether the driving force of these travelling waves can be established.

Our network relates to previous computational models that have explored the role of biologically plausible dynamics for multiplexing and inter-areal communication (Akam & Kullmann, 2014; Jensen, 2001; Lisman & Idiart, 1995; McLelland & VanRullen, 2016; VanRullen & Thorpe, 2001). We expand on this work by demonstrating how multiplexing and communication through synchronous oscillatory activity can enhance the computational versatility of neural network in the context of multi-item image classification. As we aimed to provide a proof-of-principle, we trained the network on a comparably simple classification problem involving a small training set. The non-monotonic loss function in Figure 4.2b implies that the network might have learned to solve the problem by memorizing the inputs and could thus show low generalisability to new inputs (Chollet, 2021). Our aim is to expand the presented principles to CNNs with a deeper architecture that can solve benchmark image classification problems such as (E)MNIST (Cohen et al., 2017; LeCun et al., 1998), CIFAR-10 (Krizhevsky, 2009), and ImageNet (Wu et al., 2015). One technical detail to consider is that modern DNNs typically implement non-linearities using the rectified linear unit (ReLU) function which reduces the vanishing gradient problem in deep architectures and speeds up learning (Chollet, 2021; Goodfellow et al., 2016). Since ReLUs are not bind the activations between 0 and 1, a different set of ODEs will be needed to describe the dynamics in future versions of this model.

Alternatively, the dynamics could be integrated in additional layers with sigmoid-like activation functions, between the trained network layers, as conventionally done in spiking neural networks (Sörensen et al., 2022; Zambrano et al., 2019). For instance, Sörensen et al. (2022) integrated spiking dynamics into a pre-trained CNN, which allowed the network to find a target

stimulus in a complex natural image, an ability the model did not exhibit without the spiking dynamics. As alpha oscillations have been shown to modulate spiking activity (Bollimunta et al., 2008, 2011; Haegens et al., 2011), it would be interesting to understand to what extent oscillatory dynamics could serve to modulate activations in spiking neural networks. By incorporating spiking or non-spiking dynamics into extra layers with activations constrained between 0 and 1, the concepts presented here could be explored in pre-existing deep neural networks. In sum, future versions of this network will expand to deeper architectures and modern image classification benchmarks.

The rate of change in the network nodes was defined by a set of ODEs, following conventional practice in computational neuroscience (Miller, 2018). ODEs have also found applications in the development of RNNs. For instance, in the form of neural ODEs (Chen et al., 2018), liquid-time constant neural networks (Hasani et al., 2020, 2022), and RNNs consisting of damped oscillators (Effenberger et al., 2022). These networks had great success in learning long-range dependencies in time series data (Chen et al., 2018; Hasani et al., 2020, 2022), sequences of images (Liebe et al., 2022), and image classification when the pixels of the input are transformed into a time series (sequential MNIST) (Effenberger et al., 2022; Hasani et al., 2022). The goal of our work, in comparison, was to convert spatially presented inputs into a time series. The dynamics in our model therefore do not provide information about the dependencies between inputs but rather serve to segment them in time. However, integrating biologically plausible dynamics into the training process would undoubtedly be interesting. Oscillatory activity in the theta, alpha, and gamma-band has been repeatedly shown to support learning and memory (for review see Fell & Axmacher, 2011; Hanslmayr et al., 2016). In line with this, Effenberger et al. (2022) have shown that an RNN whose nodes reflect damped oscillators outperform the performance of non-oscillatory RNNs when classifying the sequential MNIST data set. For future extensions of the presented algorithm, it would be interesting to explore if and how biologically plausible dynamics could be used to support the training process.

4.6 Conclusion

We here present a proof-of-concept showing that integrating oscillatory dynamics based on excitation, refraction, and pulses of inhibition into the hidden nodes of an ANN enables multiplexing of competing stimuli, even though the network was only trained to classify individual inputs. Our simulations predict that the visual system of humans and non-human primates handles the processing of multiple stimuli by organising their neural representations along the phase of inhibitory alpha oscillations. These predictions can be experimentally tested using simple attention paradigms and electrophysiological recordings in humans, non-human primates, and rodents. Future versions of the network will include extensions to deeper architectures and modern image classification benchmarks.

5

Discussion

Tasks such as searching for a friend in a crowd or distinguishing a passionfruit from apples at the supermarket are integral to our daily lives. The sophisticated mechanisms underpinning our visual perception enable us to effortlessly move our attention (and gaze) through the environment. Throughout this thesis, my objective has been to understand the properties of oscillatory dynamics in the visual cortex, and how they support visual perception and attention.

In chapter 2, I have demonstrated that neuronal responses to a rhythmic high-frequency flicker and endogenous gamma oscillations represent different phenomena, emerging from at least partially distinct cortical regions. In chapter 3, I have employed the high-frequency flicker again for Rapid Invisible Frequency Tagging (RIFT) to investigate the neural correlates of guided and unguided search. Consistent with recent work, I have confirmed that RIFT responses are an effective read-out of neuronal excitability in early visual regions (Ferrante et al., 2023; Gutteling et al., 2022; Minarik et al., 2023; Pan et al., 2020; Zhigalov et al., 2019). Furthermore, for the first time, I have tested this in the context of feature-based attention. Crucially, I found that

alpha oscillations in early visual regions support the search through a mechanism that we have termed *blanket inhibition*, which dampens the excitability of all stimuli irrespective of their task relevance. Finally, in chapter 4, I have drawn inspiration from my empirical work to integrate oscillatory dynamics into an Artificial Neural Network (ANN) trained on a computer vision problem. The simulations indicate that oscillations can enable a converging system to multiplex concurrently presented stimuli.

In the following, I will synthesise these results to argue that gamma oscillations are likely to be relevant for local neuronal processes, while alpha oscillations operate at a more global scale.

5.1 Summary of the core findings

In chapter 2, I used MEG to systematically investigate the properties of rhythmic flicker responses in visual cortex, both in the absence and presence of endogenous gamma oscillations (see Duecker et al., 2021, for the publication). My results demonstrate that the early visual cortex can be driven by frequencies of up to 80 Hz, whereby sufficient signal-to-noise ratio was achieved with as little as 15 trials. I reasoned that the limit on this frequency is likely imposed by low-pass filtering in the thalamocortical connections. Notably, flickers at frequenices above 60 Hz are largely imperceptible (see, for instance Griffiths et al., 2023; Minarik et al., 2023), rendering them ideal for Rapid Invisible Frequency Tagging (RIFT). Employing sensory stimulation at these high frequencies has the added benefit of allowing measures of attentional modulations with high temporal precision. This makes RIFT a versatile tool not only for research in cognitive neuroscience but also for brain-computer interfaces (Brickwedde, Bezsudnova, et al., 2022). My exploration of the flicker responses at 52 to 90 Hz suggests that an optimal frequency range for RIFT is 60 to 70 Hz, ensuring both a good signal-to-noise ratio and a largely subliminal stimulation (also see Minarik et al., 2023, for a systematic exploration of optimum parameters for RIFT).

The key finding in this chapter is that a rapid flicker did not entrain endogenous gamma oscillations, even at overlapping frequencies. Instead, our results suggest a co-existence of the two neuronal activities, with the flicker response being strongest in the primary visual cortex, and the endogenous gamma oscillations emerging from the secondary visual cortex. This finding was unexpected for several reasons: Firstly, gamma oscillations have long been theorised to implement feedforward communication within the visual system (Bastos, Vezoli, Bosman, et al., 2015; Fries, 2015; van Kerkoerle et al., 2014), with consecutive layers communicating by entraining one another's activity at a gamma rhythm. Secondly, 40 Hz photic stimulation has been reported to trigger neuroprotective mechanisms in a mouse model of Alzheimer's Disease, an effect thats has been attributed to the entrainment of ongoing gamma oscillations (Adaikkan & Tsai, 2020; Adaikkan et al., 2019; Iaccarino et al., 2016). Lastly, prior research has indicated

that oscillations at lower frequencies, for instance, in the alpha-band, can be entrained by a visual flicker (Notbohm et al., 2016; Spaak et al., 2014), but also see Keitel et al. (2014) for a critical perspective. In the context of these findings, the observed resilience of gamma oscillations to external perturbation was intriguing.

In chapter 3, I have drawn from my experience with high-frequency visual stimulation, to investigate the neural correlates of visual search. Using MEG in combination with RIFT in a classic visual search paradigm, I have uncovered three main findings:

First, I have demonstrated that the neuronal excitability in early visual cortex is modulated in line with a priority map – to boost targets and suppress distractors (Awh et al., 2012; Koch & Ullman, 1985; Navalpakkam & Itti, 2005; Serences & Yantis, 2006; Thompson & Bichot, 2005; Zelinsky & Bisley, 2015). These findings align with previous work showing that early visual cortex underlies top-down control from the visual hierarchy (Budd, 1998; Muckli, 2010; Muckli & Petro, 2013). However, the application of these ideas to priority maps and visual search has not been explicitly made before (Bisley & Mirpour, 2019).

Second, I have corroborated earlier preliminary findings linking the power of occipital alpha oscillations to reaction time (Pastuszak et al., 2018). Third, going one step further, I have revealed that alpha oscillations are associated with an overall reduced excitability to all visual inputs, irrespective of their relevance to the task. We have coined the term *blanket inhibition* for this phenomenon. The negative correlation with reaction time suggests that this global inhibition makes the search more efficient. While prior studies on signal detection paradigms have argued for a decrease in visual performance with increasing alpha power (Dijk et al., 2008; Ergenoglu et al., 2004; Hanslmayr et al., 2007; Mathewson et al., 2009), our results show that these oscillations can be beneficial in tasks where a lot of distracting stimuli are present. However, when controlling these effects for time-on-task, we found that the relationship between response times and alpha power was not robust. This confound could reflect both task-related effects, indicating that participants learned to utilise the inhibition, or task-unrelated effects, indicating increased mental fatigue (Craig et al., 2012). These interpretations will be tested in follow-up work.

The link between alpha power and fast response times, revealed in chapter 3, points to a computational benefit of these oscillations in visual processing. In chapter 4, I further delved into this mechanism, by testing the theory that pulses of inhibition segregate and organise competing visual inputs in time. Combining concepts from Dynamical Systems Theory and Machine Learning, I have presented a *dynamical ANN*, an ANN trained on a computer vision problem, that embraces the oscillatory dynamics of the visual system. As indicated by my simulations, incorporating refractory terms into the network led to rhythmic activations in the hidden nodes, oscillating at frequencies between 10 to 12 Hz. These dynamics enabled the network to segregate the simultaneously presented inputs in time. The stability of the dynamic output was further improved by pulsed inhibition akin to alpha oscillations in the visual cortex, which notably synchronised the oscillatory activity within and between the network layers. As a result, the network was able to transform the spatially presented stimuli into a temporal code, whereby the output nodes activated along the phase of the alpha inhibition, ordered according to the attentional bias to the letters. This algorithm offers an implementation of the notion that alpha oscillations serve to segregate neuronal representations of visual objects into a temporal code (Jensen, Gips, et al., 2014). As I have discussed, such a mechanism could underlie parallel and serial processing across the visual hierarchy (Jensen et al., 2021).

The presented results provide insights into the properties of oscillatory dynamics in the visual system. Gamma oscillations and responses to rhythmic visual inputs appeared to co-exist in early visual areas V1 and V2. The magnitude of the alpha oscillations in early visual regions, on the other hand, was correlated with the strength of the flicker response, suggesting that alpha oscillations did interact with the visual inputs. I have proposed that this modulation could serve as a threshold (chapter 3) or as a mechanism for temporal coordination (chapter 4). These results have important implications for the role of these neuronal oscillations in visual processing and neuronal computation.

5.2 Novel insights & future directions

5.2.1 The low-pass filter properties of neuronal integration attenuate the propagation of gamma oscillations along the visual hierarchy.

In chapter 2, I reasoned that the flicker was unable to entrain endogenous gamma oscillations, as it might not affect the inhibitory interneurons that are critically involved in the emergence of gamma oscillations (Bartos et al., 2007; Cardin et al., 2009; Traub et al., 1997; Wang & Buzsáki, 1996; Whittington et al., 2011). Furthermore, I suspected that the low-pass properties in the communication along the visual hierarchy might have prevented the response from propagating beyond early visual cortex (Douglas & Martin, 2004; Hawken et al., 1996).

Since chapter 2 was published in Duecker et al. (2021), these predictions have been explicitly tested based on intracranial recordings in rodents in combination with computational modelling (Schneider et al., 2023; Soula et al., 2023). Schneider et al. (2023) investigated responses to a visual flicker at 20, 40 and 80 Hz in mice. In line with the proposal in chapter 2, they reported that the flicker response did not propagate beyond early visual regions. Using computational modelling, Schneider et al. (2023) further investigated how inhibitory interneurons and pyramidal cells respond to excitatory inputs at the respective stimulation frequencies. While the inhibitory interneurons were able to follow the stimulation up to 80 Hz, the pyramidal neurons integrated the 40 and 80 Hz inputs and responded with an overall increase in excitability. These results corroborate the idea outlined in chapter 2 that a visual flicker might not serve to entrain endogenous gamma oscillations, as it is unable to target the inhibitory interneurons. Soula et al. (2023) have further replicated the findings in chapter 2, showing that a rhythmic flicker did not entrain endogenous gamma oscillations in the mouse brain. Going one step further, they were unable to replicate the neuroprotective mechanisms reported by Iaccarino et al. (2016) (also see Adaikkan et al., 2019; Martorell et al., 2019; Singer, 2018). The implications of this null finding will be addressed below. In sum, since its publication in Duecker et al. (2021), chapter 2 has become part of a series of studies indicating that gamma oscillations in the visual system do not

synchronise to rhythmic sensory stimulation.

This line of research has important implications for the *Communication through Coherence* theory. *Communication through Coherence* posits that gamma oscillations transmit information up the visual hierarchy in a cascading fashion, whereby each region entrains the oscillatory activity of its subsequent receiving region (Bastos, Vezoli, & Fries, 2015; Fries, 2015; van Kerkoerle et al., 2014). However, this idea is difficult to reconcile with the observation that the low-pass filter properties of pyramidal neurons prevent the gamma rhythm from propagating across the network layers (Schneider et al., 2023). In accordance with that, Schneider et al. (2021) have shown that coherence between two cortical regions is not a clear indicator of communication. Instead, coherence between two neuronal populations might spuriously emerge if the LFP recorded from the receiving population contains afferent inputs from the sending populations (Buzsáki & Schomburg, 2015). As such, coherence might give the illusion that the two populations oscillate at synchronous rhythms, even in the absence of gamma oscillations in the receiving population.

While recent findings have amplified the criticism targeted at the *Binding by Synchrony* and *Communication through Coherence* theories (Roelfsema, 2023; Vinck et al., 2023) they cannot negate the multitude of studies showing that spiking activity in V1 (Peter et al., 2019, 2021; Vinck et al., 2010; Womelsdorf et al., 2012), V4 (Gregoriou et al., 2009; Vinck et al., 2013), and FEF (Gregoriou et al., 2009) is modulated by the phase of ongoing gamma oscillations. As such, studying gamma oscillations may still be useful for understanding neuronal computation in the visual system (Cardin, 2016).

Previous work has reported neuroprotective mechanisms in response photic stimulation in the gamma-band (Adaikkan & Tsai, 2020; Adaikkan et al., 2019; Iaccarino et al., 2016; Singer et al., 2018) . These findings have led to the proposal that driving gamma oscillations with sensory stimulation may reduce neurodegeneration in Alzheimer's disease (Adaikkan & Tsai, 2020). As mentioned in the introduction, the results of first human trials have also led to encouraging findings (Chan et al., 2022; He et al., 2021; Liu, Han, et al., 2022; McNett et al., 2023). However, more recent work has demonstrated that the visual flicker does not entrain endogenous gamma

oscillations in the mouse brain (Soula et al., 2023). Moreover, this study was unable to replicate the effects on neurohistochemistry and found that the animals tended to avoid the visual flicker (Soula et al., 2023). While the roots of these discrepancies are to be determined, the recent line of work, including the findings presented in chapter 2, suggests that the compelling effects of photic stimulation on neurons on glia may not underlie an entrainment of ongoing oscillations. As I will outline in the following, it is still possible that gamma oscillations may facilitate neural processing. As such, stimulating the cortex at these frequencies may still have beneficial effects on neural activity (also see Griffiths et al., 2023).

5.2.2 Gamma oscillations may still support vision by increasing the information represented by individual spikes.

How might gamma oscillations still be involved in visual processing, if not directly through facilitating feature-binding or inter-areal communication? Recent work has suggested that gamma oscillations may carry information about the predictability of visual inputs (Vinck & Bosman, 2016). This is the case both for the uniformity of structures within an image (Peter et al., 2019), as well as repeated presentations of the same stimulus (Peter et al., 2021). Spiking activity has been shown to reduce in response to visual stimuli with a highly predictable structure (Coen-Cagli et al., 2015). Moreover, firing rates have been repeatedly demonstrated to reduce when the stimulus is presented repeatedly, a phenomenon termed neuronal adaptation (see Kohn, 2007, for review).

The rationale that gamma oscillations synchronise individual spikes for feature binding has long been criticised based on the observation that they typically coincide with a sparse spiking output (e.g. Burns et al., 2011; Xing et al., 2012). As a counterargument, it has often been pointed out that gamma oscillations do not define when a neuron must fire, but instead, they provide a window of opportunity (Börgers & Kopell, 2003; Nikolić et al., 2013). Peter et al. (2021) have proposed that while neurons indeed reduce their firing in response to a repeatedly presented stimulus, strong gamma oscillations may serve to concentrate the fewer remaining spikes within a short time interval. Consequently, the sparse spiking output may reach the postsynaptic neurons with high temporal precision, in turn increasing the impact of the individual spikes (also see Larkum, 2013; Singer, 2018; Vinck & Bosman, 2016). Through this coordination of sparse spiking activity, gamma oscillations may still be involved in organising visual processing and communication between cortical areas (Vinck et al., 2023). This notion reconciles previous work arguing in favour (for review see Engel et al., 2001; Fries, 2015; Fries et al., 2007; Singer & Gray, 1995; Singer, 1999) and in contrast (see Roelfsema, 2023; Schneider et al., 2021; Shadlen & Movshon, 1999, for review) to *Binding by Synchrony* and *Communication through Coherence*.

Furthermore, it has been argued that these modulatory gamma oscillations might emerge from feedback connections (Vinck & Bosman, 2016). Indeed, strong gamma oscillations have been repeatedly observed in the supragranular but not the granular layers; a finding that has so far been difficult to align with the idea that gamma oscillations support feedforward communication (Buffalo et al., 2011; Ray & Maunsell, 2015; Smith et al., 2013; Xing et al., 2012). The association of gamma oscillations with the temporal coordination of spike timings in response to repeated stimuli indicates that studying gamma oscillations is still informative to understanding the neural mechanisms underlying visual perception (Cardin, 2016).

5.2.3 Gamma oscillations may support local neuronal processing.

Another surprising finding in chapter 2 was the absence of resonance phenomena, i.e. a selective amplification of individual frequencies in the stimulation range (Hutcheon & Yarom, 2000). Previous work applying visual flickers at a broad range of frequencies has reported a selective amplification of stimulation frequencies below 50 Hz (Gulbinaite et al., 2019; Herrmann, 2001). These findings and the results in chapter 2 indicate that the visual cortex does not selectively amplify frequencies above 50 Hz. Moreover, this even happens to be the case in presence of endogenous gamma oscillations. This interpretation is in line with a related study, where we applied a broadband flicker (1-720 Hz) to moving grating stimuli (Zhigalov et al., 2021). Previous work has reported that the temporal response function to a broadband stimulus, which is often approximated based on the cross-correlation between the EEG or MEG signal and the time series of the stimulation, exhibits a selective response in the alpha-band, termed the perceptual echo (VanRullen & Macdonald, 2012). Our high-frequency broadband flicker revealed an additional echo in the gamma band, which preceded the one in the alpha band (Zhigalov et al., 2021). Interestingly, we found the peak frequency of this gamma echo to be lower than the frequency of the gamma oscillations elicited by the moving grating stimulus. This is in line with the results in chapter 2, showing that the flicker frequency eliciting the strongest response tended to be lower than the individual gamma frequency. These findings indicate that the dynamics of the visual cortex exhibit substantial heterogeneity in the gamma band.

The heterogeneity of neuronal gamma band activity, for instance, the observation that the peak frequency of the oscillations varies depending on the stimulus properties, has long been argued to be problematic for the *Binding by Synchrony* and *Communication through Coherence* theories (Hermes et al., 2015a; Hermes et al., 2015b; Muthukumaraswamy & Singh, 2013; Muthukumaraswamy et al., 2010; Ray & Maunsell, 2010). However, computational work has proposed a more positive stance, arguing that the spectral variability of the gamma oscillations underlies highly flexible neural circuits (Whittington et al., 2011).

This flexibility may underpin the involvement of cortical dynamics in the gamma band in inter-areal communication. The *Communication through Resonance* hypothesis posits that a sending population could drive a receiving population by shifting its energy towards the receiver's resonance frequency (Hahn et al., 2014; Izhikevich et al., 2003; Vinck et al., 2023). In comparison to *Communication through Coherence*, this mechanism does not require that both populations oscillate in synchrony (Vinck et al., 2023). Instead, the receiver integrates the incoming signal non-linearly, but may itself not exhibit oscillations at the same frequency as the sender (Vinck et al., 2023).

Intracranial recordings from the human or non-human primate brain could help to understand whether gamma oscillations indeed support inter-areal communication in this localised way. For instance, Kuzovkin et al. (2018) recorded the LFP from the visual ventral stream in 100 epilepsy patients and found that activity in the high gamma band best mapped onto hidden activations in AlexNet, a popular CNN used for image classification (Krizhevsky et al., 2012). These data could be re-analysed using non-linear synchrony measures such as explained power (Dowdall et al., 2023) and mutual information measures (Imperatori et al., 2019; King et al., 2013; Park et al., 2018), to test whether consecutive layers along the visual hierarchy might indeed drive each other's activity at frequencies in the gamma-range. My interpretation of the *Communication through Resonance* theory is that communication is facilitated by a cascade of locally synchronised assemblies. As such, I would predict that the extent to which activations in one neuronal population can be explained by another area decreases with increasing distance between them. For instance, synchrony between V2 and V4 should be higher than synchrony

between V2 and IT. This is in line with previous work arguing that gamma synchrony decays with increasing distance (Roelfsema, 2023; Roelfsema et al., 2004).

Kuzovkin et al. (2018) further used natural stimuli such as photos of landscapes, which have a highly predictable structure, and images of animals whose structure is less predictable. As such, these data may further serve to test the conclusions presented by Peter et al. (2019), who showed that gamma oscillations in primate V1 increased with increasing predictability of the structures within an image. As Kuzovkin et al. (2018) recorded data from several regions in the ventral stream, it would be possible to investigate whether the findings by Peter et al. (2019) generalise to areas beyond V1.

In summary, novel results on neuronal gamma oscillations suggest that they might still organise spiking activity and inter-areal communication in a more localised way than previously hypothesised. Re-analysis of previously recorded data by Kuzovkin et al. (2018) could allow to test the predictions of these novel ideas.

5.2.4 Gating by alpha oscillations may flexibly operate in different areas for the different forms of attention.

In chapter 3, I pointed out that previous studies have not robustly observed a link between alpha power and frequency tagging responses, which is at odds with our association of alpha oscillations with an inhibitory mechanism modulating visual inputs (Antonov et al., 2020; Gundlach et al., 2020; Morrow et al., 2023; Zhigalov et al., 2021). I argued that one of the reasons for these discrepancies may be that the visual search task investigated in chapter 3 was guided by feature-based attention, while previous work has investigated inhibition by alpha oscillations in the context of spatial attention. Accordingly, the peak sources of the alpha oscillation in previous studies were localised in parietal cortex (Zhigalov & Jensen, 2020), while we found the peak source of the alpha power in early visual cortex. I have reasoned that this could reflect a gating mechanism implemented by alpha oscillations in early visual cortex, that funnels communication between the cortical areas that are relevant for the feature-guided search (see chapter 3 and Duecker et al., 2023).

This theory could be tested using a combination of MEG and RIFT, paired with a modulated version of the visual search task presented in chapter 3. In this follow-up study, attention could either be guided toward features, as done in chapter 3, or location, for instance, the side of the screen where the target stimulus will be presented. Accordingly, RIFT could be applied based on stimulus colour, or stimulus location (left vs right). Based on the conclusions in chapter 3, I would predict that the coordinates of the peak sources in the two conditions will differ along the dorsal and lateral axes. In the colour-guided search, I would predict alpha power to increase uniformly over visual cortex, while in the spatial condition, alpha power should be lateralised as previously shown in several spatial attention paradigms (Bahramisharif et al., 2010; Gutteling et al., 2022; Kelly et al., 2006; Sauseng et al., 2005; van Gerven & Jensen, 2009; Vissers et al., 2016; Worden et al., 2000; Zhigalov & Jensen, 2020). Furthermore, I predict these lateralised sources to be localised in parietal cortex (Zhigalov & Jensen, 2020). If spatial attention indeed benefits from gating in parietal cortex, while feature-based attention relies on gating in early visual regions, then a modulation of the RIFT response may only be observed in the feature-guided condition.

Contrary to the studies discussed above, Gutteling et al. (2022) have recently demonstrated a negative correlation between alpha power and RIFT responses. In a lateralised attention paradigm, the authors manipulated perceptual load by adding noise masks to either the target or the distractor stimulus – or to both. The perceptual load was maximal when the target but not the distractor stimulus was obscured by a noise mask.

In this condition, high alpha power in the hemisphere contralateral to the distractor was linked to a reduced RIFT response. These results align well with previous proposals, suggesting that the modulation of alpha oscillations and the reduction of resources dedicated to processing the distracting stimulus, may be driven by an increased demand of processing resources for the target (Jensen, 2023; Noonan et al., 2016). This proposal could be explored using the paradigm I have outlined above. One prediction would be that a negative correlation between the RIFT response and alpha power can only be observed for difficult searches with high set sizes.

Considering previous work that could not link alpha power and flicker responses in spatial

attention paradigm, I offer the interpretation of the findings presented in chapter 3 that inhibition by alpha oscillations can be flexibly utilised to implement gating mechanisms in task-relevant regions (also see Rodriguez-Larios et al., 2022; Sokoliuk et al., 2019, for the discussion of similar ideas). I have proposed a follow-up experiment that explicitly tests whether alpha oscillations are modulated differently for different forms of attention.

5.2.5 The link between blanket inhibition and the temporal code

In chapter 3, I have reported that alpha oscillations are linked to reduced neuronal excitability to all visual inputs. We suggested that in this way, alpha oscillations serve as a threshold that is applied to all locations in the priority map (also see Duecker et al., 2023). In chapter 4, the periodicity of the inhibition imposed by the alpha oscillation is central to the emergence of a temporal code, as it defines when the hidden units activate. This model relies on the notion that alpha oscillations offer windows of opportunity for neuronal activation (Jensen et al., 2012; VanRullen, 2016). When averaging over trials without controlling for the phase of the alpha oscillations, these effects are likely to be reflected in an overall decrease in excitability as shown in chapter 3. In other words, the *blanket inhibition* mechanism may be applied in a cyclic fashion. As the *blanket inhibition* reduces periodically, the neural representations of the visual inputs may activate according to their level of excitability, thus implementing a temporal code.

This idea could be tested using cross-frequency measures on the data presented in chapter 3, to investigate whether the amplitude of the RIFT response is modulated periodically by alpha phase. One may further hypothesise that the RIFT response to the target stimuli increases at an earlier phase of the alpha cycle than the distractor stimuli, reflecting a temporal code. However, there are potential confounds in these data that might disguise any effects of alpha oscillations implementing a temporal code. First, the signal-to-noise ratio of the RIFT response may be insufficient to identify any amplitude modulations by alpha phase, especially for the suppressed distractors. Second, as explained above, the findings in chapter 2 suggest that the RIFT response does not propagate beyond early visual cortex, which was supported by recent investigations of flicker responses in mouse visual cortex (Schneider et al., 2023). Primary visual cortex has

been shown to process low-level features, such as colour, in parallel (Popovkina et al., 2021; White et al., 2017). As such, a temporal coordination of the neuronal responses to the target and distractor stimuli along the visual hierarchy may not be reflected in the RIFT response. This notion is in line with the simulations presented in chapter 4, showing that a segregation of the competing stimuli along the phase of the alpha oscillations does not occur in the first layer. Finally, the temporal code model considers a relatively small number of visual inputs, and has so far not explicitly been extended to complex task such as visual search.

A more suitable way to test the idea that alpha oscillations convert competing visual inputs into a temporal code could be achieved using relatively simple visual attention paradigms, in combination with MEG, fMRI, and decoding methods such as Multivariate Pattern Analysis (Cichy & Oliva, 2020; Cichy et al., 2014, 2016, 2017). Previous studies have used a fusion of MEG and fMRI decoding to trace neuronal representations of visual objects (Cichy et al., 2016; Mohsenzadeh et al., 2019). The decoding approach serves to relate the neuromagnetic and hemodynamic responses acquired with the MEG and fMRI, and thus allows to isolate the neuronal representations of visual stimuli with both high temporal and spatial precision (Cichy & Oliva, 2020). As such, this method serves to estimate the response latency in different regions within the visual hierarchy (Cichy et al., 2016; Mohsenzadeh et al., 2019).

As outlined in chapter 4, the temporal code has been hypothesised to result in a pipelining mechanism in visual processing, whereby attended stimuli reach higher-order visual areas with a temporal advantage over unattended stimuli (Jensen et al., 2021). This theory could be tested using the MEG/fMRI-decoder, trained on individual stimuli presented laterally on the screen. By training the decoder on stimuli presented at either position, one could isolate the neural activity associated with translation invariant core object recognition of each stimulus (see DiCarlo & Cox, 2007; DiCarlo et al., 2012, for reviews on object recognition in the ventral stream) presented at a time, and the participant is instructed to attend to one of them. Following the predictions from the pipelining model (Jensen et al., 2021, and chapter 4), the increase in decoding accuracy of the attended stimulus in object-selective cortex, such as IT, may precede the decoding of the unattended stimulus. Moreover, using this paradigm, it could be tested if the decoding

of the stimuli is modulated by the phase of ongoing alpha oscillations. Indeed, van Es et al. (2022), have recently reported that the decoding accuracy of laterally presented grating stimuli is modulated by the phase of ongoing alpha oscillations in prefrontal cortex. By aligning the time series to alpha phase, for instance, using the newly developed brain time toolbox (van Bree et al., 2022) it could be tested if any delays in the neural responses to simultaneously presented stimuli can be linked to alpha phase.

In summary, while chapter 3 argues for an approximately uniform reduction of excitability by alpha oscillations in early visual cortex, chapter 4 suggests that alpha oscillations may modulate neuronal responses in a temporally precise way. I have outlined an experiment using MEG-fMRI decoding to explicitly test whether alpha oscillations can be linked to a pipelining mechanism in visual cortex.

5.2.6 Extensions of the dynamical artificial neural network could embrace the local and global dynamics of the visual system.

Throughout this discussion, I have argued that gamma oscillations may support visual processing through localised neuronal processes, while alpha oscillations affect neural activity in a more global way. To embrace these ideas, future versions of the *dynamical ANN* could feature both local and global dynamics within and across the network layers.

For instance, previous work has shown that integrating local recurrences into brain-like ANNs can improve their object recognition abilities (Kubilius et al., 2019). Gamma oscillations have been shown to emerge from supragranular layers in the visual cortex (Buffalo et al., 2011; Smith et al., 2013; Spaak et al., 2012; Xing et al., 2012), and may therefore serve to mediate local neuronal activity (Vinck et al., 2023). Moreover, gamma oscillations are known to underlie a balance of excitation and inhibition, which emerges from an interplay between pyramidal cells and inhibitory interneurons (Cardin et al., 2009; Traub et al., 1997; Whittington et al., 2011).

Possible extensions of the dynamical ANN could therefore include the integration inhibitory nodes and recurrent connections into each network layer. These features could lead to local dynamics, akin to gamma oscillations, emerging during the training process, through a balance

of excitation (through the inputs) and inhibition by the interneuron nodes (Börgers & Kopell, 2003). Previous work has proposed that the computational purpose of gamma oscillations is to segment stimulus representations in time (Lisman & Idiart, 1995; Lisman & Jensen, 2013). This is based on the notion that the inhibitory connections momentarily allow an individual representation to activate, while others are silenced. As such, a testable prediction for this extension of the model is that competing inputs may activate in consecutive cycles of the emerging gamma oscillations.

In the current version of the model, alpha oscillations are integrated into the network by subtracting synchronous sinewaves from the hidden activations in all nodes. Previous work using intracranial recordings in humans and non-human primates, however, has proposed that alpha oscillations may propagate from frontal areas backwards through visual hierarchy toward early visual cortex (Kaneko et al., 2022; Zhang et al., 2018), or from prefrontal areas via the mediodorsal thalamus toward visual cortex (Griffiths et al., 2022). In line with that, the phase of frontal alpha oscillations has been linked to a modulation of visual perception and attention (Capotosto et al., 2009), as well as decoding accuracy of visual stimuli (van Es et al., 2022).

In the current model, we found that approximately synchronous oscillations resulted in the most stable temporal code, indicating that an inhibitory oscillatory drive emerging from one single area may be optimal to organise activations in the hidden layer. It would be interesting to explore the optimal phase relationship between the network layers, and whether it is best controlled by a common pacemaker, as is the case in the current implementation, or by a travelling wave propagating along the network layers (see Alamia & VanRullen, 2019, 2023; Alamia et al., 2023, for recent work on alpha travelling waves in humans).

Finally, previous work has proposed that gamma oscillations organise the feedforward communication along the visual hierarchy, while alpha oscillations reflect a feedback signal that modulates this feedforward sweep (Bastos, Vezoli, & Fries, 2015; Mejias et al., 2016; Michalareas et al., 2016; van Kerkoerle et al., 2014). The interplay between the activity at these different rhythms has been argued to underlie the functional relevance of alpha oscillations: in absence of ongoing task-relevant activity in the gamma-band, low-frequency oscillations such as the

alpha rhythm become detrimental to performance, as they reduce excitability over long periods (Schroeder & Lakatos, 2009). If there is a task-relevant signal these oscillations can modulate, however, they will facilitate performance by organising neuronal activity in time (Jensen, Gips, et al., 2014; Schroeder & Lakatos, 2009). As such, integrating both fast and slow oscillations into future versions of the model may help to understand the functional relevance of their interaction.

To conclude, for future versions of the *dynamical ANN*, it would be interesting to test whether oscillatory dynamics at different spectral scales, akin to gamma and alpha oscillations in the visual system, could enhance the abilities of the neural network.

6

General conclusion

The insights gathered in this thesis elucidate the involvement of gamma and alpha oscillations in visual processing. I have demonstrated that while the visual cortex can be driven at high frequencies above 50 Hz, endogenous gamma oscillations in this frequency range are unperturbed by sensory stimulation. In contrast, alpha oscillations were found to modulate visual inputs. The uncovered difference in the properties of gamma and alpha oscillations hints at a sophisticated orchestration of neural computation in visual cortex: gamma oscillations may organise activity in local circuits, while functional inhibition by alpha oscillations affects neuronal populations at a more global scale.

Based on this notion, I propose that gamma and alpha oscillations take on different roles in conducting the orchestra of neuronal firing, leading to distinct but connected sections of musicians that maintain the harmony in early visual cortex.

A

Appendix Chapter 3

A.1 Supplementary Analyses

A.1.1 Behavioural results: Guided Search is associated with better performance

We predicted that search performance would decrease for more difficult searches. Indeed, Figure 3.2c and d, showing the mean reaction time and accuracy (d') for each condition, demonstrate better performance in guided compared to unguided search and smaller (16) compared to larger (32) set sizes. We investigated these effects using a hierarchical regression approach with linear mixed models, whereby we consecutively added the factors set size and guided/unguided (dummy coded as 1 being "guided search") into a model including only subject-related random effects.

To account for the skewed distribution of the reaction time data, we used a gamma distribution to fit the linear mixed models. A model predicting reaction time using the fixed factors set size and guided/unguided, and the random effects associated with these factors in each participant ($AIC = -307.57$), was superior to a model predicting reaction time as a function of subject-related random effects and set size ($AIC = -181.72, \chi^2(4) = 133.86, p < 0.0001, R^2 = 0.96, \Delta R2 = 0.22$). This additive model reveals a fixed effect for set size ($\beta = 0.180$) and guided/unguided ($\beta = -0.138$). In short, this demonstrates an increase in reaction time for set size 32 to compared to 16 by about 180 ms, and an increase of about 138 ms for unguided compared to guided search (no interaction effect, see Table A.1).

Analogously, hierarchical regression of accuracy shows that d' is best predicted by an additive model including the factors set size ($\beta = -0.74$) and guided/unguided ($\beta = 0.56, R^2 = 0.83$) and the subject-specific random effects (see Table A.3). These results show that accuracy decreases for larger set sizes and increases for guided compared to unguided search. The results of all post hoc tests are shown in Table A.2 and Table A.4, and indicated in Fugure 3.2c and d. Notably, performance was not significantly different for unguided search, set size 16 and guided search, set size 32 (Wilcoxon signed rank test on reaction time : $V(30) = 134, z = 2.23, p = 0.15, r =$

0.4, $SE = 0.019$; sensitivity (d'), dependent sample t-test: $t(30) = 2.2, p = 0.23, d = 0.2, SE = 0.081$). This finding is in line with the notion that guided search allows the participants to focus their search on items in the target colour while ignoring the distractor colour.

In sum, the behavioural findings are consistent with a priori expectations, namely an increase in response times with set size, as well as faster responses for guided compared to unguided search.

A.1.2 RIFT responses for fast compared to slow trials

As the analyses of the RIFT responses in guided and unguided search revealed a modulation of neuronal excitability in line with the priority map, we asked if successful target boosting and distractor suppression were relevant for performance. We therefore sorted the trials in each condition according to fast and slow responses (median split on reaction time) and compared the respective RIFT signals. Figure A.2d shows the RIFT response to the target colour for fast and slow trials (orange and brown line, respectively), and to the distractor colour (light and dark blue for fast and slow trials, respectively) for guided search, set size 32. We expected fast trials to be associated with respectively a stronger response to the target colour and a weaker response to the distractor colour, however, we did not find any significant differences between the RIFT responses to targets and distractors for fast vs slow trials. Upon further post-hoc comparisons, using cluster-based Monte Carlo permutations, we did find that the difference between the RIFT responses to the target and distractor colour is significantly larger for fast compared to slow trials, at about 200 ms after search display onset (Figure A.2e, $p < 0.05$, 5,000 permutations). We conclude that there was a weak, and rather short-lived relationship between reaction time and the RIFT responses to target and distractor features, which was mainly driven by a strong initial response to the target colour.

A.1.3 Ocular artefacts and gaze bias not linked to reaction time or alpha power

While participants were instructed to perform the task without moving their eyes, we found that some eye movements were present during the search. As enhanced neural processing has been suggested to underlie microsaccades (Liu, Nobre, & van Ede, 2022; Lowet et al., 2018) and alpha oscillations have been linked to the coordination of eye movement (Liu, Nobre, & van Ede, 2022; Pan et al., 2023; Popov et al., 2021), we investigated if the reaction time effects and the modulated RIFT responses observed for fast vs slow trials and high and low alpha power can be explained by differences in ocular artefacts (Figure A.9).

We divided the trials in the eye tracking data in each condition based on the median reaction time, separately for target present and absent trials in each participant (as described in the main text). Then, we identified the number of blinks and saccades in the first 500 ms after the search display onset (the time interval included in the RIFT analyses) and averaged these over conditions. Note that the threshold of the eye tracker to identify a saccade was set to 0.6°. We again analysed all main and interaction effects using a hierarchical regression approach, by comparing the explanatory value of a model containing the factor fast/slow to the baseline model.

For the average number of blinks during the trial, we find that a model containing the factor fast/slow ($AIC = -1259.3$) did not explain a significantly larger portion of the variance than the baseline model including subject-specific random effects ($AIC = -1259.5, \chi^2(1) = 1.9, p = 0.17$, Figure A.8a). Using the same approach on the average number of saccades revealed that a model including the predictor fast/slow ($AIC = -6.8$) could indeed account for a larger portion of the variance than the baseline model ($AIC = -4.86, \chi^2(1) = 3.9, p = 0.05, \Delta R^2 = 0.0014$), however, none of the pairwise comparisons reached significance (Table A.5, Figure A.8b).

To ensure that any eye movements during the search were not over-proportionally directed at the target colour in the fast trials, we binned the eye tracking data into 100 ms intervals, and identified the stimulus closest to the location of the gaze in each of these bins. The gaze

bias towards the target colour was defined as the proportion of time the eyes were directed at a position closest to a stimulus in the target colour. A value of 0.5 indicates that the participant's gaze time on the target and the distractor colour were the same, meaning no bias. Comparing a linear regression model predicting gaze bias as a function of the factor *fast/slow* (AIC = -8.64.09), with a baseline model ($AIC = -865.9$), did not reveal any significant main effects of reaction time on the gaze bias ($\chi^2(1) = 0.19, p = 0.67, \Delta R^2 = 0.0001$). This shows that participants followed the instructions and did not solve the task by moving their eyes towards the target colour (Figure A.8c).

Applying the same analyses to trials divided according to alpha power in the -1 to 0 s baseline interval, confirmed that the link between alpha power and RIFT response described in Fig. 4 was not driven by ocular artefacts or a gaze bias towards the target colour. For the average number of blinks, we found no additional explanatory value of the factor *alpha high/low* ($AIC = -1270.5$) compared to the baseline model ($AIC = -1272.2, \chi^2(1) = 0.32, p = 0.57, \Delta R^2 = -0.0011$, Figure A.8d). For the number of saccades during the trial, we did find that a linear regression model including the factor *alpha high/low* ($AIC = -13.27$) is superior to the baseline model ($AIC = -6.27, \chi^2(1) = 9.0, p = 0.0027, \Delta R^2 = 0.004$, Figure A.8e). Pairwise comparisons indicate that only the unguided search condition, set size 32, showed significantly more saccades for high vs low alpha trials ($t(30) = -3.91, p = 0.002, d = -0.685$, Benjamini-Hochberg corrected, Table A.6). As outlined above, we did not find any influence of pre-search alpha power on RIFT responses in unguided search, meaning that the number of saccades did not seem to affect the RIFT response. None of the remaining comparisons reached significance. For gaze bias, we found that the predictor alpha *high/low* did not add any significant explanatory value to the baseline model ($AIC_{baseline} = -903.08, AIC_{alpha} = \check{}902.52, \chi^2(1) = 1.4, p = 0.23, \Delta R^2 = 0.006$, Figure A.8f).

Finally, we applied the same analyses to the eye movement data split based on alpha power during search. Again, a regression model containing the factor *alpha high/low* ($AIC = -1218.2$) did not explain any additional variance compared to the baseline model ($AIC = -1219.5, \chi^2(1) = 0.73, p = 0.39, \Delta R^2 = 0.0001$, Figure A.8g). For the average number of saccades during

search, there was an effect of alpha power ($AIC = -13.27$ vs. $AIC = -6.27$ for the baseline model, $\chi^2(1) = 9, p = 0.003, \Delta R^2 = 0.0036$). Pairwise comparisons revealed that high alpha trials were associated with significantly less saccades in unguided search, set size 32 ($t(30) = -3.91, p = 0.002, d = -0.685$, Benjamini-Hochberg corrected, Figure A.8h). Considering that the median split based on alpha power before the search revealed the exact same effect for unguided search, set size 32, but no effect on the RIFT response, and considering the absence of any saccadic effects in the guided search condition, we argue that the reduced RIFT response in unguided search, set size 32, is more likely to be linked to alpha power, rather than the number of saccades. Lastly, we found that a model of gaze bias, including alpha high/low was not superior ($AIC = -902.52$) to the baseline model ($AIC = -903.08, \chi^2(1) = 1.4, p = 0.23, \Delta R^2 = 0.006$, figure A.8i).

These analyses indicate that ocular artefacts and gaze bias are not significantly linked to reaction time or alpha power. This suggests that the differences in RIFT response for fast and slow trials, as well as trials with high alpha power in the pre-search and interval, cannot be explained by eye movement or ocular artefacts.

A.2 Supplementary Figures

Figure A.1: Topoplots showing coherence to RIFT at 60 Hz for each participant. RIFT sensors of interest are indicated by the light blue rings.

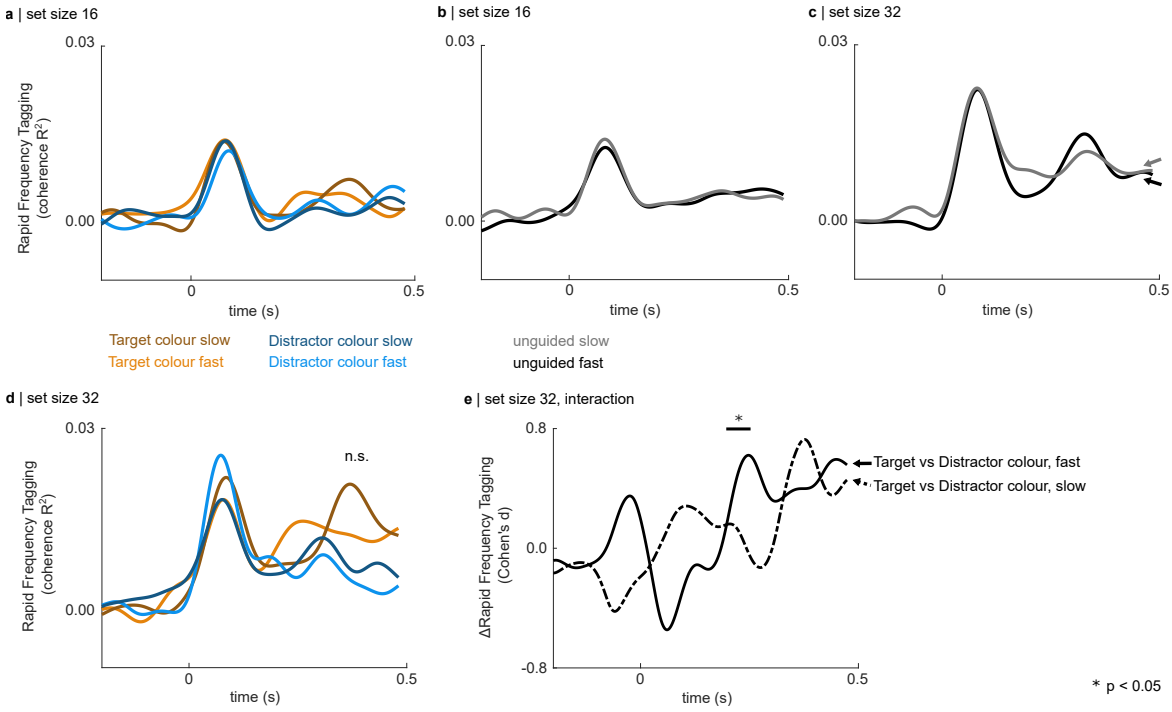

Figure A.2: RIFT responses for fast and slow trials. There is no modulation of the RIFT response for fast vs slow trials for guided search, set size 16 (**a**) or unguided search set size 16 (**b**) or 32 (**c**). **d** Visual inspection of the RIFT responses in guided search set size 32 suggests higher coherence for fast compared to slow trials, however, neither the comparisons between targets for fast vs slow nor for the distractors revealed a significant difference (cluster-based permutation t-test, 1,000 permutations). **e** Upon further inspection of the interaction effects, we find that fast trials are associated with a larger difference in the RIFT response between the target and distractor colour (cluster-based permutation Monte Carlo t-test, $p < 0.05$, 1,000 permutations). This effect seems to mainly be driven by an initial increase in RIFT response to the target colour.

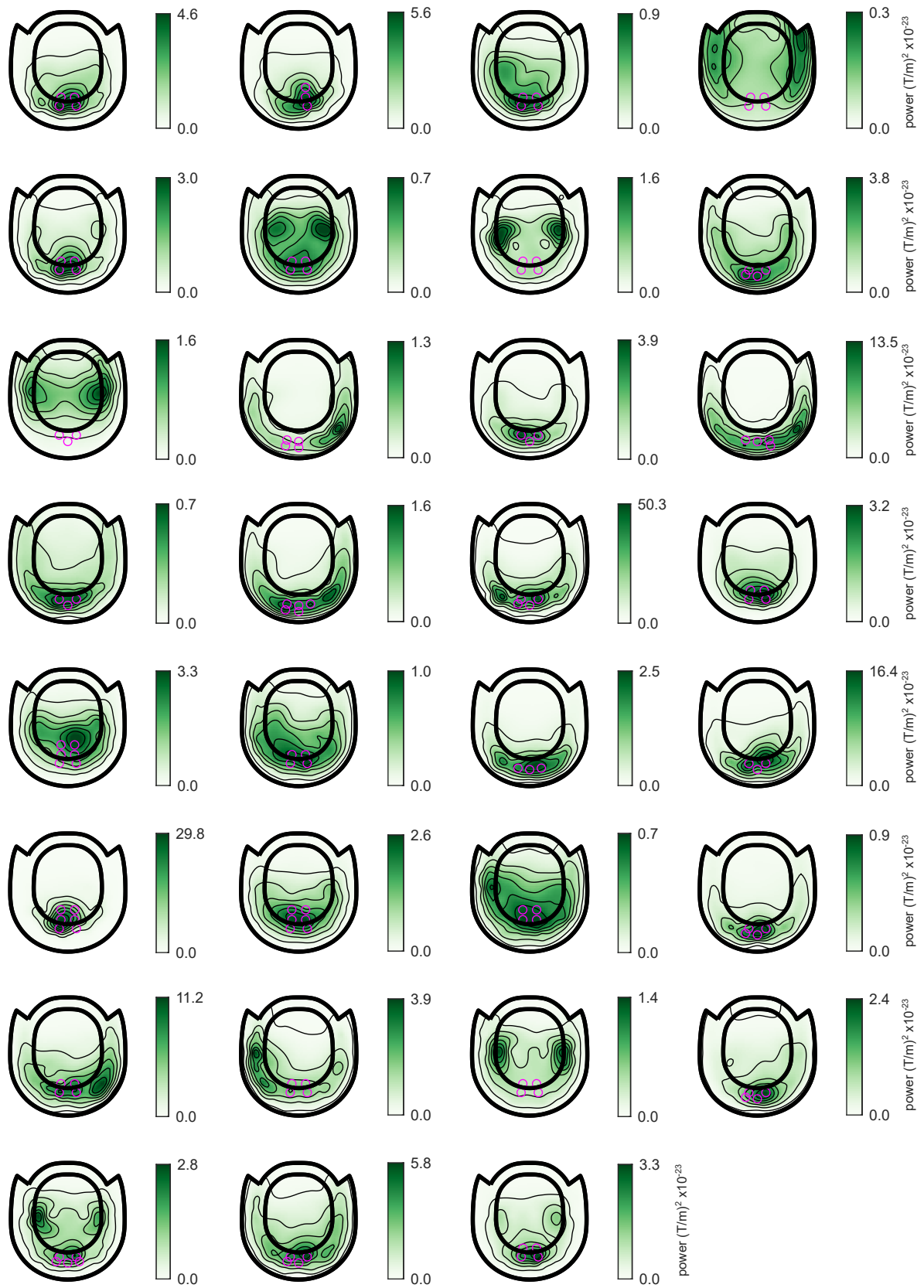

Figure A.3: Topoplots showing power at the Individual Alpha Frequency in the -1 to 0 interval. Alpha sensors of interest are indicated by the pink rings.

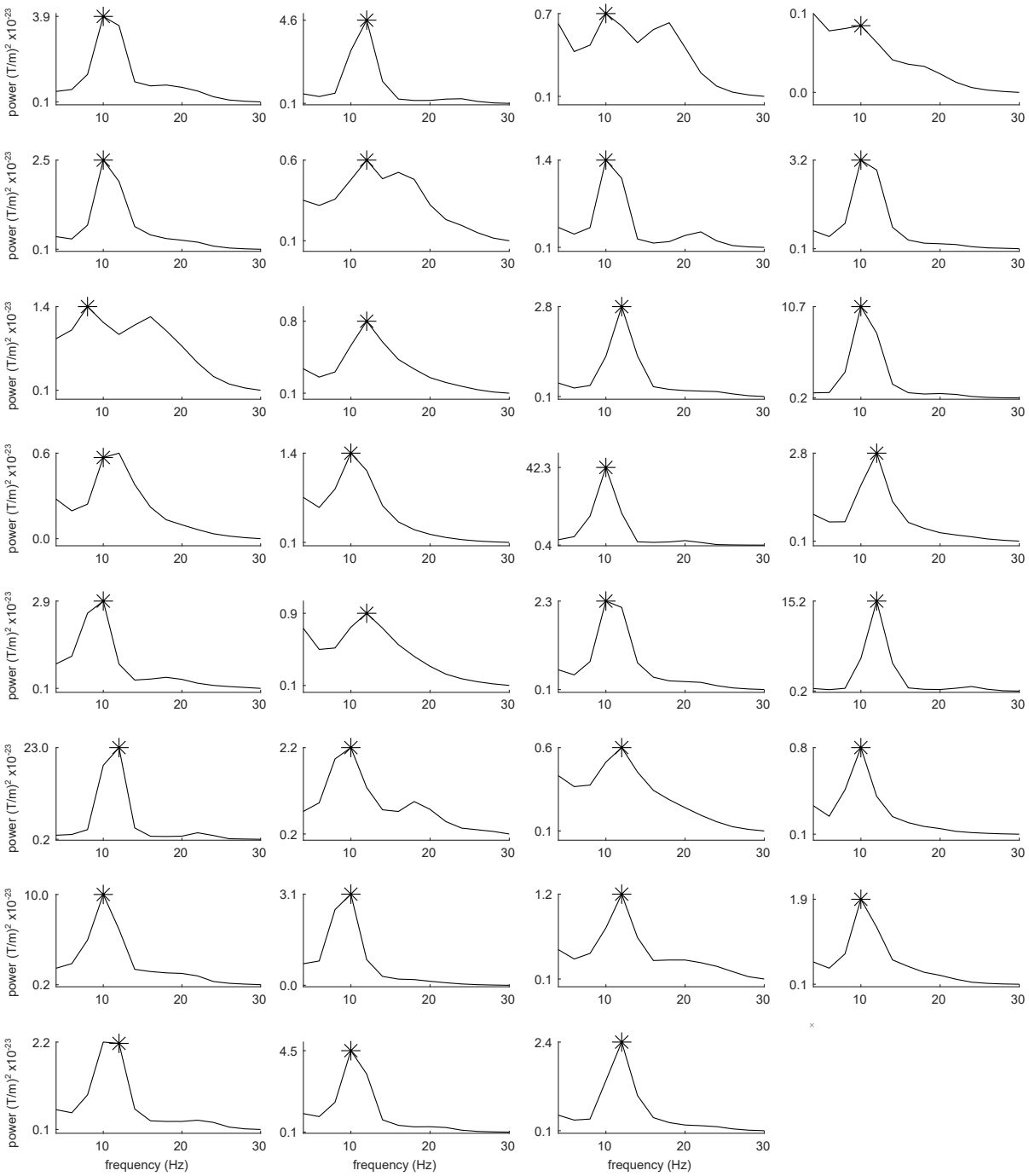

Figure A.4: Individual alpha frequency per participant. The spectra show the Time-Frequency Representations of power (obtained with a sliding time window using a complex Hanning taper of 500 ms), averaged over the -1 s to 0 interval before the onset of the search display, averaged over all trials and conditions. Individual Alpha Frequencies were identified as the peak in the spectrum in the 4-14 Hz Frequency range.

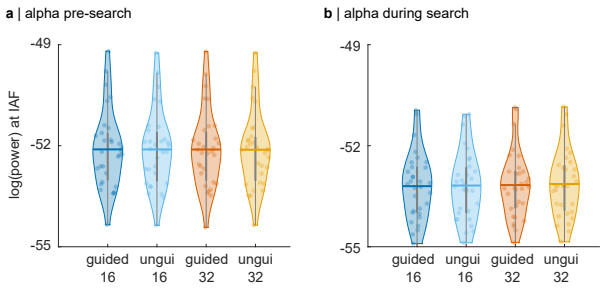

Figure A.5: Alpha power pre- and during search does not differ between conditions. **a** Power at the individual alpha frequency in the baseline, obtained from the Time-Frequency Representation of power, averaged over the -1 to 0 s interval for each condition. A repeated-measures ANOVA did not reveal any main effects factors condition (guided vs unguided search; $F(1,30) = 1.41$, $p = 0.24$) or set size ($F(1,30) = 2.52$, $p = 0.12$), nor an interaction effect ($F(1,30)=0.5$, $p = 0.48$). **b** Alpha power during search for each condition, obtained by averaging over the 0.25 to 0.5 s interval. Again, we did not find a main effect for condition $F(1,30) = 0.49$, $p = 0.49$), set size $F(1,30) = 2.4$, $p = 0.13$), or an interaction $F(1,30) = 0.26$, $p = 0.61$).

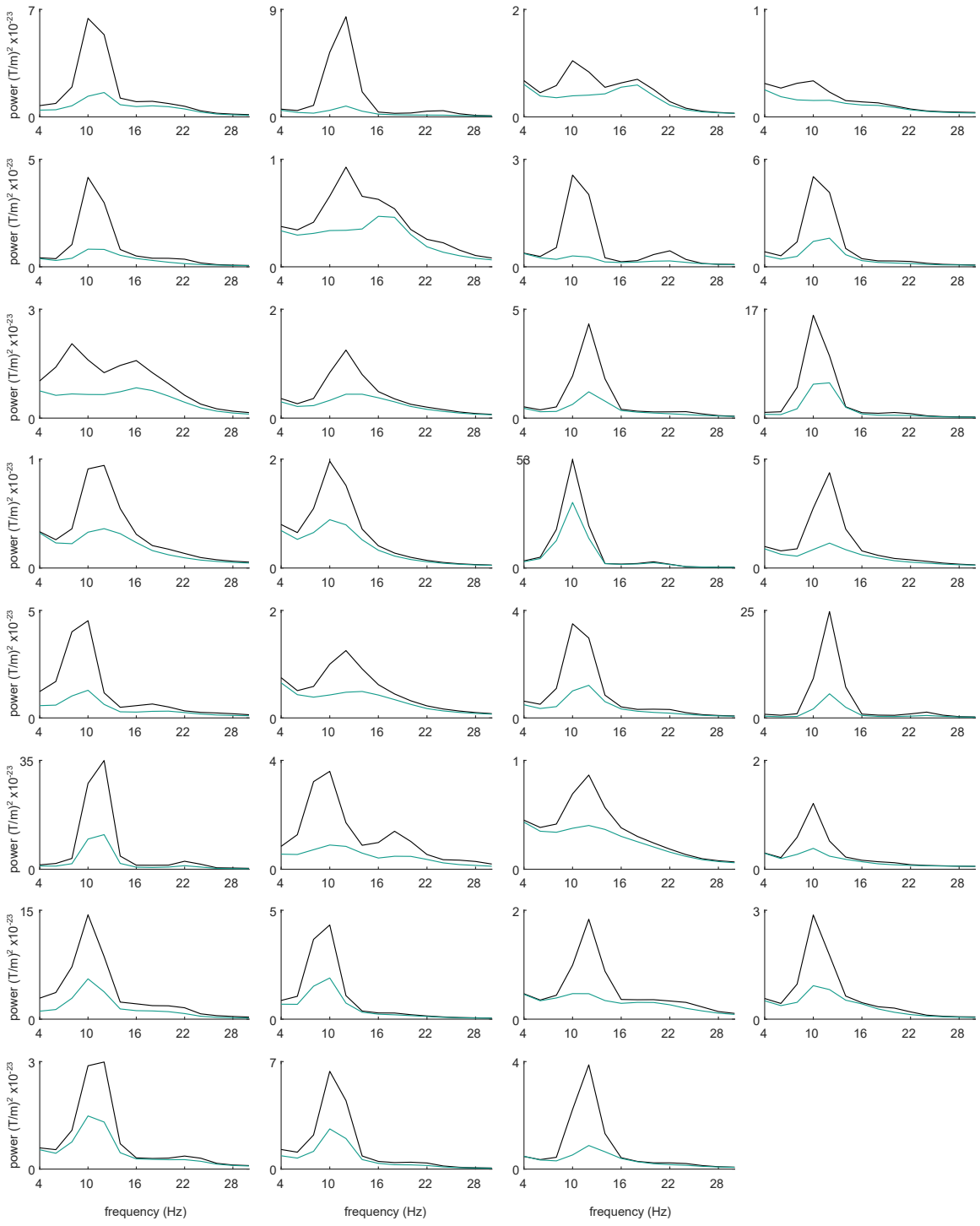

Figure A.6: Alpha power in the -1 to 0 baseline interval for high and low alpha trials, one spectrum per participant. High and low alpha trials are depicted by the black and turquoise line, respectively. The spectra were obtained by averaging Time Frequency Representations of power over the -1 to 0 s interval the onset of the search display.

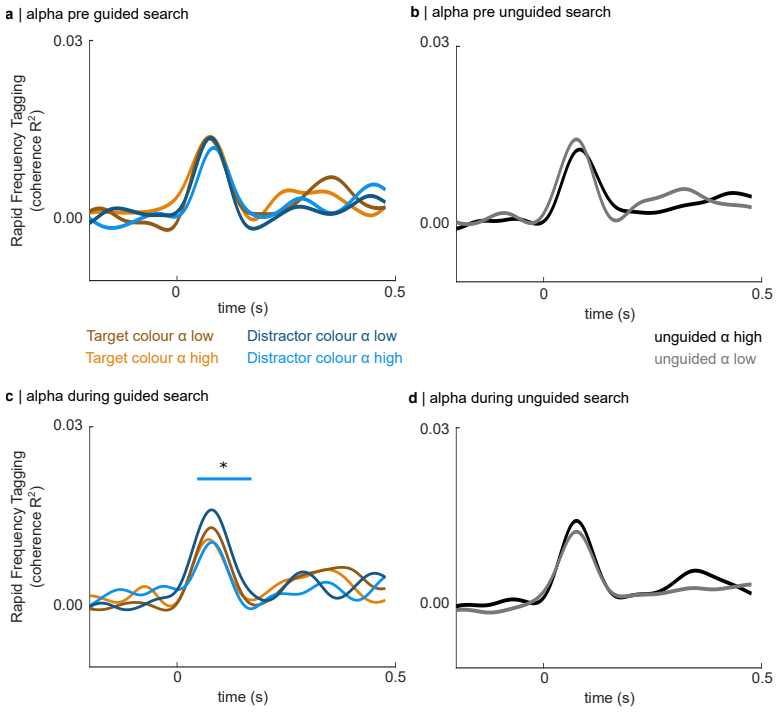

Figure A.7: RIFT responses for set size 16 show no systematic difference between trials with high and low alpha before pre-search (a,b) or during search (c,d). **c** Surprisingly, the initial event-related RIFT response to the distractor colour was significantly reduced in trials with high alpha power for guided set size 16r. This finding is the only evidence for attentional modulation in the set size 16 condition.

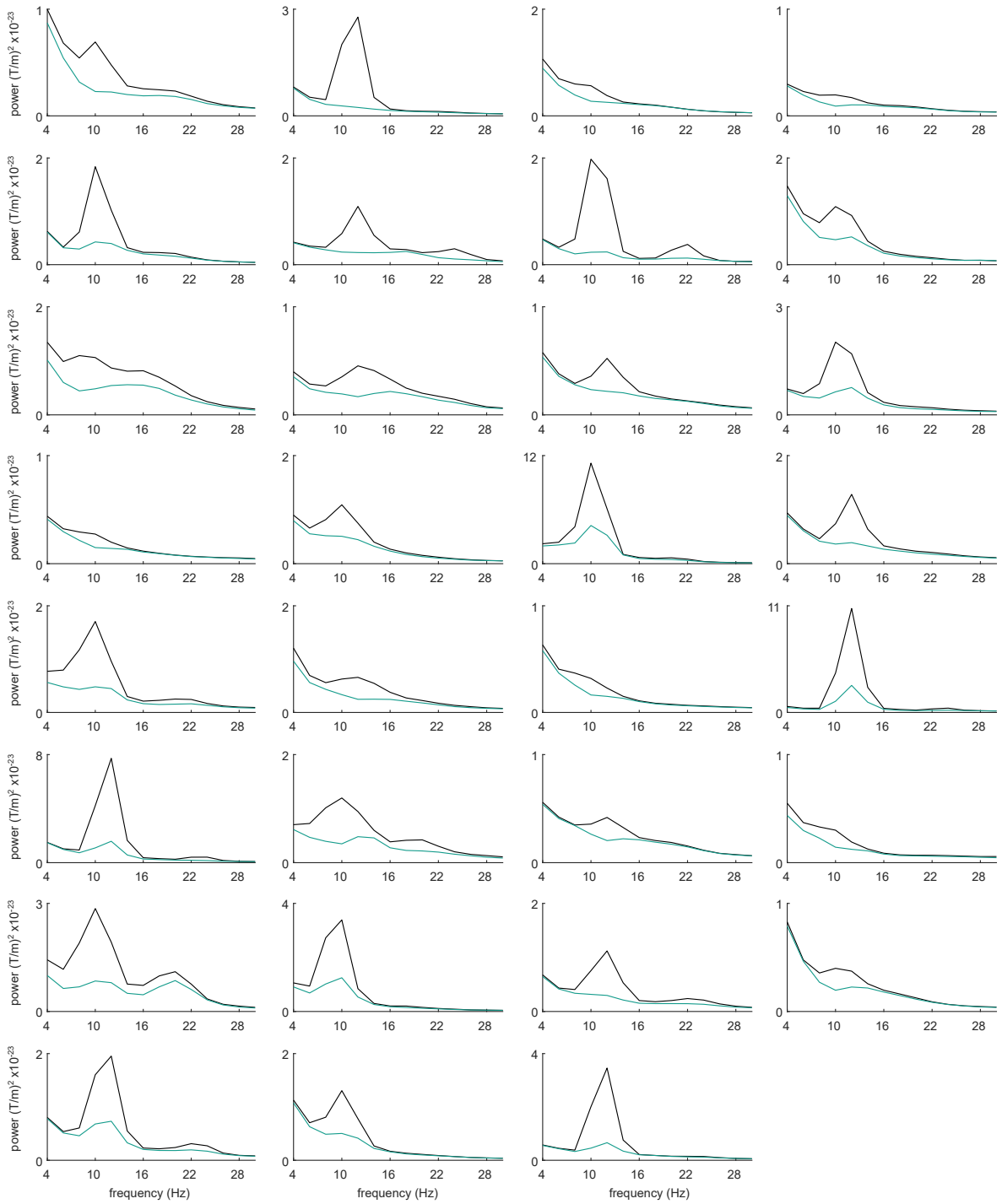

Figure A.8: Trials with high vs low alpha power during search. One spectrum per participant, the black and turquoise lines show the spectra for the high and low alpha trials, respectively. The spectra show the Time-Frequency Representations of power (obtained with a sliding time window using a complex Hanning taper of 500 ms), averaged over the 0.25 to 0.5s interval following the onset of the search display.

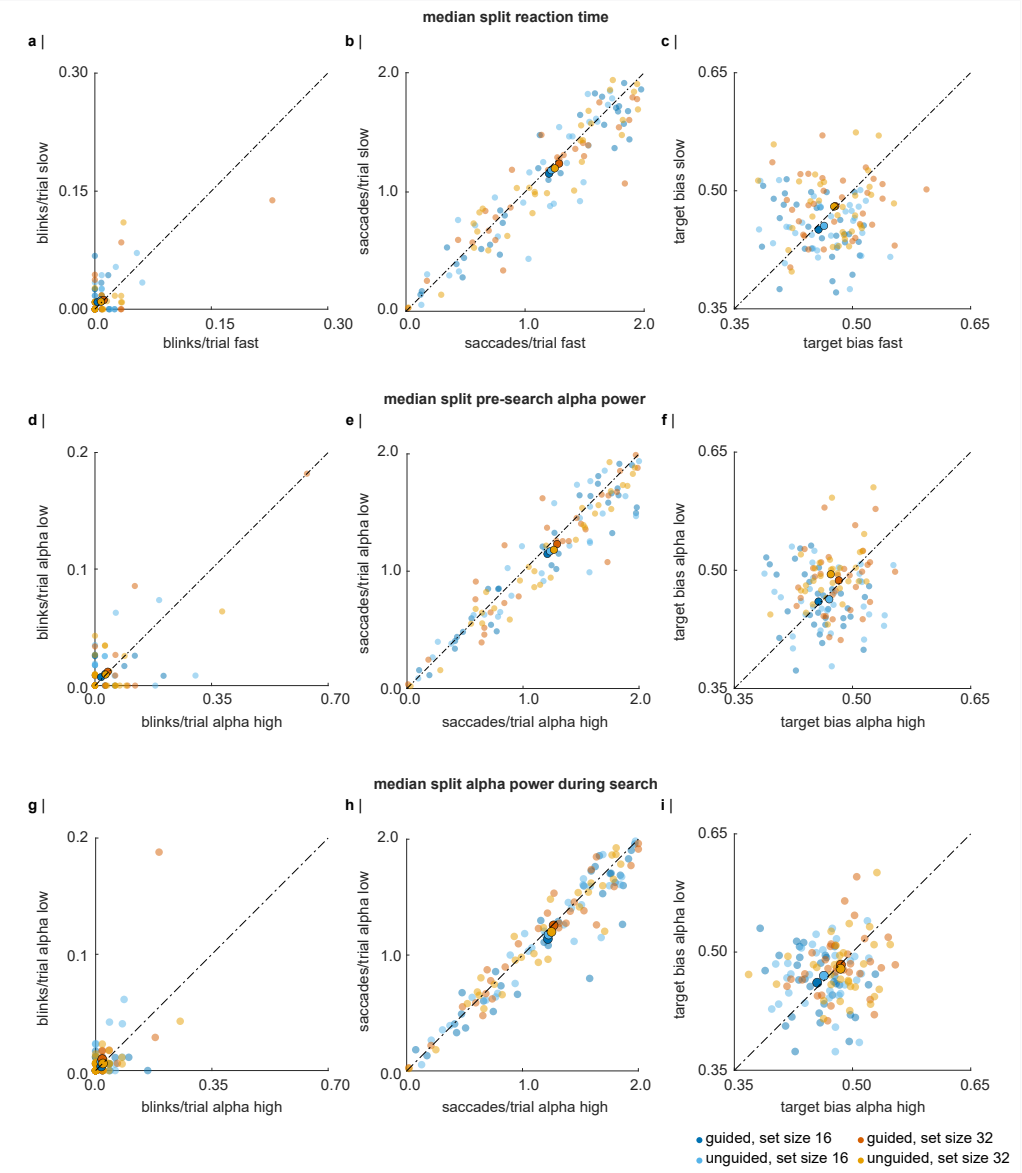

Figure A.9: Eye blinks, saccades, and gaze bias towards the target colour for fast vs slow trials (**a**-**c**) and trials with high and low alpha power before (**d**-**f**) and during the search (**g**-**h**). Individual participants and grandaverage are indicated by the opaque and solid scatters, respectively. **a** Average number of eye blinks in each condition compared for fast and slow trials. A hierarchical regression approach revealed no main effect for of reacion time fast vs. slow ($\chi^2 = 1.9, p = 0.17$. **b** Average number of saccades per trial during the search interval in each condition for fast vs slow trials. While there is a significant main effect for *fast vs slow* ($\chi^2 = 3.9, p = 0.047, \Delta R = 0.0014$), the pairwise comparisons did not show any significant differences (Table A.5) **c** Proportion of the trial the gaze spent near the target colour, again showing no difference for reaction time fast vs slow ($\chi^2 = 0.19, p = 0.67$). **d** Number of eye blinks during the search for each condition, compared for high and low alpha trials. Hierarchical regression does not reveal a main effect for *alpha high/low* $\chi^2 = 0.32, p = 0.57$. **e** Average number of saccades during search for high and low alpha trials. We found a main effect for *alpha high/low* ($\chi^2 = 9.0, p = 0.003, \Delta R = 0.004$), however, the pairwise comparisons only reveal an effect for unguided search, set size 32, where no effect of alpha on the RIFT response was observed. **f** Comparison of gaze bias in trials with high and low alpha power in the baseline, showing no effect for alpha high vs low ($\chi^2 = 1.4, p = 0.23$). **g-h** All findings shown in in **d-f** are replicated for alpha power during search.

A.3 Supplementary Tables

Table A.1: Hierarchical regression on reaction time, revealing a significant main effect for set size and guided/unguided, but no interaction effect. When fitting the regression models, we assumed that the reaction time data followed a gamma distribution.

Model	**AIC**	χ^2	**p**	$\mathbf{R^2}$
$RT = \beta_0 + \epsilon_{subj}$	−117.04			0.59
$RT = \beta_0 + \beta_1 \cdot X_{setsize} + \epsilon_{subj}$	−181.72	70.68	3×10^{-15}	0.77
$RT = \beta_0 + \beta_1 \cdot X_{setsize} + \beta_2 \cdot X_{guided} + \epsilon_{subj}$	−307.57	133.86	2×10^{-16}	0.96
$RT = \beta_0 + \beta_1 \cdot X_{setsize} + \beta_2 \cdot X_{guided} + \beta_3 \cdot X_{interaction} + \epsilon_{subj_setsize}$	−306.08	0.51	0.47	0.96

with:

ϵ_{subj_*} being the subject-specific random effects on the different variables, and

$$X_{setsize} = \begin{cases} 1, & \text{set size 16.} \\ 2, & \text{set size 32.} \end{cases} \tag{A.1}$$

$$X_{guided} = \begin{cases} 0, & \text{unguided.} \\ 1, & \text{guided.} \end{cases} \tag{A.2}$$

Table A.2: Reaction time contrasts between conditions (dependent-sample Wilcoxon signed rank test). SE indicates the standard of the difference between means. All comparisons are Bonferroni corrected.

	unguided search, 16	**guided search, 16**	**unguided search, 32**
guided search, 16	$V(30) = 481$ $z = 4.57$ $p = 8 \times 10^{-6}$ $r = 0.82$ $SE_{diff} = 0.02$		
unguided search, 32	$V(30) = 5$ $z = 4.76$ $p = 6 \times 10^{-7}$ $r = 0.86$ $SE_{diff} = 0.02$	$V(30) = 0$ $z = 4.86$ $p = 1 \times 10^{-11}$ $r = 0.87$ $SE_{diff} = 0.03$	
guided search, 32	$V(30) = 134$ $z = 2.34$ $p = 0.148$ **n.s.** $r = 0.40$ $SE_{diff} = 0.081$	$V(30) = 0$ $z = 4.86$ $p = 1 \times 10^{-11}$ $r = 0.87$ $SE_{diff} = 0.02$	$V(30) = 473$ $z = 4.41$ $p = 4 \times 10^{-5}$ $r = 0.79$ $SE_{diff} = 0.02$

Table A.3: Hierarchical regression on accuracy (d'), revealing a significant main effect for set size and guided/unguided, but no interaction effect.

Model	**AIC**	χ^2	**p**	$\mathbf{R^2}$
$RT = \beta_0 + \epsilon_{subj}$	307.1			0.48
$RT = \beta_0 + \beta_1 \cdot X_{setsize} + \epsilon_{subj}$	261.56	47.54	5×10^{-12}	0.68
$RT = \beta_0 + \beta_1 \cdot X_{setsize} + \beta_2 \cdot X_{guided} + \epsilon_{subj}$	217.96	45.60	1×10^{-11}	0.8
$RT = \beta_0 + \beta_1 \cdot X_{setsize} + \beta_2 \cdot X_{guided} + \beta_3 \cdot X_{interaction} + \epsilon_{subj_setsize}$	219.05	0.91	0.34	0.8

Table A.4: Sensitivity contrasts between conditions (post-hoc dependent sample t-tests, two-sided, Bonferroni-corrected).

	unguided search, 16	**guided search, 16**	**unguided search, 32**
guided search, 16	$t(30) = -5.9$ $p = 8 \times 10^{-5}$ $d = -0.84$ $SE_{diff} = 0.11$		
unguided search, 32	$t(30) = 7$ $p = 6 \times 10^{-7}$ $d = 0.8$ $SE_{diff} = 0.10$	$t(30) = 10.6$ $p = 7 \times 10^{-11}$ $d = 1.67$ $SE_{diff} = 0.12$	
guided search, 32	$t(30) = 2.2$ $p = 0.23$ **n.s.** $d = 0.8$ $SE_{diff} = 0.10$	$t(30) = 10.6$ $p = 7 \times 10^{-11}$ $d = 1.67$ $SE_{diff} = 0.12$	$t(30) = -5.6$ $p = 3 \times 10^{-6}$ $r = -0.55$ $SE_{diff} = 0.09$

Table A.5: Dependent sample t-tests on the number of saccades for fast vs slow trials reveals no significant effects of reaction time on saccades. The p-values are Benjamini-Hochberg corrected, however, none of the uncorrected p-values reached significance either.

unguided search, 16	**guided search, 16**	**unguided search, 32**	**guided search, 32**
$t(30) = -0.92$ $p = 0.34$	$t(30) = -1.70$ $p = 0.30$	$t(30) = -1.47$ $p = 0.30$	$t(30) = -1.21$ $p = 0.31$

Table A.6: Dependent sample t-tests on the number of saccades for trials with high vs low pre-search alpha power. There is only a significant difference in unguided search, set size 32 for high vs low alpha power. The p-values are Benjamini-Hochberg corrected, however, none of the results reached significance without the correction either.

unguided search, 16	**guided search, 16**	**unguided search, 32**	**guided search, 32**
$t(30) = -1.67$ $p = 0.14$	$t(30) = -1.96$ $p = 0.12$	$t(30) = -3.91$ $p = 0.002$	$t(30) = -1.53$ $p = 0.14$

Table A.7: Dependent sample t-tests on the number of saccades for trials with high vs low alpha power during search. There is only a significant difference in unguided search, set size 32 for high vs low alpha power. The p-values are Benjamini-Hochberg corrected; however none of the results reached significance without the correction either. Comparison to the table above suggests little variation in the average number of saccades.

unguided search, 16	**guided search, 16**	**unguided search, 32**	**guided search, 32**
$t(30) = -1.67$ $p = 0.14$	$t(30) = -1.96$ $p = 0.12$	$t(30) = -3.91$ $p = 0.002$	$t(30) = -1.53$ $p = 0.14$

B

Appendix Chapter 4

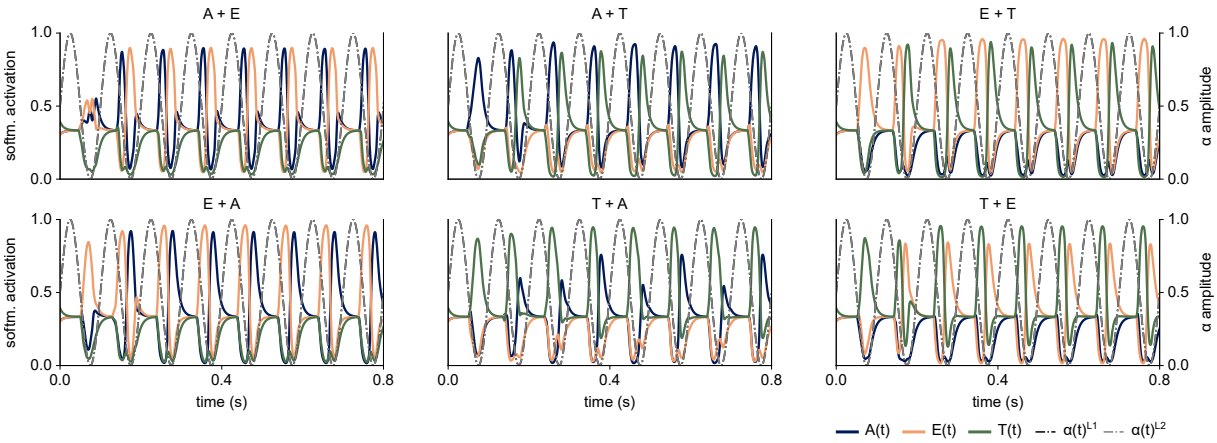

Figure B.1: Examples of the temporal code for all input combinations. The first letter in the title is the one for which input gain has been increased.

References

Adaikkan, C., Middleton, S. J., Marco, A., Pao, P.-C., Mathys, H., Kim, D. N.-W., Gao, F., Young, J. Z., Suk, H.-J., Boyden, E. S., McHugh, T. J., & Tsai, L.-H. (2019). Gamma entrainment binds higher-order brain regions and offers neuroprotection. *Neuron*, *102*(5), 929–943.e8. https://doi.org/10.1016/j.neuron.2019.04.011

Adaikkan, C., & Tsai, L.-H. (2020). Gamma entrainment: Impact on neurocircuits, glia, and therapeutic opportunities. *Trends in Neurosciences*, *43*(1), 24–41. https://doi.org/10.1016/j.tins.2019.11.001

Adrian, E. D., & Matthews, B. H. C. (1934). The berger rhythm: Potential changes from the occipital lobes in man. *Brain*, *57*(4), 355–385. https://doi.org/10.1093/brain/57.4.355

Adrian, E. D. B., & Yamagiwa, K. (1935). The origin of the berger rhythm. *Brain*, *58*(3), 323–351. https://doi.org/10.1093/brain/58.3.323

Aertsen, A., & Arndt, M. (1993). Response synchronization in the visual cortex. *Current Opinion in Neurobiology*, *3*(4), 586–594. https://doi.org/10.1016/0959-4388(93)90060-C

Akam, T. E., & Kullmann, D. M. (2012). Efficient "communication through coherence" requires oscillations structured to minimize interference between signals. *PLoS computational biology*, *8*(11), e1002760. https://doi.org/10.1371/journal.pcbi.1002760

Akam, T. E., & Kullmann, D. M. (2014). Oscillatory multiplexing of population codes for selective communication in the mammalian brain. *Nature Reviews. Neuroscience*, *15*(2), 111–122. https://doi.org/10.1038/nrn3668

Alamia, A., Terral, L., D'Ambra, M. R., & VanRullen, R. (2023). Distinct roles of forward and backward alpha-band waves in spatial visual attention. *eLife*, *12*, e85035. https://doi.org/10.7554/eLife.85035

Alamia, A., & VanRullen, R. (2019). Alpha oscillations and traveling waves: Signatures of predictive coding? *PLOS Biology*, *17*(10), e3000487. https://doi.org/10.1371/journal.pbio.3000487

Alamia, A., & VanRullen, R. (2023). A traveling waves perspective on temporal binding. *Journal of Cognitive Neuroscience*, 1–9. https://doi.org/10.1162/jocn_a_02004

Allport, A. (2011). Attention and integration. In C. Mole, D. Smithies, & W. Wu (Eds.), *Attention: Philosophical and psychological essays* (p. 24). Oxford University Press.

Andersen, S. K., & Müller, M. M. (2010). Behavioral performance follows the time course of neural facilitation and suppression during cued shifts of feature-selective attention. *Proceedings of the National Academy of Sciences of the United States of America*, *107*(31), 13878–13882. https://doi.org/10.1073/pnas.1002436107

Andersen, S. K., Hillyard, S. A., & Müller, M. M. (2008). Attention facilitates multiple stimulus features in parallel in human visual cortex. *Current Biology*, *18*(13), 1006–1009. https://doi.org/10.1016/j.cub.2008.06.030

Anderson, J., Lampl, I., Reichova, I., Carandini, M., & Ferster, D. (2000). Stimulus dependence of two-state fluctuations of membrane potential in cat visual cortex. *Nature Neuroscience*, *3*(6), 617–621. https://doi.org/10.1038/75797

Anderson, R. W., & Strowbridge, B. W. (2014). Alpha-band oscillations in intracellular membrane potentials of dentate gyrus neurons in awake rodents. *Learning & Memory*, *21*(12), 656–661. https://doi.org/10.1101/lm.036269.114

Andrade-Talavera, Y., Fisahn, A., & Rodríguez-Moreno, A. (2023). Timing to be precise? an overview of spike timing-dependent plasticity, brain rhythmicity, and glial cells interplay within neuronal circuits. *Molecular Psychiatry*, 1–12. https://doi.org/10.1038/s41380-023-02027-w

Antonov, P. A., Chakravarthi, R., & Andersen, S. K. (2020). Too little, too late, and in the wrong place: Alpha band activity does not reflect an active mechanism of selective attention. *NeuroImage*, 117006. https://doi.org/10.1016/j.neuroimage.2020.117006

Appelbaum, L. G., & Norcia, A. M. (2009). Attentive and pre-attentive aspects of figural processing. *Journal of Vision*, *9*(11), 18. https://doi.org/10.1167/9.11.18

Averbeck, B. B., Latham, P. E., & Pouget, A. (2006). Neural correlations, population coding and computation. *Nature Reviews Neuroscience*, *7*(5), 358–366. https://doi.org/10.1038/nrn1888

Awh, E., Belopolsky, A. V., & Theeuwes, J. (2012). Top-down versus bottom-up attentional control: A failed theoretical dichotomy. *Trends in Cognitive Sciences*, *16*(8), 437–443. https://doi.org/10.1016/j.tics.2012.06.010

Ayzenberg, V., & Behrmann, M. (2022). Does the brain's ventral visual pathway compute object shape? *Trends in Cognitive Sciences*, *26*(12), 1119–1132. https://doi.org/10.1016/j.tics.2022.09.019

Bahramisharif, A., Van Gerven, M., Heskes, T., & Jensen, O. (2010). Covert attention allows for continuous control of brain–computer interfaces. *European Journal of Neuroscience*, *31*(8), 1501–1508. https://doi.org/10.1111/j.1460-9568.2010.07174.x

Bahramisharif, A., van Gerven, M. A. J., Aarnoutse, E. J., Mercier, M. R., Schwartz, T. H., Foxe, J. J., Ramsey, N. F., & Jensen, O. (2013). Propagating neocortical gamma bursts are coordinated by traveling alpha waves. *Journal of Neuroscience*, *33*(48), 18849–18854. https://doi.org/10.1523/JNEUROSCI.2455-13.2013

Baillet, S. (2013). Forward and inverse problems of MEG/EEG. In D. Jaeger & R. Jung (Eds.), *Encyclopedia of computational neuroscience* (pp. 1–8). Springer New York. https://doi.org/10.1007/978-1-4614-7320-6_529-1

Bartoli, E., Bosking, W., Chen, Y., Li, Y., Sheth, S. A., Beauchamp, M. S., Yoshor, D., & Foster, B. L. (2019). Functionally distinct gamma range activity revealed by stimulus tuning in human visual cortex. *Current Biology*, *29*, 3345–3358. https://doi.org/10.1016/j.cub.2019.08.004

Bartos, M., Vida, I., & Jonas, P. (2007). Synaptic mechanisms of synchronized gamma oscillations in inhibitory interneuron networks, 12.

Başar, E. (2013). Brain oscillations in neuropsychiatric disease. *Dialogues in Clinical Neuroscience*, *15*(3), 291–300. Retrieved July 14, 2023, from https://www.ncbi.nlm.nih.gov/pmc/articles/PMC3811101/

Başar, E., Başar-Eroğlu, C., Karakaş, S., & Schürmann, M. (2000). Brain oscillations in perception and memory. *International Journal of Psychophysiology*, *35*(2), 95–124. https://doi.org/10.1016/S0167-8760(99)00047-1

Başar-Eroglu, C., Strüber, D., Schürmann, M., Stadler, M., & Başar, E. (1996). Gamma-band responses in the brain: A short review of psychophysiological correlates and functional significance. *International Journal of Psychophysiology*, *24*(1), 101–112. https://doi.org/10.1016/S0167-8760(96)00051-7

Bastos, A. M., Vezoli, J., & Fries, P. (2015). Communication through coherence with inter-areal delays. *Current Opinion in Neurobiology*, *31*, 173–180. https://doi.org/10.1016/j.conb.2014.11.001

Bastos, A. M., & Schoffelen, J.-M. (2016). A tutorial review of functional connectivity analysis methods and their interpretational pitfalls. *Frontiers in Systems Neuroscience*, *9*, 175. https://doi.org/10.3389/fnsys.2015.00175

Bastos, A. M., Vezoli, J., Bosman, C. A., Schoffelen, J.-M., Oostenveld, R., Dowdall, J. R., De Weerd, P., Kennedy, H., & Fries, P. (2015). Visual areas exert feedforward and feedback influences through distinct frequency channels. *Neuron*, *85*(2), 390–401. https://doi.org/10.1016/j.neuron.2014.12.018

Bauer, M., Akam, T., Joseph, S., Freeman, E., & Driver, J. (2012). Does visual flicker phase at gamma frequency modulate neural signal propagation and stimulus selection? *Journal of Vision*, *12*, 1–10. https://doi.org/10.1167/12.4.5

Bayguinov, P. O., Ghitani, N., Jackson, M. B., & Basso, M. A. (2015). A hard-wired priority map in the superior colliculus shaped by asymmetric inhibitory circuitry. *Journal of Neurophysiology*, *114*(1), 662–676. https://doi.org/10.1152/jn.00144.2015

Beck, D. M., & Kastner, S. (2005). Stimulus context modulates competition in human extrastriate cortex. *Nature Neuroscience*, *8*(8), 1110–1116. https://doi.org/10.1038/nn1501

Belardinelli, P., Ortiz, E., & Braun, C. (2012). Source activity correlation effects on LCMV beamformers in a realistic measurement environment. *Computational and Mathematical Methods in Medicine*, *2012*, 190513. https://doi.org/10.1155/2012/190513

Benwell, C. S. Y., Keitel, C., Harvey, M., Gross, J., & Thut, G. (2018). Trial-by-trial co-variation of pre-stimulus EEG alpha power and visuospatial bias reflects a mixture of stochastic and deterministic effects. *European Journal of Neuroscience*, *48*(7), 2566–2584. https://doi.org/10.1111/ejn.13688

Benwell, C. S. Y., London, R. E., Tagliabue, C. F., Veniero, D., Gross, J., Keitel, C., & Thut, G. (2019). Frequency and power of human alpha oscillations drift systematically with time-on-task. *NeuroImage*, *192*, 101–114. https://doi.org/10.1016/j.neuroimage.2019.02.067

Berger, H. (1929). Über das Elektrenkephalogramm des Menschen. *Archiv für Psychiatrie und Nervenkrankheiten*, *87*(1), 527–570. https://doi.org/10.1007/BF01797193

Berger, H. (1931). Über das Elektrenkephalogramm des Menschen. *Archiv für Psychiatrie und Nervenkrankheiten*, *94*(1), 16–60. https://doi.org/10.1007/BF01835097

Berger, H. (1932). Über das Elektrenkephalogramm des Menschen. *Archiv für Psychiatrie und Nervenkrankheiten*, *97*(1), 6–26. https://doi.org/10.1007/BF01815532

Berger, H. (1933a). Über das Elektrenkephalogramm des Menschen. *Archiv für Psychiatrie und Nervenkrankheiten*, *98*(1), 231–254. https://doi.org/10.1007/BF01814645

Berger, H. (1933b). Über das Elektrenkephalogramm des Menschen. *Archiv für Psychiatrie und Nervenkrankheiten*, *99*(1), 555–574. https://doi.org/10.1007/BF01814320

Berger, H. (1933c). Über das Elektrenkephalogramm des Menschen. *Archiv für Psychiatrie und Nervenkrankheiten*, *100*(1), 301–320. https://doi.org/10.1007/BF01814740

Berger, H. (1934). Über das Elektrenkephalogramm des Menschen. *Archiv für Psychiatrie und Nervenkrankheiten*, *102*(1), 538–557. https://doi.org/10.1007/BF01813827

Berger, H. (1935). Über das Elektrenkephalogramm des Menschen. *Archiv für Psychiatrie und Nervenkrankheiten*, *103*(1), 444–454. https://doi.org/10.1007/BF02024891

Besl, P., & McKay, N. D. (1992). A method for registration of 3-d shapes. *IEEE Transactions on Pattern Analysis and Machine Intelligence*, *14*(2), 239–256. https://doi.org/10.1109/34.121791

Bichot, N. P., Andrew F. Rossi, Rossi, A. F., & Desimone, R. (2005). Parallel and serial neural mechanisms for visual search in macaque area v4. *Science*, *308*(5721), 529–534. https://doi.org/10.1126/science.1109676

Bichot, N. P., & Schall, J. D. (1999). Effects of similarity and history on neural mechanisms of visual selection. *Nature Neuroscience*, *2*(6), 549–554. https://doi.org/10.1038/9205

Bisley, J. W. (2011). The neural basis of visual attention. *The Journal of Physiology*, *589*(1), 49–57. https://doi.org/10.1113/jphysiol.2010.192666

Bisley, J. W., & Goldberg, M. E. (2010). Attention, intention, and priority in the parietal lobe. *Annual review of neuroscience*, *33*, 1–21. https://doi.org/10.1146/annurev-neuro-060909-152823

Bisley, J. W., & Mirpour, K. (2019). The neural instantiation of a priority map. *Current opinion in psychology*, *29*, 108–112. https://doi.org/10.1016/j.copsyc.2019.01.002

Bollimunta, A., Chen, Y., Schroeder, C. E., & Ding, M. (2008). Neuronal mechanisms of cortical alpha oscillations in awake-behaving macaques. *The Journal of Neuroscience: The Official Journal of the Society for Neuroscience*, *28*(40), 9976–9988. https://doi.org/10.1523/JNEUROSCI.2699-08.2008

Bollimunta, A., Mo, J., Schroeder, C. E., & Ding, M. (2011). Neuronal mechanisms and attentional modulation of corticothalamic α oscillations. *The Journal of Neuroscience: The Official Journal of the Society for Neuroscience*, *31*(13), 4935–4943. https://doi.org/10.1523/JNEUROSCI.5580-10.2011

Bonnefond, M., Kastner, S., & Jensen, O. (2017). Communication between brain areas based on nested oscillations. *eNeuro*, *4*(2). https://doi.org/10.1523/ENEURO.0153-16.2017

Börgers, C., Epstein, S., & Kopell, N. J. (2008). Gamma oscillations mediate stimulus competition and attentional selection in a cortical network model. *Proceedings of the National Academy of Sciences*, *105*(46), 18023–18028. https://doi.org/10.1073/pnas.0809511105

Börgers, C., & Kopell, N. (2003). Synchronization in networks of excitatory and inhibitory neurons with sparse, random connectivity. *Neural Computation*, *15*(3), 509–538. https://doi.org/10.1162/089976603321192059

Borgiotti, G., & Kaplan, L. (1979). Superresolution of uncorrelated interference sources by using adaptive array techniques. *IEEE Transactions on Antennas and Propagation*, *27*(6), 842–845. https://doi.org/10.1109/TAP.1979.1142176

Bosman, C. A., Schoffelen, J.-M., Brunet, N., Oostenveld, R., Bastos, A. M., Womelsdorf, T., Rubehn, B., Stieglitz, T., De Weerd, P., & Fries, P. (2012). Attentional stimulus selection through selective synchronization between monkey visual areas. *Neuron*, *75*(5), 875–888. https://doi.org/10.1016/j.neuron.2012.06.037

Bouwkamp, F. G., Lange, F. P. d., & Spaak, E. (2023, July 14). Spatial predictive context speeds up visual search by biasing local attentional competition. https://doi.org/10.1101/2023.07.14.548976

Brainard, D. H. (1997). The psychophysics toolbox. *Spatial Vision*, *10*(4), 433–436. https://doi.org/10.1163/156856897X00357

Bressler, S. L. (1990). The gamma wave: A cortical information carrier? *Trends in Neurosciences*, *13*, 161–162. https://doi.org/10.1016/0166-2236(90)90039-D

Bressler, S. L., Coppola, R., & Nakamura, R. (1993). Episodic multiregional cortical coherence at multiple frequencies during visual task performance. *Nature*, *366*(6451), 153–156. https://doi.org/10.1038/366153a0

Bressler, S. L., & Kelso, J. A. S. (2001). Cortical coordination dynamics and cognition. *Trends in Cognitive Sciences*, *5*(1), 26–36. https://doi.org/10.1016/S1364-6613(00)01564-3

Brickwedde, M., Bezsudnova, Y., Kowalczyk, A., Jensen, O., & Zhigalov, A. (2022). Application of rapid invisible frequency tagging for brain computer interfaces. *Journal of Neuroscience Methods*, *382*, 109726. https://doi.org/10.1016/j.jneumeth.2022.109726

Brickwedde, M., Limachya, R., Markiewicz, R., Sutton, E., Shapiro, K. L., Jensen, O., & Mazaheri, A. (2022, April 19). Cross-modal alterations of alpha activity do not reflect

inhibition of early sensory processing: A frequency tagging study. https://doi.org/10.1101/2022.04.19.488727

Broadbent, D. E. (1958). *Perception and communication*. Pergamon Press. https://doi.org/10.1037/10037-000

Brosch, M., Budinger, E., & Scheich, H. (2002). Stimulus-related gamma oscillations in primate auditory cortex. *Journal of Neurophysiology*, *87*, 2715–2725. https://doi.org/10.1152/jn.2002.87.6.2715

Brunet, N., Bosman, C. A., Roberts, M., Oostenveld, R., Womelsdorf, T., De Weerd, P., & Fries, P. (2015). Visual cortical gamma-band activity during free viewing of natural images. *Cerebral cortex*, *25*, 918–926. https://doi.org/10.1093/cercor/bht280

Brunet, N., Vinck, M., Bosman, C. A., Singer, W., & Fries, P. (2014). Gamma or no gamma, that is the question. *Trends in Cognitive Sciences*, *18*(10), 507–509. https://doi.org/10.1016/j.tics.2014.08.006

Brunet, N. M., & Fries, P. (2019). Human visual cortical gamma reflects natural image structure. *NeuroImage*, *200*, 635–643. https://doi.org/10.1016/j.neuroimage.2019.06.051

Budd, J. M. (1998). Extrastriate feedback to primary visual cortex in primates: A quantitative analysis of connectivity. *Proceedings of the Royal Society of London. Series B: Biological Sciences*, *265*(1400), 1037–1044. https://doi.org/10.1098/rspb.1998.0396

Buergers, S., & Noppeney, U. (2022). The role of alpha oscillations in temporal binding within and across the senses. *Nature Human Behaviour*, *6*(5), 732–742. https://doi.org/10.1038/s41562-022-01294-x

Buffalo, E. A., Fries, P., Landman, R., Buschman, T. J., & Desimone, R. (2011). Laminar differences in gamma and alpha coherence in the ventral stream. *Proceedings of the National Academy of Sciences*, *108*(27), 11262–11267. https://doi.org/10.1073/pnas.1011284108

Bundesen, C. (1990). A theory of visual attention. *Psychological Review*, *97*(4), 523–547. https://doi.org/10.1037/0033-295x.97.4.523

Burns, S. P., Xing, D., & Shapley, R. M. (2011). Is gamma-band activity in the local field potential of v1 cortex a "clock" or filtered noise? *Journal of Neuroscience*, *31*(26), 9658–9664. https://doi.org/10.1523/JNEUROSCI.0660-11.2011

Busch, N. A., & VanRullen, R. (2010). Spontaneous EEG oscillations reveal periodic sampling of visual attention. *Proceedings of the National Academy of Sciences*, *107*(37), 16048–16053. https://doi.org/10.1073/pnas.1004801107

Busch, N. A., Debener, S., Kranczioch, C., Engel, A. K., & Herrmann, C. S. (2004). Size matters: Effects of stimulus size, duration and eccentricity on the visual gamma-band response. *Clinical Neurophysiology: Official Journal of the International Federation of Clinical Neurophysiology*, *115*(8), 1810–1820. https://doi.org/10.1016/j.clinph.2004.03.015

Buschman, T. J., & Miller, E. K. (2007). Top-down versus bottom-up control of attention in the prefrontal and posterior parietal cortices. *Science (New York, N.Y.)*, *315*(5820), 1860–1862. https://doi.org/10.1126/science.1138071

Buzsáki, G. (2010). Neural syntax: Cell assemblies, synapsembles, and readers. *Neuron*, *68*(3), 362–385. https://doi.org/10.1016/j.neuron.2010.09.023

Buzsáki, G., Anastassiou, C. A., & Koch, C. (2012). The origin of extracellular fields and currents–EEG, ECoG, LFP and spikes. *Nature Reviews. Neuroscience*, *13*(6), 407–420. https://doi.org/10.1038/nrn3241

Buzsáki, G., & Draguhn, A. (2004). Neuronal oscillations in cortical networks. *Science*, *304*(5679), 1926–1929. https://doi.org/10.1126/science.1099745

Buzsáki, G., Logothetis, N., & Singer, W. (2013). Scaling brain size, keeping timing: Evolutionary preservation of brain rhythms. *Neuron*, *80*(3), 751–764. https://doi.org/10.1016/j.neuron.2013.10.002

Buzsáki, G., & Schomburg, E. W. (2015). What does gamma coherence tell us about inter-regional neural communication? *Nature Neuroscience*, *18*(4), 484–489. https://doi.org/10.1038/nn.3952

Buzsáki, G., & Vöröslakos, M. (2023). Brain rhythms have come of age. *Neuron*, *111*(7), 922–926. https://doi.org/10.1016/j.neuron.2023.03.018

Buzsáki, G., & Wang, X.-J. (2012). Mechanisms of gamma oscillations. *Annual Review of Neuroscience*, *35*(1), 203–225. https://doi.org/10.1146/annurev-neuro-062111-150444

Buzsáki, G., & Watson, B. O. (2012). Brain rhythms and neural syntax: Implications for efficient coding of cognitive content and neuropsychiatric disease. *Dialogues in Clinical Neuroscience*, *14*(4), 345–367. https://doi.org/10.31887/DCNS.2012.14.4/gbuzsaki

Cajochen, C., Brunner, D. P., Krauchi, K., Graw, P., & Wirz-Justice, A. (1995). Power density in theta/alpha frequencies of the waking EEG progressively increases during sustained wakefulness. *Sleep*, *18*(10), 890–894. https://doi.org/10.1093/sleep/18.10.890

Callaway, E., & Yeager, C. L. (1960). Relationship between reaction time and electroencephalographic alpha phase. *Science*, *132*(3441), 1765–1766. https://doi.org/10.1126/science.132.3441.1765

Capotosto, P., Babiloni, C., Romani, G. L., & Corbetta, M. (2009). Frontoparietal cortex controls spatial attention through modulation of anticipatory alpha rhythms. *The Journal of Neuroscience: The Official Journal of the Society for Neuroscience*, *29*(18), 5863–5872. https://doi.org/10.1523/JNEUROSCI.0539-09.2009

Carandini, M. (2005). Do we know what the early visual system does? *Journal of Neuroscience*, *25*(46), 10577–10597. https://doi.org/10.1523/JNEUROSCI.3726-05.2005

Carandini, M., Heeger, D. J., & Movshon, J. A. (1997). Linearity and normalization in simple cells of the macaque primary visual cortex. *Journal of Neuroscience*, *17*, 8621–8644. https://doi.org/10.1523/jneurosci.17-21-08621.1997

Cardin, J. A. (2016). Snapshots of the brain in action: Local circuit operations through the lens of γ oscillations. *Journal of Neuroscience*, *36*(41), 10496–10504. https://doi.org/10.1523/JNEUROSCI.1021-16.2016

Cardin, J. A., Carlén, M., Meletis, K., Knoblich, U., Zhang, F., Deisseroth, K., Tsai, L.-H., & Moore, C. I. (2009). Driving fast-spiking cells induces gamma rhythm and controls sensory responses. *Nature*, *459*(7247), 663–667. https://doi.org/10.1038/nature08002

Carrasco, M. (2011). Visual attention: The past 25 years. *Vision Research*, *51*(13), 1484–1525. https://doi.org/10.1016/j.visres.2011.04.012

Caruso, V. C., Mohl, J. T., Glynn, C., Lee, J., Willett, S. M., Zaman, A., Ebihara, A. F., Estrada, R., Freiwald, W. A., Tokdar, S. T., & Groh, J. M. (2018). Single neurons may encode simultaneous stimuli by switching between activity patterns. *Nature Communications*, *9*(1), 2715. https://doi.org/10.1038/s41467-018-05121-8

Chan, D., Suk, H.-J., Jackson, B. L., Milman, N. P., Stark, D., Klerman, E. B., Kitchener, E., Avalos, V. S. F., Weck, G. d., Banerjee, A., Beach, S. D., Blanchard, J., Stearns, C., Boes, A. D., Uitermarkt, B., Gander, P., Iii, M. H., Sternberg, E. J., Nieto-Castanon, A., . . . Tsai, L.-H. (2022). Gamma frequency sensory stimulation in mild probable alzheimer's dementia patients: Results of feasibility and pilot studies. *PLOS ONE*, *17*(12), e0278412. https://doi.org/10.1371/journal.pone.0278412

Chelazzi, L., Miller, E. K., Duncan, J., & Desimone, R. (1993). A neural basis for visual search in inferior temporal cortex. *Nature*, *363*(6427), 345–347. https://doi.org/10.1038/363345a0

Chen, R. T. Q., Rubanova, Y., Bettencourt, J., & Duvenaud, D. K. (2018). Neural ordinary differential equations. *Advances in Neural Information Processing Systems*, *31*. Retrieved April 7, 2022, from https://proceedings.neurips.cc/paper/2018/hash/69386f6bb1dfed68692a24c8686939b9-Abstract.html

Chen, Y., Seth, A. K., Gally, J. A., & Edelman, G. M. (2003). The power of human brain magnetoencephalographic signals can be modulated up or down by changes in an attentive visual task. *Proceedings of the National Academy of Sciences*, *100*(6), 3501–3506. https://doi.org/10.1073/pnas.0337630100

Chen, Y., & Seidemann, E. (2012). Attentional modulations related to spatial gating but not to allocation of limited resources in primate v1. *Neuron*, *74*(3), 557–566. https://doi.org/10.1016/j.neuron.2012.03.033

Chollet, F. (2021). *Deep learning with python*. Simon; Schuster.

Cichy, R. M., Khosla, A., Pantazis, D., & Oliva, A. (2017). Dynamics of scene representations in the human brain revealed by magnetoencephalography and deep neural networks. *NeuroImage*, *153*, 346–358. https://doi.org/10.1016/j.neuroimage.2016.03.063

Cichy, R. M., Khosla, A., Pantazis, D., Torralba, A., & Oliva, A. (2016). Comparison of deep neural networks to spatio-temporal cortical dynamics of human visual object recognition reveals hierarchical correspondence. *Scientific Reports*, *6*(1), 27755. https://doi.org/10.1038/srep27755

Cichy, R. M., & Oliva, A. (2020). A m/EEG-fMRI fusion primer: Resolving human brain responses in space and time. *Neuron*, *107*(5), 772–781. https://doi.org/10.1016/j.neuron.2020.07.001

Cichy, R. M., Pantazis, D., & Oliva, A. (2014). Resolving human object recognition in space and time. *Nature Neuroscience*, *17*(3), 455–462. https://doi.org/10.1038/nn.3635

Clark, J. H. (1924). The ishihara test for color blindness. *American Journal of Physiological Optics*, *5*, 269–276.

Coen-Cagli, R., Kohn, A., & Schwartz, O. (2015). Flexible gating of contextual influences in natural vision. *Nature Neuroscience*, *18*(11), 1648–1655. https://doi.org/10.1038/nn.4128

Cohen, G., Afshar, S., Tapson, J., & van Schaik, A. (2017). EMNIST: Extending MNIST to handwritten letters. *2017 International Joint Conference on Neural Networks (IJCNN)*, 2921–2926. https://doi.org/10.1109/IJCNN.2017.7966217

Cohen, M. R., & Maunsell, J. H. R. (2009). Attention improves performance primarily by reducing interneuronal correlations. *Nature Neuroscience*, *12*(12), 1594–1600. https://doi.org/10.1038/nn.2439

Cohen, M. X. (2014, January 17). *Analyzing neural time series data: Theory and practice*. The MIT Press. https://doi.org/10.7551/mitpress/9609.001.0001

Colavita, F. B. (1974). Human sensory dominance. *Perception & Psychophysics*, *16*(2), 409–412. https://doi.org/10.3758/BF03203962

Collins, N. (2017, August 21). *Carla shatz, her breakthrough discovery in vision and the developing brain* [Stanford medicine magazine]. Retrieved November 2, 2023, from https://stanmed.stanford.edu/carla-shatz-vision-brain/

Connelly, W. M., Laing, M., Errington, A. C., & Crunelli, V. (2016). The thalamus as a low pass filter: Filtering at the cellular level does not equate with filtering at the network level. *Frontiers in Neural Circuits*, *9*. https://doi.org/10.3389/fncir.2015.00089

Conway, B. R. (2014). Color signals through dorsal and ventral visual pathways. *Visual Neuroscience*, *31*(2), 197–209. https://doi.org/10.1017/S0952523813000382

Cooper, N. R., Croft, R. J., Dominey, S. J. J., Burgess, A. P., & Gruzelier, J. H. (2003). Paradox lost? exploring the role of alpha oscillations during externally vs. internally directed attention and the implications for idling and inhibition hypotheses. *International Journal of Psychophysiology*, *47*(1), 65–74. https://doi.org/10.1016/S0167-8760(02)00107-1

Cormack, L. K. (2005). Computational models of early human vision. In *Handbook of image and video processing* (pp. 325–345). Elsevier. https://doi.org/10.1016/B978-012119792-6/50083-8

Cosman, J. D., Lowe, K. A., Zinke, W., Woodman, G. F., & Schall, J. D. (2018). Prefrontal control of visual distraction. *Current Biology*, *28*(3), 1330–1330. https://doi.org/10.1016/j.cub.2017.12.023

Craig, A., Tran, Y., Wijesuriya, N., & Nguyen, H. (2012). Regional brain wave activity changes associated with fatigue. *Psychophysiology*, *49*(4), 574–582. https://doi.org/10.1111/j.1469-8986.2011.01329.x

Daniel, R. S. (1967). Alpha and theta EEG in vigilance. *Perceptual and Motor Skills*. https://doi.org/10.2466/pms.1967.25.3.697

Davis, Z. W., Muller, L., Trujillo, J.-M., Sejnowski, T., & Reynolds, J. H. (2020). Spontaneous traveling cortical waves gate perception in behaving primates. *Nature*, *587*(7834), 432–436. https://doi.org/10.1038/s41586-020-2802-y

Desimone, R., & Duncan, J. (1995). Neural mechanisms of selective visual attention. *Annual Review of Neuroscience*, *18*(1), 193–222. https://doi.org/10.1146/annurev.ne.18.030195.001205

de Vries, S. E. J., Lecoq, J. A., Buice, M. A., Groblewski, P. A., Ocker, G. K., Oliver, M., Feng, D., Cain, N., Ledochowitsch, P., Millman, D., Roll, K., Garrett, M., Keenan, T.,

Kuan, L., Mihalas, S., Olsen, S., Thompson, C., Wakeman, W., Waters, J., . . . Koch, C. (2020). A large-scale standardized physiological survey reveals functional organization of the mouse visual cortex. *Nature Neuroscience*, *23*(1), 138–151. https://doi.org/10.1038/s41593-019-0550-9

DiCarlo, J. J., & Cox, D. D. (2007). Untangling invariant object recognition. *Trends in Cognitive Sciences*, *11*(8), 333–341. https://doi.org/10.1016/j.tics.2007.06.010

DiCarlo, J. J., Zoccolan, D., & Rust, N. C. (2012). How does the brain solve visual object recognition? *Neuron*, *73*(3), 415–434. https://doi.org/10.1016/j.neuron.2012.01.010

Diehl, P. U., Martel, J., Buhmann, J., & Cook, M. (2018). Factorized computation: What the neocortex can tell us about the future of computing. *Frontiers in Computational Neuroscience*, *12*. Retrieved September 20, 2023, from https://www.frontiersin.org/articles/10.3389/fncom.2018.00054

Dijk, H. v., Schoffelen, J.-M., Oostenveld, R., & Jensen, O. (2008). Prestimulus oscillatory activity in the alpha band predicts visual discrimination ability. *Journal of Neuroscience*, *28*(8), 1816–1823. https://doi.org/10.1523/JNEUROSCI.1853-07.2008

Donohue, S. E., Bartsch, M. V., Heinze, H.-J., Schoenfeld, M. A., & Hopf, J.-M. (2018). Cortical mechanisms of prioritizing selection for rejection in visual search. *The Journal of Neuroscience*, *38*(20), 4738–4748. https://doi.org/10.1523/JNEUROSCI.2407-17.2018

Donohue, S. E., Schoenfeld, M. A., & Hopf, J.-M. (2020). Parallel fast and slow recurrent cortical processing mediates target and distractor selection in visual search. *Communications Biology*, *3*(1), 1–10. https://doi.org/10.1038/s42003-020-01423-0

Dougherty, K., Cox, M. A., Ninomiya, T., Leopold, D. A., & Maier, A. (2017). Ongoing alpha activity in v1 regulates visually driven spiking responses. *Cerebral Cortex*, *27*, 1113–1124. https://doi.org/10.1093/cercor/bhv304

Douglas, R. J., & Martin, K. A. C. (2004). Neuronal circuits of the neocortex. *Annual Review of Neuroscience*, *27*, 419–451. https://doi.org/10.1146/annurev.neuro.27.070203.144152

Dowdall, J. R., Schneider, M., & Vinck, M. (2023). Attentional modulation of inter-areal coherence explained by frequency shifts. *NeuroImage*, *277*, 120256. https://doi.org/10.1016/j.neuroimage.2023.120256

Drijvers, L., Spaak, E., & Jensen, O. (2020). Rapid invisible frequency tagging reveals nonlinear integration of auditory and visual semantic information. *bioRxiv*. https://doi.org/10.1101/2020.04.29.067454

Duecker, K., Gutteling, T. P., Herrmann, C. S., & Jensen, O. (2020, September 26). No evidence for entrainment: Endogenous gamma oscillations and rhythmic flicker responses coexist in visual cortex. https://doi.org/10.1101/2020.09.02.279497

Duecker, K., Gutteling, T. P., Herrmann, C. S., & Jensen, O. (2021). No evidence for entrainment: Endogenous gamma oscillations and rhythmic flicker responses coexist in visual cortex. *Journal of Neuroscience*, *41*(31), 6684–6698. https://doi.org/10.1523/JNEUROSCI.3134-20.2021

Duecker, K., Shapiro, K. L., Hanslmayr, S., Wolfe, J., Pan, Y., & Jensen, O. (2023, August 3). Alpha oscillations support the efficiency of guided visual search by inhibiting both target and distractor features in early visual cortex. https://doi.org/10.1101/2023.08.03.551520

Dugué, L., Marque, P., & VanRullen, R. (2011). The phase of ongoing oscillations mediates the causal relation between brain excitation and visual perception. *Journal of Neuroscience*, *31*(33), 11889–11893. https://doi.org/10.1523/JNEUROSCI.1161-11.2011

Dustman, R. E., & Beck, E. C. (1965). Phase of alpha brain waves, reaction time and visually evoked potentials. *Electroencephalography and Clinical Neurophysiology*, *18*(5), 433–440. https://doi.org/10.1016/0013-4694(65)90123-9

Eckhorn, R., Bauer, R., Jordan, W., Brosch, M., Kruse, W., Munk, M., & Reitboeck, H. J. (1988). Coherent oscillations: A mechanism of feature linking in the visual cortex? - multiple electrode and correlation analyses in the cat. *Biological Cybernetics*, *60*, 121–130. https://doi.org/10.1007/BF00202899

Effenberger, F., Carvalho, P., Dubinin, I., & Singer, W. (2022, November 29). A biology-inspired recurrent oscillator network for computations in high-dimensional state space. https://doi.org/10.1101/2022.11.29.518360

Egeth, H. E., Virzi, R. A., & Garbart, H. (1984). Searching for conjunctively defined targets. *Journal of Experimental Psychology: Human Perception and Performance*, *10*(1), 32–39. https://doi.org/10.1037/0096-1523.10.1.32

Einevoll, G. T., Kayser, C., Logothetis, N. K., & Panzeri, S. (2013). Modelling and analysis of local field potentials for studying the function of cortical circuits. *Nature Reviews Neuroscience*, *14*(11), 770–785. https://doi.org/10.1038/nrn3599

Engel, A. K., Fries, P., & Singer, W. (2001). Dynamic predictions: Oscillations and synchrony in top–down processing. *Nature Reviews Neuroscience*, *2*(10), 704–716. https://doi.org/10.1038/35094565

Engel, A. K., König, P., Gray, C. M., & Singer, W. (1990). Stimulus-dependent neuronal oscillations in cat visual cortex: Inter-columnar interaction as determined by cross-correlation analysis. *European Journal of Neuroscience*, *2*(7), 588–606. https://doi.org/10.1111/j.1460-9568.1990.tb00449.x

Engel, A. K., König, P., Kreiter, A. K., & Singer, W. (1991). Interhemispheric synchronization of oscillatory neuronal responses in cat visual cortex. *Science*, *252*(5009), 1177–1179. https://doi.org/10.1126/science.252.5009.1177

Engel, A. K., & Singer, W. (2001). Temporal binding and the neural correlates of sensory awareness. *Trends in Cognitive Sciences*, *5*(1), 16–25. https://doi.org/10.1016/S1364-6613(00)01568-0

Ergenoglu, T., Demiralp, T., Bayraktaroglu, Z., Ergen, M., Beydagi, H., & Uresin, Y. (2004). Alpha rhythm of the EEG modulates visual detection performance in humans. *Brain Research. Cognitive Brain Research*, *20*(3), 376–383. https://doi.org/10.1016/j.cogbrainres.2004.03.009

Fan, X., Zhou, Q., Liu, Z., & Xie, F. (2015). Electroencephalogram assessment of mental fatigue in visual search. *Bio-Medical Materials and Engineering*, *26*, S1455–S1463. https://doi.org/10.3233/BME-151444

Fara, P. (1995). An atttractive therapy: Animal magnetism in eighteenth-century england. *History of Science*, *33*(2), 127–177. https://doi.org/10.1177/007327539503300201

Fecteau, J. H., & Munoz, D. P. (2006). Salience, relevance, and firing: A priority map for target selection. *Trends in Cognitive Sciences*, *10*(8), 382–390. https://doi.org/10.1016/j.tics.2006.06.011

Feldmann-Wüstefeld, T., & Awh, E. (2020). Alpha-band activity tracks the zoom lens of attention. *Journal of Cognitive Neuroscience*, *32*(2), 272–282. https://doi.org/10.1162/jocn_a_01484

Feldmann-Wüstefeld, T., Weinberger, M., & Awh, E. (2021). Spatially guided distractor suppression during visual search. *The Journal of Neuroscience: The Official Journal of the Society for Neuroscience*, *41*(14), 3180–3191. https://doi.org/10.1523/JNEUROSCI.2418-20.2021

Fell, J., & Axmacher, N. (2011). The role of phase synchronization in memory processes. *Nature Reviews Neuroscience*, *12*(2), 105–118. https://doi.org/10.1038/nrn2979

Felleman, D. J., & Van Essen, D. C. (1991). Distributed hierarchical processing in the primate cerebral cortex. *Cerebral Cortex (New York, N.Y.: 1991)*, *1*(1), 1–47. https://doi.org/10.1093/cercor/1.1.1-a

Ferrante, O., Zhigalov, A., Hickey, C., & Jensen, O. (2023). Statistical learning of distractor suppression downregulates prestimulus neural excitability in early visual cortex. *Journal of Neuroscience*, *43*(12), 2190–2198. https://doi.org/10.1523/JNEUROSCI.1703-22.2022

Finger, S. (2005a, March 3). Edgar d. adrian: Coding in the nervous system. In S. Finger (Ed.), *Minds behind the brain: A history of the pioneers and their discoveries* (pp. 239–258). Oxford University Press. https://doi.org/10.1093/acprof:oso/9780195181821.003.0015

Finger, S. (2005b, March 3). Luigi galvani: Electricity and the nerves. In S. Finger (Ed.), *Minds behind the brain: A history of the pioneers and their discoveries* (pp. 101–118). Oxford University Press. https://doi.org/10.1093/acprof:oso/9780195181821.003.0008

Forschack, N., Gundlach, C., Hillyard, S., & Müller, M. M. (2022). Dynamics of attentional allocation to targets and distractors during visual search. *NeuroImage*, *264*, 119759. https://doi.org/10.1016/j.neuroimage.2022.119759

Foster, J. J., & Awh, E. (2019). The role of alpha oscillations in spatial attention: Limited evidence for a suppression account. *Current Opinion in Psychology*, *29*, 34–40. https://doi.org/10.1016/j.copsyc.2018.11.001

Foster, J. J., Sutterer, D. W., Serences, J. T., Vogel, E. K., & Awh, E. (2017). Alpha-band oscillations enable spatially and temporally resolved tracking of covert spatial attention. *Psychological Science*, *28*(7), 929–941. https://doi.org/10.1177/0956797617699167

Foxe, J., Simpson, G., & Ahlfors, S. (1998). Parieto-occipital ~10 hz activity reflects anticipatory state of visual attention mechanisms. *NeuroReport*, *9*(17), 3929–3933. https://doi.org/10.1097/00001756-199812010-00030

Foxe, J., & Snyder, A. (2011). The role of alpha-band brain oscillations as a sensory suppression mechanism during selective attention. *Frontiers in Psychology*, *2*. Retrieved June 1, 2022, from https://www.frontiersin.org/article/10.3389/fpsyg.2011.00154

Freud, E., Plaut, D. C., & Behrmann, M. (2016). 'what' is happening in the dorsal visual pathway. *Trends in Cognitive Sciences*, *20*(10), 773–784. https://doi.org/10.1016/j.tics.2016.08.003

Friedl, W. M., & Keil, A. (2020). Effects of experience on spatial frequency tuning in the visual system: Behavioral, visuocortical, and alpha-band responses. *Journal of Cognitive Neuroscience*, *32*, 1153–1169. https://doi.org/10.1162/jocn_a_01524

Fries, P. (2005). A mechanism for cognitive dynamics: Neuronal communication through neuronal coherence. *Trends in cognitive sciences*, *9*(10). https://doi.org/10.1016/j.tics.2005.08.011

Fries, P. (2015). Rhythms for cognition: Communication through coherence. *Neuron*, *88*(1), 220–235. https://doi.org/10.1016/j.neuron.2015.09.034

Fries, P., Neuenschwander, S., Engel, A. K., Goebel, R., & Singer, W. (2001). Rapid feature selective neuronal synchronization through correlated latency shifting. *Nature Neuroscience*, *4*(2), 194–200. https://doi.org/10.1038/84032

Fries, P., Nikolić, D., & Singer, W. (2007). The gamma cycle. *Trends in Neurosciences*, *30*(7), 309–316. https://doi.org/10.1016/j.tins.2007.05.005

Fries, P., Reynolds, J. H., Rorie, A. E., & Desimone, R. (2001). Modulation of oscillatory neuronal synchronization by selective visual attention. *Science*, *291*(5508), 1560–1563. https://doi.org/10.1126/science.1055465

Fries, P., Womelsdorf, T., Oostenveld, R., & Desimone, R. (2008). The effects of visual stimulation and selective visual attention on rhythmic neuronal synchronization in macaque area v4. *Journal of Neuroscience*, *28*(18), 4823–4835. https://doi.org/10.1523/JNEUROSCI.4499-07.2008

Fröhlich, F. (2016). *Network neuroscience*. Academic Press. https://doi.org/10.1515/9781400851935-012

Fu, K.-M. G., Foxe, J. J., Murray, M. M., Higgins, B. A., Javitt, D. C., & Schroeder, C. E. (2001). Attention-dependent suppression of distracter visual input can be cross-modally cued as indexed by anticipatory parieto–occipital alpha-band oscillations. *Cognitive Brain Research*, *12*(1), 145–152. https://doi.org/10.1016/S0926-6410(01)00034-9

Galuske, R. A. W., Munk, M. H. J., & Singer, W. (2019). Relation between gamma oscillations and neuronal plasticity in the visual cortex. *Proceedings of the National Academy of Sciences*, *116*(46), 23317–23325. https://doi.org/10.1073/pnas.1901277116

Gaspar, J. M., & McDonald, J. J. (2014). Suppression of salient objects prevents distraction in visual search. *The Journal of Neuroscience: The Official Journal of the Society for Neuroscience*, *34*(16), 5658–5666. https://doi.org/10.1523/JNEUROSCI.4161-13.2014

Gaspelin, N., & Luck, S. J. (2018a). Distinguishing among potential mechanisms of singleton suppression. *Journal of Experimental Psychology. Human Perception and Performance*, *44*(4), 626–644. https://doi.org/10.1037/xhp0000484

Gaspelin, N., & Luck, S. J. (2018b). Combined electrophysiological and behavioral evidence for the suppression of salient distractors. *Journal of Cognitive Neuroscience*, *30*(9), 1265–1280. https://doi.org/10.1162/jocn_a_01279

Gattass, R., Nascimento-Silva, S., Soares, J. G., Lima, B., Jansen, A. K., Diogo, A. C. M., Farias, M. F., Botelho, M. M., Eliã P, Mariani, O. S., Azzi, J., & Fiorani, M. (2005). Cortical visual areas in monkeys: Location, topography, connections, columns, plasticity and cortical dynamics. *Philosophical Transactions of the Royal Society B: Biological Sciences*, *360*(1456), 709–731. https://doi.org/10.1098/rstb.2005.1629

Gazzaniga, M. S. (Ed.). (2009). *The cognitive neurosciences* (4th ed). MIT Press.

Gencer, N., & Williamson, S. (1998). Differential characterization of neural sources with the bimodal truncated SVD pseudo-inverse for EEG and MEG measurements. *IEEE Transactions on Biomedical Engineering*, *45*(7), 827–838. https://doi.org/10.1109/10.686790

Geng, J. J. (2014). Attentional mechanisms of distractor suppression. *Current Directions in Psychological Science*, *23*(2), 147–153. https://doi.org/10.1177/0963721414525780

Gieselmann, M. A., & Thiele, A. (2008). Comparison of spatial integration and surround suppression characteristics in spiking activity and the local field potential in macaque v1. *European Journal of Neuroscience*, *28*(3), 447–459. https://doi.org/10.1111/j.1460-9568.2008.06358.x

Glorot, X., & Bengio, Y. (2010). Understanding the difficulty of training deep feedforward neural networks. *Proceedings of the Thirteenth International Conference on Artificial Intelligence and Statistics*, 249–256. Retrieved September 23, 2023, from https://proceedings.mlr.press/v9/glorot10a.html

Goodale, M. A., & Milner, A. D. (1992). Separate visual pathways for perception and action. *Trends in Neurosciences*, *15*(1), 20–25. https://doi.org/10.1016/0166-2236(92)90344-8

Goodfellow, I., Bengio, Y., & Courville, A. (2016). *Deep learning*. MIT Press.

Gottlieb, J. P., Kusunoki, M., & Goldberg, M. E. (1998). The representation of visual salience in monkey parietal cortex. *Nature*, *391*(6666), 481–484. https://doi.org/10.1038/35135

Gray, C. M., & Singer, W. (1989). Stimulus-specific neuronal oscillations in orientation columns of cat visual cortex. *Proceedings of the National Academy of Sciences*, *86*(5), 1698–1702. https://doi.org/10.1073/pnas.86.5.1698

Gray, C. M. (1994). Synchronous oscillations in neuronal systems: Mechanisms and functions. *Journal of Computational Neuroscience*, *1*(1), 11–38. https://doi.org/10.1007/BF00962716

Gray, C. M., Engel, A. K., König, P., & Singer, W. (1990). Stimulus-dependent neuronal oscillations in cat visual cortex: Receptive field properties and feature dependence. *European Journal of Neuroscience*, *2*(7), 607–619. https://doi.org/10.1111/j.1460-9568.1990.tb00450.x

Gray, C. M., & Prisco, G. V. D. (1997). Stimulus-dependent neuronal oscillations and local synchronization in striate cortex of the alert cat. *Journal of Neuroscience*, *17*(9), 3239–3253. https://doi.org/10.1523/JNEUROSCI.17-09-03239.1997

Gregoriou, G. G., Gotts, S. J., Zhou, H., & Desimone, R. (2009). High-frequency, long-range coupling between prefrontal and visual cortex during attention. *Science*, *324*(5931), 1207–1210. https://doi.org/10.1126/science.1171402

Griffiths, B. J., Parish, G., Roux, F., Michelmann, S., van der Plas, M., Kolibius, L. D., Chelvarajah, R., Rollings, D. T., Sawlani, V., Hamer, H., Gollwitzer, S., Kreiselmeyer, G., Staresina, B., Wimber, M., & Hanslmayr, S. (2019). Directional coupling of slow and fast hippocampal gamma with neocortical alpha/beta oscillations in human episodic memory. *Proceedings of the National Academy of Sciences*, *116*(43), 21834–21842. https://doi.org/10.1073/pnas.1914180116

Griffiths, B. J., Weinert, D. E., Jensen, O., & Staudigl, T. (2023, July 25). Imperceptible gamma-band sensory stimulation enhances episodic memory retrieval. https://doi.org/10.1101/2023.07.21.550057

Griffiths, B. J., Zaehle, T., Repplinger, S., Schmitt, F. C., Voges, J., Hanslmayr, S., & Staudigl, T. (2022). Rhythmic interactions between the mediodorsal thalamus and prefrontal cortex precede human visual perception. *Nature Communications*, *13*(1), 3736. https://doi.org/10.1038/s41467-022-31407-z

Gross, J., Kujala, J., Hämäläinen, M., Timmermann, L., Schnitzler, A., & Salmelin, R. (2001). Dynamic imaging of coherent sources: Studying neural interactions in the human brain. *Proceedings of the National Academy of Sciences*, *98*(2), 694–699. https://doi.org/10.1073/pnas.98.2.694

Grothe, I., Neitzel, S. D., Mandon, S., & Kreiter, A. K. (2012). Switching neuronal inputs by differential modulations of gamma-band phase-coherence. *Journal of Neuroscience*, *32*(46), 16172–16180. https://doi.org/10.1523/JNEUROSCI.0890-12.2012

Gruber, T., Tsivilis, D., Montaldi, D., & Müller, M. M. (2004). Induced gamma band responses: An early marker of memory encoding and retrieval. *NeuroReport*, *15*(11), 1837. https://doi.org/10.1097/01.wnr.0000137077.26010.12

Gruber, W. R., Zauner, A., Lechinger, J., Schabus, M., Kutil, R., & Klimesch, W. (2014). Alpha phase, temporal attention, and the generation of early event related potentials. *NeuroImage*, *103*, 119–129. https://doi.org/10.1016/j.neuroimage.2014.08.055

Grützner, C., Wibral, M., Sun, L., Rivolta, D., Singer, W., Maurer, K., & Uhlhaas, P. (2013). Deficits in high-(> 60 hz) gamma-band oscillations during visual processing in schizophrenia. *Frontiers in Human Neuroscience*, *7*, 88. https://doi.org/10.3389/fnhum.2013.00088

Güçlü, U., & van Gerven, M. A. J. (2015). Deep neural networks reveal a gradient in the complexity of neural representations across the ventral stream. *Journal of Neuroscience*, *35*(27), 10005–10014. https://doi.org/10.1523/JNEUROSCI.5023-14.2015

Guggenmos, M., Sterzer, P., & Cichy, R. M. (2018). Multivariate pattern analysis for MEG: A comparison of dissimilarity measures. *NeuroImage*, *173*, 434–447. https://doi.org/10.1016/j.neuroimage.2018.02.044

Gulbinaite, R., İlhan, B., & VanRullen, R. (2017). The triple-flash illusion reveals a driving role of alpha-band reverberations in visual perception. *Journal of Neuroscience*, *37*(30), 7219–7230. https://doi.org/10.1523/JNEUROSCI.3929-16.2017

Gulbinaite, R., Roozendaal, D. H., & VanRullen, R. (2019). Attention differentially modulates the amplitude of resonance frequencies in the visual cortex. *NeuroImage*, *203*, 116–146. https://doi.org/10.1016/j.neuroimage.2019.116146

Gundlach, C., Moratti, S., Forschack, N., & Müller, M. M. (2020). Spatial attentional selection modulates early visual stimulus processing independently of visual alpha modulations. *Cerebral Cortex*, *30*(6), 3686–3703. https://doi.org/10.1093/cercor/bhz335

Gur, M., & Nodderly, D. M. (1997). Visual receptive fields of neurons in primary visual cortex (v1) move in space with the eye movements of fixation. *Vision Research*, *37*, 257–265. https://doi.org/10.1016/S0042-6989(96)00182-4

Gutteling, T. P., Sillekens, L., Lavie, N., & Jensen, O. (2022). Alpha oscillations reflect suppression of distractors with increased perceptual load. *Progress in Neurobiology*, *214*, 102285. https://doi.org/10.1016/j.pneurobio.2022.102285

Haegens, S., Nácher, V., Luna, R., Romo, R., & Jensen, O. (2011). α-oscillations in the monkey sensorimotor network influence discrimination performance by rhythmical inhibition of neuronal spiking. *Proceedings of the National Academy of Sciences*, *108*(48), 19377–19382.

Hahn, G., Bujan, A. F., Frégnac, Y., Aertsen, A., & Kumar, A. (2014). Communication through resonance in spiking neuronal networks. *PLoS computational biology*, *10*(8), e1003811. https://doi.org/10.1371/journal.pcbi.1003811

Händel, B. F., Haarmeier, T., & Jensen, O. (2011). Alpha oscillations correlate with the successful inhibition of unattended stimuli. *Journal of Cognitive Neuroscience*, *23*(9), 2494–2502. https://doi.org/10.1162/jocn.2010.21557

Händel, B. F., & Jensen, O. (2014). Spontaneous local alpha oscillations predict motion-induced blindness. *European Journal of Neuroscience*, *40*(9), 3371–3379. https://doi.org/10.1111/ejn.12701

Hanna, T. N., Zygmont, M. E., Peterson, R., Theriot, D., Shekhani, H., Johnson, J.-O., & Krupinski, E. A. (2018). The effects of fatigue from overnight shifts on radiology search patterns and diagnostic performance. *Journal of the American College of Radiology*, *15*(12), 1709–1716. https://doi.org/10.1016/j.jacr.2017.12.019

Hanslmayr, S., Aslan, A., Staudigl, T., Klimesch, W., Herrmann, C. S., & Bäuml, K.-H. (2007). Prestimulus oscillations predict visual perception performance between and within subjects. *NeuroImage*, *37*(4), 1465–1473. https://doi.org/10.1016/j.neuroimage.2007.07.011

Hanslmayr, S., Staresina, B. P., & Bowman, H. (2016). Oscillations and episodic memory: Addressing the synchronization/desynchronization conundrum. *Trends in Neurosciences*, *39*(1), 16–25. https://doi.org/10.1016/j.tins.2015.11.004

Harris, K. D., Csicsvari, J., Hirase, H., Dragoi, G., & Buzsáki, G. (2003). Organization of cell assemblies in the hippocampus. *Nature*, *424*(6948), 552–556. https://doi.org/10.1038/nature01834

Hasani, R., Lechner, M., Amini, A., Liebenwein, L., Ray, A., Tschaikowski, M., Teschl, G., & Rus, D. (2022). Closed-form continuous-time neural networks. *Nature Machine Intelligence*, *4*(11), 992–1003. https://doi.org/10.1038/s42256-022-00556-7

Hasani, R., Lechner, M., Amini, A., Rus, D., & Grosu, R. (2020, December 14). Liquid time-constant networks. Retrieved December 7, 2022, from http://arxiv.org/abs/2006.04439

Havenith, M. N., Yu, S., Biederlack, J., Chen, N.-H., Singer, W., & Nikolic, D. (2011). Synchrony makes neurons fire in sequence, and stimulus properties determine who is ahead. *Journal of Neuroscience*, *31*(23), 8570–8584. https://doi.org/10.1523/JNEUROSCI.2817-10.2011

Hawken, M. J., Shapley, R. M., & Grosof, D. H. (1996). Temporal-frequency selectivity in monkey visual cortex. *Visual Neuroscience*, *13*(3), 477–492. https://doi.org/10.1017/s0952523800008154

Haxby, J. V., Connolly, A. C., & Guntupalli, J. S. (2014). Decoding neural representational spaces using multivariate pattern analysis. *Annual Review of Neuroscience*, *37*, 435–456. https://doi.org/10.1146/annurev-neuro-062012-170325

He, Q., Colon-Motas, K. M., Pybus, A. F., Piendel, L., Seppa, J. K., Walker, M. L., Manzanares, C. M., Qiu, D., Miocinovic, S., Wood, L. B., Levey, A. I., Lah, J. J., & Singer, A. C. (2021). A feasibility trial of gamma sensory flicker for patients with prodromal alzheimer's disease. *Alzheimer's & Dementia: Translational Research & Clinical Interventions*, *7*(1), e12178. https://doi.org/10.1002/trc2.12178

Hebb, D. O. (2002, May 1). *The organization of behavior: A neuropsychological theory*. Psychology Press. https://doi.org/10.4324/9781410612403

Helfrich, R. F., Breska, A., & Knight, R. T. (2019). Neural entrainment and network resonance in support of top-down guided attention. *Current Opinion in Psychology*, *29*, 82–89. https://doi.org/10.1016/j.copsyc.2018.12.016

Hermes, D., Miller, K., Wandell, B., & Winawer, J. (2015a). Stimulus dependence of gamma oscillations in human visual cortex. *Cerebral Cortex*, *25*(9), 2951–2959. https://doi.org/10.1093/cercor/bhu091

Hermes, D., Miller, K. J., Wandell, B. A., & Winawer, J. (2015b). Gamma oscillations in visual cortex: The stimulus matters. *Trends in Cognitive Sciences*, *19*(2), 57–58. https://doi.org/10.1016/j.tics.2014.12.009

Herrmann, B., Maess, B., Hahne, A., Schröger, E., & Friederici, A. D. (2011). Syntactic and auditory spatial processing in the human temporal cortex: An MEG study. *Neuroimage*, *57*, 624–633. https://doi.org/10.1016/j.neuroimage.2011.04.034

Herrmann, C. S. (2001). Human EEG responses to 1-100 hz flicker: Resonance phenomena in visual cortex and their potential correlation to cognitive phenomena. *Experimental Brain Research*, *137*, 346–353. https://doi.org/10.1007/s002210100682

Herrmann, C. S., & Demiralp, T. (2005). Human EEG gamma oscillations in neuropsychiatric disorders. *Clinical Neurophysiology*, *116*, 2719–2733. https://doi.org/10.1016/j.clinph.2005.07.007

Herrmann, C. S., Fründ, I., & Lenz, D. (2010). Human gamma-band activity: A review on cognitive and behavioral correlates and network models. *Neuroscience & Biobehavioral Reviews*, *34*, 981–992. https://doi.org/10.1016/j.neubiorev.2009.09.001

Herrmann, C. S., & Mecklinger, A. (2001). Gamma activity in human EEG is related to highspeed memory comparisons during object selective attention. *Visual Cognition*, *8*, 593–608. https://doi.org/10.1080/13506280143000142

Herrmann, C. S., Munk, M. H. J., & Engel, A. K. (2004). Cognitive functions of gamma-band activity: Memory match and utilization. *Trends in Cognitive Sciences*, *8*(8), 347–355. https://doi.org/10.1016/j.tics.2004.06.006

Hickey, C., Di Lollo, V., & McDonald, J. J. (2009). Electrophysiological indices of target and distractor processing in visual search. *Journal of Cognitive Neuroscience*, *21*(4), 760–775. https://doi.org/10.1162/jocn.2009.21039

Hodgkin, A. L., & Huxley, A. F. (1952). A quantitative description of membrane current and its application to conduction and excitation in nerve. *The Journal of Physiology*, *117*(4), 500–544. Retrieved September 30, 2023, from https://www.ncbi.nlm.nih.gov/pmc/articles/PMC1392413/

Hogan, K., & Fitzpatrick, J. (1988). The cerebral origin of the alpha rhythm. *Electroencephalography and Clinical Neurophysiology*, *69*(1), 79–81. https://doi.org/10.1016/0013-4694(88)90037-5

Hoogenboom, N., Schoffelen, J. M., Oostenveld, R., & Fries, P. (2010). Visually induced gamma-band activity predicts speed of change detection in humans. *NeuroImage*, *51*, 1162–1167. https://doi.org/10.1016/j.neuroimage.2010.03.041

Hoogenboom, N., Schoffelen, J.-M., Oostenveld, R., Parkes, L. M., & Fries, P. (2006). Localizing human visual gamma-band activity in frequency, time and space. *NeuroImage*, *29*, 764–773. https://doi.org/10.1016/j.neuroimage.2005.08.043

Hopfield, J. J. (1982). Neural networks and physical systems with emergent collective computational abilities. *Proceedings of the National Academy of Sciences*, *79*(8), 2554–2558. https://doi.org/10.1073/pnas.79.8.2554

Hoppensteadt, F. C., & Izhikevich, E. M. (1998). Thalamo-cortical interactions modeled by weakly connected oscillators: Could the brain use FM radio principles? *Bio Systems*, *48*(1), 85–94. https://doi.org/10.1016/s0303-2647(98)00053-7

Horwitz, G. D. (2020). Signals related to color in the early visual cortex. *Annual Review of Vision Science*, *6*(1), 287–311. https://doi.org/10.1146/annurev-vision-121219-081801

Howard, M. W., Rizzuto, D. S., Caplan, J. B., Madsen, J. R., Lisman, J., Aschenbrenner-Scheibe, R., Schulze-Bonhage, A., & Kahana, M. J. (2003). Gamma oscillations correlate with working memory load in humans. *Cerebral Cortex*, *13*(12), 1369–1374. https://doi.org/10.1093/cercor/bhg084

Hubel, D. H., & Livingstone, M. S. (1987). Segregation of form, color, and stereopsis in primate area 18. *Journal of Neuroscience*, *7*(11), 3378–3415. https://doi.org/10.1523/JNEUROSCI.07-11-03378.1987

Hubel, D. H., & Wiesel, T. N. (1962). Receptive fields, binocular interaction and functional architecture in the cat's visual cortex. *The Journal of Physiology*, *160*(1), 106–154.2. Retrieved July 12, 2020, from https://www.ncbi.nlm.nih.gov/pmc/articles/PMC1359523/

Hutcheon, B., & Yarom, Y. (2000). Resonance, oscillation and the intrinsic frequency preferences of neurons. *Trends in Neurosciences*, *23*, 216–222. https://doi.org/10.1016/S0166-2236(00)01547-2

Hutt, A., Griffiths, J. D., Herrmann, C. S., & Lefebvre, J. (2018). Effect of stimulation waveform on the non-linear entrainment of cortical alpha oscillations. *Frontiers in Neuroscience*, *12*. https://doi.org/10.3389/fnins.2018.00376

Iaccarino, H. F., Singer, A. C., Martorell, A. J., Rudenko, A., Gao, F., Gillingham, T. Z., Mathys, H., Seo, J., Kritskiy, O., Abdurrob, F., Adaikkan, C., Canter, R. G., Rueda, R., Brown, E. N., Boyden, E. S., & Tsai, L.-H. (2016). Gamma frequency entrainment attenuates amyloid load and modifies microglia. *Nature*, *540*(7632), 230–235. https://doi.org/10.1038/nature20587

Iemi, L., Chaumon, M., Crouzet, S. M., & Busch, N. A. (2017). Spontaneous neural oscillations bias perception by modulating baseline excitability. *Journal of Neuroscience*, *37*(4), 807–819. https://doi.org/10.1523/JNEUROSCI.1432-16.2016

Iemi, L., Gwilliams, L., Samaha, J., Auksztulewicz, R., Cycowicz, Y. M., King, J.-R., Nikulin, V. V., Thesen, T., Doyle, W., Devinsky, O., Schroeder, C. E., Melloni, L., & Haegens, S. (2022). Ongoing neural oscillations influence behavior and sensory representations by suppressing neuronal excitability. *NeuroImage*, *247*, 118746. https://doi.org/10.1016/j.neuroimage.2021.118746

Imperatori, L. S., Betta, M., Cecchetti, L., Canales-Johnson, A., Ricciardi, E., Siclari, F., Pietrini, P., Chennu, S., & Bernardi, G. (2019). EEG functional connectivity metrics wPLI and wSMI account for distinct types of brain functional interactions. *Scientific Reports*, *9*(1), 8894. https://doi.org/10.1038/s41598-019-45289-7

International Brain Laboratory, Benson, B., Benson, J., Birman, D., Bonacchi, N., Carandini, M., Catarino, J. A., Chapuis, G. A., Churchland, A. K., Dan, Y., Dayan, P., DeWitt, E. E., Engel, T. A., Fabbri, M., Faulkner, M., Fiete, I. R., Findling, C., Freitas-Silva, L., Gerçek, B., . . . Witten, I. B. (2023, July 4). *A brain-wide map of neural activity during complex behaviour* (preprint). Neuroscience. https://doi.org/10.1101/2023.07.04.547681

Ipata, A. E., Gee, A. L., Bisley, J. W., & Goldberg, M. E. (2009). Neurons in the lateral intraparietal area create a priority map by the combination of disparate signals. *Experimental Brain Research*, *192*(3), 479–488. https://doi.org/10.1007/s00221-008-1557-8

Ipata, A. E., Gee, A. L., Goldberg, M. E., & Bisley, J. W. (2006). Activity in the lateral intraparietal area predicts the goal and latency of saccades in a free-viewing visual search task. *Journal of Neuroscience*, *26*(14), 3656–3661. https://doi.org/10.1523/JNEUROSCI.5074-05.2006

Ipata, A. E., Gee, A. L., Gottlieb, J., Bisley, J. W., & Goldberg, M. E. (2006). LIP responses to a popout stimulus are reduced if it is overtly ignored. *Nature Neuroscience*, *9*, 1071–1076. https://doi.org/10.1038/nn1734

Izhikevich, E. M., Desai, N. S., Walcott, E. C., & Hoppensteadt, F. C. (2003). Bursts as a unit of neural information: Selective communication via resonance. *Trends in Neurosciences*, *26*(3), 161–167. https://doi.org/10.1016/S0166-2236(03)00034-1

Jannati, A., Gaspar, J. M., & McDonald, J. J. (2013). Tracking target and distractor processing in fixed-feature visual search: Evidence from human electrophysiology. *Journal of Experimental Psychology: Human Perception and Performance*, *39*, 1713–1730. https://doi.org/10.1037/a0032251

Jansen, B. H., & Brandt, M. E. (1991). The effect of the phase of prestimulus alpha activity on the averaged visual evoked response. *Electroencephalography and Clinical Neurophysiology/Evoked Potentials Section*, *80*(4), 241–250. https://doi.org/10.1016/0168-5597(91)90107-9

Jensen, O. (2001). Information transfer between rhythmically coupled networks: Reading the hippocampal phase code. *Neural Computation*, *13*(12), 2743–2761. https://doi.org/10.1162/089976601317098510

Jensen, O. (2023, January 20). Gating by alpha band inhibition revised: A case for a secondary control mechanism. https://doi.org/10.31234/osf.io/7bk32

Jensen, O., Bonnefond, M., & VanRullen, R. (2012). An oscillatory mechanism for prioritizing salient unattended stimuli. *Trends in Cognitive Sciences*, *16*(4), 200–206. https://doi.org/10.1016/j.tics.2012.03.002

Jensen, O., Gelfand, J., Kounios, J., & Lisman, J. E. (2002). Oscillations in the alpha band (9-12 hz) increase with memory load during retention in a short-term memory task. *Cerebral Cortex (New York, N.Y.: 1991)*, *12*(8), 877–882. https://doi.org/10.1093/cercor/12.8.877

Jensen, O., Gips, B., Bergmann, T. O., & Bonnefond, M. (2014). Temporal coding organized by coupled alpha and gamma oscillations prioritize visual processing. *Trends in Neurosciences*, *37*(7), 357–369. https://doi.org/10.1016/j.tins.2014.04.001

Jensen, O., & Hanslmayr, S. (2020). The role of alpha oscillations for attention and working memory. https://doi.org/10.7551/mitpress/11442.003.0038

Jensen, O., Kaiser, J., & Lachaux, J.-P. (2007). Human gamma-frequency oscillations associated with attention and memory. *Trends in Neurosciences*, *30*(7), 317–324. https://doi.org/10.1016/j.tins.2007.05.001

Jensen, O., & Lisman, J. E. (1996). Hippocampal CA3 region predicts memory sequences: Accounting for the phase precession of place cells. *Learning & Memory (Cold Spring Harbor, N.Y.)*, *3*(2), 279–287. https://doi.org/10.1101/lm.3.2-3.279

Jensen, O., & Lisman, J. E. (2000). Position reconstruction from an ensemble of hippocampal place cells: Contribution of theta phase coding. *Journal of Neurophysiology*, *83*(5), 2602–2609. https://doi.org/10.1152/jn.2000.83.5.2602

Jensen, O., & Mazaheri, A. (2010). Shaping functional architecture by oscillatory alpha activity: Gating by inhibition. *Frontiers in Human Neuroscience*, *4*. Retrieved May 5, 2022, from https://www.frontiersin.org/article/10.3389/fnhum.2010.00186

Jensen, O., Pan, Y., Frisson, S., & Wang, L. (2021). An oscillatory pipelining mechanism supporting previewing during visual exploration and reading. *Trends in Cognitive Sciences*, *25*(12), 1033–1044. https://doi.org/10.1016/j.tics.2021.08.008

Jensen, O., Spaak, E., & Zumer, J. M. (2014, July 1). Human brain oscillations: From physiological mechanisms to analysis and cognition. In *Magnetoencephalography* (pp. 359–403, Vol. 9783642330452). Springer. https://doi.org/10.1007/978-3-642-33045-2_17

Jezek, K., Henriksen, E. J., Treves, A., Moser, E. I., & Moser, M.-B. (2011). Theta-paced flickering between place-cell maps in the hippocampus. *Nature*, *478*(7368), 246–249. https://doi.org/10.1038/nature10439

Jia, X., Smith, M. A., & Kohn, A. (2011). Stimulus selectivity and spatial coherence of gamma components of the local field potential. *Journal of Neuroscience*, *31*(25), 9390–9403. https://doi.org/10.1523/JNEUROSCI.0645-11.2011

Jia, X., Xing, D., & Kohn, A. (2013). No consistent relationship between gamma power and peak frequency in macaque primary visual cortex. *Journal of Neuroscience*, *33*, 17–25. https://doi.org/10.1523/JNEUROSCI.1687-12.2013

Kahneman, D. (1973). *Attention and effort*. Prentice-Hall.

Kahneman, D., Treisman, A., & Gibbs, B. J. (1992). The reviewing of object files: Object-specific integration of information. *Cognitive Psychology*, *24*(2), 175–219. https://doi.org/10.1016/0010-0285(92)90007-o

Kaiser, J., Ripper, B., Birbaumer, N., & Lutzenberger, W. (2003). Dynamics of gamma-band activity in human magnetoencephalogram during auditory pattern working memory. *NeuroImage*, *20*(2), 816–827. https://doi.org/10.1016/S1053-8119(03)00350-1

Kamiński, J., Brzezicka, A., Mamelak, A. N., & Rutishauser, U. (2020). Combined phase-rate coding by persistently active neurons as a mechanism for maintaining multiple items in working memory in humans. *Neuron*, *106*(2), 256–264.e3. https://doi.org/10.1016/j.neuron.2020.01.032

Kamiyama, A., Fujita, K., & Kashimori, Y. (2016). A neural mechanism of dynamic gating of task-relevant information by top-down influence in primary visual cortex. *Biosystems*, *150*, 138–148. https://doi.org/10.1016/j.biosystems.2016.09.009

Kaneko, T., Komatsu, M., Yamamori, T., Ichinohe, N., & Okano, H. (2022). Cortical neural dynamics unveil the rhythm of natural visual behavior in marmosets. *Communications Biology*, *5*(1), 1–13. https://doi.org/10.1038/s42003-022-03052-1

Kastner, S., Pinsk, M. A., Weerd, P. D., Desimone, R., & Ungerleider, L. G. (1999). Increased activity in human visual cortex during directed attention in the absence of visual stimulation. *Neuron*, *22*(4), 751–761. https://doi.org/10.1016/S0896-6273(00)80734-5

Kastner, S., & Ungerleider, L. G. (2000). Mechanisms of visual attention in the human cortex. *Annual Review of Neuroscience*, *23*(1), 315–341. https://doi.org/10.1146/annurev.neuro.23.1.315

Kastner, S., & Ungerleider, L. G. (2001). The neural basis of biased competition in human visual cortex. *Neuropsychologia*, *39*(12), 1263–1276. https://doi.org/10.1016/S0028-3932(01)00116-6

Katyal, S., He, S., He, B., & Engel, S. A. (2019). Frequency of alpha oscillation predicts individual differences in perceptual stability during binocular rivalry. *Human Brain Mapping*, *40*(8), 2422. https://doi.org/10.1002/hbm.24533

Kayser, C. (2009). Phase resetting as a mechanism for supramodal attentional control. *Neuron*, *64*(3), 300–302. https://doi.org/10.1016/j.neuron.2009.10.022

Keitel, C., Keitel, A., Benwell, C. S., Daube, C., Thut, G., & Gross, J. (2019). Stimulus-driven brain rhythms within the alpha band: The attentional-modulation conundrum. *Journal of Neuroscience*, *39*, 3119–3129. https://doi.org/10.1523/JNEUROSCI.1633-18.2019

Keitel, C., Quigley, C., & Ruhnau, P. (2014). Stimulus-driven brain oscillations in the alpha range: Entrainment of intrinsic rhythms or frequency-following response? *Journal of Neuroscience*, *34*(31), 10137–10140. https://doi.org/10.1523/JNEUROSCI.1904-14.2014

Kelly, S. P., Lalor, E. C., Reilly, R. B., & Foxe, J. J. (2006). Increases in alpha oscillatory power reflect an active retinotopic mechanism for distracter suppression during sustained visuospatial attention. *Journal of Neurophysiology*, *95*(6), 3844–3851. https://doi.org/10.1152/jn.01234.2005

Kim, H., Ährlund-Richter, S., Wang, X., Deisseroth, K., & Carlén, M. (2016). Prefrontal parvalbumin neurons in control of attention. *Cell*, *164*(1), 208–218. https://doi.org/10.1016/j.cell.2015.11.038

King, J.-R., Sitt, J. D., Faugeras, F., Rohaut, B., El Karoui, I., Cohen, L., Naccache, L., & Dehaene, S. (2013). Information sharing in the brain indexes consciousness in noncommunicative patients. *Current Biology*, *23*(19), 1914–1919. https://doi.org/10.1016/j.cub.2013.07.075

Kingma, D. P., & Ba, J. (2017, January 29). Adam: A method for stochastic optimization. https://doi.org/10.48550/arXiv.1412.6980

Kirchberger, L., Mukherjee, S., Schnabel, U. H., Beest, E. H. v., Barsegyan, A., Levelt, C. N., Heimel, J. A., Lorteije, J. A. M., Togt, C. v. d., Self, M. W., & Roelfsema, P. R. (2021). The essential role of recurrent processing for figure-ground perception in mice. *Science Advances*, *7*(27), eabe1833. https://doi.org/10.1126/sciadv.abe1833

Klimesch, W., Doppelmayr, M., Schwaiger, J., Auinger, P., & Winkler, T. (1999). 'paradoxical' alpha synchronization in a memory task. *Cognitive Brain Research*, *7*(4), 493–501. https://doi.org/10.1016/S0926-6410(98)00056-1

Klimesch, W. (2012). Alpha-band oscillations, attention, and controlled access to stored information. *Trends in Cognitive Sciences*, *16*(12), 606–617. https://doi.org/10.1016/j.tics.2012.10.007

Klimesch, W., Fellinger, R., & Freunberger, R. (2011). Alpha oscillations and early stages of visual encoding. *Frontiers in Psychology*, *2*. https://doi.org/10.3389/fpsyg.2011.00118

Klimesch, W., Sauseng, P., & Hanslmayr, S. (2007). EEG alpha oscillations: The inhibition–timing hypothesis. *Brain Research Reviews*, *53*(1), 63–88. https://doi.org/10.1016/j.brainresrev.2006.06.003

Klink, P. C., Teeuwen, R. R. M., Lorteije, J. A. M., & Roelfsema, P. R. (2023). Inversion of pop-out for a distracting feature dimension in monkey visual cortex. *Proceedings of the National Academy of Sciences*, *120*(9), e2210839120. https://doi.org/10.1073/pnas.2210839120

Knyazev, G. G., Slobodskoj-Plusnin, J. Y., Bocharov, A. V., & Pylkova, L. V. (2011). The default mode network and EEG α oscillations: An independent component analysis. *Brain Research*, *1402*, 67–79. https://doi.org/10.1016/j.brainres.2011.05.052

Koch, C., & Ullman, S. (1985). Shifts in selective visual attention: Towards the underlying neural circuitry. *Human Neurobiology*, *4*(4), 219–227.

Kohn, A. (2007). Visual adaptation: Physiology, mechanisms, and functional benefits. *Journal of Neurophysiology*, *97*(5), 3155–3164. https://doi.org/10.1152/jn.00086.2007

Konen, C. S., & Kastner, S. (2008). Two hierarchically organized neural systems for object information in human visual cortex. *Nature Neuroscience*, *11*(2), 224–231. https://doi.org/10.1038/nn2036

König, P., Engel, A. K., & Singer, W. (1995). Relation between oscillatory activity and long-range synchronization in cat visual cortex. *Proceedings of the National Academy of Sciences*, *92*(1), 290–294. https://doi.org/10.1073/pnas.92.1.290

Kopell, N., & Ermentrout, B. (2004). Chemical and electrical synapses perform complementary roles in the synchronization of interneuronal networks. *Proceedings of the National Academy of Sciences of the United States of America*, *101*(43), 15482–15487. https://doi.org/10.1073/pnas.0406343101

Kriegeskorte, N. (2015). Deep neural networks: A new framework for modeling biological vision and brain information processing. *Annual Review of Vision Science*, *1*, 417–446. https://doi.org/10.1146/annurev-vision-082114-035447

Kristan, W. B., & Shaw, B. K. (1997). Population coding and behavioral choice. *Current Opinion in Neurobiology*, *7*(6), 826–831. https://doi.org/10.1016/S0959-4388(97)80142-0

Krizhevsky, A. (2009). Learning multiple layers of features from tiny images. Retrieved October 23, 2023, from https://www.semanticscholar.org/paper/Learning-Multiple-Layers-of-Features-from-Tiny-Krizhevsky/5d90f06bb70a0a3dced62413346235c02b1aa086

Krizhevsky, A., Sutskever, I., & Hinton, G. E. (2012). ImageNet classification with deep convolutional neural networks. *Advances in Neural Information Processing Systems*, *25*. Retrieved March 22, 2023, from https://papers.nips.cc/paper_files/paper/2012/hash/c399862d3b9d6b76c8436e924a68c45b-Abstract.html

Kruger, N., Janssen, P., Kalkan, S., Lappe, M., Leonardis, A., Piater, J., Rodriguez-Sanchez, A. J., & Wiskott, L. (2013). Deep hierarchies in the primate visual cortex: What can we learn for computer vision? *IEEE Transactions on Pattern Analysis and Machine Intelligence*, *35*(8), 1847–1871. https://doi.org/10.1109/TPAMI.2012.272

Kubilius, J., Schrimpf, M., Kar, K., Hong, H., Majaj, N. J., Rajalingham, R., Issa, E. B., Bashivan, P., Prescott-Roy, J., Schmidt, K., Nayebi, A., Bear, D., Yamins, D. L. K., & DiCarlo, J. J. (2019). Brain-like object recognition with high-performing shallow recurrent ANNs. *arXiv:1909.06161 [cs, eess, q-bio]*. Retrieved January 20, 2022, from http://arxiv.org/abs/1909.06161

Kuffler, S. W. (1953). Discharge patterns and functional organization of mammalian retina. *Journal of Neurophysiology*, *16*, 37–68. https://doi.org/10.1152/jn.1953.16.1.37

Kujala, J., Jung, J., Bouvard, S., Lecaignard, F., Lothe, A., Bouet, R., Ciumas, C., Ryvlin, P., & Jerbi, K. (2015). Gamma oscillations in v1 are correlated with GABA a receptor density: A multi-modal MEG and flumazenil-PET study. *Scientific Reports*, *5*, 16347. https://doi.org/10.1038/srep16347

Kuzovkin, I., Vicente, R., Petton, M., Lachaux, J.-P., Baciu, M., Kahane, P., Rheims, S., Vidal, J. R., & Aru, J. (2018). Activations of deep convolutional neural networks are aligned with gamma band activity of human visual cortex. *Communications Biology*, *1*(1), 1–12. https://doi.org/10.1038/s42003-018-0110-y

Lacadie, C. M., Fulbright, R. K., Arora, J., Constable, R. T., & Papademetris, X. (2007). Brodmann areas defined in MNI space using new tracing tool in BioImage suite. *Proceedings of the 14th Annual Meeting of the Organization for Human Brain Mapping*, *36*, 6494.

Lacadie, C. M., Fulbright, R. K., Rajeevan, N., Constable, R. T., & Papademetris, X. (2008). More accurate talairach coordinates for neuroimaging using non-linear registration. *NeuroImage*, *42*, 717–725. https://doi.org/10.1016/j.neuroimage.2008.04.240

Lachaux, J. P., Rodriguez, E., Martinerie, J., & Varela, F. J. (1999). Measuring phase synchrony in brain signals. *Human Brain Mapping*, *8*, 194–208. https://doi.org/10.1002/(SICI)1097-0193(1999)8:4<194::AID-HBM4>3.0.CO;2-C

Lachaux, J.-P., George, N., Tallon-Baudry, C., Martinerie, J., Hugueville, L., Minotti, L., Kahane, P., & Renault, B. (2005). The many faces of the gamma band response to complex visual stimuli. *NeuroImage*, *25*(2), 491–501. https://doi.org/10.1016/j.neuroimage.2004.11.052

Lachaux, J.-P., Rodriguez, E., Martinerie, J., Adam, C., Hasboun, D., & Varela, F. J. (2000). A quantitative study of gamma-band activity in human intracranial recordings triggered by visual stimuli. *European Journal of Neuroscience*, *12*(7), 2608–2622. https://doi.org/10.1046/j.1460-9568.2000.00163.x

Lakatos, P., Gross, J., & Thut, G. (2019). A new unifying account of the roles of neuronal entrainment. *Current Biology*, *29*(18), R890–R905. https://doi.org/10.1016/j.cub.2019.07.075

Landman, R. (2004, August 31). *Electronics in the development of modern medicine*. https://doi.org/10.13140/2.1.4639.2328

Larkum, M. (2013). A cellular mechanism for cortical associations: An organizing principle for the cerebral cortex. *Trends in Neurosciences*, *36*(3), 141–151. https://doi.org/10.1016/j.tins.2012.11.006

LeCun, Y., & Bengio, Y. (1995). Convolutional networks for images, speech, and time-series. In M. Arbib (Ed.), *The handbook of brain theory and neural networks*. MIT Press.

LeCun, Y., Bottou, L., Bengio, Y., & Haffner, P. (1998). Gradient-based learning applied to document recognition. *Proceedings of the IEEE*, *86*(11), 2278–2324. https://doi.org/10.1109/5.726791

Lee, S., & Jones, S. R. (2013). Distinguishing mechanisms of gamma frequency oscillations in human current source signals using a computational model of a laminar neocortical network. *Frontiers in Human Neuroscience*, *7*. https://doi.org/10.3389/fnhum.2013.00869

Legewie, H., Simonova, O., & Creutzfeldt, O. D. (1969). EEG changes during performance of various tasks under open- and closed-eyed conditions. *Electroencephalography and Clinical Neurophysiology*, *27*(5), 470–479. https://doi.org/10.1016/0013-4694(69)90187-4

Li, K., Kozyrev, V., Kyllingsbæk, S., Treue, S., Ditlevsen, S., & Bundesen, C. (2016). Neurons in primate visual cortex alternate between responses to multiple stimuli in their receptive field. *Frontiers in Computational Neuroscience*, *10*. Retrieved September 21, 2023, from https://www.frontiersin.org/articles/10.3389/fncom.2016.00141

Liebe, S., Niediek, J., Pals, M., Reber, T. P., Faber, J., Bostroem, J., Elger, C. E., Macke, J. H., & Mormann, F. (2022, September 27). Phase of firing does not reflect temporal order in sequence memory of humans and recurrent neural networks. https://doi.org/10.1101/2022.09.25.509370

Liesefeld, H. R., & Müller, H. J. (2019). Distractor handling via dimension weighting. *Current Opinion in Psychology*, *29*, 160–167. https://doi.org/10.1016/j.copsyc.2019.03.003

Limbach, K., & Corballis, P. M. (2016). Prestimulus alpha power influences response criterion in a detection task. *Psychophysiology*, *53*(8), 1154–1164. https://doi.org/10.1111/psyp.12666

Lindsley, D. B. (1952). Psychological phenomena and the electroencephalogram. *Electroencephalography and Clinical Neurophysiology*, *4*(4), 443–456. https://doi.org/10.1016/0013-4694(52)90075-8

Lippold, O. (1970). Origin of the alpha rhythm. *Nature*, *226*(5246), 616–618. https://doi.org/10.1038/226616a0

Lisman, J., & Buzsáki, G. (2008). A neural coding scheme formed by the combined function of gamma and theta oscillations. *Schizophrenia Bulletin*, *34*(5), 974–980. https://doi.org/10.1093/schbul/sbn060

Lisman, J. E., & Idiart, M. A. (1995). Storage of 7 +/- 2 short-term memories in oscillatory subcycles. *Science (New York, N.Y.)*, *267*(5203), 1512–1515. https://doi.org/10.1126/science.7878473

Lisman, J. E., & Jensen, O. (2013). The theta-gamma neural code. *Neuron*, *77*(6), 1002–1016. https://doi.org/10.1016/j.neuron.2013.03.007

Liu, B., Nobre, A. C., & van Ede, F. (2022). Functional but not obligatory link between microsaccades and neural modulation by covert spatial attention. *Nature Communications*, *13*(1), 3503. https://doi.org/10.1038/s41467-022-31217-3

Liu, B., Nobre, A. C., & van Ede, F. (2023). Microsaccades transiently lateralise EEG alpha activity. *Progress in Neurobiology*, *224*, 102433. https://doi.org/10.1016/j.pneurobio.2023.102433

Liu, C., Han, T., Xu, Z., Liu, J., Zhang, M., Du, J., Zhou, Q., Duan, Y., Li, Y., Wang, J., Cui, D., & Wang, Y. (2022). Modulating gamma oscillations promotes brain connectivity to improve cognitive impairment. *Cerebral Cortex*, *32*(12), 2644–2656. https://doi.org/10.1093/cercor/bhab371

Livingstone, M., & Hubel, D. (1988). Segregation of form, color, movement, and depth: Anatomy, physiology, and perception. *Science*, *240*(4853), 740–749. https://doi.org/10.1126/science.3283936

Llinás, R. R. (1988). The intrinsic electrophysiological properties of mammalian neurons: Insights into central nervous system function. *Science (New York, N.Y.)*, *242*(4886), 1654–1664. https://doi.org/10.1126/science.3059497

Lopes Da Silva, F. H., & Storm Van Leeuwen, W. (1977). The cortical source of the alpha rhythm. *Neuroscience Letters*, *6*(2), 237–241. https://doi.org/10.1016/0304-3940(77)90024-6

Lopes da Silva, F. (2022). EEG: Origin and measurement. In C. Mulert & L. Lemieux (Eds.), *EEG - fMRI: Physiological basis, technique, and applications* (pp. 23–48). Springer International Publishing. https://doi.org/10.1007/978-3-031-07121-8_2

Lopour, B. A., Tavassoli, A., Fried, I., & Ringach, D. L. (2013). Coding of information in the phase of local field potentials within human medial temporal lobe. *Neuron*, *79*(3), 594–606. https://doi.org/10.1016/j.neuron.2013.06.001

Lowet, E., Gomes, B., Srinivasan, K., Zhou, H., Schafer, R. J., & Desimone, R. (2018). Enhanced neural processing by covert attention only during microsaccades directed toward the attended stimulus. *Neuron*, *99*(1), 207–214.e3. https://doi.org/10.1016/j.neuron.2018.05.041

Lozano-Soldevilla, D., ter Huurne, N., Cools, R., & Jensen, O. (2014). GABAergic modulation of visual gamma and alpha oscillations and its consequences for working memory performance. *Current biology: CB*, *24*(24), 2878–2887. https://doi.org/10.1016/j.cub.2014.10.017

Lucas, K., & Adrian, E. D. A. B. (1917). *The conduction of the nervous impulse* (Vol. 3). Longmans, Green; Company.

Luck, S. J., & Hillyard, S. A. (1994a). Electrophysiological correlates of feature analysis during visual search. *Psychophysiology*, *31*(3), 291–308. https://doi.org/10.1111/j.1469-8986.1994.tb02218.x

Luck, S. J., & Hillyard, S. A. (1994b). Spatial filtering during visual search: Evidence from human electrophysiology. *Journal of Experimental Psychology. Human Perception and Performance*, *20*(5), 1000–1014. https://doi.org/10.1037//0096-1523.20.5.1000

Luck, S. J., Gaspelin, N., Folk, C. L., Remington, R. W., & Theeuwes, J. (2021). Progress toward resolving the attentional capture debate. *Visual Cognition*, *29*(1), 1–21. https://doi.org/10.1080/13506285.2020.1848949

Mainy, N., Kahane, P., Minotti, L., Hoffmann, D., Bertrand, O., & Lachaux, J.-P. (2007). Neural correlates of consolidation in working memory. *Human Brain Mapping*, *28*(3), 183–193. https://doi.org/10.1002/hbm.20264

Maldonado, P. E., Friedman-Hill, S., & Gray, C. M. (2000). Dynamics of striate cortical activity in the alert macaque: II. fast time scale synchronization. *Cerebral Cortex*, *10*(11), 1117–1131. https://doi.org/10.1093/cercor/10.11.1117

Maris, E., & Oostenveld, R. (2007). Nonparametric statistical testing of EEG- and MEG-data. *Journal of Neuroscience Methods*, *164*(1), 177–190. https://doi.org/10.1016/j.jneumeth.2007.03.024

Marques, T., Schrimpf, M., & DiCarlo, J. J. (2021, March 2). *Multi-scale hierarchical neural network models that bridge from single neurons in the primate primary visual cortex to object recognition behavior* (preprint). Neuroscience. https://doi.org/10.1101/2021.03.01.433495

Martinez-Trujillo, J. C., & Treue, S. (2004). Feature-based attention increases the selectivity of population responses in primate visual cortex. *Current biology: CB*, *14*(9), 744–751. https://doi.org/10.1016/j.cub.2004.04.028

Martorell, A. J., Paulson, A. L., Suk, H.-J., Abdurrob, F., Drummond, G. T., Guan, W., Young, J. Z., Kim, D. N.-W., Kritskiy, O., Barker, S. J., Mangena, V., Prince, S. M., Brown, E. N., Chung, K., Boyden, E. S., Singer, A. C., & Tsai, L.-H. (2019). Multi-sensory gamma stimulation ameliorates alzheimer's-associated pathology and improves cognition. *Cell*, *177*(2), 256–271.e22. https://doi.org/10.1016/j.cell.2019.02.014

Mathewson, K. E., Gratton, G., Fabiani, M., Beck, D. M., & Ro, T. (2009). To see or not to see: Prestimulus alpha phase predicts visual awareness. *The Journal of Neuroscience: The Official Journal of the Society for Neuroscience*, *29*(9), 2725–2732. https://doi.org/10.1523/JNEUROSCI.3963-08.2009

Maunsell, J. H. R., & Treue, S. (2006). Feature-based attention in visual cortex. *Trends in Neurosciences*, *29*(6), 317–322. https://doi.org/10.1016/j.tins.2006.04.001

Mazaheri, A., van Schouwenburg, M. R., Dimitrijevic, A., Denys, D., Cools, R., & Jensen, O. (2014). Region-specific modulations in oscillatory alpha activity serve to facilitate processing in the visual and auditory modalities. *NeuroImage*, *87*, 356–362. https://doi.org/10.1016/j.neuroimage.2013.10.052

Mazurek, M. E., & Shadlen, M. N. (2002). Limits to the temporal fidelity of cortical spike rate signals. *Nature Neuroscience*, *5*(5), 463–471. https://doi.org/10.1038/nn836

McAdams, C. J., & Maunsell, J. H. (2000). Attention to both space and feature modulates neuronal responses in macaque area v4. *Journal of Neurophysiology*, *83*(3), 1751–1755. https://doi.org/10.1152/jn.2000.83.3.1751

McClelland, G. H., Lynch, J. G., Irwin, J. R., Spiller, S. A., & Fitzsimons, G. J. (2015). Median splits, type II errors, and false–positive consumer psychology: Don't fight the power. *Journal of Consumer Psychology*, *25*(4), 679–689. https://doi.org/10.1016/j.jcps.2015.05.006

McCormick, D. A., Shu, Y., & Yu, Y. (2007). Hodgkin and huxley model — still standing? *Nature*, *445*(7123), E1–E2. https://doi.org/10.1038/nature05523

McLelland, D., & VanRullen, R. (2016). Theta-gamma coding meets communication-through-coherence: Neuronal oscillatory multiplexing theories reconciled. *PLOS Computational Biology*, *12*(10), e1005162. https://doi.org/10.1371/journal.pcbi.1005162

McNett, S. D., Vyshedskiy, A., Savchenko, A., Durakovic, D., Heredia, G., Cahn, R., & Kogan, M. (2023). A feasibility study of AlzLife 40 hz sensory therapy in patients with MCI and early AD. *Healthcare*, *11*(14), 2040. https://doi.org/10.3390/healthcare11142040

Mehrpour, V., Martinez-Trujillo, J. C., & Treue, S. (2020). Attention amplifies neural representations of changes in sensory input at the expense of perceptual accuracy. *Nature Communications*, *11*(1), 2128. https://doi.org/10.1038/s41467-020-15989-0

Mejias, J. F., Murray, J. D., Kennedy, H., & Wang, X.-J. (2016). Feedforward and feedback frequency-dependent interactions in a large-scale laminar network of the primate cortex. *Science Advances*, *2*(11), e1601335. https://doi.org/10.1126/sciadv.1601335

Michalareas, G., Vezoli, J., van Pelt, S., Schoffelen, J.-M., Kennedy, H., & Fries, P. (2016). Alpha-beta and gamma rhythms subserve feedback and feedforward influences among human visual cortical areas. *Neuron*, *89*(2), 384–397. https://doi.org/10.1016/j.neuron.2015.12.018

Miller, P. (2018). *An introductory course in computational neuroscience*. MIT Press.

Milner, A. D., & Goodale, M. A. (2008). Two visual systems re-viewed. *Neuropsychologia*, *46*(3), 774–785. https://doi.org/10.1016/j.neuropsychologia.2007.10.005

Milner, P. M. (1974). A model for visual shape recognition. *Psychological Review*, *81*(6), 521–535. https://doi.org/10.1037/h0037149

Minarik, T., Berger, B., & Jensen, O. (2023). Optimal parameters for rapid (invisible) frequency tagging using MEG. *NeuroImage*, *281*, 120389. https://doi.org/10.1016/j.neuroimage.2023.120389

Mirpour, K., Arcizet, F., Ong, W. S., & Bisley, J. W. (2009). Been there, seen that: A neural mechanism for performing efficient visual search. *Journal of Neurophysiology*, *102*(6), 3481–3491. https://doi.org/10.1152/jn.00688.2009

Mishkin, M., Ungerleider, L. G., & Macko, K. A. (1983). Object vision and spatial vision: Two cortical pathways. *Trends in Neurosciences*, *6*, 414–417. https://doi.org/10.1016/0166-2236(83)90190-X

Mohsenzadeh, Y., Mullin, C., Lahner, B., Cichy, R. M., & Oliva, A. (2019). Reliability and generalizability of similarity-based fusion of MEG and fMRI data in human ventral and dorsal visual streams. *Vision*, *3*(1), 8. https://doi.org/10.3390/vision3010008

Montemurro, M. A., Rasch, M. J., Murayama, Y., Logothetis, N. K., & Panzeri, S. (2008). Phase-of-firing coding of natural visual stimuli in primary visual cortex. *Current Biology*, *18*(5), 375–380. https://doi.org/10.1016/j.cub.2008.02.023

Moore, C. I., Carlen, M., Knoblich, U., & Cardin, J. A. (2010). Neocortical interneurons: From diversity, strength. *Cell*, *142*(2), 189–193. https://doi.org/10.1016/j.cell.2010.07.005

Moran, J., & Desimone, R. (1985). Selective attention gates visual processing in the extrastriate cortex. *Science (New York, N.Y.)*, *229*(4715), 782–784. https://doi.org/10.1126/science.4023713

Morey, R. D., & Rouder, J. N. (2018). *BayesFactor: Computation of bayes factors for common designs*. https://CRAN.R-project.org/package=BayesFactor

Morgan, S. T., Hansen, J. C., & Hillyard, S. A. (1996). Selective attention to stimulus location modulates the steady-state visual evoked potential. *Proceedings of the National Academy of Sciences of the United States of America*, *93*(10), 4770–4774. Retrieved August 18, 2022, from https://www.ncbi.nlm.nih.gov/pmc/articles/PMC39354/

Morris, J. S., Friston, K. J., & Dolan, R. J. (1997). Neural responses to salient visual stimuli. *Proceedings of the Royal Society B: Biological Sciences*, *264*(1382), 769–775. Retrieved October 20, 2023, from https://www.ncbi.nlm.nih.gov/pmc/articles/PMC1688407/

Morrow, A., Elias, M., & Samaha, J. (2023). Evaluating the evidence for the functional inhibition account of alpha-band oscillations during preparatory attention. *Journal of Cognitive Neuroscience*, *35*(8), 1195–1211. https://doi.org/10.1162/jocn_a_02009

Motter, B. C. (1994). Neural correlates of attentive selection for color or luminance in extrastriate area v4. *Journal of Neuroscience*, *14*(4), 2178–2189. https://doi.org/10.1523/JNEUROSCI.14-04-02178.1994

Muckli, L. (2010). What are we missing here? brain imaging evidence for higher cognitive functions in primary visual cortex v1. *International Journal of Imaging Systems and Technology*, *20*(2), 131–139. https://doi.org/10.1002/ima.20236

Muckli, L., & Petro, L. S. (2013). Network interactions: Non-geniculate input to v1. *Current Opinion in Neurobiology*, *23*(2), 195–201. https://doi.org/10.1016/j.conb.2013.01.020

Müller, M. M., Andersen, S., Trujillo, N. J., Valdés-Sosa, P., Malinowski, P., & Hillyard, S. A. (2006). Feature-selective attention enhances color signals in early visual areas of the human brain. *Proceedings of the National Academy of Sciences*, *103*(38), 14250–14254. https://doi.org/10.1073/pnas.0606668103

Müller, M. M., Junghöfer, M., Elbert, T., & Rochstroh, B. (1997). Visually induced gamma-band responses to coherent and incoherent motion: A replication study. *NeuroReport*, *8*, 2575–2579. https://doi.org/10.1097/00001756-199707280-00031

Muthukumaraswamy, S. D., & Singh, K. D. (2013). Visual gamma oscillations: The effects of stimulus type, visual field coverage and stimulus motion on MEG and EEG recordings. *NeuroImage*, *69*. https://doi.org/10.1016/j.neuroimage.2012.12.038

Muthukumaraswamy, S. D., Singh, K. D., Swettenham, J. B., & Jones, D. K. (2010). Visual gamma oscillations and evoked responses: Variability, repeatability and structural MRI correlates. *NeuroImage*, *49*, 3349–3357. https://doi.org/10.1016/j.neuroimage.2009.11.045

Navalpakkam, V., & Itti, L. (2005). Modeling the influence of task on attention. *Vision Research*, *45*(2), 205–231. https://doi.org/10.1016/j.visres.2004.07.042

Nichols, T. E., & Holmes, A. P. (2002). Nonparametric permutation tests for functional neuroimaging: A primer with examples. *Human Brain Mapping*, *15*(1), 1–25. https://doi.org/10.1002/hbm.1058

Nikolić, D., Fries, P., & Singer, W. (2013). Gamma oscillations: Precise temporal coordination without a metronome. *Trends in Cognitive Sciences*, *17*(2), 54–55. https://doi.org/10.1016/j.tics.2012.12.003

Nolte, G. (2003). The magnetic lead field theorem in the quasi-static approximation and its use for magnetoencephalography forward calculation in realistic volume conductors. *Physics in Medicine and Biology*, *48*(22), 3637–3652. https://doi.org/10.1088/0031-9155/48/22/002

Noonan, M. P., Adamian, N., Pike, A., Printzlau, F., Crittenden, B. M., & Stokes, M. G. (2016). Distinct mechanisms for distractor suppression and target facilitation. *The Journal of*

Neuroscience: The Official Journal of the Society for Neuroscience, *36*(6), 1797–1807. https://doi.org/10.1523/JNEUROSCI.2133-15.2016

Notbohm, A., Kurths, J., & Herrmann, C. S. (2016). Modification of brain oscillations via rhythmic light stimulation provides evidence for entrainment but not for superposition of event-related responses. *Frontiers in Human Neuroscience*, *10*, 10. https://doi.org/10.3389/fnhum.2016.00010

Nunn, C. M. H., & Osselton, J. W. (1974). The influence of the EEG alpha rhythm on the perception of visual stimuli. *Psychophysiology*, *11*(3), 294–303. https://doi.org/10.1111/j.1469-8986.1974.tb00547.x

O'Keefe, J., & Recce, M. L. (1993). Phase relationship between hippocampal place units and the EEG theta rhythm. *Hippocampus*, *3*(3), 317–330. https://doi.org/10.1002/hipo.450030307

Oldfield, R. C. (1971). The assessment and analysis of handedness: The edinburgh inventory. *Neuropsychologia*, *9*(1), 97–113. https://doi.org/10.1016/0028-3932(71)90067-4

Olufsen, M. S., Whittington, M. A., Camperi, M., & Kopell, N. (2003). New roles for the gamma rhythm: Population tuning and preprocessing for the beta rhythm. *Journal of Computational Neuroscience*, *14*(1), 33–54. https://doi.org/10.1023/A:1021124317706

Oostenveld, R., Fries, P., Maris, E., & Schoffelen, J.-M. (2010). FieldTrip: Open source software for advanced analysis of MEG, EEG, and invasive electrophysiological data. *Computational Intelligence and Neuroscience*, *2011*, e156869. https://doi.org/10.1155/2011/156869

Osipova, D., Hermes, D., & Jensen, O. (2008). Gamma power is phase-locked to posterior alpha activity. *PLOS ONE*, *3*(12), e3990. https://doi.org/10.1371/journal.pone.0003990

Osipova, D., Takashima, A., Oostenveld, R., Fernández, G., Maris, E., & Jensen, O. (2006). Theta and gamma oscillations predict encoding and retrieval of declarative memory. *Journal of Neuroscience*, *26*(28), 7523–7531. https://doi.org/10.1523/JNEUROSCI.1948-06.2006

Otero, M., Prado-Gutiérrez, P., Weinstein, A., Escobar, M.-J., & El-Deredy, W. (2020). Persistence of eeg alpha entrainment depends on stimulus phase at offset. *Frontiers in Human Neuroscience*, *14*, 139. https://doi.org/10.3389/fnhum.2020.00139

Palmer, E. M., Van Wert, M. J., Horowitz, T. S., & Wolfe, J. M. (2019). Measuring the time course of selection during visual search. *Attention, Perception, & Psychophysics*, *81*(1), 47–60. https://doi.org/10.3758/s13414-018-1596-6

Palmer, J. (1994). Set-size effects in visual search: The effect of attention is independent of the stimulus for simple tasks. *Vision Research*, *34*(13), 1703–1721. https://doi.org/10.1016/0042-6989(94)90128-7

Palva, S., & Palva, J. M. (2007). New vistas for alpha-frequency band oscillations. *Trends in Neurosciences*, *30*(4), 150–158. https://doi.org/10.1016/j.tins.2007.02.001

Pan, Y., Frisson, S., & Jensen, O. (2020). Lexical parafoveal previewing predicts reading speed. *bioRxiv*. https://doi.org/10.1101/2020.10.05.326314

Pan, Y., Popov, T., Frisson, S., & Jensen, O. (2023). Saccades are locked to the phase of alpha oscillations during natural reading. *PLOS Biology*, *21*(1), e3001968. https://doi.org/10.1371/journal.pbio.3001968

Panzeri, S., Brunel, N., Logothetis, N. K., & Kayser, C. (2010). Sensory neural codes using multiplexed temporal scales. *Trends in Neurosciences*, *33*(3), 111–120. https://doi.org/10.1016/j.tins.2009.12.001

Panzeri, S., Macke, J. H., Gross, J., & Kayser, C. (2015). Neural population coding: Combining insights from microscopic and mass signals. *Trends in Cognitive Sciences*, *19*(3), 162–172. https://doi.org/10.1016/j.tics.2015.01.002

Park, H., Ince, R. A. A., Schyns, P. G., Thut, G., & Gross, J. (2018). Representational interactions during audiovisual speech entrainment: Redundancy in left posterior superior temporal gyrus and synergy in left motor cortex. *PLOS Biology*, *16*(8), e2006558. https://doi.org/10.1371/journal.pbio.2006558

Pastuszak, A., Shapiro, K., & Hanslmayr, S. (2018). The role of pre-stimulus alpha oscillation in distractor filtering during a visual search task. *Journal of Vision*, *18*(10), 979. https://doi.org/10.1167/18.10.979

Payne, L., & Sekuler, R. (2014). The importance of ignoring: Alpha oscillations protect selectivity. *Current directions in psychological science*, *23*(3), 171–177. https://doi.org/10.1177/0963721414529145

Perry, G., Hamandi, K., Brindley, L. M., Muthukumaraswamy, S. D., & Singh, K. D. (2013). The properties of induced gamma oscillations in human visual cortex show individual variability in their dependence on stimulus size. *NeuroImage*, *68*, 83–92. https://doi.org/10.1016/j.neuroimage.2012.11.043

Peter, A., Stauch, B. J., Shapcott, K., Kouroupaki, K., Schmiedt, J. T., Klein, L., Klon-Lipok, J., Dowdall, J. R., Schölvinck, M. L., Vinck, M., Schmid, M. C., & Fries, P. (2021). Stimulus-specific plasticity of macaque v1 spike rates and gamma. *Cell Reports*, *37*(10), 110086. https://doi.org/10.1016/j.celrep.2021.110086

Peter, A., Uran, C., Klon-Lipok, J., Roese, R., van Stijn, S., Barnes, W., Dowdall, J. R., Singer, W., Fries, P., & Vinck, M. (2019). Surface color and predictability determine contextual modulation of v1 firing and gamma oscillations (L. Colgin, Ed.). *eLife*, *8*, e42101. https://doi.org/10.7554/eLife.42101

Peylo, C., Hilla, Y., & Sauseng, P. (2021). Cause or consequence? alpha oscillations in visuospatial attention. *Trends in Neurosciences*, *44*(9), 705–713. https://doi.org/10.1016/j.tins.2021.05.004

Pfurtscheller, G. (2001). Functional brain imaging based on ERD/ERS. *Vision Research*, *41*(10), 1257–1260. https://doi.org/10.1016/S0042-6989(00)00235-2

Pfurtscheller, G., & Lopes da Silva, F. H. (1999). Event-related EEG/MEG synchronization and desynchronization: Basic principles. *Clinical Neurophysiology*, *110*(11), 1842–1857. https://doi.org/10.1016/S1388-2457(99)00141-8

Pfurtscheller, G., Stancak, A., Neuper, C., & C. Neuper. (1996). Event-related synchronization (ERS) in the alpha band - an electrophysiological correlate of cortical idling: A review.

International Journal of Psychophysiology, *24*(1), 39–46. https://doi.org/10.1016/s0167-8760(96)00066-9

Piccolino, M., & Bresadola, M. (2013, November 1). *Shocking frogs: Galvani, volta, and the electric origins of neuroscience*. Oxford University Press. https://doi.org/10.1093/acprof:oso/9780199782161.001.0001

Piccolino, M., Bresadola, M., & Wade, N. (2013, November 1). From galvani to hodgkin and beyond: The central problem of electrophysiology in the last two centuries. In M. Piccolino & M. Bresadola (Eds.), *Shocking frogs: Galvani, volta, and the electric origins of neuroscience* (pp. 269–298). Oxford University Press. https://doi.org/10.1093/acprof:oso/9780199782161.003.0009

Pikovsky, A., Kurths, J., Rosenblum, M., & Kurths, J. (2003). *Synchronization: A universal concept in nonlinear sciences* (Vol. 12). Cambridge University Press.

Pinel, J. P., & Barnes, S. (2017). *Biopsychology*. Pearson Higher Ed.

Popov, T., Gips, B., Kastner, S., & Jensen, O. (2019). Spatial specificity of alpha oscillations in the human visual system. *Human Brain Mapping*, *40*(15), 4432–4440. https://doi.org/10.1002/hbm.24712

Popov, T., Miller, G. A., Rockstroh, B., Jensen, O., & Langer, N. (2021, September 24). *Alpha oscillations link action to cognition: An oculomotor account of the brain's dominant rhythm*. bioRxiv. https://doi.org/10.1101/2021.09.24.461634

Popovkina, D. V., Palmer, J., Moore, C. M., & Boynton, G. M. (2021). Is there a serial bottleneck in visual object recognition? *Journal of Vision*, *21*(3), 15. https://doi.org/10.1167/jov.21.3.15

Ptak, R. (2012). The frontoparietal attention network of the human brain: Action, saliency, and a priority map of the environment. *The Neuroscientist: A Review Journal Bringing Neurobiology, Neurology and Psychiatry*, *18*(5), 502–515. https://doi.org/10.1177/1073858411409051

Quintana, D. S., & Williams, D. R. (2018). Bayesian alternatives for common null-hypothesis significance tests in psychiatry: A non-technical guide using JASP. *BMC Psychiatry*, *18*, 1–8. https://doi.org/10.1186/s12888-018-1761-4

Quiquempoix, M., Fayad, S. L., Boutourlinsky, K., Leresche, N., Lambert, R. C., & Bessaih, T. (2018). Layer 2/3 pyramidal neurons control the gain of cortical output. *Cell Reports*, *24*(11), 2799–2807.e4. https://doi.org/10.1016/j.celrep.2018.08.038

R Core Team. (2020). *R: A language and environment for statistical computing*. R Foundation for Statistical Computing. https://www.R-project.org/

Rager, G., & Singer, W. (1998). The response of cat visual cortex to flicker stimuli of variable frequency. *European Journal of Neuroscience*, *10*, 1856–1877. https://doi.org/10.1046/j.1460-9568.1998.00197.x

Ray, S., & Maunsell, J. H. R. (2015). Do gamma oscillations play a role in cerebral cortex? *Trends in Cognitive Sciences*, *19*(2), 78–85. https://doi.org/10.1016/j.tics.2014.12.002

Ray, S., & Maunsell, J. H. (2010). Differences in gamma frequencies across visual cortex restrict their possible use in computation. *Neuron*, *67*(5), 885–896. https://doi.org/10.1016/j.neuron.2010.08.004

Ray, S., & Maunsell, J. H. (2011). Different origins of gamma rhythm and high-gamma activity in macaque visual cortex. *PLoS Biology*, *9*. https://doi.org/10.1371/journal.pbio.1000610

Ray, W. J., & Cole, H. W. (1985). EEG alpha activity reflects attentional demands, and beta activity reflects emotional and cognitive processes. *Science (New York, N.Y.)*, *228*(4700), 750–752. https://doi.org/10.1126/science.3992243

Reynolds, J. H., Chelazzi, L., & Desimone, R. (1999). Competitive mechanisms subserve attention in macaque areas v2 and v4. *The Journal of Neuroscience*, *19*(5), 1736–1753. https://doi.org/10.1523/JNEUROSCI.19-05-01736.1999

Reynolds, J. H., & Desimone, R. (1999). The role of neural mechanisms of attention in solving the binding problem. *Neuron*, *24*(1), 19–29. https://doi.org/10.1016/S0896-6273(00)80819-3

Ringach, D. L. (2004). Mapping receptive fields in primary visual cortex. *The Journal of Physiology*, *558*, 717–728. https://doi.org/10.1113/jphysiol.2004.065771

Rodriguez, E., George, N., Lachaux, J. P., Martinerie, J., Renault, B., & Varela, F. J. (1999). Perception's shadow: Long-distance synchronization of human brain activity. *Nature*, *397*, 430–433. https://doi.org/10.1038/17120

Rodriguez-Larios, J., ElShafei, A., Wiehe, M., & Haegens, S. (2022). Visual working memory recruits two functionally distinct alpha rhythms in posterior cortex. *eNeuro*, *9*(5), ENEURO.0159–22.2022. https://doi.org/10.1523/ENEURO.0159-22.2022

Roelfsema, P. R. (2023). Solving the binding problem: Assemblies form when neurons enhance their firing rate—they don't need to oscillate or synchronize. *Neuron*, *111*(7), 1003–1019. https://doi.org/10.1016/j.neuron.2023.03.016

Roelfsema, P. R., Engel, A. K., König, P., & Singer, W. (1997). Visuomotor integration is associated with zero time-lag synchronization among cortical areas. *Nature*, *385*(6612), 157–161. https://doi.org/10.1038/385157a0

Roelfsema, P., Lamme, V., & Spekreijse, H. (2004). Synchrony and covariation of firing rates in the primary visual cortex during contour grouping. *Nature Neuroscience*, *7*(9), 982–991. https://doi.org/10.1038/nn1304

Rolls, E. T., & Baylis, G. C. (1986). Size and contrast have only small effects on the responses to faces of neurons in the cortex of the superior temporal sulcus of the monkey. *Experimental Brain Research*, *65*(1), 38–48. https://doi.org/10.1007/BF00243828

Rolls, E. T., Aggelopoulos, N. C., & Zheng, F. (2003). The receptive fields of inferior temporal cortex neurons in natural scenes. *The Journal of Neuroscience*, *23*(1), 339–348. https://doi.org/10.1523/JNEUROSCI.23-01-00339.2003

Romei, V., Brodbeck, V., Michel, C., Amedi, A., Pascual-Leone, A., & Thut, G. (2008). Spontaneous fluctuations in posterior α-band EEG activity reflect variability in excitability of human visual areas. *Cerebral Cortex*, *18*(9), 2010–2018. https://doi.org/10.1093/cercor/bhm229

Romei, V., Gross, J., & Thut, G. (2010). On the role of prestimulus alpha rhythms over occipito-parietal areas in visual input regulation: Correlation or causation? *The Journal of Neuroscience: The Official Journal of the Society for Neuroscience*, *30*(25), 8692–8697. https://doi.org/10.1523/JNEUROSCI.0160-10.2010

Rosenblatt, F. (1958). The perceptron: A probabilistic model for information storage and organization in the brain. *Psychological Review*, *65*(6), 386–408. https://doi.org/10.1037/h0042519

Rouhinen, S., Panula, J., Palva, J. M., & Palva, S. (2013). Load dependence of β and γ oscillations predicts individual capacity of visual attention. *Journal of Neuroscience*, *33*(48), 19023–19033. https://doi.org/10.1523/JNEUROSCI.1666-13.2013

Roux, F., Wibral, M., Mohr, H. M., Singer, W., & Uhlhaas, P. J. (2012). Gamma-band activity in human prefrontal cortex codes for the number of relevant items maintained in working memory. *Journal of Neuroscience*, *32*(36), 12411–12420. https://doi.org/10.1523/JNEUROSCI.0421-12.2012

Rutishauser, U., Ross, I. B., Mamelak, A. N., & Schuman, E. M. (2010). Human memory strength is predicted by theta-frequency phase-locking of single neurons. *Nature*, *464*(7290), 903–907. https://doi.org/10.1038/nature08860

Sadaghiani, S., Scheeringa, R., Lehongre, K., Morillon, B., Giraud, A.-L., D'Esposito, M., & Kleinschmidt, A. (2012). Alpha-band phase synchrony is related to activity in the fronto-parietal adaptive control network. *Journal of Neuroscience*, *32*(41), 14305–14310. https://doi.org/10.1523/JNEUROSCI.1358-12.2012

Saenz, M., Buracas, G. T., & Boynton, G. M. (2002). Global effects of feature-based attention in human visual cortex. *Nature Neuroscience*, *5*(7), 631–632. https://doi.org/10.1038/nn876

Sah, P., & Louise Faber, E. S. (2002). Channels underlying neuronal calcium-activated potassium currents. *Progress in Neurobiology*, *66*(5), 345–353. https://doi.org/10.1016/S0301-0082(02)00004-7

Salinas, E., & Sejnowski, T. J. (2000). Impact of correlated synaptic input on output firing rate and variability in simple neuronal models. *The Journal of Neuroscience: The Official*

Journal of the Society for Neuroscience, *20*(16), 6193–6209. https://doi.org/10.1523/JNEUROSCI.20-16-06193.2000

Salinas, E., & Sejnowski, T. J. (2001). Correlated neuronal activity and the flow of neural information. *Nature Reviews Neuroscience*, *2*(8), 539–550. https://doi.org/10.1038/35086012

Samaha, J., & Postle, B. R. (2015). The speed of alpha-band oscillations predicts the temporal resolution of visual perception. *Current Biology*, *25*(22), 2985–2990. https://doi.org/10.1016/j.cub.2015.10.007

Sauseng, P., Klimesch, W., Stadler, W., Schabus, M., Doppelmayr, M., Hanslmayr, S., Gruber, W. R., & Birbaumer, N. (2005). A shift of visual spatial attention is selectively associated with human EEG alpha activity. *European Journal of Neuroscience*, *22*(11), 2917–2926. https://doi.org/10.1111/j.1460-9568.2005.04482.x

Sawaki, R., & Luck, S. J. (2010). Capture versus suppression of attention by salient singletons: Electrophysiological evidence for an automatic attend-to-me signal. *Attention, Perception & Psychophysics*, *72*(6), 1455–1470. https://doi.org/10.3758/APP.72.6.1455

Schadow, J., Lenz, D., Thaerig, S., Busch, N. A., Fründ, I., Rieger, J. W., & Herrmann, C. S. (2007). Stimulus intensity affects early sensory processing: Visual contrast modulates evoked gamma-band activity in human EEG. *International Journal of Psychophysiology*, *66*, 28–36. https://doi.org/10.1016/j.ijpsycho.2007.05.010

Scheeringa, R., Petersson, K. M., Kleinschmidt, A., Jensen, O., & Bastiaansen, M. C. (2012). EEG alpha power modulation of fMRI resting-state connectivity. *Brain Connectivity*, *2*(5), 254–264. https://doi.org/10.1089/brain.2012.0088

Schmidgen, H. (2014, September 15). A research machine. In H. Schmidgen & N. F. Schot (Eds.), *The helmholtz curves: Tracing lost time* (pp. 55–84). Fordham University Press. https://doi.org/10.5422/fordham/9780823261949.003.0004

Schneider, M., Broggini, A. C., Dann, B., Tzanou, A., Uran, C., Sheshadri, S., Scherberger, H., & Vinck, M. (2021). A mechanism for inter-areal coherence through communication

based on connectivity and oscillatory power. *Neuron*, *109*(24), 4050–4067.e12. https://doi.org/10.1016/j.neuron.2021.09.037

Schneider, M., Tzanou, A., Uran, C., & Vinck, M. (2023). Cell-type-specific propagation of visual flicker. *Cell Reports*, *42*(5). https://doi.org/10.1016/j.celrep.2023.112492

Schnitzler, A., & Gross, J. (2005). Normal and pathological oscillatory communication in the brain. *Nature Reviews Neuroscience*, *6*(4), 285–296. https://doi.org/10.1038/nrn1650

Schrimpf, M., Kubilius, J., Hong, H., Majaj, N. J., Rajalingham, R., Issa, E. B., Kar, K., Bashivan, P., Prescott-Roy, J., Geiger, F., Schmidt, K., Yamins, D. L. K., & DiCarlo, J. J. (2020). Brain-score: Which artificial neural network for object recognition is most brain-like? *bioRxiv*, 407007. https://doi.org/10.1101/407007

Schroeder, C. E., & Lakatos, P. (2009). Low-frequency neuronal oscillations as instruments of sensory selection. *Trends in Neurosciences*, *32*(1), 9–18. https://doi.org/10.1016/j.tins.2008.09.012

Schupp, H. T., Lutzenberger, W., Birbaumer, N., Miltner, W., & Braun, C. (1994). Neurophysiological differences between perception and imagery. *Cognitive Brain Research*, *2*(2), 77–86. https://doi.org/10.1016/0926-6410(94)90004-3

Schwab, K., Ligges, C., Jungmann, T., Hilgenfeld, B., Haueisen, J., & Witte, H. (2006). Alpha entrainment in human electroencephalogram and magnetoencephalogram recordings. *NeuroReport*, *17*, 1829–1833. https://doi.org/10.1097/01.wnr.0000246326.89308.ec

Schweigger, J. S. C. (1836). *Einleitung in die Mythologie auf dem Standpunkte der Naturwissenschaft*. Bei Eduard Anton.

Sederberg, P. B., Schulze-Bonhage, A., Madsen, J. R., Bromfield, E. B., Litt, B., Brandt, A., & Kahana, M. J. (2007). Gamma oscillations distinguish true from false memories: Research report. *Psychological Science*, *18*, 927–932. https://doi.org/10.1111/j.1467-9280.2007.02003.x

Sederberg, P. B., Schulze-Bonhage, A., Madsen, J. R., Bromfield, E. B., McCarthy, D. C., Brandt, A., Tully, M. S., & Kahana, M. J. (2007). Hippocampal and neocortical gamma

oscillations predict memory formation in humans. *Cerebral Cortex*, *17*(5), 1190–1196. https://doi.org/10.1093/cercor/bhl030

Seidemann, E., & Newsome, W. T. (1999). Effect of spatial attention on the responses of area MT neurons. *Journal of Neurophysiology*, *81*(4), 1783–1794. https://doi.org/10.1152/jn.1999.81.4.1783

Self, M. W., Peters, J. C., Possel, J. K., Reithler, J., Goebel, R., Ris, P., Jeurissen, D., Reddy, L., Claus, S., Baayen, J. C., & Roelfsema, P. R. (2016). The effects of context and attention on spiking activity in human early visual cortex. *PLOS Biology*, *14*(3), e1002420. https://doi.org/10.1371/journal.pbio.1002420

Serences, J. T., & Yantis, S. (2006). Selective visual attention and perceptual coherence. *Trends in Cognitive Sciences*, *10*(1), 38–45. https://doi.org/10.1016/j.tics.2005.11.008

Serences, J. T., Yantis, S., Culberson, A., & Awh, E. (2004). Preparatory activity in visual cortex indexes distractor suppression during covert spatial orienting. *Journal of Neurophysiology*, *92*(6), 3538–3545. https://doi.org/10.1152/jn.00435.2004

Seyfarth, E.-A. (2006). Julius bernstein (1839–1917): Pioneer neurobiologist and biophysicist. *Biological Cybernetics*, *94*(1), 2–8. https://doi.org/10.1007/s00422-005-0031-y

Shadlen, M. N., & Movshon, J. A. (1999). Synchrony unbound: A critical evaluation of the temporal binding hypothesis. *Neuron*, *24*(1), 67–77, 111–125. https://doi.org/10.1016/s0896-6273(00)80822-3

Sharp, P., Gutteling, T., Melcher, D., & Hickey, C. (2022). Spatial attention tunes temporal processing in early visual cortex by speeding and slowing alpha oscillations. *Journal of Neuroscience*. https://doi.org/10.1523/JNEUROSCI.0509-22.2022

Sherrington, C. (1949). Man and his nature: Broadcast talks in religion and philosophy.

Shin, D., Peelman, K., Lien, A. D., Del Rosario, J., & Haider, B. (2023). Narrowband gamma oscillations propagate and synchronize throughout the mouse thalamocortical visual system. *Neuron*, *111*(7), 1076–1085.e8. https://doi.org/10.1016/j.neuron.2023.03.006

Siegle, J. H., Jia, X., Durand, S., Gale, S., Bennett, C., Graddis, N., Heller, G., Ramirez, T. K., Choi, H., Luviano, J. A., Groblewski, P. A., Ahmed, R., Arkhipov, A., Bernard, A., Billeh,

Y. N., Brown, D., Buice, M. A., Cain, N., Caldejon, S., ... Koch, C. (2021). Survey of spiking in the mouse visual system reveals functional hierarchy. *Nature*, *592*(7852), 86–92. https://doi.org/10.1038/s41586-020-03171-x

Singer, A. C., Martorell, A. J., Douglas, J. M., Abdurrob, F., Attokaren, M. K., Tipton, J., Mathys, H., Adaikkan, C., & Tsai, L.-H. (2018). Noninvasive 40-hz light flicker to recruit microglia and reduce amyloid beta load. *Nature Protocols*, *13*(8), 1850–1868. https://doi.org/10.1038/s41596-018-0021-x

Singer, W., & Gray, C. M. (1995). Visual feature integration and the temporal correlation hypothesis. *Annual Review of Neuroscience*, *18*, 555–586. https://doi.org/10.1146/annurev.ne.18.030195.003011

Singer, W. (1999). Neuronal synchrony: A versatile code for the definition of relations? *Neuron*, *24*(1), 49–65. https://doi.org/10.1016/S0896-6273(00)80821-1

Singer, W. (2009). Distributed processing and temporal codes in neuronal networks. *Cognitive Neurodynamics*, *3*, 189–196. https://doi.org/10.1007/s11571-009-9087-z

Singer, W. (2018). Neuronal oscillations: Unavoidable and useful? *The European Journal of Neuroscience*, *48*(7), 2389–2398. https://doi.org/10.1111/ejn.13796

Skaggs, W. E., McNaughton, B. L., Wilson, M. A., & Barnes, C. A. (1996). Theta phase precession in hippocampal neuronal populations and the compression of temporal sequences. *Hippocampus*, *6*(2), 149–172. https://doi.org/10.1002/(SICI)1098-1063(1996)6:2<149::AID-HIPO6>3.0.CO;2-K

Smith, A. T., Singh, K. D., Williams, A. L., & Greenlee, M. W. (2001). Estimating receptive field size from fMRI data in human striate and extrastriate visual cortex. *Cerebral Cortex (New York, N.Y.: 1991)*, *11*(12), 1182–1190. https://doi.org/10.1093/cercor/11.12.1182

Smith, M. A., Jia, X., Zandvakili, A., & Kohn, A. (2013). Laminar dependence of neuronal correlations in visual cortex. *Journal of Neurophysiology*, *109*(4), 940–947. https://doi.org/10.1152/jn.00846.2012

Snyder, A. C., & Foxe, J. J. (2010). Anticipatory attentional suppression of visual features indexed by oscillatory alpha-band power increases: A high-density electrical mapping

study. *The Journal of Neuroscience: The Official Journal of the Society for Neuroscience*, *30*(11), 4024–4032. https://doi.org/10.1523/JNEUROSCI.5684-09.2010

Sohal, V. S. (2016). How close are we to understanding what (if anything) γ oscillations do in cortical circuits? *Journal of Neuroscience*, *36*(41), 10489–10495. https://doi.org/10.1523/JNEUROSCI.0990-16.2016

Sokoliuk, R., Mayhew, S. D., Aquino, K. M., Wilson, R., Brookes, M. J., Francis, S. T., Hanslmayr, S., & Mullinger, K. J. (2019). Two spatially distinct posterior alpha sources fulfill different functional roles in attention. *The Journal of Neuroscience: The Official Journal of the Society for Neuroscience*, *39*(36), 7183–7194. https://doi.org/10.1523/JNEUROSCI.1993-18.2019

Sörensen, L. K. A., Zambrano, D., Slagter, H. A., Bohté, S. M., & Scholte, H. S. (2022). Leveraging spiking deep neural networks to understand the neural mechanisms underlying selective attention. *Journal of Cognitive Neuroscience*, *34*(4), 655–674. https://doi.org/10.1162/jocn_a_01819

Soula, M., Martín-Ávila, A., Zhang, Y., Dhingra, A., Nitzan, N., Sadowski, M. J., Gan, W.-B., & Buzsáki, G. (2023). Forty-hertz light stimulation does not entrain native gamma oscillations in alzheimer's disease model mice. *Nature Neuroscience*, 1–9. https://doi.org/10.1038/s41593-023-01270-2

Spaak, E., Bonnefond, M., Maier, A., Leopold, D. A., & Jensen, O. (2012). Layer-specific entrainment of gamma-band neural activity by the alpha rhythm in monkey visual cortex. *Current Biology*, *22*, 2313–2318. https://doi.org/10.1016/j.cub.2012.10.020

Spaak, E., de Lange, F. P., & Jensen, O. (2014). Local entrainment of α oscillations by visual stimuli causes cyclic modulation of perception. *The Journal of Neuroscience: The Official Journal of the Society for Neuroscience*, *34*(10), 3536–3544. https://doi.org/10.1523/JNEUROSCI.4385-13.2014

Spaak, E., Fonken, Y., Jensen, O., & de Lange, F. P. (2016). The neural mechanisms of prediction in visual search. *Cerebral Cortex (New York, N.Y.: 1991)*, *26*(11), 4327–4336. https://doi.org/10.1093/cercor/bhv210

Sprague, T. C., & Serences, J. T. (2013). Attention modulates spatial priority maps in the human occipital, parietal and frontal cortices. *Nature Neuroscience*, *16*(12), 1879–1887. https://doi.org/10.1038/nn.3574

Stauch, B. J., Peter, A., Ehrlich, I., Nolte, Z., & Fries, P. (2022). Human visual gamma for color stimuli (L. L. Colgin & C. I. Moore, Eds.). *eLife*, *11*, e75897. https://doi.org/10.7554/eLife.75897

Staudigl, T., Hartl, E., Noachtar, S., Doeller, C. F., & Jensen, O. (2017). Saccades are phase-locked to alpha oscillations in the occipital and medial temporal lobe during successful memory encoding (F. Tong, Ed.). *PLOS Biology*, *15*(12), e2003404. https://doi.org/10.1371/journal.pbio.2003404

Steinmetz, N. A., Aydin, C., Lebedeva, A., Okun, M., Pachitariu, M., Bauza, M., Beau, M., Bhagat, J., Böhm, C., Broux, M., Chen, S., Colonell, J., Gardner, R. J., Karsh, B., Kloosterman, F., Kostadinov, D., Mora-Lopez, C., O'Callaghan, J., Park, J., . . . Harris, T. D. (2021). Neuropixels 2.0: A miniaturized high-density probe for stable, long-term brain recordings. *Science*, *372*(6539), eabf4588. https://doi.org/10.1126/science.abf4588

Stenroos, M., Hunold, A., Eichardt, R., & Haueisen, J. (2012). Comparison of three- and single-shell volume conductor models in magnetoencephalography. *Biomedical Engineering*, *57*, 311. https://doi.org/10.1515/bmt-2012-4396

Storm, J. F. (1990). Potassium currents in hippocampal pyramidal cells. *Progress in Brain Research*, *83*, 161–187. https://doi.org/10.1016/s0079-6123(08)61248-0

Tallon, C., Bertrand, O., Bouchet, P., & Pernier, J. (1995). Gamma-range activity evoked by coherent visual stimuli in humans. *European Journal of Neuroscience*, *7*, 1285–1291. https://doi.org/10.1111/j.1460-9568.1995.tb01118.x

Tallon-Baudry, C. (2009). The roles of gamma-band oscillatory synchrony in human visual cognition. *Frontiers in Bioscience (Landmark Edition)*, *14*(1), 321–332. https://doi.org/10.2741/3246

Tallon-Baudry, C., Bertrand, O., Tallon-Baudry, C., Bertrand, O., Tallon-Baudry, C., & Bertrand, O. (1999). Oscillatory gamma activity in humans and its role in object representa-

tion. *Trends in Cognitive Sciences*, *3*(4), 151–162. https://doi.org/10.1016/S1364-6613(99)01299-1

Tan, H. R., Gross, J., & Uhlhaas, P. J. (2016). MEG sensor and source measures of visually induced gamma-band oscillations are highly reliable. *NeuroImage*, *137*, 34–44. https://doi.org/10.1016/j.neuroimage.2016.05.006

Tass, P., Rosenblum, M. G., Weule, J., Kurths, J., Pikovsky, A., Volkmann, J., Schnitzler, A., & Freund, H. J. (1998). Detection of n:m phase locking from noisy data: Application to magnetoencephalography. *Physical Review Letters*, *81*, 3291–3294. https://doi.org/10.1103/PhysRevLett.81.3291

Taylor, K., Mandon, S., Freiwald, W., & Kreiter, A. (2005). Coherent oscillatory activity in monkey area v4 predicts successful allocation of attention. *Cerebral Cortex*, *15*(9), 1424–1437. https://doi.org/10.1093/cercor/bhi023

Thayer, D. D., Miller, M., Giesbrecht, B., & Sprague, T. C. (2022). Learned feature regularities enable suppression of spatially overlapping stimuli. *Attention, Perception, & Psychophysics*. https://doi.org/10.3758/s13414-022-02612-1

Thompson, K. G., & Bichot, N. P. (2005). A visual salience map in the primate frontal eye field. *Progress in Brain Research*, *147*, 251–262. https://doi.org/10.1016/S0079-6123(04)47019-8

Thompson, K. G., Bichot, N. P., & Sato, T. R. (2005). Frontal eye field activity before visual search errors reveals the integration of bottom-up and top-down salience. *Journal of Neurophysiology*, *93*(1), 337–351. https://doi.org/10.1152/jn.00330.2004

Thut, G., Schyns, P., & Gross, J. (2011). Entrainment of perceptually relevant brain oscillations by non-invasive rhythmic stimulation of the human brain. *Frontiers in Psychology*, *2*, 170. https://doi.org/10.3389/fpsyg.2011.00170

Tiesinga, P. H. E. (2012). Motifs in health and disease: The promise of circuit interrogation by optogenetics. *European Journal of Neuroscience*, *36*(2), 2260–2272. https://doi.org/ https://doi.org/10.1111/j.1460-9568.2012.08186.x

Tovee, M. J., Rolls, E. T., & Azzopardi, P. (1994). Translation invariance in the responses to faces of single neurons in the temporal visual cortical areas of the alert macaque. *Journal of Neurophysiology*, *72*(3), 1049–1060. https://doi.org/10.1152/jn.1994.72.3.1049

Traikapi, A., & Konstantinou, N. (2021). Gamma oscillations in alzheimer's disease and their potential therapeutic role. *Frontiers in Systems Neuroscience*, *15*. Retrieved July 25, 2023, from https://www.frontiersin.org/articles/10.3389/fnsys.2021.782399

Traub, R. D., Jefferys, J. G., & Whittington, M. A. (1997). Simulation of gamma rhythms in networks of interneurons and pyramidal cells. *Journal of Computational Neuroscience*, *4*(2), 141–150. https://doi.org/10.1023/a:1008839312043

Traub, R. D., & Whittington, M. (2010). *Cortical oscillations in health and disease*. Oxford University Press. https://doi.org/10.1093/acprof:oso/9780195342796.001.0001

Traub, R. D., Whittington, M. A., Stanford, I. M., & Jefferys, J. G. R. (1996). A mechanism for generation of long-range synchronous fast oscillations in the cortex. *Nature*, *383*(6601), 621–624. https://doi.org/10.1038/383621a0

Treisman, A., Garry Gelade, Garry Gelade, & Gelade, G. A. (1980). A feature-integration theory of attention. *Cognitive Psychology*, *12*(1), 97–136. https://doi.org/10.1016/0010-0285(80)90005-5

Treue, S. (2001). Neural correlates of attention in primate visual cortex. *Trends in Neurosciences*, *24*(5), 295–300. https://doi.org/10.1016/s0166-2236(00)01814-2

Uhlhaas, P., Pipa, G., Lima, B., Melloni, L., Neuenschwander, S., Nikolić, D., & Singer, W. (2009). Neural synchrony in cortical networks: History, concept and current status. *Frontiers in Integrative Neuroscience*, *3*. https://doi.org/10.3389/neuro.07.017.2009

Uhlhaas, P. J., Haenschel, C., Nikolić, D., & Singer, W. (2008). The role of oscillations and synchrony in cortical networks and their putative relevance for the pathophysiology of schizophrenia. *Schizophrenia Bulletin*, *34*(5), 927–943. https://doi.org/10.1093/schbul/sbn062

Uhlhaas, P. J., & Singer, W. (2006). Neural synchrony in brain disorders: Relevance for cognitive dysfunctions and pathophysiology. *Neuron*, *52*(1), 155–168. https://doi.org/10.1016/j.neuron.2006.09.020

Uhlhaas, P. J., & Singer, W. (2010). Abnormal neural oscillations and synchrony in schizophrenia. *Nature Reviews Neuroscience*, *11*(2), 100–113. https://doi.org/10.1038/nrn2774

Underwood, E. A. (1955). Galvani and the discovery of 'animal electricity'. *Nature*, *175*(4454), 441–442. https://doi.org/10.1038/175441a0

Ungerleider, L. G., & Haxby, J. V. (1994). 'what' and 'where' in the human brain. *Current Opinion in Neurobiology*, *4*(2), 157–165. https://doi.org/10.1016/0959-4388(94)90066-3

Upton, A., & Payan, J. (1970). Dr. lippold and the alpha rhythm. *Nature*, *226*(5250), 1073. https://doi.org/10.1038/2261073a0

Valera, F. J., Toro, A., Roy John, E., & Schwartz, E. L. (1981). Perceptual framing and cortical alpha rhythm. *Neuropsychologia*, *19*(5), 675–686. https://doi.org/10.1016/0028-3932(81)90005-1

Van Diepen, R. M., Foxe, J. J., & Mazaheri, A. (2019). The functional role of alpha-band activity in attentional processing: The current zeitgeist and future outlook. *Current Opinion in Psychology*, *29*, 229–238. https://doi.org/10.1016/j.copsyc.2019.03.015

Van Essen, D. C., Anderson, C. H., & Felleman, D. J. (1992). Information processing in the primate visual system: An integrated systems perspective. *Science*, *255*(5043), 419–423. https://doi.org/10.1126/science.1734518

Van Essen, D. C., Olshausen, B. A., Anderson, C. H., & Gallant, J. T. (1991, July 9). Pattern recognition, attention, and information bottlenecks in the primate visual system. In B. P. Mathur & C. Koch (Eds.). https://doi.org/10.1117/12.45537

van Bree, S., Melcón, M., Kolibius, L. D., Kerrén, C., Wimber, M., & Hanslmayr, S. (2022). The brain time toolbox, a software library to retune electrophysiology data to brain dynamics. *Nature Human Behaviour*, *6*(10), 1430–1439. https://doi.org/10.1038/s41562-022-01386-8

van Es, M. W. J., Marshall, T. R., Spaak, E., Jensen, O., & Schoffelen, J.-M. (2022). Phasic modulation of visual representations during sustained attention. *European Journal of Neuroscience*, *55*(11), 3191–3208. https://doi.org/10.1111/ejn.15084

van Gerven, M. A. J., & Jensen, O. (2009). Attention modulations of posterior alpha as a control signal for two-dimensional brain-computer interfaces. *Journal of Neuroscience Methods*, *179*(1), 78–84. https://doi.org/10.1016/j.jneumeth.2009.01.016

van Kerkoerle, T., Self, M. W., Dagnino, B., Gariel-Mathis, M.-A., Poort, J., van der Togt, C., & Roelfsema, P. R. (2014). Alpha and gamma oscillations characterize feedback and feedforward processing in monkey visual cortex. *Proceedings of the National Academy of Sciences*, *111*(40), 14332–14341. https://doi.org/10.1073/pnas.1402773111

van Pelt, S., Boomsma, D. I., & Fries, P. (2012). Magnetoencephalography in twins reveals a strong genetic determination of the peak frequency of visually induced gamma-band synchronization. *Journal of Neuroscience*, *32*(10), 3388–3392. https://doi.org/10.1523/JNEUROSCI.5592-11.2012

van Pelt, S., & Fries, P. (2013). Visual stimulus eccentricity affects human gamma peak frequency. *NeuroImage*, *78*, 439–447. https://doi.org/10.1016/j.neuroimage.2013.04.040

VanRullen, R. (2016). Perceptual cycles. *Trends in Cognitive Sciences*, *20*(10), 723–735. https://doi.org/10.1016/j.tics.2016.07.006

VanRullen, R., & Macdonald, J. S. (2012). Perceptual echoes at 10 hz in the human brain. *Current Biology*, *22*(11), 995–999. https://doi.org/10.1016/j.cub.2012.03.050

VanRullen, R., & Thorpe, S. J. (2001). Is it a bird? is it a plane? ultra-rapid visual categorisation of natural and artifactual objects. *Perception*, *30*(6), 655–668. https://doi.org/10.1068/p3029

VanRullen, R., Zoefel, B., & Ilhan, B. (2014). On the cyclic nature of perception in vision versus audition. *Philosophical Transactions of the Royal Society B: Biological Sciences*, *369*(1641), 20130214. https://doi.org/10.1098/rstb.2013.0214

van Zoest, W., Huber-Huber, C., Weaver, M. D., & Hickey, C. (2021). Strategic distractor suppression improves selective control in human vision. *The Journal of Neuroscience*, *41*(33), 7120–7135. https://doi.org/10.1523/JNEUROSCI.0553-21.2021

Varela, F., Lachaux, J.-P., Rodriguez, E., & Martinerie, J. (2001). The brainweb: Phase synchronization and large-scale integration. *Nature Reviews Neuroscience*, *2*(4), 229–239. https://doi.org/10.1038/35067550

Veen, B., Joseph, J., & Hecox, K. (1992). Localization of intra-cerebral sources of electrical activity via linearly constrained minimum variance spatial filtering. *1992 IEEE 6th SP Workshop on Statistical Signal and Array Processing, SSAP 1992 - Conference Proceedings*, *44*, 526–529. https://doi.org/10.1109/SSAP.1992.246899

Verret, L., Mann, E. O., Hang, G. B., Barth, A. M. I., Cobos, I., Ho, K., Devidze, N., Masliah, E., Kreitzer, A. C., Mody, I., Mucke, L., & Palop, J. J. (2012). Inhibitory interneuron deficit links altered network activity and cognitive dysfunction in alzheimer model. *Cell*, *149*(3), 708–721. https://doi.org/10.1016/j.cell.2012.02.046

Vidal, J. R., Chaumon, M., O'Regan, J. K., & Tallon-Baudry, C. (2006). Visual grouping and the focusing of attention induce gamma-band oscillations at different frequencies in human magnetoencephalogram signals. *Journal of Cognitive Neuroscience*, *18*(11), 1850–1862. https://doi.org/10.1162/jocn.2006.18.11.1850

Vinck, M., & Bosman, C. A. (2016). More gamma more predictions: Gamma-synchronization as a key mechanism for efficient integration of classical receptive field inputs with surround predictions. *Frontiers in Systems Neuroscience*, *10*. Retrieved October 7, 2023, from https://www.frontiersin.org/articles/10.3389/fnsys.2016.00035

Vinck, M., Lima, B., Womelsdorf, T., Oostenveld, R., Singer, W., Neuenschwander, S., & Fries, P. (2010). Gamma-phase shifting in awake monkey visual cortex. *Journal of Neuroscience*, *30*(4), 1250–1257. https://doi.org/10.1523/JNEUROSCI.1623-09.2010

Vinck, M., Uran, C., Spyropoulos, G., Onorato, I., Broggini, A. C., Schneider, M., & Canales-Johnson, A. (2023). Principles of large-scale neural interactions. *Neuron*, *111*(7), 987–1002. https://doi.org/10.1016/j.neuron.2023.03.015

Vinck, M., Womelsdorf, T., Buffalo, E. A., Desimone, R., & Fries, P. (2013). Attentional modulation of cell-class-specific gamma-band synchronization in awake monkey area v4. *Neuron*, *80*(4), 1077–1089. https://doi.org/10.1016/j.neuron.2013.08.019

Vinken, K., Boix, X., & Kreiman, G. (2020). Incorporating intrinsic suppression in deep neural networks captures dynamics of adaptation in neurophysiology and perception. *Science Advances*, *6*(42), eabd4205. https://doi.org/10.1126/sciadv.abd4205

Virtanen, P., Gommers, R., Oliphant, T. E., Haberland, M., Reddy, T., Cournapeau, D., Burovski, E., Peterson, P., Weckesser, W., Bright, J., van der Walt, S. J., Brett, M., Wilson, J., Millman, K. J., Mayorov, N., Nelson, A. R. J., Jones, E., Kern, R., Larson, E., . . . van Mulbregt, P. (2020). SciPy 1.0: Fundamental algorithms for scientific computing in python. *Nature Methods*, *17*(3), 261–272. https://doi.org/10.1038/s41592-019-0686-2

Vissers, M. E., van Driel, J., & Slagter, H. A. (2016). Proactive, but not reactive, distractor filtering relies on local modulation of alpha oscillatory activity. *Journal of Cognitive Neuroscience*, *28*(12), 1964–1979. https://doi.org/10.1162/jocn_a_01017

Vogels, T. P., & Abbott, L. F. (2009). Gating multiple signals through detailed balance of excitation and inhibition in spiking networks. *Nature Neuroscience*, *12*(4), 483–491. https://doi.org/10.1038/nn.2276

von der Malsburg, C. (1981). *The correlation theory of brain function* (Departmental Technical Report). MPI. Retrieved October 20, 2023, from https://web-archive.southampton.ac.uk/cogprints.org/1380/

von der Malsburg, C. (1985). Nervous structures with dynamical links. *Berichte der Bunsen-gesellschaft für physikalische Chemie*, *89*(6), 703–710. https://doi.org/10.1002/bbpc.19850890625

von der Malsburg, C. (1995). Binding in models of perception and brain function. *Current Opinion in Neurobiology*, *5*(4), 520–526. https://doi.org/10.1016/0959-4388(95)80014-X

von der Malsburg, C. (1999). The what and why of binding: The modeler's perspective. *Neuron*, *24*, 95–104.

von Helmholtz, H. (2021). Messungen über den zeitlichen Verlauf der Zuckung animalischer Muskeln und die Fortpflanzungsgeschwindigkeit der Reizung in den Nerven. In H. Schmidgen (Ed.), *Hermann von Helmholtz: Versuche zur Fortpflanzungsgeschwindigkeit der Reizung in den Nerven* (pp. 63–122). Springer. https://doi.org/10.1007/978-3-662-63833-0_4

Voulodimos, A., Doulamis, N., Doulamis, A., & Protopapadakis, E. (2018). Deep learning for computer vision: A brief review. *Computational Intelligence and Neuroscience*, *2018*, e7068349. https://doi.org/10.1155/2018/7068349

Voytek, B., Canolty, R., Shestyuk, A., Crone, N., Parvizi, J., & Knight, R. (2010). Shifts in gamma phase–amplitude coupling frequency from theta to alpha over posterior cortex during visual tasks. *Frontiers in Human Neuroscience*, *4*. Retrieved October 11, 2023, from https://www.frontiersin.org/articles/10.3389/fnhum.2010.00191

Wang, X.-J., & Buzsáki, G. (1996). Gamma oscillation by synaptic inhibition in a hippocampal interneuronal network model. *Journal of Neuroscience*, *16*(20), 6402–6413. https://doi.org/10.1523/JNEUROSCI.16-20-06402.1996

Watson, B. O., Ding, M., & Buzsáki, G. (2018). Temporal coupling of field potentials and action potentials in the neocortex. *European Journal of Neuroscience*, *48*(7), 2482–2497. https://doi.org/10.1111/ejn.13807

Wehr, M., & Laurent, G. (1996). Odour encoding by temporal sequences of firing in oscillating neural assemblies. *Nature*, *384*, 162–166. https://doi.org/10.1038/384162a0

Westner, B. U., Dalal, S. S., Gramfort, A., Litvak, V., Mosher, J. C., Oostenveld, R., & Schoffelen, J.-M. (2022). A unified view on beamformers for m/EEG source reconstruction. *NeuroImage*, *246*, 118789. https://doi.org/10.1016/j.neuroimage.2021.118789

White, A. L., Palmer, J., Boynton, G. M., & Yeatman, J. D. (2019). Parallel spatial channels converge at a bottleneck in anterior word-selective cortex. *Proceedings of the National Academy of Sciences*, *116*(20), 10087–10096. https://doi.org/10.1073/pnas.1822137116

White, A. L., Runeson, E., Palmer, J., Ernst, Z. R., & Boynton, G. M. (2017). Evidence for unlimited capacity processing of simple features in visual cortex. *Journal of Vision*, *17*(6), 19. https://doi.org/10.1167/17.6.19

Whittington, M. A., Cunningham, M. O., LeBeau, F. E., Racca, C., & Traub, R. D. (2011). Multiple origins of the cortical gamma rhythm. *Developmental Neurobiology*, *71*(1), 92–106. https://doi.org/10.1002/dneu.20814

Williams, P. E., Mechler, F., Gordon, J., Shapley, R., & Hawken, M. J. (2004). Entrainment to video displays in primary visual cortex of macaque and humans. *Journal of Neuroscience*, *24*(38), 8278–8288. https://doi.org/10.1523/JNEUROSCI.2716-04.2004

Wilson, H. R., & Cowan, J. D. (1972). Excitatory and inhibitory interactions in localized populations of model neurons. *Biophysical Journal*, *12*, 1–24. https://doi.org/10.1016/S0006-3495(72)86068-5

Wolfe, J. M. (1994). Guided search 2.0 a revised model of visual search. *Psychonomic Bulletin & Review*, *1*(2), 202–238. https://doi.org/10.3758/BF03200774

Wolfe, J. M. (1998). What can 1 million trials tell us about visual search? *Psychological Science*, *9*(1), 33–39. https://doi.org/10.1111/1467-9280.00006

Wolfe, J. M. (2021). Guided search 6.0: An updated model of visual search. *Psychonomic Bulletin & Review*, *28*(4), 1060–1092. https://doi.org/10.3758/s13423-020-01859-9

Wolfe, J. M., Cave, K. R., & Franzel, S. L. (1989). Guided search: An alternative to the feature integration model for visual search. *Journal of Experimental Psychology: Human Perception and Performance*, *15*(3), 419–433. https://doi.org/10.1037/0096-1523.15.3.419

Wolfe, J. M., & Horowitz, T. S. (2017). Five factors that guide attention in visual search. *Nature Human Behaviour*, *1*(3), 1–8. https://doi.org/10.1038/s41562-017-0058

Wolfe, J. M., Palmer, E. M., & Horowitz, T. S. (2010). Reaction time distributions constrain models of visual search. *Vision Research*, *50*(14), 1304–1311. https://doi.org/10.1016/j.visres.2009.11.002

Wolfe, J. M., Reinecke, A., & Brawn, P. (2006). Why don't we see changes?: The role of attentional bottlenecks and limited visual memory. *Visual cognition*, *14*(4), 749–780. https://doi.org/10.1080/13506280500195292

Womelsdorf, T., Fries, P., Mitra, P. P., & Desimone, R. (2006). Gamma-band synchronization in visual cortex predicts speed of change detection. *439*, 15.

Womelsdorf, T., Lima, B., Vinck, M., Oostenveld, R., Singer, W., Neuenschwander, S., & Fries, P. (2012). Orientation selectivity and noise correlation in awake monkey area v1 are modulated by the gamma cycle. *Proceedings of the National Academy of Sciences*, *109*(11), 4302–4307. https://doi.org/10.1073/pnas.1114223109

Womelsdorf, T., Schoffelen, J.-M., Oostenveld, R., Singer, W., Desimone, R., Engel, A. K., & Fries, P. (2007). Modulation of neuronal interactions through neuronal synchronization. *Science (New York, N.Y.)*, *316*(5831), 1609–1612. https://doi.org/10.1126/science.1139597

Wong, R. K., Prince, D. A., & Basbaum, A. I. (1979). Intradendritic recordings from hippocampal neurons. *Proceedings of the National Academy of Sciences of the United States of America*, *76*(2), 986–990. https://doi.org/10.1073/pnas.76.2.986

Worden, M. S., Foxe, J. J., Wang, N., & Simpson, G. V. (2000). Anticipatory biasing of visuospatial attention indexed by retinotopically specific α-bank electroencephalography increases over occipital cortex. *Journal of Neuroscience*, *20*(6), RC63–RC63. https://doi.org/10.1523/JNEUROSCI.20-06-j0002.2000

Wu, R., Yan, S., Shan, Y., Dang, Q., & Sun, G. (2015, July 5). Deep image: Scaling up image recognition. https://doi.org/10.48550/arXiv.1501.02876

Wutz, A., Melcher, D., & Samaha, J. (2018). Frequency modulation of neural oscillations according to visual task demands. *Proceedings of the National Academy of Sciences*, *115*(6), 1346–1351. https://doi.org/10.1073/pnas.1713318115

Xing, D., Yeh, C.-I., Burns, S., & Shapley, R. M. (2012). Laminar analysis of visually evoked activity in the primary visual cortex. *Proceedings of the National Academy of Sciences*, *109*(34), 13871–13876. https://doi.org/10.1073/pnas.1201478109

Yamins, D. L. K., & DiCarlo, J. J. (2016). Using goal-driven deep learning models to understand sensory cortex. *Nature Neuroscience*, *19*(3), 356–365. https://doi.org/10.1038/nn.4244

Yamins, D. L. K., Hong, H., Cadieu, C. F., Solomon, E. A., Seibert, D., & DiCarlo, J. J. (2014). Performance-optimized hierarchical models predict neural responses in higher visual cortex. *Proceedings of the National Academy of Sciences*, *111*(23), 8619–8624. https://doi.org/10.1073/pnas.1403112111

Yuasa, K., Groen, I. I. A., Piantoni, G., Montenegro, S., Flinker, A., Devore, S., Devinsky, O., Doyle, W., Dugan, P., Friedman, D., Ramsey, N., Petridou, N., & Winawer, J. (2023, April 6). Precise spatial tuning of visually driven alpha oscillations in human visual cortex. https://doi.org/10.1101/2023.02.11.528137

Zaehle, T., Rach, S., & Herrmann, C. S. (2010). Transcranial alternating current stimulation enhances individual alpha activity in human EEG. *Public Library of Science One*, *5*, e13766. https://doi.org/10.1371/journal.pone.0013766

Zambrano, D., Nusselder, R., Scholte, H. S., & Bohté, S. M. (2019). Sparse computation in adaptive spiking neural networks. *Frontiers in Neuroscience*, *12*. https://doi.org/10.3389/fnins.2018.00987

Zelinsky, G. J., & Bisley, J. W. (2015). The what, where, and why of priority maps and their interactions with visual working memory. *Annals of the New York Academy of Sciences*, *1339*(1), 154–164. https://doi.org/10.1111/nyas.12606

Zhang, H., Watrous, A. J., Patel, A., & Jacobs, J. (2018). Theta and alpha oscillations are traveling waves in the human neocortex. *Neuron*, *98*(6), 1269–1281.e4. https://doi.org/10.1016/j.neuron.2018.05.019

Zhao, C., Kong, Y., Li, D., Huang, J., Kong, L., Li, X., Jensen, O., & Song, Y. (2023). Suppression of distracting inputs by visual-spatial cues is driven by anticipatory alpha activity. *PLOS Biology*, *21*(3), e3002014. https://doi.org/10.1371/journal.pbio.3002014

Zhigalov, A., Duecker, K., & Jensen, O. (2021). The visual cortex produces gamma band echo in response to broadband visual flicker. *PLOS Computational Biology*, *17*(6), e1009046. https://doi.org/10.1371/journal.pcbi.1009046

Zhigalov, A., Herring, J. D., Herpers, J., Bergmann, T. O., & Jensen, l. (2019). Probing cortical excitability using rapid frequency tagging. *NeuroImage*, *195*, 59–66. https://doi.org/10.1016/j.neuroimage.2019.03.056

Zhigalov, A., & Jensen, O. (2020). Alpha oscillations do not implement gain control in early visual cortex but rather gating in parieto-occipital regions. *Human Brain Mapping*, *41*(18), 5176–5186. https://doi.org/10.1002/hbm.25183

Zhigalov, A., & Jensen, O. (2023). Perceptual echoes as travelling waves may arise from two discrete neuronal sources. *NeuroImage*, *272*, 120047. https://doi.org/10.1016/j.neuroimage.2023.120047

Zumer, J. M., Scheeringa, R., Schoffelen, J.-M., Norris, D. G., & Jensen, O. (2014). Occipital alpha activity during stimulus processing gates the information flow to object-selective cortex. *PLOS Biology*, *12*(10), e1001965. https://doi.org/10.1371/journal.pbio.1001965